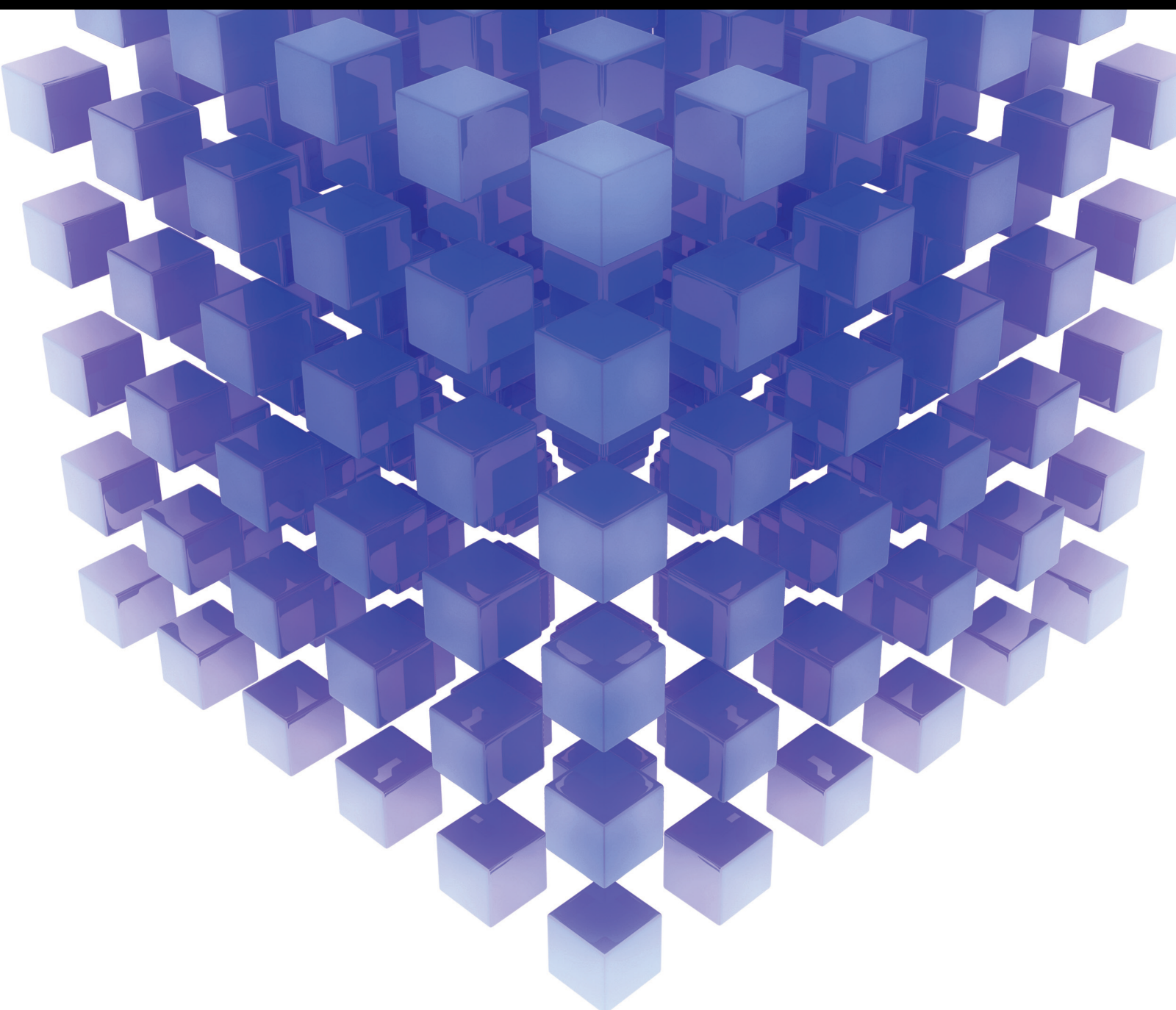# Optimisation of Contactless Delivery

Lead Guest Editor: Yandong He
Guest Editors: Lin Zhou, Fuli Zhou, and Sunil Tiwari

Optimisation of Contactless Delivery

Optimisation of Contactless Delivery

Lead Guest Editor: Yandong He
Guest Editors: Lin Zhou, Fuli Zhou, and Sunil Tiwari

Paolo Boscariol, Italy
Daniela Boso (iD), Italy
Guillermo Botella-Juan, Spain
Abdesselem Boulkroune (iD), Algeria
Boulaïd Boulkroune, Belgium
Fabio Bovenga (iD), Italy
Francesco Braghin (iD), Italy
Ricardo Branco, Portugal
Julien Bruchon (iD), France
Matteo Bruggi (iD), Italy
Michele Brun (iD), Italy
Maria Elena Bruni, Italy
Maria Angela Butturi (iD), Italy
Bartłomiej Błachowski (iD), Poland
Dhanamjayulu C (iD), India
Raquel Caballero-Águila (iD), Spain
Filippo Cacace (iD), Italy
Salvatore Caddemi (iD), Italy
Zuowei Cai (iD), China
Roberto Caldelli (iD), Italy
Francesco Cannizzaro (iD), Italy
Maosen Cao (iD), China
Ana Carpio, Spain
Rodrigo Carvajal (iD), Chile
Caterina Casavola, Italy
Sara Casciati, Italy
Federica Caselli (iD), Italy
Carmen Castillo (iD), Spain
Inmaculada T. Castro (iD), Spain
Miguel Castro (iD), Portugal
Giuseppe Catalanotti (iD), United Kingdom
Alberto Cavallo (iD), Italy
Gabriele Cazzulani (iD), Italy
Fatih Vehbi Celebi, Turkey
Miguel Cerrolaza (iD), Venezuela
Gregory Chagnon (iD), France
Ching-Ter Chang (iD), Taiwan
Kuei-Lun Chang (iD), Taiwan
Qing Chang (iD), USA
Xiaoheng Chang (iD), China
Prasenjit Chatterjee (iD), Lithuania
Kacem Chehdi, France
Peter N. Cheimets, USA
Chih-Chiang Chen (iD), Taiwan
He Chen (iD), China

Kebing Chen (iD), China
Mengxin Chen (iD), China
Shyi-Ming Chen (iD), Taiwan
Xizhong Chen (iD), Ireland
Xue-Bo Chen (iD), China
Zhiwen Chen (iD), China
Qiang Cheng, USA
Zeyang Cheng, China
Luca Chiapponi (iD), Italy
Francisco Chicano (iD), Spain
Tirivanhu Chinyoka (iD), South Africa
Adrian Chmielewski (iD), Poland
Seongim Choi (iD), USA
Gautam Choubey (iD), India
Hung-Yuan Chung (iD), Taiwan
Yusheng Ci, China
Simone Cinquemani (iD), Italy
Roberto G. Citarella (iD), Italy
Joaquim Ciurana (iD), Spain
John D. Clayton (iD), USA
Piero Colajanni (iD), Italy
Giuseppina Colicchio, Italy
Vassilios Constantoudis (iD), Greece
Enrico Conte, Italy
Alessandro Contento (iD), USA
Mario Cools (iD), Belgium
Gino Cortellessa, Italy
Carlo Cosentino (iD), Italy
Paolo Crippa (iD), Italy
Erik Cuevas (iD), Mexico
Guozeng Cui (iD), China
Mehmet Cunkas (iD), Turkey
Giuseppe D'Aniello (iD), Italy
Peter Dabnichki, Australia
Weizhong Dai (iD), USA
Zhifeng Dai (iD), China
Purushothaman Damodaran (iD), USA
Sergey Dashkovskiy, Germany
Adiel T. De Almeida-Filho (iD), Brazil
Fabio De Angelis (iD), Italy
Samuele De Bartolo (iD), Italy
Stefano De Miranda (iD), Italy
Filippo De Monte (iD), Italy

Francisco J. Martos, Spain
Elio Masciari, Italy
Paolo Massioni, France
Alessandro Mauro, Italy
Jonathan Mayo-Maldonado, Mexico
Pier Luigi Mazzeo, Italy
Laura Mazzola, Italy
Driss Mehdi, France
Zahid Mehmood, Pakistan
Roderick Melnik, Canada
Xiangyu Meng, USA
Jose Merodio, Spain
Alessio Merola, Italy
Mahmoud Mesbah, Iran
Luciano Mescia, Italy
Laurent Mevel, France
Constantine Michailides, Cyprus
Mariusz Michta, Poland
Prankul Middha, Norway
Aki Mikkola, Finland
Giovanni Minafò, Italy
Edmondo Minisci, United Kingdom
Hiroyuki Mino, Japan
Dimitrios Mitsotakis, New Zealand
Ardashir Mohammadzadeh, Iran
Francisco J. Montáns, Spain
Francesco Montefusco, Italy
Gisele Mophou, France
Rafael Morales, Spain
Marco Morandini, Italy
Javier Moreno-Valenzuela, Mexico
Simone Morganti, Italy
Caroline Mota, Brazil
Aziz Moukrim, France
Shen Mouquan, China
Dimitris Mourtzis, Greece
Emiliano Mucchi, Italy
Taseer Muhammad, Saudi Arabia
Ghulam Muhiuddin, Saudi Arabia
Amitava Mukherjee, India
Josefa Mula, Spain
Jose J. Muñoz, Spain
Giuseppe Muscolino, Italy
Marco Mussetta, Italy

Hariharan Muthusamy, India
Alessandro Naddeo, Italy
Raj Nandkeolyar, India
Keivan Navaie, United Kingdom
Soumya Nayak, India
Adrian Neagu, USA
Erivelton Geraldo Nepomuceno, Brazil
AMA Neves, Portugal
Ha Quang Thinh Ngo, Vietnam
Nhon Nguyen-Thanh, Singapore
Papakostas Nikolaos, Ireland
Jelena Nikolic, Serbia
Tatsushi Nishi, Japan
Shanzhou Niu, China
Ben T. Nohara, Japan
Mohammed Nouari, France
Mustapha Nourelfath, Canada
Kazem Nouri, Iran
Ciro Núñez-Gutiérrez, Mexico
Wlodzimierz Ogryczak, Poland
Roger Ohayon, France
Krzysztof Okarma, Poland
Mitsuhiro Okayasu, Japan
Murat Olgun, Turkey
Diego Oliva, Mexico
Alberto Olivares, Spain
Enrique Onieva, Spain
Calogero Orlando, Italy
Susana Ortega-Cisneros, Mexico
Sergio Ortobelli, Italy
Naohisa Otsuka, Japan
Sid Ahmed Ould Ahmed Mahmoud, Saudi Arabia
Taoreed Owolabi, Nigeria
EUGENIA PETROPOULOU, Greece
Arturo Pagano, Italy
Madhumangal Pal, India
Pasquale Palumbo, Italy
Dragan Pamučar, Serbia
Weifeng Pan, China
Chandan Pandey, India
Rui Pang, United Kingdom
Jürgen Pannek, Germany
Elena Panteley, France
Achille Paolone, Italy

Bekir Sahin, Turkey
Laxminarayan Sahoo (iD), India
John S. Sakellariou (iD), Greece
Michael Sakellariou (iD), Greece
Salvatore Salamone, USA
Jose Vicente Salcedo (iD), Spain
Alejandro Salcido (iD), Mexico
Alejandro Salcido, Mexico
Nunzio Salerno (iD), Italy
Rohit Salgotra (iD), India
Miguel A. Salido (iD), Spain
Sinan Salih (iD), Iraq
Alessandro Salvini (iD), Italy
Abdus Samad (iD), India
Sovan Samanta, India
Nikolaos Samaras (iD), Greece
Ramon Sancibrian (iD), Spain
Giuseppe Sanfilippo (iD), Italy
Omar-Jacobo Santos, Mexico
J Santos-Reyes (iD), Mexico
José A. Sanz-Herrera (iD), Spain
Musavarah Sarwar, Pakistan
Shahzad Sarwar, Saudi Arabia
Marcelo A. Savi (iD), Brazil
Andrey V. Savkin, Australia
Tadeusz Sawik (iD), Poland
Roberta Sburlati, Italy
Gustavo Scaglia (iD), Argentina
Thomas Schuster (iD), Germany
Hamid M. Sedighi (iD), Iran
Mijanur Rahaman Seikh, India
Tapan Senapati (iD), China
Lotfi Senhadji (iD), France
Junwon Seo, USA
Michele Serpilli, Italy
Silvestar Šesnić (iD), Croatia
Gerardo Severino, Italy
Ruben Sevilla (iD), United Kingdom
Stefano Sfarra (iD), Italy
Dr. Ismail Shah (iD), Pakistan
Leonid Shaikhet (iD), Israel
Vimal Shanmuganathan (iD), India
Prayas Sharma, India
Bo Shen (iD), Germany
Hang Shen, China

Xin Pu Shen, China
Dimitri O. Shepelsky, Ukraine
Jian Shi (iD), China
Amin Shokrollahi, Australia
Suzanne M. Shontz (iD), USA
Babak Shotorban (iD), USA
Zhan Shu (iD), Canada
Angelo Sifaleras (iD), Greece
Nuno Simões (iD), Portugal
Mehakpreet Singh (iD), Ireland
Piyush Pratap Singh (iD), India
Rajiv Singh, India
Seralathan Sivamani (iD), India
S. Sivasankaran (iD), Malaysia
Christos H. Skiadas, Greece
Konstantina Skouri (iD), Greece
Neale R. Smith (iD), Mexico
Bogdan Smolka, Poland
Delfim Soares Jr. (iD), Brazil
Alba Sofi (iD), Italy
Francesco Soldovieri (iD), Italy
Raffaele Solimene (iD), Italy
Yang Song (iD), Norway
Jussi Sopanen (iD), Finland
Marco Spadini (iD), Italy
Paolo Spagnolo (iD), Italy
Ruben Specogna (iD), Italy
Vasilios Spitas (iD), Greece
Ivanka Stamova (iD), USA
Rafał Stanisławski (iD), Poland
Miladin Stefanović (iD), Serbia
Salvatore Strano (iD), Italy
Yakov Strelniker, Israel
Kangkang Sun (iD), China
Qiuqin Sun (iD), China
Shuaishuai Sun, Australia
Yanchao Sun (iD), China
Zong-Yao Sun (iD), China
Kumarasamy Suresh (iD), India
Sergey A. Suslov (iD), Australia
D.L. Suthar, Ethiopia
D.L. Suthar (iD), Ethiopia
Andrzej Swierniak, Poland
Andras Szekrenyes (iD), Hungary
Kumar K. Tamma, USA

Zaoli Yang ![ORCID], China
Jun Ye ![ORCID], China
Min Ye ![ORCID], China
Luis J. Yebra ![ORCID], Spain
Peng-Yeng Yin ![ORCID], Taiwan
Muhammad Haroon Yousaf ![ORCID], Pakistan
Yuan Yuan, United Kingdom
Qin Yuming, China
Elena Zaitseva ![ORCID], Slovakia
Arkadiusz Zak ![ORCID], Poland
Mohammad Zakwan ![ORCID], India
Ernesto Zambrano-Serrano ![ORCID], Mexico
Francesco Zammori ![ORCID], Italy
Jessica Zangari ![ORCID], Italy
Rafal Zdunek ![ORCID], Poland
Ibrahim Zeid, USA
Nianyin Zeng ![ORCID], China
Junyong Zhai ![ORCID], China
Hao Zhang ![ORCID], China
Haopeng Zhang ![ORCID], USA
Jian Zhang ![ORCID], China
Kai Zhang, China
Lingfan Zhang ![ORCID], China
Mingjie Zhang ![ORCID], Norway
Qian Zhang ![ORCID], China
Tianwei Zhang ![ORCID], China
Tongqian Zhang ![ORCID], China
Wenyu Zhang ![ORCID], China
Xianming Zhang ![ORCID], Australia
Xuping Zhang ![ORCID], Denmark
Yinyan Zhang, China
Yifan Zhao ![ORCID], United Kingdom
Debao Zhou, USA
Heng Zhou ![ORCID], China
Jian G. Zhou ![ORCID], United Kingdom
Junyong Zhou ![ORCID], China
Xueqian Zhou ![ORCID], United Kingdom
Zhe Zhou ![ORCID], China
Wu-Le Zhu, China
Gaetano Zizzo ![ORCID], Italy
Mingcheng Zuo, China

Contents

Research Article

Study on the Path of Three-Chain Integration of the Logistics Service Industry in Zhengzhou

Qingxiu Peng [1] and **Yujie Wang** [2]

¹*College of Economics and Management, Zhengzhou University of Light Industry, Zhengzhou 450008, Henan, China*
²*Zhengzhou Shengda Economic and Trade Management College, Zhengzhou 450008, Henan, China*

Correspondence should be addressed to Qingxiu Peng; pengqingxiu@163.com and Yujie Wang; 408169810@qq.com

To optimize the spatial layout of modern logistics services in Zhengzhou, build a driving mechanism for the professional development of logistics services, and promote logistics services to give full play to the driving force of coordinated development of regional economy, we must base ourselves on the logistics service industry chain, strengthen industrial innovation, value innovation and integration innovation, and realize the reconstruction of the value chain of logistics service industry. Based on the three-chain integration theory, this paper constructs a fuzzy comprehensive evaluation model for the three-chain integration of logistics service industry, adopts a combination of qualitative and quantitative methods, evaluates the effect of the three-chain integration of logistics service industry in Zhengzhou, and aims at the problems existing in the process of three-chain integration, such as lack of systematic planning, weak competitiveness, and low profitability. Measures such as improving fiscal and tax incentives, clarifying strategic positioning, overall planning of industry layout, strengthening innovation, and integrating new driving forces for the development of logistics service industry will further promote the in-depth integration of logistics service industry chain, value chain, and innovation chain in Zhengzhou.

1. Problem Presentation

With the proposal of "One Belt And One Road" strategy and the approval of Zhengzhou national central cities, Zhengzhou has been entrusted with the important task of building an international logistics center by its superior geographical position and good transportation system; the National Development and Reform Commission has pointed out that Zhengzhou national central city should be built as a logistics center. Therefore, improving the infrastructure construction of logistics service industry, building a large-scale logistics service center and logistics information hub, innovating the operation and management mode of logistics service industry, and promoting the cost reduction and efficiency increase of logistics service industry are the key measures to accelerate the development of modern intelligent logistics service industry in Zhengzhou, so as to meet the expansion of the demand for logistics service industry by the optimization and upgrading of regional economic structure, realize the optimal allocation of resources in Zhengzhou, and improve the efficiency and effect of economic operation. The key measures to improve the efficiency and effect of economic operation [1]. By promoting the effective integration of the value chain, industrial chain, and innovation chain of the logistics service industry, this can effectively promote the rapid development of the logistics service industry in Henan Province and comprehensively build Zhengzhou into an international logistics hub city and a domestic logistics hub city.

Based on the development status of Zhengzhou's logistics service industry, this paper combines the research trends of the three-chain integration of logistics service industry, builds an evaluation model of the three-chain integration level of Zhengzhou's logistics service industry, explores the specific reasons that affect the integration of industrial chain, logistics chain, and innovation chain in the

development process of Zhengzhou's logistics service industry, and plays a certain role in promoting Zhengzhou's logistics planning optimization, comprehensive allocation of logistics resources, and strategic adjustment of logistics enterprises.

2. Research Review and Research Trends on the Three-Chain Integration of Logistics Service Industry

The task of optimizing and upgrading China's economic structure in the next five years is to deploy the innovation chain around the industrial chain and promote the restructuring and upgrading of the value chain of traditional industries by relying on the innovation chain. The logistics service industry optimizes the allocation of resources at each node of the industrial chain through basic means such as storage, transportation, distribution, and information processing to realize the effect of $1 + 1 > 2$ (Jing) [2].

2.1. Research Status of Three-Chain Integration of Logistics Service Industry. The research results of the three-chain integration of the logistics service industry include connotation definition, internal logic, and mechanism of action, but the results are relatively scarce. Given the development trend of the financial industry, manufacturing industry, agriculture, and other industries and the attempt of three-chain integration development, combined with the development status and development trend of the logistics service industry, this paper elaborates from three dimensions:

(1) Definition of the connotation of three-chain fusion. As for the connotation of three-chain fusion, different scholars emphasize the definition of three-chain fusion due to their different research perspectives. For example, Yee and Seog [3], David et al. [4], and Lee et al. [5] believe that the key of three-chain integration is the integration of innovation chain, which can promote the transformation of scientific research achievements through the reconstruction of innovation chain and further promote the innovation of products and technologies in the industrial chain. Realize the optimization and promotion of the industrial value chain; Jixin et al. Zhijian Lin [6] think that the three-chain integration refers to the integration of industrial chain, innovation chain, and capital chain, and the mechanism of the integration of the three is the interaction mechanism of the three. Taking Zhejiang smart health industry as the research object, it is proposed to optimize financing channels and improve capital chain to promote technological innovation and knowledge innovation and then provide support for industrial development. Zhou [7] proposed that, by integrating all resources in the industrial chain, including capital and scientific and technological innovation, operating costs can be effectively reduced. Market competitiveness and profitability can be improved [7]. Zijing [8], from the perspective of the

unbalanced situation of logistics space, believes that the development of the logistics service industry can only be stimulated by the coordinated development of the industrial chain, innovation chain, and value chain [8].

(2) Study on the interaction mechanism of three-chain fusion. This paper studies the development status of the logistics service industry and, through empirical analysis, identifies the key variables that restrict the development of the logistics service industry and then explores the development trend of the logistics service industry. Yao [9] takes the development of Internet e-commerce shopping platform as the logistics supply chain must be integrated with the development of e-commerce industry to build development advantages [9]. Mahour et al. [10], Manuel et al. [11], and Rivera et al. [12] demonstrated empirically that logistics service industry plays a key role in promoting the optimization and upgrading of industrial value chain from the perspective of resource sharing. Yafei [13] used grey correlation analysis degree to analyze the motivation of logistics development in each node city of "One Belt And One Road" and further pointed out that the key to the development of modern logistics service industry was to promote the improvement of the value chain of the logistics service industry by improving the innovation chain [13]. Wenfu [14] used the annual data of logistics development and GDP to establish a mathematical model after taking the natural logarithm of GDP and goods turnover and pointed out that the logistics service industry could effectively promote economic development through the integration of industrial chain, value chain, and innovation chain [14].

(3) Study on the implementation path of three-chain fusion. As for the implementation path of three-chain fusion, scholars at home and abroad have achieved abundant research results. Rivera et al. [15] and Kumar et al. [16] took the American logistics industry agglomeration as the research object to analyze the integrated development path of logistics service industry in shaping the advantages of industrial agglomeration. Cui and Song [17], Heitz and Dablanc [18], Sakai et al. [19, 20], Dubie et al. [21], Giuliano et al. [22], and Heitz et al. [23] took China, Paris, Tokyo, Chicago, California, Sweden, and other countries or cities as the research objects, combined with the advantages of regional factors. Research and analyze the specific implementation path in the development process of logistics service industry; Liu and Pingfan [24] started from the perspective of upgrading the value chain of traditional industries. Through empirical analysis, it is believed that the key to promoting the industrial agglomeration effect is to develop the eco-industrial chain with advantageous industries as the core, to improve the innovation chain based on technology and knowledge creation,

and to build an interactive mode among the three by promoting the upgrading of the value chain [24]; Fan [25], from the perspective of steel logistics resource integration, proposed strengthening resource sharing and information exchange among relevant nodes of the industry chain to realize the comprehensive improvement of economic benefits, management benefits, and economic benefits of the logistics service industry [25]. Dongfang [26] made an in-depth analysis of the development status of the logistics industry from the aspects of location conditions, infrastructure, logistics services and industrial environment, government support, and so forth and pointed out that the logistics service industry should strengthen innovation and promote the integrated development of multiple industries [26].

To sum up, although there are few research theories and achievements on the three-chain integration of the logistics service industry, there are many attempts to develop three-chain integration, the development status, and innovation of the logistics service industry, which will provide theoretical support for the research of this topic.

2.2. Internal Mechanism of the Three-Chain Integration of Logistics Service Industry.

At each node of logistics service industry chain, there are circulation of innovation and transfer of value. That is, through the innovation of knowledge, technology, products, management methods, and operation mode, the theoretical achievements of logistics development can be transformed into operation management technology of logistics service industry, technology application can promote product innovation, product innovation can strengthen the reform and innovation of development mode of logistics industry, and the innovation chain construction of management innovation of logistics service industry can be realized. Drive the integration and innovation of logistics service content and business modules to promote the increase of added value of the logistics industry, accelerate the structure optimization and development drive mechanism construction of logistics service industry, and realize the systematic development of logistics service industry. The theoretical model of the action mechanism of the three-chain integration of logistics service industry is shown in Figure 1.

First, enhance the industrial value chain based on the value chain. As can be seen from Figure 1, in the logistics service industry chain, demand analysis, design, and development, logistics service and after-sales service belong to high value-added nodes, while the added value of technological innovation, manufacturing, and sales operation is low. On the basis of value chain reconstruction, through innovative operation and management methods and effective use of intelligent information technology, promote the value improvement of each node of the industrial chain and realize the value chain improvement of logistics service industry; that is, realize the integration of industrial chain and value chain [27].
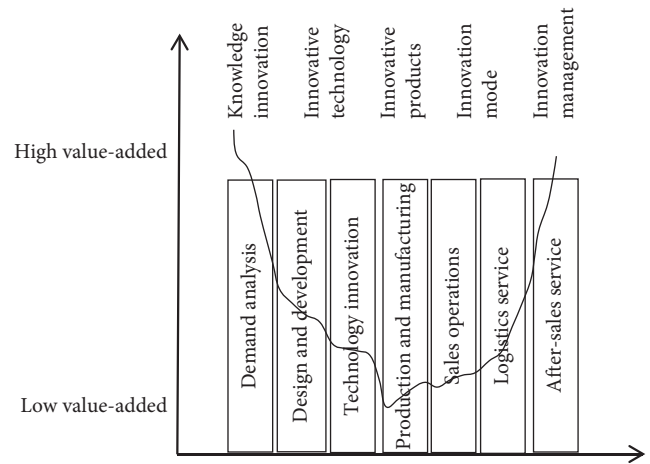
FIGURE 1: Theoretical model of the mechanism of three-chain fusion.

Second, relying on the industrial value chain, accelerate the integration of innovation chain. In the process of upgrading the industrial value chain, relying on the demand for innovation achievements in the layout of the industrial chain, promote more innovation subjects to join the industrial value chain and make accurate positioning, establish cooperative alliances, connect innovation activities, innovation resources, and innovation technologies, and enrich the connotation and forms of innovation activities, so as to optimize and improve the innovation chain and promote the transformation of innovation achievements to meet the development needs of the industrial value chain. At the same time, when the industry develops to a certain extent, it will put forward new requirements for the promotion of the value chain and innovation achievements. Such repetition will realize the coupling and interaction of the industrial chain, the value chain, and the innovation chain, forming a virtuous cycle process of synergy and mutual promotion.

Three-logistics-service-chain integration is the essence of logistics industry value chain, based on the value chain analysis, the traditional industrial chain of a link or entering a new industry chain industry to choose a location, match the knowledge, technology, products, management, and build innovation chain mechanism innovation, with further promotion of industrial value chain [2]. That is to deploy an innovation chain based on the original innovation chain, to realize the codependence and mutual transmission of material, energy, and information among different industries and enterprises, and to realize the flow and circulation of innovation results in different links of the industrial value chain, thus realizing the integration of the three chains. However, the process of three-chain fusion is not one-dimensional. After the innovation chain design, a new industrial chain layout should be started, and then a new value chain analysis and innovation chain design should be carried out. Therefore, the essence of the integration of the industrial chain, value chain, and innovation chain is a dynamic coupling mechanism, which presents a spiral development among the three to meet the needs of industrial economic development at different stages. The dynamic logic model of three-chain fusion is shown in Figure 2.
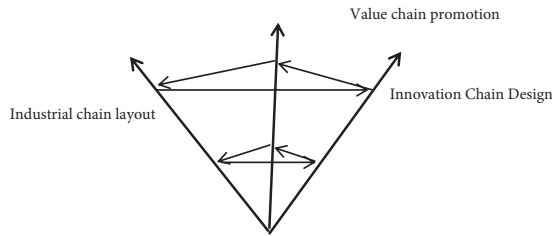
FIGURE 2: Dynamic logic model of three-chain fusion.

3. The Foundation of the Three-Chain Integration of the Logistics Service Industry in Zhengzhou

The logistics service industry plays a key role in promoting industrial integration and industrial structure optimization and upgrading, promoting foreign economic and trade activities, and driving more employment. As a key node city in central China and One Belt And One Road, Zhengzhou is located from east to west and from south to north, and the development of the logistics service industry is of great significance for promoting the optimization and upgrading of industrial structure and accelerating the construction of central China urban agglomeration. However, the logistics service industry in Zhengzhou has not yet formed an intelligent, intensive, and collaborative management mode, and there are problems such as high logistics cost and lack of new technology application, through the guidance of perfect logistics services to support and management system, and vigorously to build large international logistics center development, pay attention to the introduction of big data and cloud platform and Internet technology. A relatively intelligent management mode of logistics service industry has been initially formed. Therefore, the basis of promoting the three-chain integration of Zhengzhou logistics service industry is mainly presented in the following aspects.

3.1. Focus on Regional Advantages and Strengthen the Radiation-Driven Effect of the Logistics Service Industry. By virtue of its location advantage, Zhengzhou has become an important transportation hub city in China. There are not only two railway arteries, Beijing-Guangzhou and Longhai, which meet here, but also many national and provincial trunk roads, such as 310 National Highway and Lianhuo Expressway, which run through Zhengzhou, and Xinzheng International Airport. Convenient traffic conditions lay the foundation for the development of logistics service industry. By the end of March 2021, the number of enterprises engaged in logistics-related business in Zhengzhou was 32,713, accounting for 2/5 of the total number of logistics service enterprises in Henan Province. More than 100 logistics enterprises have a certain scale of development. Through industrial agglomeration, Zhengzhou's modern logistics service industry has begun to take shape, and its industrial driving capacity has been significantly enhanced. At the same time, relying on the "One Belt And One Road" strategy, we will implement the strategy; Zhengzhou vigorously

develops air rail intermodal transport and sea rail intermodal transport to connect the maritime Silk Road. The development of economic and trade activities along the Silk Road and the operation of Zhengzhou-Europe trains have promoted the rapid development of Zhengzhou's logistics service industry. Its business radiates to 34 provinces, autonomous regions, and municipalities directly under the central government and more than 100 foreign countries. The internationalization of the logistics service industry extends the industrial chain of Zhengzhou's logistics service industry and strengthens the construction of value chain and innovation chain to provide a basis for development.

3.2. Promote the Adjustment of Industrial Structure and Strengthen the Agglomeration Effect of the Logistics Service Industry. Under the organization and guidance of the provincial party committee and the provincial government, Zhengzhou has accelerated the construction scale and speed of Zhengzhou logistics service industry park by actively undertaking the advantageous industries of coastal cities, increasing the investment in the infrastructure construction of logistics service industry, improving the management policies of logistics service industry, and attracting investment, so as to continuously optimize the logistics service industry structure of Zhengzhou and improve the overall economic development situation. With the optimization of industrial structure and commercial reform in Zhengzhou, Zhengzhou has undergone qualitative changes in international trade. At present, the ten characteristic industries in Zhengzhou, such as medical medicine, food cold chain, automobile manufacturing, textile and clothing, and grain and flowers, have a good development momentum. The logistics parks and third-party logistics enterprises based on the ten characteristic industries have also entered a stage of rapid development, innovating the operation mode of new business forms of the logistics industry, such as cross-border e-commerce, cold chain distribution, and assembly manufacturing and distribution industry. It provides a basic guarantee for Zhengzhou to cultivate and expand logistics enterprises, establish an international logistics service system in line with the world, promote the intelligent and intensive development of logistics service industry, and improve the core position of Zhengzhou in China's logistics service industry structure.

3.3. Increase the Investment Scale and Make the Distribution of the Logistics Service Industry Reasonable. Clarify the strategic positioning of logistics service industry in Zhengzhou, increase investment, and improve the function of logistics comprehensive information platform through the introduction of modern equipment. Effectively strengthen the service capacity of logistics informatization, build a modern logistics hub, and make the industrial layout of logistics service industry in Zhengzhou more reasonable. Five international logistics hub service areas will be formed, namely, the North Logistics Service Area, the West Logistics Service Area, the South Logistics Service Area, the International Logistics Service Area, and the Aviation Logistics

Service Area. At the same time, Zhengzhou and Henan Investment Group Co., Ltd. have jointly established Henan Zhongyuan Modern Logistics Co., Ltd. and plan to complete the development and operation of five modern logistics hubs in Zhanyang, Xuedian, Shangjie, Guangwu, and Zhengzhou International Logistics Park in Zhengzhou by 2023. The total investment scale of the project reaches 12 billion yuan, and the annual freight service volume is expected to exceed 50 million tons. It provides power for extending the material strip of Zhengzhou logistics service industry and promoting the value promotion of logistics industry chain. In particular, the construction of the international inland port in the economic development zone, which connects the railway port, highway port, port, and airport to realize the linkage of four ports, not only promotes the integration of logistics resources and the agglomeration of the logistics industry in Zhengzhou but also promotes the development of the export-oriented economy in the inland areas. Through several measures, the layout of the logistics service industry in Zhengzhou is more reasonable, and multimodal transport, information intelligence, and cost minimization are realized. Among them, Zhengzhou international inland port core opening support is Zhengzhou-Europe international freight train.

4. Establishment of Evaluation Mechanism Model of Three-Chain Integration in Logistics Service Industry

4.1. Thoughts on Evaluation of the Three-Chain Integration Level of the Logistics Service Industry. The evaluation of the three-chain integration level of the logistics service industry is a comprehensive evaluation of the effect of the three-chain integration of the logistics service industry. According to the goal of three-chain integration of logistics service industry in Zhengzhou, this paper comprehensively evaluates the effect of three-chain integration of logistics service industry by constructing a scientific and reasonable evaluation index system and selecting appropriate evaluation methods. The purpose of the evaluation of the three-chain integration level of logistics service industry is to scientifically and objectively reflect the effect of the three-chain integration of logistics service industry, timely find the problems existing in the process of the three-chain integration of logistics service industry in Zhengzhou, and take corresponding measures for correction and improvement, so as to continuously improve the three-chain integration level of logistics service industry in Zhengzhou. The specific evaluation ideas can be as follows: determine the evaluation index system, collect and process data, determine the evaluation method and model, model evaluation, and output evaluation results.

4.2. Construction of the Evaluation Index System for the Three-Chain Integration Level of the Logistics Service Industry. The evaluation index system of the three-chain integration level of the logistics service industry is the premise and foundation of the evaluation of the three-chain integration level of the logistics service industry. Therefore, it is necessary to construct a scientific and reasonable evaluation index system for the three-chain integration of the logistics service industry according to the connotation, mode, and operation mechanism of the integration of the logistics service industry.

According to the research status at home and abroad and the development status of logistics service industry in Zhengzhou, this paper constructs the evaluation index system of three-chain integration level of logistics service industry from the perspective of supply and demand from four aspects: logistics infrastructure resource integration level, industrial chain related organization resource integration level, logistics innovation service integration level, and logistics organization income level, as shown in Table 1.

4.2.1. Integration Level of the Logistics Infrastructure Resources. The main goal of the three-chain integration of the logistics service industry is to effectively improve the value positioning of the logistics service industry in the industrial chain by innovating the mode and connotation of the logistics service industry. According to the characteristics of the logistics industry, the operation process mainly involves the use of storage, transportation, and information integrated system platform. Therefore, the utilization efficiency of resources such as storage, transportation, and information integrated system platform is used to measure the resource integration level of logistics infrastructure.

① Warehouse logistics utilization rate reflects the efficiency level of storage resources, expressed by the ratio of the total logistics demand to the total storage facilities.

Warehouse logistics utilization rate = total demand for steel logistics/total storage facilities.

② The average logistics utilization rate of freight vehicles reflects the efficiency level of transport resources, which is expressed by the ratio of the total logistics demands to the number of freight vehicles.

The average logistics utilization rate of freight vehicles = the total demand of steel logistics/the number of freight vehicles.

③ Utilization rate of information integrated system platform reflects the use of information platform, which is expressed by the ratio of the total amount of information integrated system platform to the demand of the logistics platform.

The utilization rate of information integrated system platform = demands of logistics platform/total amount of information integrated system platform.

4.2.2. Resource Integration Level of Industrial Chain Related Organizations. Integrating the three chains of the logistics service industry needs the cooperation of all enterprises in the industry chain. To some extent, the level of resource integration of industrial chain related organizations is determined by cooperation among various organizations, on the one hand, technology research and development service

TABLE 1: Evaluation index system of three-chain integration of logistics service industry in Zhengzhou.

Evaluation index system of three-chain integration of logistics service industry in Zhengzhou	Integration level of logistics infrastructure resources	Utilization rate of warehouse logistics
		Average logistics utilization rate of freight vehicles
		Utilization rate of information integrated system platform
	Resource integration level of industrial chain related organizations	Organizational resource sharing level
		Complementation of logistics resources
		Cooperation trust
	Logistics innovation service integration level	Logistics demand response speed
		Accuracy of logistics activities
		Logistics service flexibility
	The level of profitability of the logistics organization	Economic benefits
		Management of earnings
		Technical benefits

enterprises, manufacturing enterprises, logistics and distribution enterprises, after-sales service enterprises, and other related enterprises under the guidance of a certain operation mechanism, to achieve the common, sharing, and complementary logistics service resources and, on the other hand, production enterprises, marketing enterprises, logistics enterprises, and other related enterprises through cooperation can quickly respond to the logistics service demand and can share or disperse part of the risk. Given this, the resource integration level of related organizations in the industrial chain is measured by the indexes of resource sharing level, complementation, cooperation trust, and so on.

① Sharing level of organizational resources: it reflects the sharing degree of organizational resources among relevant subjects of the industrial chain. The greater the openness of information and resources of each subject, the higher the level of sharing income.

② Complementation of logistics resources: it reflects the differentiation and complementation of logistics resources. The integration of logistics resources of different organizations in the industrial chain can promote and realize the complementation of the logistics resources of various enterprises.

③ Cooperative trust: cooperative trust is the premise of cooperation between enterprises. The higher the trust of each enterprise through cooperation, the more conducive to the improvement of the three-chain integration level of the logistics service industry.

4.2.3. Logistics Innovation Service Integration Level.
Logistics service innovation on the integration of industrial chain of each node resources position, function, demand, state, and target customers to effectively integrate organizational relationships and service already achieved the goal of service innovation; logistics service mode innovation is the content of the response speed and accuracy of logistics activities by logistics demand and flexible logistics services to measure.

① Logistics demand response speed: It reflects the service demand of the logistics enterprise and the

processing speed of the logistics demands of the enterprise, and it is expressed by the time to complete the relevant service.

② Accuracy of logistics activities: It is the basic requirement of logistics services. Accuracy of logistics activities is by customer requirements, the product by the specified time and place of good delivery.

③ Logistics service flexibility: It reflects the ability to adapt to the change of logistics demand and service.

4.2.4. The Income Level of Logistics Organization.
Through the integration of the three chains of the logistics services, it can not only give play to the function of logistics service industry in the whole industrial chain but also further expand the scope of the logistics service through service innovation and value innovation, comprehensively improve the service level of the logistics service industry, and effectively reduce and avoid the repeated investment and construction of logistics resources. The fundamental purpose of the three-chain integration of the logistics service industry is to maximize the economic benefits of all parties in the logistics service industry, maintain a cooperative game relationship through innovation and value reconstruction of the industrial chain, and realize the goal of bringing benefits to all parties of supply and demand. Therefore, the income analysis in the integration of logistics resources is used to measure the income level of the logistics service industry from three aspects: economic income, management income, and technical income.

① Economic income: Reflecting the integration of the three chains of the logistics service industry for technical service enterprises, production enterprises, marketing enterprises, logistics enterprises, and other interest related enterprises brought the most direct income, which is also the most important income, that is, economic income. The profit growth rate is used to measure the direct benefits generated by the integration of three chains in the logistics service industry.

Economic income = (profit after the enterprise participates in the three-chain fusion − profit before the

enterprise participates in the three-chain fusion)/ profit before the enterprise participates in the three-chain fusion.

② Management benefit: The management benefit brought by integrating the three chains of the logistics service industry for production enterprises, iron and steel trading enterprises, logistics enterprises, and other related enterprises. Through the three-chain integration of logistics service industry, relevant cooperative enterprises can learn from each other's advanced business concepts, management methods, and systems to improve their management level. For example, when the third-party logistics enterprises cooperate with the production enterprises, the logistics enterprises can learn from the modern operation and management concepts of the production enterprises. The production enterprises can learn from the professional logistics management methods of the logistics enterprises.

Management income = (the management level after the enterprise participates in the three-chain fusion – the management level before the enterprise participates in the three-chain fusion)/the management level before the enterprise participates in the three-chain fusion

③ Technical benefits: Through the integration of three chains of the logistics service industry, related cooperative enterprises can obtain economic benefits and management benefits as well as various technical benefits. Through the application of modern information technology, such as logistics management information system and positioning system, logistics resources can be scientifically and effectively allocated and then improve the income level of related organizations in the logistics service industry.

Technical benefit = (the technical level after the enterprise participates in the three-chain fusion – the technical level before the enterprise participates in the three-chain fusion)/the technical level before the enterprise participates in the integration.

4.3. Establishment of Evaluation Model for the Three-Chain Integration Level of Logistics Service Industry.
In the evaluation index system of the three-chain integration level of the logistics service industry, there are qualitative and quantitative indexes, and the fuzzy comprehensive evaluation method can well integrate the two indexes into the evaluation system. The fuzzy comprehensive evaluation method can deal with the indexes that are difficult to be quantified. The fuzzy

comprehensive evaluation method is used to evaluate the three-chain integration level of the logistics service industry, which makes the evaluation more consistent with the actual situation and more reasonable. A fuzzy comprehensive evaluation is adopted to make the comprehensive evaluation of three-chain fusion transform between qualitative and quantitative indexes. Combined with the mathematical membership theory, the evaluation is more systematic, and the evaluation results are relatively clear. Steps of fuzzy comprehensive evaluation method are demonstrated as follows.

4.3.1. Determine the Evaluation Object Factor Set.
The evaluation object factor set consists of several evaluation indexes, and the factor set $U = \{u_1, u_2, u_3, \ldots\ldots, u_n\}$, where $u_1, u_2, u_3, \ldots\ldots, u_n$, represents different influencing factors. If the factors affecting the target layer are stratified in the evaluation system, a multilevel model can be adopted.

4.3.2. Determine the Evaluation Set.
The evaluation set is used to represent the degree of the merits and demerits of the evaluated objects. According to the specific research needs, the number of the registered merits and demerits of the evaluated objects can be positively defined and represented by V. The evaluation set is $V = \{v_1, v_2, v_3, \ldots\ldots, v_n\}$.

4.3.3. Establish Fuzzy Membership Matrix.
According to the evaluation set, the factor set is evaluated; that is, the fuzzy mapping from U to V is established, which can be described by the fuzzy management matrix R. R_{ij} indicates the degree of subordination to grade J comments on the ith indicator.

$$R = \begin{bmatrix} r_{11} & r_{11} & \cdots & r_{1n} \\ r_{21} & r_{21} & \cdots & r_{2n} \\ \cdots & \cdots & \cdots & \cdots \\ r_{m1} & r_{m1} & \cdots & r_{mn} \end{bmatrix}. \quad (1)$$

4.3.4. Determine the Weight Vector of Evaluation Factors.
$A = (a_1, a_2, \ldots\ldots, a_m)$ is a weight set, and a_i represents the weight of the ith indicator in the indicator set U.

$$\sum_{i=1}^{m} a_i = 1. \quad (2)$$

4.3.5. Synthesis Result Vector.
Using the operator to synthesize the matrix, the evaluation results based on a fuzzy algorithm can be obtained.

$$A * R = (a_1, a_2, \ldots\ldots, a_m) * \begin{bmatrix} r_{11} & r_{11} & \cdots & r_{1n} \\ r_{21} & r_{21} & \cdots & r_{2n} \\ \cdots & \cdots & \cdots & \cdots \\ r_{m1} & r_{m1} & \cdots & r_{mn} \end{bmatrix} = (b_1, b_2, \ldots\ldots, b_m) = B. \quad (3)$$

The corresponding results can be obtained by calculating column J of A and R and can be represented by b_j. In contrast, V_j can be used to represent the fuzzy subset of the evaluated object as a whole.

4.3.6. Analyze the Result Vector of the Fuzzy Comprehensive Evaluation. The maximum membership principle is used to analyze the result vector of fuzzy comprehensive evaluation.

4.4. Evaluation on the Effect of Three-Chain Integration of Logistics Service Industry in Zhengzhou. Based on the logistics industry, through value chain reconstruction and innovation chain integration, Zhengzhou's logistics service industry has gathered stakeholders such as technology research and development enterprises, production enterprises, trade enterprises, logistics enterprises, and logistics parks and built an industrial network with certain integration capabilities. Users of the logistics service industry can choose their own products and related logistics services on the platform according to their needs, thus realizing the organic and dynamic integration of the value chain, industrial chain, and innovation chain of the logistics service industry [28]. Through the investigation of major logistics industrial parks and representative logistics enterprises in Zhengzhou, the rationality and feasibility of the evaluation index system and evaluation model of the three-chain integration level of the logistics service industry are verified.

4.4.1. Constructing the Hierarchy Chart of the Evaluation Index of the Three-Chain Integration Level of Zhengzhou Logistics Service Industry. According to the evaluation index system of the three-chain integration level of the logistics service industry in Zhengzhou, the fuzzy comprehensive evaluation hierarchy is constructed, as shown in Table 2.

4.4.2. Determine the Weight of Evaluation Indicators. According to the hierarchical structure diagram of fuzzy comprehensive evaluation in Table 2, the analytic hierarchy process (AHP) was adopted to calculate the weight of the two-level evaluation indexes.

(i) $w = (0.135, 0.357, 0.265, 0.243)$

(ii) $W_1 = (0.282, 0.285, 0.433)$

(iii) $W_2 = (0.242, 0.295, 0.463)$

(iv) $W_3 = (0.275, 0.358, 0.367)$

(v) $W_4 = (0.171, 0.286, 0.543)$

4.4.3. Determine the Evaluation Set. The comprehensive evaluation is divided into five levels, from good to bad, that is, the evaluation set. $V = (v_1, v_2, v_3, v_4, v_5) = $ (Excellent, Good, Normal, Poor, Worse).

4.4.4. Determine the Fuzzy Evaluation Matrix. The membership matrix of the second-level evaluation index is obtained by experts after statistical processing of the evaluation data of each index according to the rating set.

$$R_1 = \begin{bmatrix} 0.1 & 0.3 & 0.1 & 0.2 & 0.2 \\ 0.1 & 0.2 & 0.2 & 0.3 & 0.2 \\ 0.1 & 0.2 & 0.2 & 0.3 & 0.2 \end{bmatrix},$$

$$R_2 = \begin{bmatrix} 0.2 & 0.1 & 0.2 & 0.3 & 0.2 \\ 0.1 & 0.1 & 0.1 & 0.3 & 0.4 \\ 0.1 & 0.2 & 0.3 & 0.3 & 0.1 \end{bmatrix},$$

$$R_3 = \begin{bmatrix} 0.2 & 0.3 & 0.1 & 0.3 & 0.1 \\ 0 & 0.2 & 0.2 & 0.4 & 0.2 \\ 0.1 & 0.1 & 0.3 & 0.4 & 0.1 \end{bmatrix},$$

$$R_4 = \begin{bmatrix} 0 & 0.1 & 0.2 & 0.3 & 0.2 \\ 0.1 & 0.2 & 0.2 & 0.3 & 0.2 \\ 0 & 0.2 & 0.2 & 0.4 & 0.2 \end{bmatrix}. \tag{4}$$

4.4.5. Fuzzy Comprehensive Evaluation Calculation. According to the membership matrix, the membership vector of the first level index can be obtained.

$$V_1 = W_1 * R_1 = (0.282, 0.285, 0.433) * \begin{bmatrix} 0.2 & 0.3 & 0.1 & 0.2 & 0.2 \\ 0.1 & 0.2 & 0.2 & 0.3 & 0.2 \\ 0.1 & 0.2 & 0.2 & 0.3 & 0.2 \end{bmatrix} = (0.128, 0.228, 0.172, 0.272, 0.200). \tag{5}$$

According to this algorithm, the membership vectors of the other four dimensions are obtained.

$$V_2 = (0.124, 0.146, 0.217, 0.300, 0.213),$$
$$V_3 = (0.092, 0.191, 0.209, 0.372, 0.136), \tag{6}$$
$$V_4 = (0.029, 0.183, 0.200, 0.388, 0.200).$$

The fuzzy comprehensive evaluation matrix is obtained.

$$R = \begin{bmatrix} 0.128 & 0.228 & 0.172 & 0.272 & 0.200 \\ 0.124 & 0.146 & 0.217 & 0.300 & 0.213 \\ 0.092 & 0.191 & 0.209 & 0.372 & 0.136 \\ 0.029 & 0.183 & 0.200 & 0.388 & 0.200 \end{bmatrix}. \tag{7}$$

TABLE 2: Fuzzy comprehensive evaluation hierarchy structure of three-chain fusion in Zhengzhou logistics service industry.

Evaluation index system of three-chain integration of logistics service industry in Zhengzhou	Integration level of logistics infrastructure resources	Utilization rate of warehouse logistics (I_{11})
		Average logistics utilization rate of freight vehicles (I_{12})
		Utilization rate of information integrated system platform (I_{13})
	Resource integration level of industrial chain related organizations	Organizational resource sharing level (I_{21})
		Complementation of logistics resources (I_{22})
		Cooperation trust (I_{23})
	Logistics innovation service integration level	Logistics demand response speed (I_{31})
		Accuracy of logistics activities (I_{32})
		Logistics service flexibility (I_{33})
	The level of profitability of the logistics organization	Economic benefits (I_{41})
		Management of earnings (I_{42})
		Technical benefits (I_{43})

The comprehensive evaluation results are obtained further.

$$V = W^* R = (0.135, 0.357, 0.265, 0.243)^* \begin{bmatrix} 0.128 & 0.228 & 0.172 & 0.272 & 0.200 \\ 0.124 & 0.146 & 0.217 & 0.300 & 0.213 \\ 0.092 & 0.191 & 0.209 & 0.372 & 0.136 \\ 0.029 & 0.183 & 0.200 & 0.388 & 0.200 \end{bmatrix} = (0.093, 0.178, 0.204, 0.337, 0.188). \quad (8)$$

Combined with the survey data of logistics service industry related enterprises and parks in Zhengzhou, according to the principle of maximum membership degree, the evaluation results show that the three-chain integration level of the logistics service industry in Zhengzhou is poor. From the four dimensions of influencing factors of Zhengzhou logistics service industry's three-chain integration level, the three-chain integration of Zhengzhou logistics service industry is poor, which can be seen as follows: the integration efficiency of Zhengzhou logistics service industry's value chain and industrial chain is low, the integration of innovation chain and industrial chain is disjointed, and the integration effect of innovation chain and value chain is poor. Zhengzhou chain present situation and the effect evaluation, and can guide the government in formulating the logistics services guide support policy system construction and logistics enterprise strategy planning is of great significance.

5. Analysis of the Reasons Influencing the Three-Chain Integration of the Logistics Service Industry in Zhengzhou

The integration of the three chains of the logistics service industry in Zhengzhou can promote the logistics service industry, the transformation and upgrading of logistics enterprises, and the construction of the new modern logistics service system and the upgrading of the value chain of the logistics industry. According to the comprehensive effect evaluation of the three-chain integration of Zhengzhou logistics service industry, it can be seen that the integration effect of Zhengzhou logistics service industry chain, value chain, and innovation chain is poor. The poor integration effect can be analyzed from three aspects: the integration efficiency of value chain and industry chain, the convergence degree of innovation chain and industry chain, and the integration effect of innovation chain and value chain.

5.1. Low Efficient Integration for Value Chain and Industry Chain in Logistics Service Industry. The relationship of each link in the value chain is interrelated. The importance of any link and its influence on other links are reflected in its position in the value chain. Given the logistics service, industry value chain can be divided into three links, namely, the upstream link, the intermediate link, and the downstream link, logistics is integration, service development and integration of logistics technology belong to the upstream link, and the ability to create logistics services and supply belong to the intermediate links, and logistics service belongs to the downstream link sales and after-sales service. The core of the upstream link is knowledge creation and technology integration, the core of the midstream link is infrastructure construction and capacity construction, and the core of the downstream link is market demand.

Therefore, it can be seen that the key to the integration of value chain and industrial chain of logistics service industry lies in the reconstruction of the entire industrial value chain, technology application, management innovation and infrastructure configuration, and so forth. The reasons for the low efficiency of the integration of the two can be further analyzed from the following aspects:

(1) Lack of systematic planning for the development of the logistics industry. Although Zhengzhou occupies a regional advantage, due to the lack of policy guidance and support, the city positioning is not clear enough at the early stage, leading to the late start of the development of modern logistics; the logistics market in the unified supervision and overall planning still need to be strengthened, and the distinctive and professional logistics business mode still needs to be innovated and reconstructed. At the same time, with the established as a national central city of Zhengzhou city, building "three areas, a group of" and "area", the implementation of the strategic national logistics service function has carried on the relocation of Zhengzhou, the logistics service industry to develop rapidly, but too fast speed makes the development of logistics industry policies and regulations innovation relatively lagging. There are some links of the absence of laws and regulations and the lack of policy and illegal phenomenon.

(2) Backwardness of intelligent information technology. Zhengzhou's logistics information technology and equipment are still a bit backward, and the distribution infrastructure is weak. Most logistics companies have not introduced intelligent logistics management information system, which leads to the lack of information chain and the inability to connect information among logistics industries, resulting in the ineffective allocation of resources among logistics industries, which leads to vicious competition between logistics enterprises and the inside and outside of logistics industries. The degree of mechanization and automation of logistics enterprises in some logistics parks needs to be strengthened. The logistics operation is still operated by manual labour, and the office automation technology has not been widely promoted, which leads to the low efficiency of the overall logistics operation and the dilution of the operating benefits of logistics enterprises.

(3) Low management level. Most of Zhengzhou city logistics park and logistics enterprises lack innovation in the management of service, service content, and the methods of the single, backward management model, business mode, and content of the lack of overall innovation consciousness, transport, and warehousing business content single only for service-oriented business such as foundation, the service, and a lack of internal management rules and regulations, as well as lack of their brand building awareness and brand management concept. Logistics enterprises exist independently among departments and regions so that rights and responsibilities overlap among departments and regions, and unclear responsibilities and rights lead to low management efficiency.

(4) The air-ground connection needs to be improved. The development of logistics service industry cannot be separated from the effective support of basic transportation network and information service network. Because of the obvious modularity of administrative management, Zhengzhou's basic transportation network, integrated information service platform, aviation hub, and other functions lack integration, and there is no effective connection between industries, insufficient interaction, and virtuous circle, which greatly reduces the accuracy and safety of logistics, weakens the speed and efficiency of air logistics transportation, and restricts the improvement of logistics service level and the expansion of service scope.

5.2. Disintegration between Innovation Chain and Industrial Chain of Logistics Service Industry. Due to the low degree of connection between the educational mechanism and the market economic mechanism, innovation activities are decoupled from economic activities. On the one hand, economic activities have no mechanism to guide the demand for innovation activities, which leads to the blind lack of systematic planning and direction for the development of entrepreneurial activities. Innovation achievements are independent of each other, and repeated and worthless innovation development consumes many resources. On the other hand, due to the lack of practical support from economic activities, the transformation rate of innovation achievements is low, and the value function of innovation cannot be fully exerted. As a result, many achievements are difficult or not transformed into actual products, and it is difficult to realize the industrialization of scientific research achievements. As a result, the logistics service industry in Zhengzhou has some several problems such as low business innovation ability, lagging business integration innovation mode, and weak competition ability.

(1) Weak competitiveness. Zhengzhou's logistics service industry is still in the period of development and construction, the agglomeration effect of logistics parks has not been effectively exerted, and the service content, scope, and radiation function of logistics enterprises are still at a low level. For example, the additional services of logistics are relatively lacking, the spatial distribution of service resources is relatively discrete, the scale effect is insufficient, and the business services are scattered and unitary. As a result, domestic logistics services cannot effectively compete with some developed countries. Given this situation, the main reason lies in the lack of effective matching between the logistics service industry and

innovation activities, which leads to the single path of service innovation, scope innovation, and function innovation of the logistics service industry.

(2) Lack of innovation in the integration mode of the logistics service industry chain. The construction of logistics infrastructure and network system in Zhengzhou needs to be strengthened. On the one hand, the single function of logistics information service platform leads to the lack of integration of logistics resources, lack of sharing among logistics industries and low efficiency, and low utilization rate of transportation and storage facilities. On the other hand, the current logistics transportation mode is backward, the circulation speed is slow, the efficiency is low, the cost is high, and the consumption rate is high. As a result, Zhengzhou logistics service industry has not yet reached the due effect of the international logistics network.

(3) Low attraction ability of logistics service industry. Although Zhengzhou is currently a key node city of One Belt And One Road and a national central city and strives to build an inland airport in central China, there is still a certain lack of attraction in terms of the city. Internationally renowned logistics enterprises, including transportation enterprises, logistics service enterprises, and professional logistics real estate developers, will prioritize Wuhan, Xi'an, and other inland cities. The main reason for the lack of attraction of the logistics service industry lies in the lack of innovation in the construction of logistics infrastructure and logistics development environment, making the logistics resource foundation weak, and it has not yet formed a perfect logistics ecosystem.

5.3. Poor Integration of Innovation Chain and Value Chain in the Logistics Service Industry. With the establishment of Zhengzhou as an international logistics hub and central city, the competition of the international logistics service industry has entered the stage of innovation value chain competition from product competition. Only by upgrading and improving the service value chain can the development of the low-end circular logistics service industry be broken through. However, there are still some problems in the process of the integration of the innovation chain and value chain of the logistics service industry in Zhengzhou. Due to the poor integration effect of the innovation chain and value chain, the profit level, management income, and technical income level of the logistics industry have decreased significantly.

(1) The profit level of logistics enterprises declines. Take Zhengzhou International Logistics Park, one of the four state-level demonstration logistics parks in Henan Province, as an example. In 2020, Zhengzhou International Logistics Park completed the fixed asset investment of 12.58 billion yuan, with a year-on-year growth of 11.3%. Revenue from the service sector reached 45.7 billion yuan, up 13% year on year. However, the growth rate of the main business cost is significantly higher than the growth rate of the income level, leading to the decline of the profit level. The main reason for its existence is that the rapid growth of workforce, management, rent, and other costs results in a sharp increase in the operating pressure of logistics enterprises and the contraction of profit space, and even some warehousing enterprises and logistics parks appear to suffer from losses.

(2) Low management efficiency. Due to the lack of guidance, logistics parks and logistics enterprises in Zhengzhou lack effective integration planning, the fragmented phenomenon is still relatively serious, laws, regulations, and policies system and industry integrity system still need to be strengthened and improved, and the market order is relatively chaotic. At the same time, the proportion of traditional logistics is large, the number of logistics enterprises is large, the scale is small, the strength is weak, the function is single, resulting in the logistics service industry concentration being not high, the business is not centralized, the service consciousness is weak, and the maturity is not high.

(3) The technical efficiency has not been effectively played. For most of the logistics park of Zhengzhou city is still in the initial stage of development, the aviation logistics talent shortage, uneven levels, lack of aviation logistics service concept, service business and service level consciousness, lack of boast, the global consciousness, and the lack of standardized service rules, relative foreign logistics industry service level is low, causing a bigger effect on our country's aviation logistics.

6. Suggestions for Promoting the Three-Chain Integration of Logistics Service Industry in Zhengzhou

Combined with the specific reason why the Zhengzhou logistics service industry value chain, industry chain, and innovation chain fusion effect is poorer, use comprehensive fuzzy analysis matrix involved in the four dimensions of the 12 indicators, the government policy level, logistics service level, and logistics enterprises from the following aspects, to guide the coordination of Zhengzhou city logistics services; for example, at the policy level, the government should improve the policy support and guidance mechanism, expand the scope and validity of the guidance and support to the logistics service industry, and promote the shape and improvement of the value chain of the logistics service industry. At the level of industry development, it is necessary to define the industry development orientation, make overall planning of industrial development layout, and realize the matching and reconstruction of logistics service industry value chain and industry chain. At the enterprise level, we should strengthen innovation, pay attention to the introduction and application of innovative services, and

comprehensively promote the deep integration of value chain, industrial chain, and innovation chain.

6.1. Improve the Policy Support and Guidance Mechanism and Expand the Scope and Validity of Policy Radiation. During the 14th Five-Year Plan period, Zhengzhou should rely on representative industrial parks such as Zhengzhou Airport National Logistics Hub and International Logistics Park to build a hub economy pioneer zone with international influence, improve the policy support and guidance mechanism in promoting the innovative, integrated, and characteristic development of logistics service industry, and realize the expansion and promotion of the radiation range and validity of policies to the logistics industry. This can be done through the following ways:

(1) We improved the functioning of government policies. Promote the construction of the supervision organization of the logistics service industry in Zhengzhou, enrich the functions and responsibilities of the organization, and play specific functions in the development planning, policy formulation, and integrated information system construction of the logistics service industry. At the same time, improve the identification system of key logistics enterprise projects and logistics parks, optimize the logistics project examination and approval management process, and promote the logistics service industry to be more standardized and effective.

(2) Strengthen guidance and support. In order to effectively promote the three-chain integration of the logistics service industry in Zhengzhou, the guidance and support for the logistics service industry should focus on three aspects: financial support, preferential land use, and project investment. First, terms of financial support, for enterprises engaged in the logistics business, such as warehousing and transportation enterprise, in the given preferential tax, can be in accordance with the range of 3% to 5% of subsidies for profit.

7. Conclusion

On the basis of defining the logistics service industry and the three-chain integration theory, this paper systematically analyzes the development environment and current situation of the logistics service industry in Zhengzhou. On the whole, Zhengzhou logistics service industry has more opportunities than challenges and more advantages than disadvantages in the future development process. Based on many influencing factors of Zhengzhou logistics service industry, how to build an international logistics center city and a logistics transshipment hub city? From the perspective of logistics service industry value chain, we must dig deep into industrial value and extend industrial value chain. From the perspective of industrial chain, it is necessary to strengthen supporting industries, support deep integration among industries, promote industrial upgrading, and then build industrial networks. From innovation chain's point of

view, it is necessary to strengthen research and development to promote the transformation of scientific and technological achievements. Based on the theory of three-chain integration, through the integration of innovation chain and value chain, the added value of Zhengzhou logistics service industry can be promoted. Through the integration of industrial chain and innovation chain, the degree of industrial integration can be promoted, and then the cost can be reduced and the competitiveness of logistics service industry can be enhanced. Through the integration of value chain and industrial chain, the logistics industry environment can be optimized, and the logistics service industry can be upgraded and transformed.

Data Availability

No data were used to support this study.

Conflicts of Interest

The authors declare that they have no conflicts of interest.

Acknowledgments

References

[1] Y. Li, Y. Liu, and X. Wang, "Research on radiation range and pattern evolution of aviation logistics in mainland airports," *Journal of Zhengzhou University (Engineering Edition)*, vol. 42, 2021.

[2] L. Jing, "Development strategy of logistics industry in Zhengzhou under the strategy of "big hub"," *Cooperative Economy and Science & Technology*, vol. 9, no. 5, 2017.

[3] J. T. Yee and C. O. Seog, "Technology integration needs for manufacturing, logistics, and supply chain management," *Technology Integration to Business*, vol. 50, no. 08, 2012.

[4] D. Bennett and F. Klug, "Logistics supplier integration in the automotive," *Industry International Journal of Operations & Production Management*, vol. 32, no. 11, 2012.

[5] H. Y. Lee, Y. J. Seo, and D. John, "Supply chain integration logistics performance: the role of supply chain dynamism," *International Journal Logistics Management*, vol. 27, no. 03, 2016.

[6] J. Yuan, X. Wang, Z. Lin, and J. Ye, "An empirical study on the integration of industrial chain, innovation chain and capital chain; a case study of Zhejiang smart health industry," *Science and Technology Management Research*, vol. 36, no. 14, 2016.

[7] X. Zhou, *Spatial Effects of Regional Technological Innovation Driving Industrial Structure Optimization and Upgrading under Knowledge Spillover*, Jiangxi University of Finance and Economics, Nanchang, China, 2017.

[8] Z. Liang, *Research on Spatial Disequilibrium Situation and Evolution Mechanism of Regional Logistics in Jiangsu Province*, China University of Mining and Technology, Xuzhou, China, 2020.

[9] J. M. Yao, "Supply chain resources integration optimization in B2C online shopping," *International Journal of Production Research*, vol. 55, pp. 1–16, 2015.

[10] M. Mellat-Parast and E. John, "Logistics and supply chain process integration as a source of competitive advantage: an empirical analysis," *The International Journal of Logistics Management*, vol. 25, no. 2, 2014.

[11] M. Scavarda, H. Seok, and Y. Simon, "The constrained-collaboration algorithm for intelligent resource distribution in supply networks," *Computers & Industrial Engineering*, vol. 133, no. 7, 2017.

[12] L. Rivera, Y. Sheffi, and D. Knoppen, "Logistics clusters: the impact of further agglomeration, training and firm size on collaboration and value added services," *International Journal of Production Economics*, vol. 179, 2016.

[13] Y. Zhang, "Analysis on influencing factors of logistics industry in "one belt and one road" inland node cities- a case study of Zhengzhou," *Journal of Xinxiang University*, vol. 34, no. 7, 2017.

[14] W. Mao, *Evaluation Research on the Coordinated Development of Logistics Industry and Regional Economy in China*, Capital University of Economics and Business, Beijing, China, 2017.

[15] L. Rivera, Y. Sheffi, and R. E. Welsch, "Logistics agglomeration in the US," *Transportation Research Part A-Policy and Practice*, vol. 59, 2014.

[16] I. Kumar, A. Zhalnin, A. Kim, and L. J. Beaulieu, "Transportation and logistics cluster competitive advantages in the US regions: a cross-sectional and spatio-temporal analysis," *Research in Transportation Economics*, vol. 61, 2016.

[17] Y. Cui and B. Song, "Logistics agglomeration and its impacts in China," *Transportation Research Procedia*, vol. 25, 2017.

[18] A. Heitz and L. Dablanc, "Logistics spatial patterns in Paris: rise of paris basin as logistics megaregion," *Transportation Research Record*, vol. 2477, no. 01, 2015.

[19] T. Sakai, K. Kawamura, and T. Hyodo, "Locational dynamics of logistics facilities: evidence from Tokyo," *Journal of Transport Geography*, vol. 46, no. 07, 2015.

[20] T. Sakai, K. Kawamura, and T. Hyodo, "Spatial reorganization of urban logistics system and its impacts: case of Tokyo," *Journal of Transport Geography*, vol. 60, 2017.

[21] M. Dubie, K. C. Kuo, G. Giron-Valderrama, and A. Goodchild, "An evaluation of logistics sprawl in Chicago and Phoenix," *Journal of Transport Geography*, vol. 50, no. 8, 2018.

[22] G. Giuliano and S. Kang, "Spatial dynamics of the logistics industry: evidence from California," *Journal of Transport Geography*, vol. 66, 2018.

[23] A. Heitz, L. Dablanc, J. Olsson, I. Sanchez-Diaz, and J. Woxenius, "Spatial patterns of logistics facilities in Gothenburg, Sweden," *Journal of Transport Geography*, vol. 88, no. 03, 2018.

[24] C. Liu and L. Pingfan, "An empirical study of lighting clustering in Guzhen town of Guangdong province," *Southern Economics*, vol. 308, no. 5, 2015.

[25] Y. Fan, *Research on the Integration Mode and Operation Mechanism of Iron and Steel Logistics Resources from the Perspective of Supply and Demand*, Beijing Jiaotong University, Beijing, China, 2018.

[26] D. Wang, *Research on the Evolution and Mechanism of Spatial Structure of Urban Logistics Development in China*, Chang'an University, Xi'an, China, 2019.

[27] Y. Zhang, *Research on the Development Status and Talent Demand of Modern Logistics Industry in Zhengzhou*, Henan Agricultural University, Zhengzhou, China, 2016.

[28] J. Tao and X. Guo, "Collaborative location of logistics park and industrial park based on total cost and carbon emission reduction," *Chinese Journal of Management Science*, vol. 26, no. 12, pp. 124–134, 2018.

Research Article

Algorithms for Picking and Distribution of Online Orders in New Retail Enterprises

Weiya Zhong ⬤ and **Jia Cui** ⬤

School of Management, Shanghai University, Shanghai 200444, China

Correspondence should be addressed to Weiya Zhong; wyzhong@i.shu.edu.cn

This paper studies joint algorithms of order picking and distribution in new retail enterprises. The problem will consider many factors, such as the type of goods, picking time, batch capacity of distribution, distribution time, and distribution cost. First of all, the research problems are summarized as mathematical programming problems. Then, a genetic algorithm and comparison algorithms are proposed. Finally, the rationality of the model and the effectiveness of the algorithms are verified by computational experiments, and management enlightenments are revealed.

1. Introduction

In the first quarter of 2020, communities in China were closed for management, and since then, the public has been buying fresh food and daily necessities online because of the outbreak of COVID-19. The number of customers in traditional stores has reduced, and orders from new fresh e-commerce have increased rapidly. The new mode of door-to-door delivery has become popular. "It's not the alarm clock that wakes me up every day, but the desire for fresh vegetables." After the outbreak of the epidemic, many people living at home chose to stay away from the grocery market temporarily and "embrace" the Internet, so "online shopping" has become the main choice for supplying daily necessities. This has led to the rise of various online fresh food retail platform merchants against the trend, with the number of users, orders, and sales reaching a new height. According to public information, Dingdong (an APP for online fresh food shopping) saw a 291.42% increase in the number of new users and an overall volume growth of approximately 80%; the order volume of Meituan (an APP for online fresh food shopping) increased by more than 200% in some sites in Shanghai; and the number for HEMA (an APP for online fresh food shopping) was 290%. While the business volume of each online retail platform is booming, the supply chain including logistics and distribution is also under great pressure.

On January 15, 2016, HEMA opened its first store in Shanghai Jinqiao Square and quickly became an "Internet celebrity." HEMA is a new retail format completely reconstructed by Alibaba for offline supermarkets that is different from other fresh e-commerce. It is a supermarket, a restaurant, and a vegetable market. However, such descriptions seem to be inaccurate. Consumers can buy goods in-store or place orders through HEMA APP. This feature is also known as "warehouse-store-integration," and HEMA's warehouse is also its store. Compared to traditional warehouse, the interior merchandise is placed differently. The traditional warehouse stores goods in the standard shelf-stacking pattern. However, each customer can see all goods in HEMA. The display and placement of commercial products are different according to the preferences of consumers in the area where the store is located.

By observing online orders' picking process of HEMA, we found that once a customer places an order in HEMA APP, the information processing center will divide the order into several suborders according to commodity types, such as river fresh, fruit, pasta, and daily necessities. (*This is determined by the goods location and attributes of the commodity. For example, fresh river food products need to be*

dehydrated and processed. It must also be sealed and packed to prevent contamination of other goods.) The information of each suborder is first sent to the handheld device of the staff in the area where the goods are located. The staff selects goods and puts them into a bag. The bag is hung on the hook at the starting position of a conveyor belt, which transfers the bag to the packaging area. In the packaging area, items from the same order are assembled together and passed on to the deliverymen, who distribute customers' orders in batches. One of the biggest characteristics of HEMA is fast delivery: within 3 kilometers around the store, it takes only 30 minutes to deliver goods to your door.

From the above description, we can see that, in the order processing system, the flow of information drives the flow of goods: receiving information from the information processing center, sending instructions to the staff, and sending the goods to the customers by deliverymen. Each of the above steps is important in order to achieve the goal of rapid delivery. In this paper, we formulate the above order processing as a joint scheduling problem of online order picking and distribution.

Order picking is a process of picking the required products from the shelves accurately and quickly, according to the information of customers' orders. It is one of the most important operations in the distribution center. An appropriate order picking system helps improve working efficiency and customer satisfaction [1]. Many literatures have studied such problems, mainly involving design of goods location [2], picking routes [3], order batching [4, 5], and partition picking [6]. In the "online shopping" mode, logistics distribution business poses a lot of new challenges. Researchers have studied the decision-making and route optimization of e-commerce logistics distribution, such as [7, 8]. In order to deliver goods to customers quickly, it is necessary to manage order picking and distribution as a whole. This is because the starting time of vehicle distribution is directly related to the completion time of order picking. Wang et al. [9] constructed a joint scheduling model of picking and distribution to minimize orders' fulfillment time. Peng [10] studied a joint scheduling problem of order batching and distribution routing and took the shortest total fulfillment time from order picking to distribution completion as the goal of B2C e-commerce distribution center. Zhang et al. [11] studied the online integrated order picking and delivery problem with the multizone routing method to minimize the sum of the maximum delivery completion time and the total delivery cost.

The order picking in this paper is different from the traditional warehouse order picking. A HEMA offline store is also a warehouse, which increases the difficulty of order fulfillment due to the variety of commodity demand and small batch sizes. All orders submitted through HEMA app are picked by the staff in the sales area. The placement of goods in the sales area is different from that in traditional warehouses. There is no unified standard shelf. The display and the placement of goods varies from shop to shop according to the preferences of consumers in the area where the store is located. Therefore, we study the picking and distribution problem of orders generated in HEMA APP from a different

view. It is assumed that, in a certain period of time, there are some orders to be picked out and distributed to customers. These orders are regarded as jobs, the staff and conveyor belts in HEMA stores are regarded as machines, and the deliverymen are regarded as vehicles. We analyze the combined problem of order picking and distribution and establish the model with the goal of minimizing the sum of orders' total completion time and total delivery cost.

From the view of scheduling research, we study a machine scheduling problem with transportation of finished jobs. Hall and Potts [12] were the first to propose a joint machine scheduling problem with job transportation. Chen [13] gave a detailed review on the joint problems of machine scheduling and product transportation published before 2008. Zhong et al. [14] and Fu et al. [15] studied scheduling problems of outsourcing the transportation of products to third-party logistics companies. Ullrich [16] considered machine scheduling and job transportation problems with path planning. In this paper, we consider orders' picking and distribution in HEMA as a joint scheduling problem with distribution coordination. Orders are first processed in dedicated flow shops followed by assembly lines and then are distributed to the customers by deliverymen. To the best of our knowledge, this machine scheduling problem has not been covered in any previous literature.

The remaining sections of this paper are organized as follows: In Section 2, we give the problem description; in Section 3, we construct a MP model for the case with one machine at each stage and one deliveryman; in Section 4, we devise algorithms to solve the problem; in Section 5, numerical experiments are carried out to verify the rationality of the model and the effectiveness of the algorithms; in Section 6, we conclude this paper.

2. Problem Descriptions

Suppose that, during a certain period of time, there are several orders waiting to be processed in the online order system of HEMA. Each order is composed of several types of suborders and processed in four stages in sequence. The first and second stages are order processing within the shop: a subjob is first processed on a stage 1 machine (the staff picks out the products and put them into a bag) and then processed on a stage 2 machine (the conveyor belt transfers the bag to packing area); then, in the packing area, suborders belonging to the same order are assembled together for distribution; this is stage 3. In stage 4, completed orders are distributed to their customers in batches by deliverymen with electric power carts. The full process is shown in Figure 1.

We regard each order as a job, and a suborder as a subjob (order and job, and suborder and subjob will be used interchangeably in the following). The staff and conveyor belts are regarded as machines, and the deliverymen are regarded as vehicles.

Next, we describe the above process of orders' picking and distribution as a joint machine scheduling and transportation problem. At the beginning of the planning horizon, n orders $\{O_1, O_2, \ldots, O_n\}$ are placed by n customers. Job O_i may contain one or more subjobs O_i^l (item type-l),
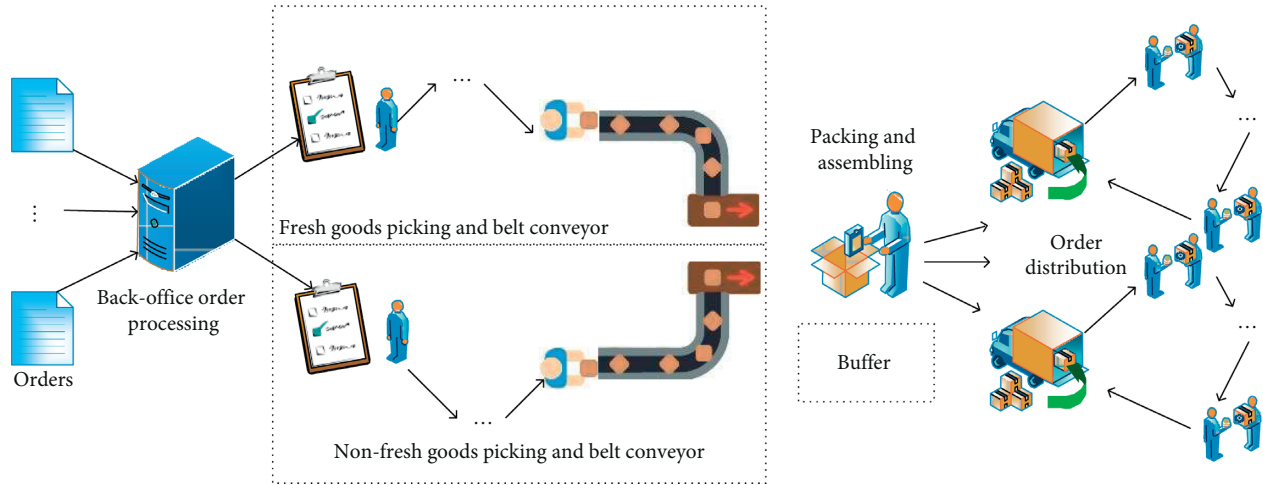
FIGURE 1: Order processing and distribution.

$i = 1, 2, \ldots, n, l = 1, 2, \ldots, k$, where each type of suborders is processed by a dedicated two-stage flow-shop machine $F_l(1,1)$. For $l = 1, 2, \ldots, k$, each subjob O_i^l is first processed by a stage 1 machine M_1^l with processing time p_{i1}^l (time needed for staff's picking) and then processed by a stage 2 machine M_2^l with processing time p_{i2}^l (time needed for belt conveying). When subjobs $O_i^l, i = 1, 2, \ldots, n, l = 1, 2, \ldots, k$ are all finished, they need to be assembled together for distribution. The processing time for job O_i's assembling operation is p_i^3. Each vehicle contains a batch of jobs when it departs from the store. It delivers the jobs to the customers one by one and returns to the store after it delivers the last job. Then, it is ready for the next batch's delivery. It can carry no more than Q jobs in one batch. In this paper, a complete undirected graph $G = (V, E)$ with $n + 1$ vertices is used to represent the geographical locations and distances between the HEMA store and n customers, $V = \{V_0, V_1, V_2, \ldots, V_n\}$, $E = \{e_{ij}, i \neq j, \ i, \ j = 1, 2, \cdots, n\}$, where V_0 is the HEMA store, and $V_1, V_2, \ldots, V_n$ represent n customers. It takes time of t_{ij} $(i, j = 1, 2, \ldots, n)$ for the vehicle travelling between V_i and V_j. The vehicle starts from V_0, distributes the orders in the current batch to their customers one by one, and returns to V_0. We assume that the triangle inequality is satisfied between any three points in the distribution network. Since a batch may contain a variety of orders (e.g., requiring refrigeration or additional packaging), each order occurs a distribution cost d_i. If several orders are contained in one batch, the distribution cost of this batch equals the arithmetic mean of the cost of all orders in the batch.

Our goal in this paper is to design a solution for the above joint machine scheduling and distribution problem, such that the total arrival time (sum of the times when the customers receive their orders) and the total distribution cost are minimized.

We need to make the following decisions: (1) subjobs' arrangement on the dedicated flow-shop machines and the assembly machines; (2) batching decision before distribution, including the number of batches and jobs contained in each batch; (3) the time when each batch leaves the machine and the routes of distributing orders in each batch.

3. MP Model for a Special Case

In this section, we study the case when each job contains two subjobs (subjob A and subjob B denote fresh goods and nonfresh goods, respectively), and there are one assembly machine and one vehicle. We construct a mathematical programming model for this problem. It seems that it is a bit special; however, we can see that it reveals the meaning for the coordinated consideration of order picking and distribution. We first list parameters and variables for this model.

Parameters

N: the set of jobs, $N = \{O_1, O_2, \ldots, O_n\}$

O_i: the ith job

O_i^A: subjob A of job O_i

O_i^B: subjob B of job O_i

p_{i1}^A: processing time of subjob A of job O_i at the first stage

p_{i1}^B: processing time of subjob B of job O_i at the first stage

p_{i2}^A: processing time of subjob A of job O_i at the second stage

p_{i2}^B: processing time of subjob B of job O_i at the second stage

p_{i3}: processing time of job O_i on the assembling machine

V: the set of vertices in the distribution network

t_{ij}: transportation time for a vehicle travelling between V_i and V_j

Q: capacity constraint of a distribution batch

d_i: distribution cost for each job

y_i $y_i = 1$ if job O_i contains subjob A; otherwise, $y_i = 0$

z_i $z_i = 1$ if job O_i contains subjob B; otherwise $z_i = 0$

Variables

s_{i1}^A: starting time of subjob A of job O_i at the first stage

c_{i1}^A: finishing time of subjob A of job O_i at the first stage

s_{i1}^B: starting time of subjob B of job O_i at the first stage

c_{i1}^B: finishing time of subjob B of job O_i at the first stage

s_{i2}^A: starting time of subjob A of job O_i at the second stage

c_{i2}^A: finishing time of subjob A of job O_i at the second stage

s_{i2}^B: starting time of subjob B of job O_i at the second stage

c_{i2}^B: finishing time of subjob B of job O_i at the second stage

s_{i3}: starting time of job O_i on the assembling machine

c_{i3}: finishing time of job O_i on the assembling machine

s_{i4}: departure time of job O_i (departure time of the batch that job O_i belongs to)

c_{i4}: completion time of job O_i (when it is delivered to its customer)

s_f: starting time of the distribution of batch B_f

c_f: finishing time of the distribution of batch B_f (when the last job is delivered, and the vehicle returns to the store)

F: the number of batches, $\lceil n/Q \rceil \leq F \leq n$

B: the set of distribution batches, $B = \{B_1, B_2, \ldots, B_F\}$

b_f: number of jobs in batch B_f, $f = 1, 2, \ldots, F$

$e_{ij}^{A1} = 1$ if O_i^A precedes O_j^A at the first stage, else $= 0$

$e_{ij}^{A2} = 1$ if O_i^A precedes O_j^A at the second stage, else $= 0$

$e_{ij}^{B1} = 1$ if O_i^B precedes O_j^B at the first stage, else $= 0$

$e_{ij}^{B2} = 1$ if O_i^B precedes O_j^B at the second stage, else $= 0$

$e_{ij}^3 = 1$ if O_i precedes O_j at the third stage, else $= 0$

$v_{ij}^f = 1$ if vehicle travels from V_i to V_j in batch B_f, else $= 0$

$x_{if} = 1$ if job O_i is allocated to batch B_f, else $= 0$

$v_{ij} = 1$ if vehicle travels from V_i to V_j in some batch, else $= 0$ (For ease of presentation, let $v_{jj} = 1$)

D_f: distribution cost for batch B_f

Mathematical programming model is as follows:

$$\min \quad \sum_{i=1}^{n} c_{i4} + \sum_{f=1}^{F} D_f, \tag{1}$$

$$\text{s.t.} \quad s_{i1}^A \geq 0, \quad i = 1, 2, \ldots, n, \tag{2}$$

$$s_{i1}^B \geq 0, \quad i = 1, 2, \ldots, n, \tag{3}$$

$$c_{i1}^A = \left(s_{i1}^A + p_{i1}^A\right) \times y_i, \quad i = 1, 2, \ldots, n, \tag{4}$$

$$c_{i2}^A = \left(s_{i2}^A + p_{i2}^A\right) \times y_i, \quad i = 1, 2, \ldots, n, \tag{5}$$

$$c_{i1}^A - s_{i2}^A \leq 0, \quad i = 1, 2, \ldots, n, \tag{6}$$

$$c_{i1}^B - s_{i2}^B \leq 0, \quad i = 1, 2, \ldots, n, \tag{7}$$

$$c_{i1}^B = \left(s_{i1}^B + p_{i1}^B\right) \times z_i, \quad i = 1, 2, \ldots, n, \tag{8}$$

$$c_{i2}^B = \left(s_{i2}^B + p_{i2}^B\right) \times z_i, \quad i = 1, 2, \ldots, n, \tag{9}$$

$$c_{i3} = s_{i3} + p_{i3}, \quad i = 1, 2, \ldots, n, \tag{10}$$

$$\max\left\{c_{i2}^A, c_{i2}^B\right\} - s_{i3} \leq 0, \quad i = 1, 2, \ldots, n, \tag{11}$$

$$s_{j1}^A \geq c_{i1}^A - \left(1 - e_{ij}^{A1}\right)M, \quad i, j = 1, 2, \ldots, n, i \neq j, \tag{12}$$

$$s_{j1}^B \geq c_{i1}^B - \left(1 - e_{ij}^{B1}\right)M, \quad i, j = 1, 2, \ldots, n, i \neq j, \tag{13}$$

$$s_{j2}^A \geq c_{i2}^A - \left(1 - e_{ij}^{A2}\right)M, \quad i, j = 1, 2, \ldots, n, i \neq j, \tag{14}$$

$$s_{j2}^B \geq c_{i2}^B - \left(1 - e_{ij}^{B2}\right)M, \quad i, j = 1, 2, \ldots, n, i \neq j, \tag{15}$$

$$s_{j3} \geq c_{i3} - \left(1 - e_{ij}^3\right)M, \quad i, j = 1, 2, \ldots, n, i \neq j, \tag{16}$$

$$\sum_{f=1}^{F} x_{if} = 1, \quad i = 1, 2, \ldots, n, \tag{17}$$

$$\sum_{O_i \in B_f} x_{if} \leq Q, \quad f = 1, 2, \ldots, F, \tag{18}$$

$$\left\lceil \frac{n}{Q} \right\rceil \leq F \leq n, \tag{19}$$

$$s_f = \max_{i \in \{1, 2, \ldots, n\}} \left\{c_{i3} - \left(1 - x_{if}\right)M\right\}, f = 1, 2, \ldots, F, \tag{20}$$

$$s_{i4} = \max_{i \in \{1, 2, \ldots, n\}} \left\{s_f - \left(1 - x_{if}\right)M\right\}, \quad f = 1, 2, \ldots, F, \tag{21}$$

$$D_f = \frac{\sum_{i=1}^{n} x_{if} d_i}{b_f}, \quad f = 1, 2, \ldots, F, \tag{22}$$

$$s_f - c_{f-1} \geq 0, \quad f = 2, 3, \ldots, F, \tag{23}$$

$$x_{if} = \sum_{j \in N \bigcup \{0\} \setminus \{i\}} v_{ij}^f, \quad i = 1, 2, \ldots, n, f = 1, 2, \ldots, F, \tag{24}$$

$$\sum_{f=1}^{F} \sum_{i=0}^{n} v_{ij}^f = 1, \quad j = 1, 2, \ldots, n, \tag{25}$$

$$\sum_{f=1}^{F} \sum_{j=0}^{n} v_{ij}^f = 1, \quad i = 1, 2, \ldots, n, \tag{26}$$

$$\sum_{j=1}^{n} v_{0j}^f = 1, \quad f = 1, 2, \ldots, F, \tag{27}$$

$$\sum_{j=1}^{n} v_{j0}^{f} = 1, \quad f = 1, 2, \ldots, F, \tag{28}$$

$$c_f = s_f + \sum_{i=0}^{n} \sum_{j=1}^{n+1} t_{ij} v_{ij}^{f}, \quad f = 1, 2, \ldots, F, \tag{29}$$

$$c_{i4} + t_{ij} v_{ij}^{f} - M\left(1 - v_{ij}^{f}\right) \leq c_{j4}, \quad i = 1, \ldots, n, j = 1, \ldots, n,$$
$$f = 1, 2, \ldots, F, \tag{30}$$

$$s_f + t_{0j} v_{0j}^{f} - M\left(1 - v_{0j}^{f}\right) \leq c_{j4}, \quad j = 1, \ldots, n, f = 1, 2, \ldots, F. \tag{31}$$

Objective function (1) is to minimize the sum of the total completion time and the total distribution cost of jobs. Constraints (2) and (3) ensure that each subjob starts processing after time zero. Constraints (4) and (5) denote the finishing time of type A subjobs at the first stage and second stage. Constraints (6) and (7) indicate that a subjob can be started on stage 2 machine only after it has been finished on the corresponding stage 1 machine. Constraints (8) and (9) denote the finishing time of type B sub jobs at the first stage and second stage. Constraint (10) denotes the finishing time of the jobs at the third stage. Constraint (11) ensures that a job can be assembled only after its two subjobs have been completed. Constraints (12) to (16) ensure that, at any time, only one job can be processed on a machine. Constraint (17) ensures that a job is contained in exactly one batch. Constraint (18) ensures that the number of jobs in one batch is no larger than the capacity constraint. Constraint (19) denotes the bound for the number of distribution batches. Constraint (20) ensures that the vehicle can start travelling only after all jobs in one batch are completed. Constraint (21) indicates that, for each job, the departure time is the starting time of corresponding batch distribution. Constraint (22) denotes the cost of distribution for each batch. Constraint (23) ensures that the vehicle starts a new distribution batch only if he has distributed all the jobs in the last batch and returns to the store. Constraints (24) to (26) indicate that each customer is visited exactly once. Constraints (27) and (28) indicate that the vehicle travels from/to the store exactly F times. Constraint (29) denotes the time when the vehicle returns to the store equal to its starting time of the current batch plus the total travel time in the routing. Constraints (30) to (31) denote the delivery time of job O_i in batch B_f.

4. A Genetic Algorithm

Note that the two-stage assembly scheduling problem with two parallel machines in the first stage and no delivery is strongly NP-hard [17]. Therefore, the problem in this paper with two dedicated flow shops in the first stage and delivery coordination is obviously strongly NP-hard. Only relatively small instances can be optimally solved in reasonable computational time. Consequently, in this section, we develop a genetic algorithm to find good solutions [18].

For a given sequence of $\{O_1, O_2, \ldots, O_n\}$, we first devise algorithm CA-D (Algorithm 1) to arrange the jobs' processing and distribution.

Note that algorithm CA-D generates a feasible schedule for our problem; however, this schedule is not that good. This is because the processing sequence and delivery sequence are the same in one batch. Next, we propose algorithm LGP (Algorithm 2) to improve this problem. LGP does not change the batching decisions but tries to reduce the completion time on the machines as well as the total transportation time of each batch.

Next, we list the details of our genetic algorithm:

(1) Coding and encoding

A chromosome represents a sequence of orders' picking and distribution based on the above algorithm CA-D. Figure 2 shows an example of a chromosome with ten genes indicating that there are ten jobs to be processed. {1, 5, 4, 2, 7, 10, 9, 8, 3, 6} is the input of algorithm CA-D in order to determine the processing sequence on each machine and the distribution batches with routing consideration.

(2) Fitness function

We define the fitness function of a chromosome as the inverse of the objective function: $1/(\sum_{i=1}^{n} c_{i4} + \sum_{f=1}^{F} D_f)$.

(3) Genetic operators

Genetic operators used in this paper include selection, crossover, mutation, reversal, and reinsertion. First, parent chromosomes are selected from the initial population, then the offspring chromosomes are generated by crossover operator, and then mutation operation is performed. In order to improve the local search ability, reverse operation is carried out. Finally, in order to handle the reduction of the number of chromosomes caused by the selection operator, reinsertion operation is carried out:

(3.1) Selection

In this paper, Roulette wheel selection is used to select offspring from the parent population. Roulette wheel selection is similar to the roulette wheel used in gambling. Table 1 shows the probability of selection of an individual based on the fitness functions for a population of ten individuals, where the probability of selection of an individual equals (the fitness of the individual ÷ the sum of the fitness of all individuals in the population of the individual) × 100%.

Each time, we randomly generate two numbers between $[0, 1]$, which is equivalent to turning the wheel twice to get the position of the pointer (the sector to which the pointer stops is the selected individual), and the two selected individuals are the parents. As shown in Figure 3, we plot the probability of each individual being selected on a roulette wheel for the

Step 1: process type A subjobs on each stage of the dedicated flow-shop in the sequence of $\{O_1^A, O_2^A, \ldots, O_n^A\}$ and process type B subjobs on each stage of the dedicated flow-shop in the sequence of $\{O_1^B, O_2^B, \ldots, O_n^B\}$. Assemble the jobs in the sequence of $\{O_1, O_2, \ldots, O_n\}$.
Step 2: jobs are delivered in $F = \lceil n/Q \rceil$ batches. For $f = 2, \ldots, F - 1$, batch B_f contains $\{O_{(f-1)\times Q+1}, O_{(f-1)\times Q+2}, \ldots, O_{f\times Q}\}$, and the last batch B_F contains $\{O_{(F-1)\times Q+1}, O_{(F-1)\times Q+2}, \ldots, O_n\}$.
Step 3: the vehicle distributes the batches in the sequence of $\{B_1, B_2, \ldots, B_F\}$, and the routing inside each batch is in the same sequence as that on the assembly machine. (The jobs are delivered in the sequence of $\{O_1, O_2, \ldots, O_n\}$.)

ALGORITHM 1: CA-D.

Input: a feasible solution of generated from CA-D with delivery batches of $\{B_1, B_2, \ldots, B_F\}$.
Output: an improved feasible solution.
Initialization: $f = 1$.
Step 1: for batch B_f, select two jobs randomly from this batch. Swap the two jobs in the processing sequence, i.e., on each machine, corresponding subjobs are swapped. Compute the completion time of the last job in B_f on the assembly machine. Repeat such swapping operation 50 times and select the processing sequence with the minimum completion time of the last job in B_f.
Step 2: for batch B_f, select two jobs randomly from this batch. Swap the two jobs in the delivery sequence and compute the total delivery time of this new sequence. Repeat such swapping operation 50 times and select the delivery sequence with the minimum total delivery time.
Step 3: if $f < F$, $f = f + 1$, go to Step 1; otherwise, stop.

ALGORITHM 2: LGP.

| 1 | 5 | 4 | 2 | 7 | 10 | 9 | 8 | 3 | 6 |
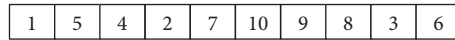
FIGURE 2: An example of a chromosome with ten genes.

TABLE 1: Calculation of selection probabilities based on individual fitness.

Individual	Chromosome	Fitness	Probability of selection	Cumulative probability
1	10, 8, 9, 5, 6, 3, 2, 1, 4, 7	5	0.060976	0.060976
2	10, 8, 9, 5, 4, 7, 6, 3, 2, 1	4	0.048780	0.109756
3	9, 5, 6, 3, 10, 8, 2, 1, 4, 7	9	0.109756	0.219512
4	4, 8, 9, 5, 6, 3, 2, 1, 10, 7	7	0.085366	0.304878
5	9, 5, 6, 10, 8, 3, 2, 1, 4, 7	8	0.097561	0.402439
6	9, 5, 6, 2, 1, 4, 7, 10, 8, 3	8	0.097561	0.500000
7	8, 3, 2, 1, 4, 7, 9, 5, 6, 10	5	0.060976	0.560976
8	3, 2, 1, 10, 8, 4, 7, 9, 5, 6	10	0.121951	0.682927
9	1, 5, 4, 2, 7, 10, 9, 8, 3, 6	15	0.182927	0.865854
10	2, 9, 7, 5, 6, 4, 3, 8, 10, 1	11	0.134146	1.000000

population in Table 1 and then select the parent individuals in turn by roulette selection.

(3.2) Crossover

In this paper, Partially Matched Crossover (PMX) method is used in the crossover. In PMX, we first select two crossover points randomly, exchange the genes between the two crossover points, and then replace the repeated genes through allele mapping. In Figure 4, we show the process of creating two offspring from a pair of parents by PMX crossover and

mutation, using individuals 9 and 10 from Table 2: first, the crossover region of the parent individual is selected, and the genes of the two chromosomes within the crossover region are crossed over. As the new chromosome contains duplicated genes, we replace the duplicated genes by mapping the alleles of the parent individuals $(4 - 7 - 10, 2 - 5, 7 - 6, 9 - 3)$. A random number in $[0, 1]$ is generated, and if it is smaller than the crossover probability c, crossover is run.
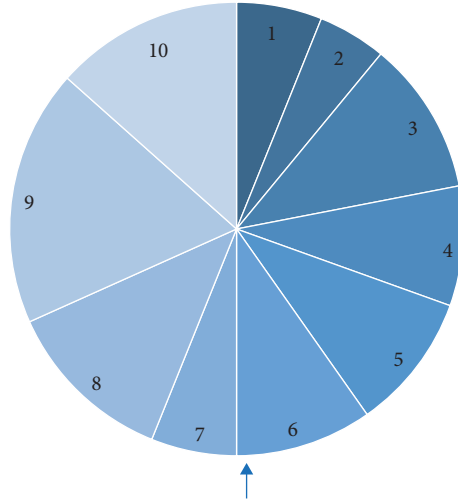
FIGURE 3: Roulette wheel selection.
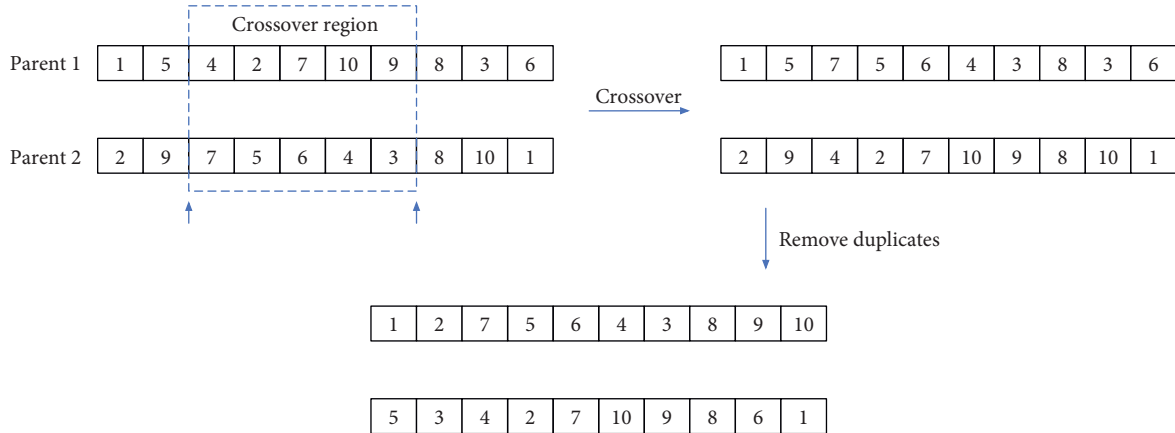
FIGURE 4: Partially matched crossover operation.

TABLE 2: Parameters for 60 instances.

Group	Instance	p_{i1}^{A}	p_{i2}^{A}	p_{i1}^{B}	p_{i2}^{B}	p_{i3}	d_i	t_{ij}
X	1–20	[5, 10]	[2, 3]	[3, 9]	[1, 2]	[2, 8]	[7, 13]	[4, 7]
Y	21–40	[0, 10]	[0, 3]	[0, 9]	[0, 2]	[2, 8]	[7, 13]	[4, 7]
Z	41–60	[0, 10]	[0, 3]	[0, 9]	[0, 2]	[2, 8]	[7, 13]	[40, 70]

(3.3) Mutation

In the mutation operation, for the two individuals after the crossover operation, we randomly select two positions in an individual to exchange genes at these two positions, as shown in Figure 5. A random number in [0, 1] is generated, and if it is smaller than the mutation probability m, mutation is run.

(4) Iteration termination conditions

The minimal fitness function value of the last generated population is denoted as LB, where the initial value of LB is the minimum fitness function value of the initial population. The minimal fitness function value of the current population is denoted as CR. If $(|LB - CR|/LB) \le \varepsilon$ (ε is a given positive number) or the number of iterations reaches 500, stop.

Now we are ready to devise a genetic algorithm DU-GA (Algorithm 3) for the integrated order picking and distribution problem.

5. Numerical Experiments and Analysis

In order to verify the rationality of the above model and test the performance of algorithm DU-GA, we conduct numerical experiments and analyze the results based on Python 3.8. All numerical experiments are performed on a personal
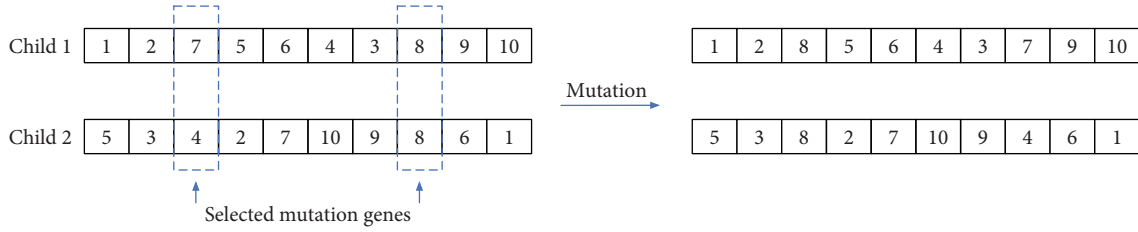
FIGURE 5: Mutation operation.

TABLE 3: Parameter settings.

Group	(50, 0.7, 0.1)	(100, 0.7, 0.1)	(150, 0.7, 0.1)	(150, 0.8, 0.1)	(150, 0.9, 0.1)	(150, 0.8, 0.2)	(150, 0.8, 0.3)
X	13455.71	12737.29	12725.33	12410.71	12411.79	12225.33	13156.88
Y	9991.83	9948.67	10067.88	10049.04	10202.08	9691.38	9739.04
Z	73821.38	73692.67	73705.42	73221.75	73667.25	72058.00	73418.88

computer with 8 GB memory and 2.70-GHz Intel Core i5 CPU.

5.1. Parameter Setting

5.1.1. Parameters for Instances.
According to different situations of these parameters, we carry out three groups of numeral experiments, where each group randomly generates 20 instances. Each instance contains 50 jobs, and the vehicle capacity is $Q = 8$.

Table 2 shows the parameter intervals for 20 instances of each Group. For example, parameters for Group-X are set as $p_{i1}^A \in [5, 10]$, $p_{i2}^A \in [2, 3]$, $p_{i1}^B \in [3, 9]$, $p_{i2}^B \in [1, 2]$, $p_{i3} \in [2, 8]$ and $d_i \in [7, 13]$ ($p_{i1}^A \in [5, 10]$ means that p_{i1}^A is a random integer uniformly generated in interval of $[5, 10]$ and the other parameter settings are similar to this).

Group-X (Instances 1–20) considers the case when orders contain both fresh and nonfresh products, where the processing time is always larger than zero. The picking time for fresh products is generally longer than that for nonfresh products due to the additional steps (i.e., dewatering and weighing) during the picking process. Group-Y (Instances 21–40) and Group-Z (Instances 41–60) allow orders containing only fresh products or only nonfresh products, in recognition of the fact that customers may need to buy only fresh or nonfresh products, where the processing time may be zero, which is more realistic. Group-Z (Instances 41–60) examines cases where the delivery time of orders is significantly longer than processing time.

5.1.2. Parameters for Genetic Operators.
Before the genetic algorithm is applied, the following parameters need to be determined: population size P, crossover probability c, and mutation probability m. P is set to be one of {50, 100, 150} and maintains the same size for each iteration. The crossover probability c is set to be one of {0.7, 0.8, 0.9}. The mutation probability m is generally set to be in [0.05, 0.1]; however, considering the strong NP-hardness of the problem, m is set to be one of {0.1, 0.2, 0.3} to expand the search space. Since the actual performance of genetic algorithm is closely related

to these parameters, we first test different combinations of (P, c, m). For each group, an instance is generated. For different parameters of GA, the algorithm is run five times for each instance. Table 3 lists the average objective value for the instances (i.e., 13477.71 online 2 column 2 denotes the average objective value of the instance of Group-X with parameter $(50, 0.7, 0.1)$, and the others are similar to this).

We observe the following:

(1) If $(c, m) \in (0.7, 0.1)$, by comparing $(P, c, m) \in \{(50, 0.7, 0.1), (100, 0.7, 0.1), (150, 0.7, 0.1)\}$, when $P = 150$, DU-GA terminates with the best objective value

(2) If $P = 150$, by comparing $(P, c, m) \in \{(150, 0.7, 0.1), (150, 0.8, 0.1), (150, 0.9, 0.1)\}$, when $c = 0.8$, DU-GA terminates with the best objective value

(3) Based on (1) and (2), we let $P = 150$ and $c = 0.8$. If $(P, c, m) \in \{(150, 0.8, 0.1), (150, 0.8, 0.2), (150, 0.8, 0.3)\}$, when $m = 0.8$, the objective value is best

Therefore, we set the parameters (P, c, m) for DU-GA to be $(150, 0.8, 0.1)$.

5.2. Analysis of Experimental Results

5.2.1. Stability Test.
To evaluate the stability of algorithm DU-GA, for Groups X, Y and Z, we run each instance five times to assess the span between the minimal solution (denoted as S_B) and the average value (denoted as S_A), which is referred to as Relative Deviation (denoted as RD), calculating by RD = $((S_A - S_B)/S_A) \times 100\%$.

Table 4 shows that the span between S_A and S_B is small, with an average RD of 1.46% for Group-X, 1.97% for Group-Z, and 2.05% for Group-Y. Therefore, DU-GA is stable in all three groups of instances.

5.2.2. Comparison Algorithm.
To evaluate the effectiveness of the algorithm DU-GA, we design comparison algorithms DU-1 (Algorithm 4) and DU-2 (Algorithm 5). Algorithm DU-1 is a genetic algorithm that is different from DU-GA in that it calculates the fitness function based on the departure

TABLE 4: Stability test of DU-GA.

Group	Min RD (%)	Max RD (%)	Average RD (%)
X	0.35	2.48	1.46
Y	1.41	3.71	1.97
Z	0.90	4.94	2.05

Step 1: determine the population size P, the crossover probability c, the mutation probability m, and the termination condition of the algorithm, followed by initializing the population (i.e., randomly generating P individuals).
Step 2: for each individual, apply algorithm CA-D. Evaluate fitness values of the chromosome and select two individuals as parents.
Step 3: perform crossover and mutation operators on the selected parents to obtain offspring individuals.
Step 4: update the population by adding the newly generated individuals to the population. Step 2 and Step 3 are repeated until the termination condition is met, and the iteration is stopped.
Step 5: select the best solution from the current population, and let it be the input of algorithm LGP. Run algorithm LGP, and output the resulted solution.

ALGORITHM 3: DU-GA.

time of each job s_{i4}. Algorithm DU-2 processes and distributes jobs in a random order.

5.2.3. Algorithm Effectiveness Analysis. In Tables 5–7, the results for instances of Groups X, Y and Z by applying DU-GA, DU-1, and DU-2 are listed. For ease of presentation, we denote the objective value of the solution obtained from DU-GA, DU-1, and DU-2 as C_{DU-GA}, C_{DU-1} and C_{DU-2}, respectively. We run each instance five times and record the mean of the objective values. The first column shows the index of the 20 instances; the second and third columns show the results of DU-2 and DU-1; the fourth column shows the objective values of the solutions obtained from DU-GA. We record the reduction of C_{DU-GA} over C_{DU-1} and C_{DU-2} in the fifth and sixth columns and show the percentage improvement of C_{DU-GA} over C_{DU-1} and C_{DU-2} in the seventh and eighth columns.

We also observe that DU-GA takes the longest time in most instances, but the maximal does not exceed 11.83 seconds; the running time of DU-1 is shorter than that of DU-GA, while the running time of DU-2 is the shortest. Compared with DU-1, DU-GA not only considers the delivery times in fitness function but also adds further optimization of the production and distribution stages based on the basic GA algorithm:

(1) Compare DU-GA with DU-1

According to Tables 5–7, the average improvement of C_{DU-GA} over C_{DU-1} for Groups X, Y and Z instances is 1.94%, 4.00%, and 5.12%.

(1.1) It is shown that the improvement of C_{DU-GA} over C_{DU-1} of Group-Y is better than that of Group-X. Note that the processing times of jobs in Group-Y are smaller than those of Group-X, and thus the distribution time is relatively larger in Group-Y. DU-GA differs from DU-1 in that it considers the delivery times as well as processing times in the fitness function;

therefore, the larger the delivery times, the more the improvement of C_{DU-GA} over C_{DU-1}.

(1.2) The improvement of C_{DU-GA} over C_{DU-1} of Group-Z is better than that of Group-Y. Note that the transportation times of instances in Group-Z are obviously higher. The same reason as in (1.1) can explain this observation.

(1.3) The results of Group-Z are significantly better than those of the other two groups, meaning that, compared to algorithm DU-1, algorithm DU-GA is highly effective for the practical case when orders may only contain fresh items or nonfresh items and take longer for distribution than processing.

(2) Compare DU-GA with DU-2

According to Tables 5–7, the average improvement of DU-GA over DU-2 for Groups X, Y and Z instances is 5.35%, 9.70%, and 10.38%.

(2.1) It is shown that the average improvement of C_{DU-GA} over C_{DU-2} of Group-Y is better than that of Group-X. DU-2 is a FIFO strategy, and no optimization skill is applied. DU-GA is a genetic algorithm, and it considers the processing times and the delivery times in the fitness function. Note that there is only one vehicle for distribution, and multiple orders are contained in one batch; thus, the optimization of the distribution stage plays a more important role than that of the production stages. Recall that the processing times of jobs in Group-Y are smaller than those of Group-X, and thus the distribution time is relatively larger in Group-Y. Therefore, the larger the delivery times, the more the improvement of C_{DU-GA} over C_{DU-2}.

(2.2) The improvement of C_{DU-GA} over C_{DU-2} of Group-Z is better than that of Group-Y. Note that the transportation times of instances in

Step 1: same as Step 1 of DU-GA;
Step 2: for each individual, apply algorithm CA-D. Calculate the fitness value for individuals in the population by taking $1/\sum_{i=1}^{n} s_{i4} \sum_{f=1}^{F} D_f$ as the fitness function.
Step 3-Step 4: same as Step 3 - Step 4 of DU-GA;
Step 5: output the processing sequence, batching decision, and delivery routings of the best solution based on fitness function $1/\sum_{i=1}^{n} s_{i4} \sum_{f=1}^{F} D_f$. Calculate the corresponding objective function $\sum_{i=1}^{n} c_{i4} + \sum_{f=1}^{F} D_f$.

ALGORITHM 4: DU-1.

Step 1: run algorithm CA-D in a random order;
Step 2: output the processing sequence, batching decision and delivery routings. Calculate the corresponding objective $\sum_{i=1}^{n} c_{i4} + \sum_{f=1}^{F} D_f$.

ALGORITHM 5: DU-2.

TABLE 5: Experimental results of 20 instances in Group-X.

Instance	C_{DU-2}	C_{DU-1}	C_{DU-GA}	$C_{DU-GA} - C_{DU-1}$	$C_{DU-GA} - C_{DU-2}$	$(C_{DU-GA} - C_{DU-1})/C_{DU-1}$ (%)	$(C_{DU-GA} - C_{DU-2})/C_{DU-2}$ (%)
ins1	13189.63	13025.50	12841.38	184.13	348.25	1.41	2.64
ins2	13173.00	12871.25	12680.50	190.75	492.50	1.48	3.74
ins3	13038.75	12852.13	12748.13	104.00	290.63	0.81	2.23
ins4	13380.00	12702.63	12537.75	164.88	842.25	1.30	6.29
ins5	13078.50	12928.00	12580.50	347.50	498.00	2.69	3.81
ins6	13361.75	12919.38	12837.88	81.50	523.88	0.63	3.92
ins7	13320.00	12870.25	12645.13	225.13	674.88	1.75	5.07
ins8	13145.75	12945.25	12643.50	301.75	502.25	2.33	3.82
ins9	13145.75	12945.25	12643.50	301.75	502.25	2.33	3.82
ins10	12851.88	12311.13	12168.38	142.75	683.50	1.16	5.32
ins11	12892.88	12153.13	11974.25	178.88	918.63	1.47	7.13
ins12	12898.50	12189.50	12022.50	167.00	876.00	1.37	6.79
ins13	13040.50	12281.88	11918.13	363.75	1122.38	2.96	8.61
ins14	13160.38	12254.00	12063.38	190.63	1097.00	1.56	8.34
ins15	13223.25	12294.25	11984.00	310.25	1239.25	2.52	9.37
ins16	12559.75	12365.63	12011.75	353.88	548.00	2.86	4.36
ins17	12969.50	12118.25	11956.50	161.75	1013.00	1.33	7.81
ins18	12733.00	12410.63	11903.25	507.38	829.75	4.09	6.52
ins19	13716.88	13627.00	13225.13	401.88	491.75	2.95	3.59
ins20	13561.63	13295.00	13046.88	248.13	514.75	1.87	3.80
Average	13122.06	12668.00	12421.62	246.38	700.44	1.94	5.35

Group-Z are obviously higher. The same reason as in (2.1) can explain this observation.

(2.3) The results of Group-Z are significantly better than those of the other two groups, meaning that, compared to algorithm DU-2, algorithm DU-GA is highly effective for the practical case when orders may only contain fresh items or nonfresh items, and the time for distribution is longer than processing.

(3) For each instance, $C_{DU-GA} - C_{DU-2}$ is always larger than $C_{DU-GA} - C_{DU-1}$. DU-2 is a FIFO strategy, and no optimization skill is applied, while DU-1 is a genetic algorithm, which considers jobs' processing

times in the fitness function. DU-1 is also an acceptable algorithm, but not as good as DU-GA.

5.2.4. The Enlightenment for the Management of New Retail Enterprises. The orders' processing sequence in each stage directly affects the order delivery time, which in turn has an impact on customer satisfaction. In order to improve customer satisfaction, we must consider different practical scenarios. The results of numerical experiments show that the genetic algorithm DU-GA is relatively stable for all instances. We also design comparison algorithms DU-1 and DU-2 to evaluate the effectiveness of DU-GA. The results show that algorithm DU-GA outperforms algorithm DU-1

TABLE 6: Experimental results of 20 instances in Group-Y.

Instance	C_{DU-2}	C_{DU-1}	C_{DU-GA}	$C_{DU-GA} - C_{DU-1}$	$C_{DU-GA} - C_{DU-2}$	$(C_{DU-GA} - C_{DU-1})/C_{DU-1}$ (%)	$(C_{DU-GA} - C_{DU-2})/C_{DU-2}$ (%)
ins21	11729.13	10633.63	10130.88	502.75	1598.25	4.73	13.63
ins22	10821.00	10077.50	9880.63	196.88	940.38	1.95	8.69
ins23	11544.13	10683.75	10340.50	343.25	1203.63	3.21	10.43
ins24	10883.38	10361.63	9816.38	545.25	1067.00	5.26	9.80
ins25	11455.38	11073.75	10707.88	365.88	747.50	3.30	6.53
ins26	11369.00	10325.00	9640.75	684.25	1728.25	6.63	14.45
ins27	10544.88	10399.63	9849.88	549.75	695.00	5.29	6.59
ins28	10915.63	10407.13	9877.88	529.25	1037.75	5.09	9.51
ins29	11418.13	10445.88	10103.13	342.75	1315.01	3.28	11.52
ins30	10843.63	10672.50	10224.00	448.50	619.63	4.20	5.71
ins31	10968.00	10574.00	9778.50	795.50	1189.50	6.58	9.93
ins32	11800.88	11006.00	10764.13	241.88	1036.75	2.20	8.79
ins33	11745.13	10813.63	10273.13	540.50	1472.00	5.00	12.53
ins34	11127.50	10227.13	9613.50	613.63	1514.00	6.00	13.61
ins35	11716.50	10931.00	10694.25	236.75	1022.25	2.17	8.72
ins36	11339.25	10513.88	10042.38	471.50	1296.88	4.48	11.44
ins37	11205.25	10787.50	10539.50	248.00	665.75	2.30	5.94
ins38	11774.25	10763.75	10635.75	128.00	1138.50	1.19	9.67
ins39	11000.25	10820.38	10659.00	161.38	341.25	1.49	3.10
ins40	11548.38	10616.75	10009.38	607.38	1539.00	5.72	13.33
Average	11287.48	10606.72	10179.07	427.65	1108.41	4.00	9.70

TABLE 7: Experimental results of 20 instances in Group-Z.

Instance	C_{DU-2}	C_{DU-1}	C_{DU-GA}	$C_{DU-GA} - C_{DU-1}$	$C_{DU-GA} - C_{DU-2}$	$C_{DU-GA} - C_{DU-1}/C_{DU-1}$ (%)	$C_{DU-GA} - C_{DU-2}/C_{DU-2}$ (%)
ins41	80295.00	74138.63	70463.13	3675.50	9831.88	4.96	12.24
ins42	80016.75	75866.75	71510.38	4356.38	8506.38	5.74	10.63
ins43	83567.00	78034.38	73665.00	4369.38	9902.00	5.60	11.85
ins44	80826.63	74994.88	70743.88	4251.00	10082.75	5.67	12.47
ins45	78806.63	74775.63	71372.88	3402.75	7433.75	4.55	9.43
ins46	83283.63	75297.75	71529.50	3768.25	11754.13	5.00	14.11
ins47	79538.88	76558.63	71696.88	4861.75	7842.00	6.35	9.86
ins48	81573.50	77321.38	73266.75	4054.63	8306.75	5.24	10.18
ins49	78296.25	74942.13	71648.13	3294.00	6648.13	4.40	8.49
ins50	81076.25	75760.25	72000.00	3760.25	9076.25	4.96	11.19
ins51	82371.63	78569.38	73763.38	4806.00	8608.25	6.12	10.45
ins52	79815.38	74644.25	71110.25	3534.00	8705.13	4.73	10.91
ins53	78848.38	75671.13	71391.25	4279.88	7457.13	5.66	9.46
ins54	80431.75	76728.88	73497.88	3231.00	6933.88	4.21	8.62
ins55	80261.38	75413.88	70473.25	4940.63	9788.13	6.55	12.20
ins56	79548.88	76709.63	73692.50	3017.13	5856.38	3.93	7.36
ins57	84032.75	78333.25	74515.25	3818.00	9517.50	4.87	11.33
ins58	77052.38	75897.00	71994.00	3903.00	5058.38	5.14	6.56
ins59	84053.75	76164.25	73829.63	2334.63	10224.13	3.07	12.16
ins60	78999.75	76957.00	72623.38	4333.63	6376.38	5.63	8.07
Average	80634.83	76138.95	72239.36	3899.59	8395.46	5.12	10.38

and algorithm DU-2 for all instances of three different groups.

From the above analysis, we can observe the following:

(1) Algorithm DU-2, based on "first-arrive-first-process" method, is easy for operation. The manager of the new retail enterprise merely processes the orders according to the arrival sequence, and the distribution cost and delivery time can be relatively high.

(2) Compared to DU-2, DU-1 takes the departure time of each job into consideration and results in a lower total order delivery time and delivery cost. This algorithm may be run in the development stage of optimizing the operation: the manager outsources the distribution to 3PL companies and focuses on the departure times and distribution costs of orders. However, when the customers receive their orders, it is out of control, and the manager has no idea of the customers' satisfaction level.

(3) Compared to DU-1, algorithm DU-GA takes both order delivery time and delivery cost into consideration. The manager determines orders' picking and delivery as a whole and can monitor the customers' satisfaction level and total delivery cost at the same time.

DU-2, DU-1, and DU-GA represent the degrees of attention to order picking and distribution at different stages:

(1) DU-2 indicates the initial stage of enterprise establishment, and the variety of goods and the number of customers are relatively small. Therefore, the enterprise starts processing orders as soon as receiving them.

(2) DU-1 represents the development stage of the enterprise. As the scale of business becomes larger, the number of orders increases. At this stage, the new retail enterprises may cooperate with 3PL companies; thus, the business managers only need to arrange the production to ensure orders' departure times.

(3) DU-GA indicates a stable period after expansion. New retail enterprises start to focus on lean management of operation. They build their own logistics instead of resorting to 3PL companies. Hence, they need to jointly consider orders' picking and distribution.

6. Summery and Prospects

Based on the characteristics of orders' picking and delivery in new retail enterprises, this paper builds a joint scheduling and distribution model. An MP model is established for a fundamental case, and we devise a genetic algorithm as well as comparison algorithms. The results of computational experiments show the rationality of the model and the effectiveness of the algorithms. Furthermore, we simulate different practical situations to verify the applicability and performance of the algorithm. It is shown that our genetic algorithm is stable and outperforms comparison algorithms.

Our study provides management insights, showing that joint scheduling algorithms can significantly improve the efficiency of order picking and distribution in new retail enterprises. Reasonable coordination of order picking and distribution can effectively reduce business operation costs and improve customer satisfaction.

The research in this paper can be further extended, such as cases with more than three types of suborders and different types of vehicles. The research model in this paper is an offline scheduling problem, and future research can consider online problems.

Data Availability

The data used to support the findings of this study are included within the article.

Conflicts of Interest

The authors declare that there are no conflicts of interest in this paper.

Acknowledgments

References

[1] R. de Koster, T. Le-Duc, and K. J. Roodbergen, "Design and control of warehouse order picking: a literature review," *European Journal of Operational Research*, vol. 182, no. 2, pp. 481–501, 2007.

[2] L. Ning, H. B. Zhang, and B. Zhang, "Optimizing the storage location assignment in a JIT-oriented parts distribution center," *Journal of Management Sciences in China*, vol. 17, no. 11, pp. 10–19, 2014, in Chinese.

[3] F. Y. Chen, H. W. Wang, C. Qi, and Y. Xie, "Routing method for multiple order pickers with congestion consideration," *Journal of Systems Engineering*, vol. 28, no. 5, pp. 581–591, 2013, in Chinese.

[4] X. P. Wang, J. Zhang, and J. Ma, "E-commerce on-line order batching model and algorithm: considering due time," *Journal of Management Science*, vol. 27, no. 6, pp. 103–113, 2014, in Chinese.

[5] J. Zhang, F. Liu, and J. Tang, "The online integrated order picking and delivery considering Pickers' learning effects for an O2O community supermarket," *Transportation Research Part E: Logs and Transportation Review*, vol. 123, pp. 180–199, 2019.

[6] M. Li, Y. H. Wu, N. N. Chen, and J. Zhang, "Items assignment optimization for array automated picking device based on serial order accumulation," *Computer Integrated Manufacturing Systems*, vol. 22, no. 9, pp. 2127–2134, 2014, in Chinese.

[7] D. Q. Wang, "Research on optimizing distribution route of single-center logistics under new retail mode," *Journal of Fuzhou University (Natural Science Edition)*, vol. 47, no. 5, pp. 695–699, 2019, in Chinese.

[8] L. H. Wu, *Research on Fresh Produce Distribution Mode Decision of Retailer's Online Channel*, Beijing Jiaotong University, Beijing, China, 2017, in Chinese.

[9] X. P. Wang, J. Zhang, and C. Y. Yi, "Integrated scheduling of order picking and delivery under B2C E-commerce," *Chinese Journal of Management Science*, vol. 24, no. 7, pp. 101–109, 2016, in Chinese.

[10] W. X. Peng, *Research on Fresh Produce Distribution Mode Decision of Retailer's Online Channel*, Wuhan University of Technology, Wuhan, China, 2017, in Chinese.

[11] J. Zhang, X. Y. Zhang, and Y. F. Zhang, "A study on online scheduling problem of integrated order picking and delivery with multizone vehicle routing method for online-to-offline supermarket," *Mathematical Problems in Engineering*, vol. 2021, Article ID 6673079, 2021.

[12] N. G. Hall and C. N. Potts, "Supply chain scheduling: batching and delivery," *Operations Research*, vol. 51, no. 4, pp. 566–584, 2003.

[13] Z. L. Chen, "Integrated production and outbound distribution scheduling: review and extensions," *Operations Research*, vol. 58, no. 1, pp. 130–148, 2010.

[14] W. Y. Zhong, Z. L. Chen, and M. Chen, "Integrated production and distribution scheduling with committed delivery dates," *Operations Research Letters*, vol. 38, no. 2, pp. 133–138, 2010.

[15] B. Fu, Y. Huo, and H. Zhao, "Coordinated scheduling of production and delivery with production window and delivery capacity constraints," *Theoretical Computer Science*, vol. 422, pp. 39–51, 2012.

[16] C. A. Ullrich, "Integrated machine scheduling and vehicle routing with time windows," *European Journal of Operational Research*, vol. 227, no. 1, pp. 152–165, 2013.

[17] F. S. Al-Anzi and A. Allahverdi, "An artificial immune system heuristic for two-stage multi-machine assembly scheduling problem to minimize total completion time," *Journal of Manufacturing Systems*, vol. 32, no. 4, pp. 825–830, 2013.

[18] D. E. Goldberg, "Genetic algorithms in search," *Optimization, and Machine Learning*, Addison-Wesley Pub. Co., Boston, MA, USA, 1989.

Research Article

Service Quality Evaluation of Terminal Express Delivery Based on an Integrated SERVQUAL-AHP-TOPSIS Approach

Panpan Ma [iD]**, Ni Yao, and Xuedong Yang**

College of Computer and Communication Engineering, Zhengzhou University of Light Industry, Zhengzhou, China

Correspondence should be addressed to Panpan Ma; mapanpan128@163.com

With the rapid development of e-commerce and information technology, the express package volume in the Chinese market keeps an explosively increasing tendency. Terminal delivery plays a significant role on the business and reputation promotion of express brand. To identify the service quality of delivery service, an integrated SERVUQAL-AHP-TOPSIS approach is developed to evaluate the quality of service (QoS) of the city express industry. Firstly, the QoS criteria system is established through SERVQUAL-based dimensions. Secondly, the AHP method is employed to derive the relative weights of criteria. Then, the two stages are embedded into the TOPSIS steps to evaluate the service quality of the express alternative. An application case study is conducted following the detailed steps of the proposed integrated decision-making framework, and results demonstrate the effectiveness and validity of the proposed approach on the QoS of terminal delivery evaluation problem.

1. Introduction

During the last decade, consumers prefer to buy goods from the online shop, contributing to the development of e-commerce. For instance, it has become a prevailing tendency to purchase commodity from Taobao, Jingdong, and other e-shops. With the rapid development of the e-commerce and online shopping, the express industry is motivated by the increasing promotion of this circumstance, and consumers show higher expectations on the logistics service of online consumption [1].

With the soaring increase of e-commerce transaction volume, the express parcel keeps an increasing tendency. For instance, the number of packages in 2019 had reached 60 billion, providing career opportunity and job vacancies for new graduates and practitioners. Different with other business activities in e-commerce, the logistics operation has been paid much attention due to it being a bottleneck activity. With the development of advanced information technologies and logistics techniques, the operational efficiency of logistics has been improved, as well as innovation management practice on logistics mode [2, 3].

Terminal delivery, regarding as the crucial process of the city logistics, plays great significance in the logistics service [4]. Terminal delivery of the express logistics is the process interacting with customers directly, and the service conditions at this phase play a great role on the logistics brand. Regarding the final link of the online shopping, the unsatisfied experience of the logistics service will exacerbate the catastrophic damage of the express brands. In practice, the last mile service and terminal delivery are not satisfied as required in Chinese express industry. There are increasing troubles occurring regarding terminal delivery of logistics service, especially during the online shopping scenarios. For instance, the unsatisfied service attitude, irregular distribution tasks, and low delivery efficiency contribute to the unsatisfied perception of online shopping consumers. The cargo damage, inaccurate delivery, and massive express volume lead to the uneven service quality during the last mile delivery. It is very common that express terminal sites usually employ extra staff to satisfy the soaring package delivery during the rush time intervals, such as at June 18 and double 11. The busy delivery tasks may lead to the unsatisfactory attitudes towards customers, and the irregular

business operation causes the low efficiency. Under this circumstance, online shopping consumers need to suffer the delay logistics distribution and the barely satisfied service attitude [5].

To improve logistics efficiency of the express delivery, many academic researches and practical applications are studied and implemented. There are a vast majority of publications that have been published focusing on city distribution mechanism and VRP optimizations in express logistics industry. The joint distribution mode is emphasized and crucial technologies of this novel operation are addressed to improve the transportation efficiency. To promote the joint distribution mode, Li studied the profit allocation mechanism of the joint alliance [6]. The innovative VRP applications and distribution modes contribute to efficiency improvement of express delivery [3,6]. The double service including home delivery and customers' pick-up are taken into consideration during the VRP optimization [7,8]. Zhou [9] developed a novel nonlinear programming model to assist logistics managers to find an optimal integrated location-routing solution by an improved GA algorithm, and the numerical case showed that it can improve the efficiency of last mile delivery by the formulated model. Li [10] designed an improved ant colony optimization algorithm to improve the logistics efficiency under multidepot scenario. In addition, various uncertain variables are taken into account to address uncertain factors during VRP issues [11–14]. The formulated programming models and designed algorithms contribute to the cost reduction and logistics efficiency improvement [12].

Many last mile delivery researches and applications focused on objectives of low cost and high service efficiency, while ignoring the service quality indicator of the logistics brands. Different with these obvious subobjectives, it is difficult to measure the quality performance of logistics operations compared with cost and transportation time indices. However, with the increasing service requirements, more online shopping consumers start focusing on the consumption experience, which is greatly affected by terminal distribution. Therefore, the QoS is measured and considered as an important optimization goal for logistics problem [9, 15, 16]. In traditional production logistics scenarios, quality performance of logistics activities is usually described by delivery time, accuracy of transported goods, and traceability.

With the booming development of online shopping, the quality of logistics service plays a significant role on consumers' experiences. It is because the logistics service provider becomes the the person who directly contacts with online consumers, instead of salesman or the merchant. Terminal distribution, regarding as the final process of e-commerce logistics service, is the link of direct communication with online shopping consumers. The investigation of customers' experience on its products will assist logistics enterprises to better understand the service they provided [17]. The QoS of terminal distribution not only affects the customers' experience of online shopping, but also influences the brand reputation and further promotion.

However, the last mile service is the direct process of logistics activities, which will be a double-edged sword for

organizations [3]. If customers could feel a better distribution service, it helps to win favor on logistics brand, while if consumers have a bad face-to-face experience, it will lead to negative comments. Those customers even share the unsatisfied experience to potential consumers around them. To the state of the art, there is little QoS evaluation practice for terminal distribution under the online shopping scenario. Therefore, we shift our eyes to quality-of-service study since it faces customers directly during terminal delivery process. Considering the great significance of terminal distribution on logistics experience, an integrated MCDM model is developed from SERVQUAL viewpoint to fill the gap, contributing to achieving QoS evaluation and continuous improvement of logistics brands.

The remainder of this research is structured as follows. In Section 2, we present a literature review on the terminal distribution of the express industry and service quality models. Then, an integrated SERVQUAL-AHP-TOPSIS approach is developed to realize the QoS of terminal distribution evaluation in Section 3. Subsequently, a case study is presented to validate the proposed approach. Finally, we close this research with some conclusions.

2. Literature Review

2.1. Terminal Distribution. The online shopping logistics driven by e-commerce business and advanced technologies has been focused by researchers and practitioners [1, 18]. Terminal distribution, as the final process of product delivery from the merchant to consumers, plays a great significant role in logistics experiences. It is also called the last mile delivery, which means the logistics activity delivering goods to online shopping customers. The increasingly prevailing online shopping experience requires a shorter logistics time and better delivery service [19, 20].

Compared with previous stages of logistics activities, the terminal distribution faces a more challenging situation due to the large scales of customers, varied positions, discrepant demands, and uncertain quantity. Besides, the multichannel delivery has increased the complexity of terminal distribution. The distribution way based on regional locations cannot meet the distribution tasks with a balanced operational efficiency. Therefore, the joint distribution has been introduced to improve operational efficiency of logistics activity by resources sharing and designed mechanisms [3].

The academic research and practical application on terminal distribution of city logistics mainly occur in urban communities, local organizations, and universities for the numerous online shopping requirements. It has become an indispensable part of daily life. Taking the terminal distribution in university campus as an example, almost every logistics service firm has its service dot and serves for faculties' delivery demands [8]. The research area regarding terminal distribution mainly focuses on depot layout, vehicle routing programming, storage optimization, multimodal transportation, stakeholders coordination, and service quality study [9, 10,14, 21, 22]. Joint distribution and innovative cloud distribution are studied by developed regions to improve the operational efficiency of terminal

distribution. Besides, the advanced information technologies are also employed to guarantee the accuracy and safety of last mile service under online shopping atmosphere [3]. The cloud logistics and lean logistics practices also contribute to efficiency improvement [16].

There are several terminal distribution modes, such as self-operated shop, supermarket mode, stall mode, self-service express cabinet, and home delivery service. These different terminal distribution modes are embedded into traditional VRP or logistics network design or optimization problems regarding last mile distribution. Laura [13] proposed a heuristic framework combined Monte Carlo simulation with a heuristic algorithm to deal with the multidepot vehicle routing problem considering constrained capacity and stochastic requirements. Zhou [21] studied a joint problem considering multiple delivery depots and VRP optimization by formulating a nonlinear programming model, which is resolved by a proposed hybrid multipopulation genetic algorithm. Li [10] formulated a multidepot green VRP programming model whose targets are revenue maximization, and cost/time/emission minimization. And an improved ant colony optimization technique was developed to improve the efficiency of the heuristic algorithm.

Apart from the cost, time indices of logistics service, the service quality is also regarded as an important optimization objective. However, the QoS evaluation is the prerequisite of the programming model of terminal distribution. There are many multicriteria decision-making methods having been widely used for logistics performance evaluation, for instance, SERVQUAL, LSQ model, AHP, and VIKOR approaches [23–27]. However, the QoS evaluation model regarding terminal distribution process is little in previous publications and practices, and this study tries to shift our eyes to the service quality evaluation on terminal distribution since its great significance on customers' experience.

2.2. Service Quality Model.

Service quality as a hot topic has been focused and studied by academic researchers and practical managers. It has been a major factor for the triumph of e-commerce and organizational brand [17,28]. To assist industrial managers to probe into the performance of organizational service and production function, quality of service (QoS) evaluation application has been developed in different industrial sectors.

Consumers' feedback, regarding as the evaluation information, has provided enough evidence on QoS identification [29]. In addition, expert-based techniques also offer an effective way to discover the current status of organizational service. Sari [30] studied the significant factors in terms of yachtsmen's satisfaction and extracted the six service quality criteria from the ten QoS dimensions to perform quality measurement and scale of the marina service. Wong [31] proposed a service quality model of urban taxis by employing a level-of-service (LOS) standard, contributing to improving publics' better understanding on taxis service situation. Tuzkaya [32] developed an IVIF-PROMETHEE model to measure healthcare service quality, and the interval valued intuitionistic fuzzy set (IVIFS) is used to describe the ambiguity of healthcare information. Hsu [33] applied KANO quality dimensions to evaluate service quality of community buying by integrating e-commerce information with electronic service quality scales.

Jafar [34] developed a QoS evaluation model for container terminal operations from the SERVQUAL dimensions, and specific ranking of all alternatives contributes to determination of industrial managers. Kim [35] proposed a service quality evaluation model for urban rail transfer facilities considering subjective perceptions of transit people, and the Rasch analysis was employed to estimate the "goodness of fit" between difficulty and individual's ability.

Both investigated consumers' data and unstructured textual comments could help industrial managers to identify functional quality and service satisfaction of objective alternatives. Apart from structured consumers' feedbacks and investigated experts' opinion, the speech analytics is also used for the QoS model to improve service quality of pharmaceutical supply chain service providers [36]. Based on the proposed 17 quality key performance indicators (KPIs), a scored-card approach was employed to perform QoS evaluation. Textual comments generated by consumers provided new broad information datasets about service quality by using data mining techniques. Luis [37] studied the airport service quality by using user generate content (UGC) and sentiment analysis method based on collected tweets in social media. Zhou [29] developed a big data-based analytical method to evaluate the vehicle product and service level in terms of online unstructured comments. Google reviews had been proven to be alternative data source for evaluating quality of service for airline industry, and the sentiment analysis and topical modeling technique were integrated to probe into the assessment of traveler consumers [38].

The negative decision information also can be regarded as the decision information for QoS study. Negative online reviews from social media are extracted to evaluate museums' service failure, and twelve service quality indicators are identified and highlighted [39]. To assist discovering the performance gaps of their products, according to the feedbacks of after-sales service systems, the quality improvement priority index was proposed and developed to identify pilot objective for further improvement [40, 41]. Through the evaluation model and proposed index, industrial managers could perform strategic plans and quality actions to achieve product function improvement and brand reputation promotion.

The SERVQUAL scale is widely used to measure quality of service in different sectors for better understanding service status and consumers' requirements of individual organizations. Alex [42] developed a service assessment model to evaluate the perceived quality of financial service conducted at a unit of a credit union. To better identify service quality attributes of Airbnb and probe into specific influences of QoS attributes on customer satisfactions, the mixed approach was developed to discover significant service quality attributes [43]. The SERVQUAL scales for QoS evaluation of different industries are summarized in Table 1.

Industrial sector	QoS scales and dimensions	Sources
Marina services	Tangibles, reliability, responsiveness, credibility, understanding, competence, courtesy, security, access, communication	[30]
Airline industry	Tangibility, reliability security and safety, responsiveness, assurance, effective communication, addition features, ticket pricing	[44–47]
Hospital service	Interaction, technology, time-dependence, physical quality, tangibility, reliability, responsiveness, assurance, empathy	[32,48]
Urban taxis	Time costed, punctuality, facilities, comfort level, attitude, ethical conduct	[31,49]
Financial sector	Tangibles, reliability, responsiveness, assurance, empathy	[42]
Container terminal operation service	Tangibles, reliability, responsiveness, assurance, empathy	[34]
E-commerce service	Site organization, platform responsiveness and agility, legal protection, trustworthiness	[50]
Urban rail transfer facilities	Information provision, mobility convenience, comfort, convenience of facilities, safety, and security	[35]
Accommodation industry	Host service quality, web responsiveness quality, web efficiency quality, facility service quality	[43]
Online shopping	Kano dimensions: attractive, one-dimensional, must-have, nondifferentiating, reverse quality	[33]
Community pharmacy	Health and medicines advice, nonprescription service, relationship quality, technical quality, environmental quality, health outcomes	[51]
Transit service of rail stations	Security, cleanliness, maintenance, integration with other transit systems, facilities for disabled, information	[52]

For QoS of terminal distribution evaluation, traditional logistics indexes could be employed to assess service quality, such as order accuracy, timely service, and intactness of purchased goods [8, 53]. Apart from the specific logistics attributes and terminal distribution metrics, SERVQUAL scales also can be cited to assist to evaluate the QoS of last mile distribution.

3. Methodology

To realize the service quality evaluation of terminal express distribution under online shopping atmosphere, the hybrid SERVQUAL-AHP-TOPSIS approach is integrated to assess the express alternatives. This section presents the integrated approach, as well as the implementation steps. The integrated SERVQUAL-AHP-TOPSIS approach is described in Figure 1.

3.1. Criteria Development by SERVQUAL Dimensions.
The SERVQUAL measurement scales have been widely used in terms of the QoS evaluation for different sectors. There are five dimensions contained in this service quality model, reflected by specific indicators for different industrial scenarios. The five criteria and specific meaning in the express terminal delivery industry are summarized in Table 2.

The Likert five scale scoring system is applied to collect the source data, illustrated in Table 3 [54]. And the specific value reflects the degree of the agreement on the criteria description.

The perceived score in terms of each SERVQUAL dimension is calculated by the following equation:

$$SQ_i = (PI_i - EI_i), \qquad (1)$$

where SQ means the perceived service quality subjecting to each criterion, PI is the average score with respect to criteria i from investigated consumers, and EI means the expect score

of each criterion ($i = 1, 2, ..., n$). There are five criteria reflecting the QoS of express terminal industry; that is, $n = 5$.

Due to the discrepancy of each individual customer, the weight of each specific meaning is different. Therefore, the weighting average operation is conducted to obtain the overall score of each alternative subject to specific criteria, found in the following equation:

$$SQ_i = \sum_{j=1}^{J} \beta_j \left(PI_{ij} - E_{ij} \right), \qquad (2)$$

where β_j is the relative criteria of each detail meaning, j represents the investigated consumer, and the average SERVQUAL score of each individual consumer is calculated by the following:

$$\text{score} = \left(\sum_{i=1}^{n} \frac{SQ_i}{n} \right). \qquad (3)$$

3.2. AHP-Weighting Method.
As the QoS evaluation of terminal delivery from the consumer-oriented SERVQUAL dimensions, a subjective weighting method called AHP is employed to derive the weights of established criteria. AHP method, proposed by Prof. Saaty, has been proven to be a powerful technique on decision-making problems by decomposing the complex issue into a multilevel hierarchical structure with various criteria [55]. The criteria weight is obtained by the pairwise comparison and is well documented in the previous literature [56, 57]. The detail implementation steps are presented as follows.

Step 1: problem and the objective definition: in this research, the five criteria based on SERVQUAL dimensions are addressed, and the objective in this stage is to determine the relative weight of each SERVQUAL criteria.
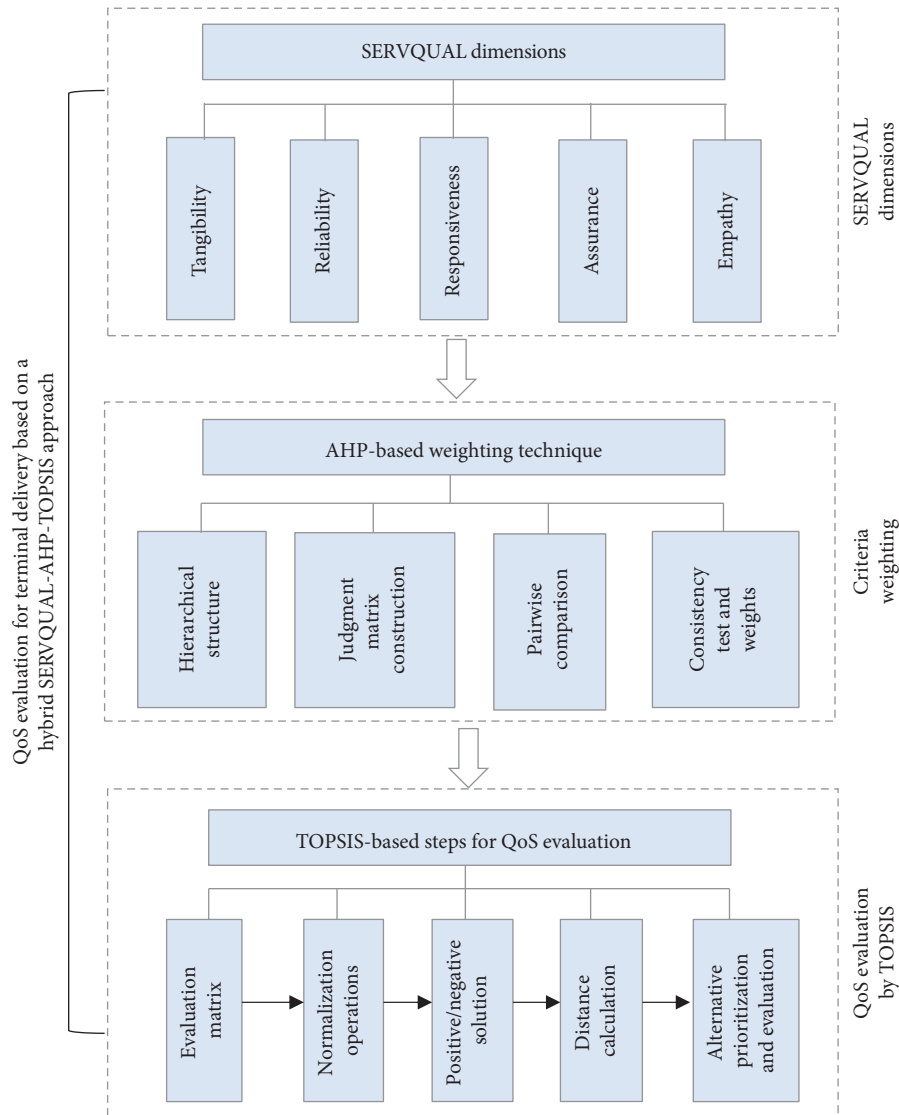
Figure 1: Implementation steps of the integrated SERVQUAL-AHP-TOPSIS approach.

Table 2: Criteria developed based on SERVQUAL dimensions and specific meanings.

Dimension	Criteria	Specific meanings in express terminal delivery
Tangibility (D1)	C1	There are modern terminal delivery facilities
	C2	The service facility with great attractiveness
	C3	The faculty has neat wearing
	C4	The facilitates match the services they provide
Reliability (D2)	C5	The company can deal with the order as required
	C6	The staff can help consumers when they are in trouble
	C7	The company is reliable and trustworthy
	C8	The company can finish the promised service on time
	C9	The order can be recorded correctly in confidential
Responsiveness (D3)	C10	The company has a precise time span about the service
	C11	The service providers could offer the required service timely
	C12	The staff is happy to assist customers
Assurance (D4)	C13	The staff is trustworthy with good reputation
	C14	Customers have a good experience during the transaction
	C15	The staff is polite and patient
	C16	The staff can get support from the company, providing better service
Empathy (D5)	C17	The company can provide personalized service specifically
	C18	The staff can give individual care
	C19	The staff can understand the customers' demands, and interests of customers have the highest priority

TABLE 3: The 1–7 scoring scale rule.

Score	1	3	5
Meaning	Unagree	Agree	Absolutely agree

Step 2: employ the pairwise comparison matrices for each of two criteria in terms of the QoS evaluation. The Saaty 1–9 scale is adopted for the pairwise comparison, illustrated in Table 4 [58].

Step 3: undertake the consistency test through equation (4).

Step 4: the relative weight calculation of each criterion through each pairwise comparison.

3.3. TOPSIS Ranking Steps.
To prioritize the QoS of terminal delivery subjecting to multiple SERVQUAL criteria, the comprehensive evaluation based multicriteria decision-making technique is usually adopted, such as VIKOR and TOPSIS method. In this study, the TOPSIS technique is employed to achieve the QoS evaluation by measuring and integrating the evaluation value of each alternative x_{ij} in terms of the specific criteria. The TOPSIS steps are similar to previous applications as follows [59].

Step 1: determination matrix establishment: the decision information of each alternative subject to established criteria is denoted as x_{ij}, and the matrix is found in the following equation:

$$p = \left(x_{ij}\right)_{m \times n} = \left\{ \begin{matrix} x_{11} & x_{12} & \cdots & x_{1n} \\ x_{21} & x_{22} & \cdots & x_{2n} \\ \vdots & \vdots & \vdots & \vdots \\ x_{m1} & x_{m2} & \cdots & x_{mn} \end{matrix} \right\}. \tag{4}$$

Step 2: normalize the decision matrix by the standardization operation. There are two operations in this step, including homogeneity and normalization in (5) and (6), respectively, the first of which makes all criteria homogeneous; that means the larger the better or the less the better, and the second of which aims at the similar measurement scale.

$$x_{ij}' = \begin{cases} x_{ij}, & \text{the more the better criterion,} \\ \dfrac{1}{x_{ij}}, & \text{the less the better criterion,} \end{cases} \tag{5}$$

$$r_{ij} = \frac{x_{ij}'}{\sqrt{\sum_{i=1}^{m} x_{ij}^2}}, \tag{6}$$

where the transformed criteria x_{ij} will become the homogeneous type; namely, the more the better one. The normalized matrix integrating the weighting vector will become

$$V = \mathbf{R} * \mathbf{W} = \left\{ \begin{matrix} w_1 r_{11} & w_2 r_{12} & \cdots & w_n r_{1n} \\ w_1 r_{21} & w_2 r_{22} & \cdots & w_n r_{2n} \\ \vdots & \vdots & \vdots & \vdots \\ w_1 r_{m1} & w_2 r_{m2} & \cdots & w_n r_{mn} \end{matrix} \right\}. \tag{7}$$

Step 3: determine the positive and negative ideal solution subject to each criterion from all alternatives. The calculation formula is found in equations (8) and (9) in terms of different types, respectively.

$$A^+ = v_1^+, v_2^+, \ldots, v_n^+,$$
$$= \left(\max v_{ij} | j \in J_1\right), \left(\min v_{ij} | j \in J_2\right) (i = 1, 2, \ldots, m), \tag{8}$$

$$A^- = v_1^-, v_2^-, \ldots, v_n^-,$$
$$= \left(\max v_{ij} | j \in J_1\right), \left(\min v_{ij} | j \in J_2\right) (i = 1, 2, \ldots, m), \tag{9}$$

where J_1 is the beneficial criteria (the more the better) and J_2 is the cost attributes (the less the better).

Step 4: the distance of alternatives from the positive and negative one is calculated by equations (10) and (11).

$$D^+ = \sqrt{\sum_{j=1}^{n} \left(v_{ij} - A^+\right)^2}, \tag{10}$$

$$D^- = \sqrt{\sum_{j=1}^{n} \left(v_{ij} - A^-\right)^2}. \tag{11}$$

Step 5: the relative closeness RC_i is derived based on the distance formula, illustrated in the following equation:

$$RC_i = \frac{D_i^M}{D_i^+ + D_i^-}, 0 \leq RC_i \leq 1. \tag{12}$$

According to the relative closeness value of each alternative, we can prioritize the QoS of express alternative and evaluate terminal delivery. In particular, when $RC_i = 1$, the alternative will be regarded as the best one. The closeness with best solution reflects the performance of the QoS of the alternatives.

4. Case Study

The campus express industry has become the important part in Chinese university daily life. The campus express is a representative application on city express with a vast

TABLE 4: 1–9 scales for pairwise comparison.

Assigned value	Meaning	Detailed explanation
1	Equally important	The two criteria have the equal importance to the QoS
3	Moderately important	The criterion is moderately important over another
5	Strongly important	The criterion is strongly important over another
7	Very strongly important	The criterion is very strongly important over another
9	Extremely important	The criterion is extremely important over another
2, 4, 6, 8	Intermediate value	Used to represent compromise within listed scale above

majority of online shopping consumers. In this section, a practical case of terminal delivery in science campus of Zhengzhou University of Light Industry (ZZULI) is conducted to verify the QoS evaluation model.

4.1. Background and Data Collection.

The university campus is a typical community with a vast majority of online shopping business for gathered faculties and students. The campus has various express terminals with many kinds of self-service cabinets and delivery outlets, including Shunfeng, Jingdong, Rookie Station, and FengNest which serves different express logistics brands (Shunfeng, Jingdong, Yuantong, and Yunda, etc.). In this section, three typical express alternatives are selected as the evaluation objectives, namely, Shunfeng (A1), Jingdong (A2), and Rookie Station (A3). The developed evaluation framework is employed to evaluate the quality of service of terminal delivery for logistics sector. The data is collected from the student consumers in the campus by the designed questionnaire from the viewpoint of SERVQUAL-based dimensions.

A pilot survey was performed before the main survey, and about 20 consumers in campus were investigated to test the survey approach and ensure the word clarity of the questionnaire. The main survey was conducted from September 2020 to February 2021. The total 597 responses were collected by mail, and the overall response rate was about 59.7%. There are two parts in the questionnaire survey: ① the demographic information of e-commerce logistics service users in the campus and ② satisfaction with the terminal delivery. The satisfaction level for each specific criterion was recorded by the Likert five-point scale scoring system [31, 54], where the higher scores represent a higher satisfaction. The decision-making information was then generated by collecting the investigation data collected from respondents, illustrated in Table 5.

4.2. Results and Comparison Analysis.

Based on the AHP-weighting steps, the comprehensive weight of influenced criteria is calculated with $W = (0.0405, 0.0193, \ldots, 0.0618, 0.0753)$. According to the detail steps of the integrated decision-making framework, the service quality of terminal distribution for objective alternatives is evaluated and calculated in Table 5. In addition, to verify the effectiveness of the proposed integrated decision-making framework, the comparison experiment is performed by exploring VIKOR steps, and the comparison results are found in Table 6 as well. The VIKOR-based method is based on the formula of L_p-metric subjecting multiple criteria in the following:

$$L_{p,i} = \left\{ \sum_{j=1}^{n} \left[\frac{w_j \left(f_j^* - f_{ij} \right)}{f_j^* - f_j^-} \right]^p \right\}^{1/p}, \quad 1 \le p \le +\infty, i = 1, 2, \ldots, m,$$

(13)

where S_1 is the max group utility value, R_i is the minimum individual regret value, and Q_i is the comprehensive utility value. The ranking rules of objective alternatives are similar to previous VIKOR applications and publications [58, 60, 61].

The alternative with higher RC to the ideal solution is regarded as with better quality service; however, candidates with minimum Q value are treated as the best one in VIKOR-based approach. According to the calculated closeness value (RC) of different alternatives, the QoS quality ranking list of terminal distribution is A1≻A2≻A3. From Table 5, the QoS level gets the same ranking result compared with the VIKOR steps. Results show that A1 provides better terminal delivery service compared to other two logistics organizations, and then follows the A2 brand. In addition, the C8, C9, C11, C14, and C17 index have higher criteria weight (0.097, 0.077, 0.081, 0.085, 0.093), and A1 has a good performance on these sectors. That is why A1 outperforms the other two brands and gets the first ranking regarding terminal delivery link. It is noteworthy that consumers in ZZULI campus tend to focus on the on-time and personalized service, and the good experience is also significant in terms of terminal delivery link. To improve the terminal delivery service, it is vital to conduct some countermeasures to make sure the punctuality of terminal delivery. Also, the flexibility of terminal delivery can be improved; for instance, the delivery time can be adjusted based on the school time. Logistics company should also pay much more attention to the professionalism cultivation for terminal delivery staffs, and improve consumers' loyalty by providing better delivery service and hospitality experience.

4.3. Theoretical Implications and Managerial Insights.

This research serves both scientific and practical contributions to domestic logistics industry by providing some theoretical contributions and practical implications regarding terminal delivery.

In this part, we address the theoretical implications to QoS evaluation of terminal delivery and provide practical insights for logistics sector. The theoretical contributions to existing research are twofold. Firstly, the comprehensive index system is constructed based on SERVQUAL dimensions, and specific 19 criteria are addressed to understand

TABLE 5: Decision-making information of investigated three alternative brands.

	C1	C2	C3	C4	C5	C6	C7	...	C18	C19
A1	0.714	0.857	0.857	0.857	0.714	0.714	0.857	...	0.429	0.857
A2	0.714	0.857	0.714	0.714	0.857	0.286	0.857	...	0.429	0.857
A3	0.429	0.571	0.429	0.429	0.429	0.429	0.571	...	0.714	0.429

TABLE 6: Results of objective alternatives.

	The proposed TOPSIS steps				The VIKOR-based approach			
	D^+	D^-	RC value	Ranking	S_i	R_i	Q_i	Ranking
A1	0.067	0.092	0.579	1	0.158	0.054	0	1
A2	0.080	0.081	0.503	2	0.834	0.093	0.461	2
A3	0.087	0.068	0.439	3	0.502	0.097	0.503	3

the QoS of terminal delivery regarding the logistics industry. Secondly, an integrated multicriteria decision-making framework is formulated to evaluate the quality of service of terminal delivery business.

From a managerial point of view, the proposed integrated SERVQUAL-AHP-TOPSIS decision-making framework enables logistics managers to better understand the existing quality service level of terminal delivery. Besides, the questionnaire investigation results also assist industrial managers to identify the advantages or disadvantages during the terminal delivery activity. Meanwhile, the unwelcome items obtained from the industrial case can also provide warning on accurate improvement for better service. It is very important for industrial managers to discover the service gap compared to benchmarking brand. This will help logistics organizations to take effective countermeasures to improve their service level.

Regarding as a significant component of online shopping experience, quality service of terminal delivery has obviously affected the consumers' loyalty and willingness to continuously choosing the same brand. From the viewpoint of logistics consumers, this study provides a decision-making framework to choose a most suitable logistics service provider. The quality service evaluation model also provides a general measurement model for logistics sector regarding terminal delivery business.

5. Conclusions

The rapid development of online shopping and e-commerce motivates the innovation of modern logistics, including concepts, distribution mode, and optimization models. These industrial applications mainly focus on transportation, distribution, inventory, and network activities, while ignoring the theoretical practices in terms of terminal delivery. As the terminal activity of modern logistics, the quality of service in this link is significant to improve organizational reputation since it provides a face-to-face opportunity to logistics consumers. To discover the QoS of terminal delivery, this study provides an integrated SERUQAL-AHP-TOPSIS framework to evaluate the quality of service. Firstly, the evaluation index system including 19 criteria is established from the viewpoint of SERUQAL

dimensions. Secondly, the AHP technique is explored to determine the criteria weight of each indicator. Then, the TOPSIS steps are used to prioritize the QoS level of alternative brands. In addition, the formulated integrated decision-making framework is verified by a practical case in the campus.

Even though the integrated approach provides an effective way to evaluate QoS of terminal delivery activity, there are still some limitations left for future research. Firstly, the influential criteria are constructed based on the basic SERUQAL dimensions, and special index can also be proposed and taken into account based on the regional and cultural discrepancy for different nations. Secondly, the criteria weighting technique is expert-oriented, and the objective-based weighting methods also can be developed by embedding with machine learning techniques. In other words, how to reduce the subjectivity of decision-making by more powerful tools needs to be discussed in the future study. Finally, other MCDM techniques can also be integrated to resolve the QoS evaluation, and the computer-based intelligent technology is also welcome to be embedded with such traditional methods, facilitating the intelligent evaluation.

Data Availability

The data used to support the findings of this study are available from the corresponding author upon request.

Conflicts of Interest

The authors declare that they have no conflicts of interest.

Acknowledgments

References

[1] X. Qin, Z. Liu, and L. Tian, "The strategic analysis of logistics service sharing in an e-commerce platform," *Omega-International Journal of Management Science*, vol. 92, 2020.

[2] A. Rai, P. A. Pavlou, G. Im, and S. Du, "Interfirm IT capability profiles and communications for cocreating relational value: evidence from the logistics industry," *MIS Quarterly*, vol. 36, no. 1, pp. 233–262, 2012.

[3] Y. He, F. Zhou, M. Qi, and X. Wang, "Joint distribution: service paradigm, key technologies and its application in the context of Chinese express industry," *International Journal of Logistics Research and Applications*, vol. 54, pp. 1–17, 2019.

[4] F. A. Tillman, "The multiple terminal delivery problem with probabilistic demands," *Transportation Science*, vol. 3, no. 3, pp. 192–204, 1969.

[5] Y. He, M. Qi, F. Zhou, and J. Su, "An effective metaheuristic for the last mile delivery with roaming delivery locations and stochastic travel times," *Computers and Industrial Engineering*, vol. 145, 2020.

[6] L. Li, X. Wang, Y. Lin, F. Zhou, and S. Chen, "Cooperative game-based profit allocation for joint distribution alliance under online shopping environment," *Asia Pacific Journal of Marketing and Logistics*, vol. 31, no. 2, pp. 302–326, 2019.

[7] Y. He, X. Wang, F. Zhou, and Y. Lin, "Dynamic vehicle routing problem considering simultaneous dual services in the last mile delivery," *Kybernetes*, vol. 10, p. 19, 2019.

[8] F. Zhou, Y. He, and L. Zhou, "Last mile delivery with stochastic travel times considering dual services," *IEEE Access*, vol. 7, pp. 159013–159021, 2019.

[9] L. Zhou, Y. Lin, X. Wang, and F. Zhou, "Model and algorithm for bilevel multisized terminal location-routing problem for the last mile delivery," *International Transactions in Operational Research*, vol. 26, no. 1, pp. 131–156, 2019.

[10] Y. Li, H. Soleimani, and M. Zohal, "An improved ant colony optimization algorithm for the multi-depot green vehicle routing problem with multiple objectives," *Journal of Cleaner Production*, vol. 227, pp. 1161–1172, 2019.

[11] F. Zhou and Y. He, "Research on pallet scheduling model with time windows and uncertain transportation time," *Engineering Letters*, vol. 28, no. 2, pp. 504–509, 2020.

[12] F. Zhou, Y. He, P. Ma, M. K. Lim, and S. Pratap, "Capacitated disassembly scheduling with random demand and operation time," *Journal of the Operational Research Society*, vol. 23, pp. 1–17, 2021.

[13] L. Calvet, D. Wang, A. Juan, and L. Bové, "Solving the multidepot vehicle routing problem with limited depot capacity and stochastic demands," *International Transactions in Operational Research*, vol. 26, no. 2, pp. 458–484, 2019.

[14] A. Almouhanna, C. L. Quintero-Araujo, J. Panadero, A. A. Juan, B. Khosravi, and D. Ouelhadj, "The location routing problem using electric vehicles with constrained distance," *Computers & Operations Research*, vol. 62, Article ID 104864, 2019.

[15] F. L. Zhou, X. Wang, Y. D. He, and M. Goh, "Production lot-sizing decision making considering bottle-neck drift in multi-stage manufacturing system," *Advances in Production Engineering & Management*, vol. 12, no. 3, pp. 213–220, 2017.

[16] F. Zhou, Y. He, L. Deng, and M. Wang, "A novel Bi-level programming model for cloud logistics resources allocation," *Journal of Computers (Taiwan)*, vol. 30, no. 6, pp. 16–30, 2019.

[17] J.-J. Wu, J.-N. Hwang, O. Sharkhuu, and B. Tsogt-Ochir, "Shopping online and off-line? complementary service quality and image congruence," *Asia Pacific Management Review*, vol. 23, no. 1, pp. 30–36, 2018.

[18] J. W. J. Weltevreden, "B2C e-commerce logistics: the rise of collection-and-delivery points in The Netherlands," *International Journal of Retail & Distribution Management*, vol. 36, no. 8-9, pp. 638–660, 2008.

[19] Y.-H. Hsu, "An effective pricing model for the congestion alleviation of e-commerce logistics," *Computers & Industrial Engineering*, vol. 129, pp. 368–376, 2019.

[20] D. A. Guerra-Zubiaga, "Intelligent E-commerce logistics platform using hybrid agent based approach," *Transportation Research*, vol. 126, pp. 15–31, 2019.

[21] D. V. W. X. Zhou Lin and R. Baldacci, "A multi-depot two-echelon vehicle routing problem with delivery options arising in the last mile distribution," *European Journal of Operational Research*, vol. 265, no. 2, pp. 765–778, 2017.

[22] Y. He, X. Wang, Y. Lin, and F. Zhou, "Optimal partner combination for joint distribution alliance using integrated fuzzy EW-AHP and TOPSIS for online shopping," *Sustainability*, vol. 8, no. 4, pp. 341–356, 2016.

[23] D. Pandit, "Determination of appropriate service delivery level for quantitative attributes of household toilets in rural settlements of India from users' perspective," *Environmental Management*, vol. 61, no. 4, pp. 637–649, 2018.

[24] F. T. S. Chan, H. K. Chan, H. C. W. Lau, and R. W. L. Ip, "An AHP approach in benchmarking logistics performance of the postal industry," *Benchmarking: An International Journal*, vol. 13, no. 6, pp. 636–661, 2006.

[25] F. Lei, G. Wei, H. Gao, J. Wu, and C. Wei, "TOPSIS method for developing supplier selection with probabilistic linguistic information," *International Journal of Fuzzy Systems*, vol. 22, no. 3, pp. 749–759, 2020.

[26] M. K. Anser, M. Mohsin, Q. Abbas, and I. S. Chaudhry, "Assessing the integration of solar power projects: SWOT-based AHP-F-TOPSIS case study of Turkey," *Environmental Science and Pollution Research*, vol. 27, no. 25, pp. 31737–31749, 2020.

[27] D. Xu, J. Ren, L. Dong, and Y. Yang, "Portfolio selection of renewable energy-powered desalination systems with sustainability perspective: a novel MADM-based framework under data uncertainties," *Journal of Cleaner Production*, vol. 275, 2020.

[28] S. Roy and S. Bhatia, "Service quality versus service experience: an empirical examination of the consequential effects in B2B services," *Industrial Marketing Management*, vol. 43, 2019.

[29] F. Zhou, M. K. Lim, Y. He, and S. Pratap, "What attracts vehicle consumers' buying: a Staay scale-based VIKOR (SSC-VIKOR) approach from after-sales textual perspective?," *Industrial Management & Data Systems*, vol. 120, no. 1, pp. 57–78, 2020.

[30] F. O. Sari, C. Bulut, and I. Pirnar, "Adaptation of hospitality service quality scales for marina services," *International Journal of Hospitality Management*, vol. 54, pp. 95–103, 2016.

[31] R. C. P. Wong and W. Y. Szeto, "An alternative methodology for evaluating the service quality of urban taxis," *Transport Policy*, vol. 69, pp. 132–140, 2018.

[32] G. Tuzkaya, B. Sennaroglu, Z. T. Kalender, and M. Mutlu, "Hospital service quality evaluation with IVIF-PROMETHEE and a case study," *Socio-Economic Planning Sciences*, vol. 44, 2019.

[33] S.-W. Hsu, F. Qing, C.-C. Wang, and H.-L. Hsieh, "Evaluation of service quality in facebook-based group-buying," *Electronic Commerce Research and Applications*, vol. 28, pp. 30–36, 2018.

[34] J. Sayareh, S. Iranshahi, and N. Golfakhrabadi, "Service quality evaluation and ranking of container terminal operators," *The Asian Journal of Shipping and Logistics*, vol. 32, no. 4, pp. 203–212, 2016.

[35] J. Kim, J.-D. Schmöcker, J. W. Yu, and J. Y. Choi, "Service quality evaluation for urban rail transfer facilities with Rasch analysis," *Travel Behaviour and Society*, vol. 13, pp. 26–35, 2018.

[36] S. Scheidt and Q. B. Chung, "Making a case for speech analytics to improve customer service quality: vision, implementation, and evaluation," *International Journal of Information Management*, vol. 45, pp. 223–232, 2019.

[37] L. Martin-Domingo, J. C. Martín, and G. Mandsberg, "Social media as a resource for sentiment analysis of Airport Service

Quality (ASQ)," *Journal of Air Transport Management*, vol. 78, pp. 106–115, 2019.

[38] K. Lee and C. Yu, "Assessment of airport service quality: a complementary approach to measure perceived service quality based on Google reviews," *Journal of Air Transport Management*, vol. 71, pp. 28–44, 2018.

[39] Y. Su and W. Teng, "Contemplating museums' service failure: extracting the service quality dimensions of museums from negative on-line reviews," *Tourism Management*, vol. 69, pp. 214–222, 2018.

[40] F. Zhou, X. Wang, and A. Samvedi, "Quality improvement pilot program selection based on dynamic hybrid MCDM approach," *Industrial Management & Data Systems*, vol. 118, no. 1, pp. 144–163, 2018.

[41] F. Zhou, X. Wang, Y. Lin, Y. He, and L. Zhou, "Strategic part prioritization for quality improvement practice using a hybrid MCDM framework: a case application in an auto factory," *Sustainability*, vol. 8, no. 6, 2016.

[42] A. F. Duarte, V. R. Moreira, A. A. Ferraresi, and A. Gerhard, "Evaluating credit union members' perception of service quality through service innovation," *RAI Revista de Administração e Inovação*, vol. 13, no. 4, pp. 242–250, 2016.

[43] Y. Ju, K.-J. Back, Y. Choi, and J.-S. Lee, "Exploring airbnb service quality attributes and their asymmetric effects on customer satisfaction," *International Journal of Hospitality Management*, vol. 77, pp. 342–352, 2019.

[44] H. Gupta, "Evaluating service quality of airline industry using hybrid best worst method and VIKOR," *Journal of Air Transport Management*, vol. 68, pp. 35–47, 2018.

[45] C. Prentice and M. Kadan, "The role of airport service quality in airport and destination choice," *Journal of Retailing and Consumer Services*, vol. 47, pp. 40–48, 2019.

[46] C.-H. Lee, X. Zhao, and Y.-C. Lee, "Service quality driven approach for innovative retail service system design and evaluation: a case study," *Computers & Industrial Engineering*, vol. 135, pp. 275–285, 2019.

[47] K. D. Atalay, B. Atalay, and F. B. Isin, "FIPIA with information entropy: a new hybrid method to assess airline service quality," *Journal of Air Transport Management*, vol. 76, pp. 67–77, 2019.

[48] A. Meesala and J. Paul, "Service quality, consumer satisfaction and loyalty in hospitals: thinking for the future," *Journal of Retailing and Consumer Services*, vol. 40, pp. 261–269, 2018.

[49] B. Alonso, R. Barreda, L. Dell'Olio, and A. Ibeas, "Modelling user perception of taxi service quality," *Transport Policy*, vol. 63, pp. 157–164, 2018.

[50] F. Marimon, J. Llach, M. Alonso-Almeida, and M. Mas-Machuca, "CC-Qual: a holistic scale to assess customer perceptions of service quality of collaborative consumption services," *International Journal of Information Management*, vol. 49, pp. 130–141, 2019.

[51] B. Grew, C. R. Schneider, A. Mirzaei, and S. R. Carter, "Validation of a questionnaire for consumers' perception of service quality in community pharmacy," *Research in Social and Administrative Pharmacy*, vol. 15, no. 6, pp. 673–681, 2019.

[52] L. Eboli, C. Forciniti, and G. Mazzulla, "Spatial variation of the perceived transit service quality at rail stations," *Transportation Research Part A: Policy and Practice*, vol. 114, pp. 67–83, 2018.

[53] Y. Yang and C. Huang, "DC fault location in multi-terminal DC distribution network based on voltage similar triangle principle," *Electric Power Systems Research*, vol. 184, Article ID 106306, 2020.

[54] F.-L. Zhou, X. Wang, Y. Lin, Y.-D. He, and N. Wu, "Influence research of multi-dimensional tech-innovation behavior on tech-innovation performance," *International Journal of Innovation Science*, vol. 8, no. 2, pp. 148–160, 2016.

[55] G. Büyüközkan and G. Çifçi, "A novel hybrid MCDM approach based on fuzzy DEMATEL, fuzzy ANP and fuzzy TOPSIS to evaluate green suppliers," *Expert Systems with Applications*, vol. 39, no. 3, pp. 3000–3011, 2012.

[56] S. K. Mangla, P. Kumar, and M. K. Barua, "Risk analysis in green supply chain using fuzzy AHP approach: a case study," *Resources, Conservation and Recycling*, vol. 104, pp. 375–390, 2015.

[57] F. Zhou, Y. Lin, X. Wang, L. Zhou, and Y. He, "ELV recycling service provider selection using the hybrid MCDM method: a case application in China," *Sustainability*, vol. 8, no. 5, 2016.

[58] D. Prajapati, F. Zhou, M. Zhang, H. Chelladurai, and S. Pratap, "Sustainable logistics network design for multi-products delivery operations in B2B e-commerce platform," *Sādhanā*, vol. 46, no. 2, pp. 1–13, 2021.

[59] Y. He, X. Wang, Y. Lin, F. Zhou, and L. Zhou, "Sustainable decision making for joint distribution center location choice," *Transportation Research Part D: Transport and Environment*, vol. 55, pp. 202–216, 2017.

[60] S. Opricovic and G.-H. Tzeng, "Compromise solution by MCDM methods: a comparative analysis of VIKOR and TOPSIS," *European Journal of Operational Research*, vol. 156, no. 2, pp. 445–455, 2004.

[61] F. Zhou, X. Wang, M. K. Lim, Y. He, and L. Li, "Sustainable recycling partner selection using fuzzy DEMATEL-AEW-FVIKOR: a case study in small-and-medium enterprises (SMEs)," *Journal of Cleaner Production*, vol. 196, pp. 489–504, 2018.

Research Article

Does Airport Preferential Policy Aggravate the Competition of Aviation Hubs in Central and Western China? Based on the Investigation of 78 Airports

Chengyu Li [iD],[1] **Xiangwu Yan** [iD],[2] **Yanbing Zhang,**[2] **Ning Xu,**[3] **Jin Chen,**[4] **and Guangliang Zhou**[5]

[1]*Industry & Innovation Research Center, Zhengzhou University of Light Industry, Zhengzhou, China*
[2]*School of Economics & Management, Zhengzhou University of Light Industry, Zhengzhou, China*
[3]*School of Tourism, Xinyang Normal University, Xinyang, China*
[4]*School of Humanities & Law, Jiangxi Institute of Economic Administrators, Nanchang, China*
[5]*Social Science Management Department, Zhengzhou University of Light Industry, Zhengzhou, China*

Correspondence should be addressed to Xiangwu Yan; xiangwu.yan@zzuli.edu.cn

China's regional economic competition is intensifying; in particular, the cluster development of air transport, high-end manufacturing, and modern service industries is closely related to the construction of regional airports. Local governments have listed aviation hubs as the hardcore advantage of high-quality growth in the new era, but it may also lead to excessive convergence and preferential system competition. Based on the "GDP competition" of local governments in China, this paper uses panel data of 78 airports in mainland China from 2001 to 2018 and tries to explore the causes of airport preferential policies. The Synthetic Control Method is used to study the influence of preferential policies on airport passenger and cargo flow, and then the Spatial Durbin Model is used to verify the spatial spillover effect of aviation hubs, which may be magnified by the preferential policies. This paper finds that the impact of preferential policies on airports in central and western China is mainly reflected in the increase of cargo throughput, and there is a spatial siphon effect on cargo throughput between airports. The implementation of the preferential policy enhances this spatial siphon effect, which in turn leads to more fierce competition. The research results show that the preferential policies, issued in central and western aviation economy, have shown a trend of evolving in the direction of vicious competition. Before the airport preferential system produces more negative effects, it should be corrected in time, and each aviation economic zone in the central and western regions should be scientifically coordinated and reasonably planned.

1. Introduction

In recent years, many aviation hub cities in central and western China have put forward plans to speed up the construction of airport economic zones or aviation metropolises, and various governments have issued various preferential policies to support the construction of airports and routes. However, judging from the service scope of the airport economic zone, after the completion of the airport economic zone, there will be certain exclusiveness within the 800-kilometer area, and the intensive construction of the

aviation economic zone in central and western China may lead to the problems of convergence competition and malicious suppression [1].

The construction of airports is usually closely related to the regional economy. Local governments generally attach great importance to investment in local airport infrastructure and adopt preferential policies to speed up the development of the regional airport economy. However, there have always been two opposing views on whether airports and airlines should be subsidized for a long time. Some scholars believe that the long-term subsidy for airports

violates the principle of fair competition, which will lead to inefficiency of airports under local protection and make the local airport never find its accurate position in the existing large international airport competition, so it will never make a profit [2, 3]. Some studies have also confirmed that if regional government subsidies are stopped, almost all German airports will not be able to make up for their annual losses [4]. Another point of view is that we should not only pay attention to the direct loss or profit of regional airports while ignoring their promoted effect on the regional economy. The evidence of airport areas, especially airports in the United States, emphasizes the huge positive impact of airport spillover effects on the surrounding economy [5–7]. European Low-Fare Airline Association also pointed out that the rapid development of airports has promoted interregional connectivity, as well as exchanges and prosperity of domestic and international trade [8]. Therefore, although the debate continues, the phenomenon of local government policy support for airport construction is an objective fact, and the economic effect of airport construction is still a hot issue, which needs to be discussed in depth [9].

This paper focuses on whether the preferential behavior of local governments will aggravate the vicious competition of airports in the central and western regions. Therefore, under the background of deepening the market-oriented reform of domestic freight rates of civil aviation, using the panel data of 78 airports in Chinese mainland from 2001 to 2018, we first utilize the Synthetic Control Method (SCM) to study the impact of preferential policies on airport passenger flow and cargo volume. Then, we add spatial related factors to the model to analyze the spatial spillover effect of passenger and cargo flow and then study whether preferential policies will expand this spatial effect. The possible marginal contribution of this paper lies in the following points. First, compared with the existing studies, the capacity of research samples has been greatly expanded, and more consistent and universal conclusions can be drawn. Secondly, through the ranking test, false experiment, and changing spatial matrix, a more robust conclusion is drawn. Thirdly, the SCM is combined with the Spatial Dubin Model (SDM), and the results of the two models confirm each other, which proves that preferential policies will aggravate the siphoning effect of airports, thus leading to more intense and even malicious competition. The conclusion of this paper has important practical significance for rationally planning the aviation economic zone in the central and western regions, exploring the differentiated development, and smoothing the domestic and international double circulation strategy through the aviation industry.

The rest of this paper is arranged as follows. The second part is the literature review. The third part is model setting and data introduction. The fourth part is the empirical study. Firstly, the SCM is used to analyze the impact of preferential policies on aviation economic zones. Then, the spatial spillover effect of the aviation economy is studied by using SDM, and the realization path of preferential policy is studied. The fifth part further discusses the reasons for the emergence of the preferential system. The last part reviews the previous content and puts forward some suggestions on the influence of aviation economic preferential policy.

2. Literature Review

2.1. The Historical Origin and Realistic Influence of Preferential Policies. In the past three decades, the promotion tournament between government officials based on GDP growth is an important source of China's rapid economic growth [10]. Under the incentive of a job promotion, local government officials give preferential policies to specific industries with high returns, so that they can quickly gather production factors, develop rapidly, and improve the regional economic level. In a catch-up economy, local governments can learn from the development experience of other countries to identify high-efficiency industries. However, the catch-up characteristics of the current economy are getting weaker and weaker. The innovative economy has become the main force for future development, and the preferential model is increasingly difficult to achieve good effects [11]. Meanwhile, in the initial stage of economic development, when society believes that economic growth is the first goal, the preferential behavior of the government is acceptable. But, as the economy enters a new stage of development, the nature of government decision-making to protect multi-interests becomes more obvious and the cost of "GDP championship" is increasing day by day. Some factors, such as vicious interregional economic competition and distorted allocation of resources, have become increasingly exposed and begun to restrict economic growth [12].

When the economic environment changes, the preferential model may change from a booster to an obstacle to economic development [11]. Some scholars had studied the return on investment of enterprises, which got more government intervention, and concluded that the return on investment of these enterprises is generally lower than that of common enterprises, which are not affected by government intervention [13, 14]. Particularly, the return on investment of private enterprises is often much higher than that of state-owned enterprises [15, 16]. The deep-seated reason for the situation is that the distorted incentives of the Chinese government and the imbalance of input-output structure lead to the low proportion of the output value of China's service industry [17], and this unreasonable industrial structure further affects the rate of return on investment [18, 19].

From the above analysis, we can find that the implementation of the preferential policy will reduce the rate of return on investment and distort the allocation of resources. For this reason, we put forward the following hypothesis.

H_1. the airport preferential policy will intensify the convergence competition of aviation hubs in the central and western regions of China, which will have a negative impact on the economy.

2.2. Reasons Why Airports Are Targeted by Preferential Subsidies. According to the early theory of regional unbalanced development, the geographical concentration of

economic activities comes from the polarization effect, and the unbalanced distribution of economic activities leads to the unbalanced pattern of regional development. Marshall (1920) used economic externalities to explain the geographical imbalance of economic activities. He noted that economic agglomeration mainly comes from labor market sharing, the scale of intermediate input, and the spillover of knowledge and technology. The development of the aviation economy made it convenient for the labor force, knowledge, and technology to gather in different regions. Cao et al. [20] analyzed the reasons for the formation of the airport economic zone from the perspective of new economic geography, which absorbed the idea of increasing scale returns of the new growth theory, and explored the internal evolutionary process of spatial economic agglomeration based on the assumptions of two departments, two regions, and two elements. They pointed out that airport economic activities are gradually strengthened around the airport, and the development of the airport economy will give feedback to the airport. Under the influence of these factors, the airport becomes the core, and other areas gradually become the periphery, which forms the airport economic zone.

The kind of literature closest to the study is the research on Mixed Oligopoly Model. Early research focused on the impact of competition on social welfare, which happened between state-owned and private enterprises in a closed market or region [21–23]. To safeguard the interests of local enterprises, the government has formulated trade protection policies. Although there are different forms of trade protection, its goal is to reduce the prices of local enterprises and make the prices of nonlocal enterprises relatively higher, thus losing their competitiveness. In central and western China, where traffic is underdeveloped, air transport investment is effective quickly, which can quickly reduce transportation costs on products with high added value and lightweight and accelerate the formation of a center-periphery pattern. So, the local governments have listed aviation hubs as the hardcore advantages of high-quality growth and subsidy objects.

From the above analysis, the reason for the government to implement the preferential policy is to enhance the competitiveness of local airports and then seize more markets. To this end, we propose the following hypothesis

H_2. the airport preferential policy will increase the passenger or cargo throughput of the local airport.

2.3. Spatial Economic Relations of Airports.

In the past, scholars are interested in the impact of the aviation economy on employment [24, 25], population [26], and industry [27, 28]. The aviation economy can accelerate the flow of population and labor capital between regions, improve the local employment situation, and finally promote the upgrading of industrial structure and regional economic transformation. Furthermore, some scholars focused on the causal relationship between airports and regional economic development. Granger test is a common method [1, 29]. However, the test results vary with the change of the test object, so this kind of research does not have universal significance.

With the progress of the theory of new economic geography and spatial econometrics, scholars gradually pay attention to the impact of spatial factors on the airport economy [30]. Generally speaking, the spillover effect of the airport on the regional economy varies with the scale and development stage of the airport [31, 32]. In terms of spatial distribution, the spillover effect of airports in eastern China is much higher than that in the west [33]. In the research on passenger volume and cargo volume, Chen et al. [34] carried out the research from the perspective of airline network and found that passenger volume has a significant positive network spillover effect on the regional economy, the spillover effect is far greater than the direct effect on the area, and freight volume only has a positive impact on the local area.

From the above discussion, most scholars have affirmed the positive impact of the aviation economic zone on the region, and some scholars have drawn some conclusions in the test of subregional and subtransport indicators. However, compared with these literature studies, the research object of this paper is richer and the sample period is longer, which ensures that this paper can draw more consistent and scientific conclusions. To sum up, we propose the following hypothesis.

H_3. the spatial spillover effect of passenger or freight volume of the airport is negative, which shows the siphoning effect in space.

3. Model Setting

3.1. Synthetic Control Method.

The Synthetic Control Method (SCM), proposed by Abadie and Gardeazabal [35], gives weight to different control groups, respectively. Based on these weights, the counterfactual control group of policy intervention individuals is constructed and used to simulate the characteristics of the treatment group before being affected by the policy. The actual value of the treatment group is compared with the composite value, to get the policy treatment effect. SCM uses a data-driven method to give weight to synthetic individuals and calculates the contribution of each synthetic individual to the counterfactual control group, which effectively overcomes the subjective and endogenous problems of sample selection and makes up for the limitations of the Difference in Difference method in policy evaluation. We will use this method to test the effectiveness of the preferential policy.

Since most of the airports in eastern China have been mature and SCM is not suitable for the study of large samples, the research object selected by SCM in this paper is the airports of the provinces and cities in the central and western. The basis of regional division comes from *China Statistical Yearbook* (2019). According to the documents released by the regional governments of the central and western, in 2012, Henan Province took the lead in issuing *Some Policies to Support the Development of the Aviation Logistics Industry in Henan Province* and *Preferential Policies for Henan Province to Support Zhengzhou Xinzheng International Airport to Introduce Base Airlines*. To speed up the construction of Zhengzhou Airport, Henan Province not

only actively strived for preferential policies from the central government but also formulated 20 additional preferential policies, which gave preferential treatment in the aspects of flight subsidy, route development reward, site rental fee reduction, and subsidy, land use, financing, talent introduction, and so on. Therefore, Xinzheng Airport in Zhengzhou becomes the experimental object of this paper. At this time, other airports in the central and western were not affected by the preferential policy or the degree of influence was not as high as Zhengzhou, so they naturally become the control group.

3.2. Spatial Econometric Model.

The setting of the spatial weight matrix is the premise and basis of spatial econometric analysis. Because the airport is a point distribution, it is an appropriate choice to use a distance-based spatial weight matrix, but it has the problem of splitting or weakening the relationship between nonneighbors. For this reason, we draw lessons from the treatment methods of Zhang et al. [36] and Gao [37] and construct a weight matrix based on economic-geographical distance. The expression is as follows

$$M = \frac{1}{d_{ij}} * \frac{1}{\left| \overline{Y}_i - \overline{Y}_j \right|}, \tag{1}$$

where Y_i is the average real GDP per capita of the city where the airport i located and d_{ij} is the large circle distance between the two airports.

Furthermore, the Global Moran's I is used to test and study the spatial correlation of airports. The test results show that each variable, including regional economic, airport passenger throughput, and airport cargo throughput, is significantly greater than 0 at 1% confidence level. Therefore, the objects studied in this paper have a strong spatial correlation, which indicates that spatial econometric analysis can be carried out.

The data, used in the spatial econometric analysis of this paper, are the data of 78 airports of the Chinese mainland from 2001 to 2018. While paying attention to the spatial autocorrelation of the whole sample airport in China, we divide the samples into eastern, central, and western for testing; the classification basis is consistent with the previous discussion. Referring to the research experience of aviation economy by Wang [32] and Chen et al. [34], in the process of selecting the model, we start from the SDM and then use Lagrange Multiplier Test and Wald Test to analyze whether the SDM can be transformed into Spatial Autocorrelation Model (SAR) or Spatial Error Model (SEM). The test results all reject the null hypothesis, which shows that the SDM is suitable for this study. Furthermore, Hausman test results show that the fixed-effects model is more appropriate than the random effects. Finally, we choose the SDM with fixed effects for research. The model is as follows

$$y_{it} = \rho W_i' y_{it} + X_{it}\beta + \theta W_i' X_{it} + \mu_i + \varepsilon_{it}, \tag{2}$$

where y is the dependent variable of the model, X is the core explanatory variable and various control variables, W is the spatial weight matrix, μ, θ, ρ, and β are the parameters to be estimated, and ε is the error term.

3.3. Variable Selection and Data Description.

Wang [32] and Chen et al. [34] collected data from 45 airports in China and researched their space spillover effect. Based on the research, this paper expands the sample and selects the balanced panel data of 78 airports in China from 2001 to 2018. The data selected in this paper are mainly from *Civil Aviation from the Perspective of Statistics (2001–2018)*, *China Urban Statistical Yearbook (2002–2019)*, and the annual *Statistical Bulletin of Civil Aviation Airport Production.* Some of the missing values are made up by consulting the *National Economic Development Bulletin* and the website of the Bureau of Statistics.

3.3.1. Airport Development Indicators.

Airport cargo traffic (lncm) and passenger flow (lntra) are the most intuitive and important indicators to measure the development level of the airport economy [38, 39]. For the case that a city has two airports, according to the experience of other scholars, the passenger and cargo throughput of the airport is combined.

3.3.2. Control Variables.

Government intervention (gov). the degree of market competition depends on the degree of government intervention [40]; under the fiscal decentralization system, the GDP tournament between regional governments and the competitive game of officials leads to incentives for the government to directly intervene in local economic activities. Particularly, since the airport ownership reform began in 2001, regional governments have regarded the aviation economy as a new economic growth pole and are more likely to carry out preferential policies. To measure the degree of government intervention, Fan and Zhang [41] used the ratio of regional government expenditure to GDP. However, the researches on the aviation economy [42, 43], which are similar to the content of this article, used the ratio of fiscal government expenditure to fiscal revenue, to reflect the degree of government intervention. The approach is adopted in this paper.

The stock of airport facilities (lnrf) is expressed by the number of takeoffs and landings of aircraft. There are two main ideas in the selection of representative variables of airport infrastructure qualification. First, according to the neoclassical concept of capital, it can be reflected in monetary form, which is mostly used in the existing literature. Second, it can be reflected in the kind form. Percoco [44] used the physical form of the number of takeoffs and landings to measure the airport qualification. Li [33] proved the necessity of using this measure; first of all, the airport has externalities, and its investment decision is not merely based on profit maximization but also based on social benefits. Secondly, the main economic source of airport investment is a central investment, so it is difficult to obtain statistical data and measure it in a unified monetary form. Finally, the construction period of the airport is long, which usually takes 2–3 years, and inaccurate results may be obtained by

measuring it in the form of currency. Therefore, to measure the qualification of airport facilities, it is an appropriate way to use the index of the number of takeoffs and landings at the airport.

Regional economic status (lngdp) is expressed by regional GDP, which has been reduced based on 2001. In the case that the radiation scope of the airport economic zone is fuzzy, it is a feasible and common method to use the GDP of the city where the airport is located, to represent the hinterland development level of the airport. Population indicator (lnpop) is expressed by the year-end population. Human capital (lntea) is generally represented by the number of college students. Based on the availability of data, this paper uses the number of full-time teachers in colleges instead. Tourist attraction (lnta) is represented by the number of lodging meal business employees. The research studies of Yang et al. [27] and David and Saporito [28] proved that tourism and aviation economy are closely linked. The industrial structure (sec) is expressed as the ratio of the added value of the secondary industry to regional GDP. Employment in the secondary industry (esis) is expressed by the proportion of manufacturing industry employees and the year-end population. Population density (pd) is expressed by the proportion of the number of people at the end of the year to the area of administrative area. This indicator can be used to reflect the degree of economic prosperity in the hinterland of the airport. Per capita urban road area (proad) is expressed by the proportion of the urban road area to the number of people at the end of the year, which can reflect the convenience of regional transportation. Table 1 is the main index and calculation method of data; Table 2 is the descriptive statistics of the main indicators in this paper. It should be noted that SCM only selected airports in the central and western as the research objects.

4. Empirical Results and Discussion

4.1. Empirical Analysis of the Effect of Preferential Policy. By the data-driven method, SCM obtains the weight of the control group, which can minimize the mean square error (the root mean square prediction error, RMSPE) of the experimental subjects and the synthetic control group before the implementation of the preferential policy. The fitting results of predictive control variables are shown in Table 3.

The passenger and cargo throughput of the Xinzheng Airport in Zhengzhou shown in Table 3 is similar to that of synthetic areas. The RMSPE of freight volume and passenger flow is less than 0.1, and the predictive control variables, such as lngdp, gov, lnpop, and sec, are very close to the real level. The airport development index of the synthetic area, in 2001 and 2006, is highly similar to that of the experimental area, which can prove that the fitting effect of the SCM method is appropriate.

The weights of the synthesized areas are listed in Table 4. According to the cargo traffic of Zhengzhou Airport, the synthetic areas include Nanchang (0.287), Chengdu (0.562), Luoyang (0.057), and Ganzhou (0.095), which indicates that Zhengzhou is the closest to Chengdu in the level of cargo traffic. As for the passenger flow of Zhengzhou Airport, the

synthetic areas are Nanchang (0.032), Harbin (Harbin), Wuhan (0.158), Luoyang (0.082), and Changsha (0.543), indicating that the passenger throughput of Changsha Airport is close to that of Zhengzhou.

Then the SCM is carried out, and the estimated results are shown in Figure 1. It is shown that, before the implementation of the preferential policy, the passenger and cargo throughput of the experimental airport and the synthetic airport had a good fit, and after the implementation of preferential policy, the passenger and cargo throughput of Xinzheng Airport showed an increasing trend. Among them, it can be observed that there is a difference in the observed values between the experimental object and the synthetic object before the implementation of the policy, which may be the advanced effect of the policy. Before the Zhengzhou government officially announced the preferential policy, some enterprises had got the news and quickly signed cooperation projects. However, compared with the freight volume, the change of passenger throughput is relatively not obvious, which may due to the orders of goods transportation mainly come from enterprises, and the passenger flow is more spontaneous, which confirms the advance effect of this policy on a certain extent.

4.1.1. Effectiveness Analysis. According to the content, the passenger and cargo transport throughput of the experimental and synthetic subjects is different after the implementation of the policy, but the influence of other factors may not be ruled out. To eliminate the interference of other policy factors and contingency, the ranking test method is adopted. It is mainly used to analyze the robustness of the counterevent experiment, its principle is assuming that the control group airports implement preferential policies, respectively, and in 2012, we applied the SCM to construct the synthetic objects and then compared them with the actual development indicators of each airport. If there is a significant difference in the degree of standard change, measured by the difference between the actual observed value of the experimental object and the observed value of the synthetic object, the policy effect difference between the two is large, and the preferential policy can significantly affect the experimental area. On the contrary, further research is needed.

In this paper, the ranking test is carried out on 37 control group samples outside Xinzheng Airport. However, if the RMSPE of the experimental object is large, which shows that the appropriate weight cannot be found to fit the observed values of the control object, the hypothesis of the SCM is not satisfied. Referring to the practice of Abadie et al. [45], we excluded the airport with RMSPE five times larger than the experimental object in the control group and finally got 25 samples and 32 samples on the cargo and passenger throughput indicators, respectively. In Figure 2, line charts of the standard changes of the experimental subjects, the cargo and passenger throughput of Xinzheng Airport, and the standard changes of other airports are drawn.

As shown in Figure 2, before the implementation of the preferential policy, the difference in cargo traffic volume

TABLE 1: The main indicators and calculation methods.

Variable type	Variable name	Variable symbol	Variable definition
Dependent variables	Airport cargo traffic	lncm	The logarithm of airport cargo throughput
	Airport passenger flow	lntra	The logarithm of airport passenger throughput
	Economic level	lngdp	The logarithm of actual regional gross domestic product
	Industrial structure	sec	Added value of manufacturing industry/regional GDP
Control variables	Population	lnpop	The logarithm of the population at the end of the year
	Facilities qualification of airports	lnrf	The logarithm of the number of airport takeoffs and landings
	Population density	pd	Population/administrative area
	Tourism attraction ability	lnta	The logarithm of the number of people employed in the accommodation and catering business
	Per capita urban road area	proad	Urban road area/population
	Human capital	lntea	The logarithm of the number of full-time teachers in colleges
	Employment situation of secondary industry	esis	The number of employed people in the manufacturing industry/ population
	Government intervention	gov	Government budget expenditure/government budget revenue

TABLE 2: Descriptive statistics of main indicators.

Variables	N	Mean	SD	Min	Max
lntra	1,404	13.900	2.314	2.773	18.580
lncm	1,404	8.844	2.984	0.095	15.260
sec	1,404	45.310	10.870	14.950	82.280
lnrf	1,404	9.716	1.915	1.792	13.560
lngdp	1,404	16.510	1.219	12.670	19.600
lnpop	1,404	6.066	0.690	3.884	7.297
pd	1,404	0.049	0.037	0.002	0.271
esis	1,404	0.078	0.088	0.008	0.958
lntea	1,404	8.493	1.385	2.773	11.160
proad	1,404	5.826	6.403	0.049	64.000
lnta	1,404	0.903	0.742	0.044	4.633
gov	1,404	1.974	1.144	0.649	12.400

TABLE 3: RMSPE comparison chart.

Objects	The predictive quality of the application of SCM before the implementation of the policy										
	RMSPE	lncm (2001)	lncm (2006)	gov	lnta	lnpop	pd	esis	sec	lntea	proad
Cargo flow at Xinzheng Airport	0.0931	9.85	10.84	1.13	1.49	6.62	0.10	0.07	53.45	10.05	3.40
Synthetic cargo flow at Xinzheng Airport		9.86	10.73	1.54	1.11	6.72	0.07	0.06	47.75	9.82	3.84
Passenger flow of Xinzheng Airport	0.0806	14.24	15.17	1.13	1.49	6.62	0.10	0.07	53.45	10.05	3.40
Synthetic passenger flow of Xinzheng Airport		14.27	15.26	1.39	1.50	6.57	0.05	0.07	46.35	9.98	4.17

TABLE 4: Synthesized regional weight of development indicators of Xinzheng Airport.

Subjects affected by preferential policies	Synthesized area (weight)			
Cargo flow at Xinzheng Airport	Nanchang	0.287	Chengdu	0.562
	Luoyang	0.057	Ganzhou	0.095
Passenger flow of Xinzheng Airport	Nanchang	0.032	Harbin	0.186
	Wuhan	0.158	Luoyang	0.082
	Changsha	0.543		

between Xinzheng Airport and other airports is relatively small. However, after the policy, the difference in the standard change degree of cargo traffic volume between Xinzheng Airport and other airports is gradually increasing. The cargo volume distribution curve of Xinzheng Airport is

located outside other airports, which proves the effectiveness of the preferential policy effect. If given random disposal, there is a 1/25 or 4% probability that a similar degree of variation between a certain airport and its synthetic airport in cargo throughput will appear. Therefore, the effect of

(a)

(b)
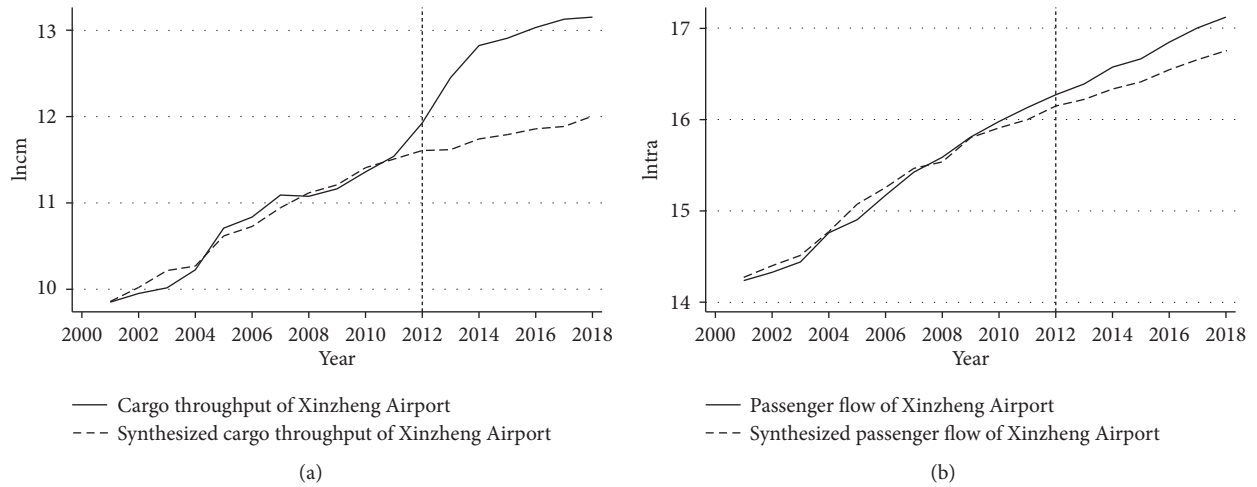
Figure 1: Cargo and passenger flow of Xinzheng Airport and its synthetic control objects.

(a)

(b)
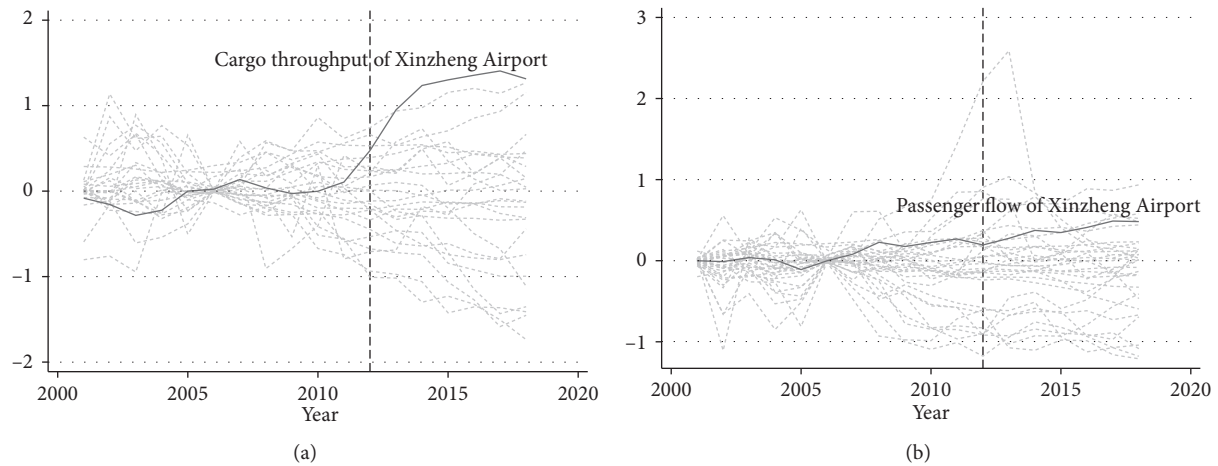
Figure 2: Distribution map of standard change degree of passenger and cargo flow at Xinzheng Airport and other airports.

preferential policies on airport cargo traffic is significant at the level of 4%.

However, in Figure 2, after the implementation of the policy, the gap between Xinzheng Airport and other airports in the standard change of passenger flow has not increased significantly, and its distribution curve is in the interior of other airports, indicating that the policy effect of preferential policy on the passenger throughput of Xinzheng Airport is not significant. This reflects that the transport cost reduction effect, which is brought about by the preferential policy, may only be effective for airport cargo traffic, and passengers will not significantly increase the number of plane trips because of lower ticket prices. However, whether the preferential policy is ineffective to the airport passenger throughput still needs to be further tested.

4.1.2. Robustness Test. To avoid the deviation of the ranking test results due to the lack of randomness, we further utilize the falsification test method to inspect the robustness. The

principle is that if the airport without preferential policy is selected for analysis, the passenger and cargo throughput of the airport is similar to that of Xinzheng Airport before the implementation of the policy, and there is a great difference between the real value and the composite value after the implementation of the policy; it shows that the result of the previous policy effect analysis is not robust. Otherwise, the analysis results of this paper are credible.

Considering two extreme cases, we construct airports with the largest weight and zero weight in the synthetic experiment objects. The largest weight indicates that the airport is most similar to the experimental subject, and a weight of zero indicates that the two are quite different. The robustness test results of the cargo and passenger throughput indicators of Xinzheng Airport are shown in Figures 3 and 4. From Figure 3, it can be found that the difference between the actual observation value and the composite value of the false experimental objects of Xinzheng Airport cargo throughput index, Chengdu and Xi'an, does not show a trend similar to Xinzheng Airport cargo throughput after 2012. However, in Figure 4, the
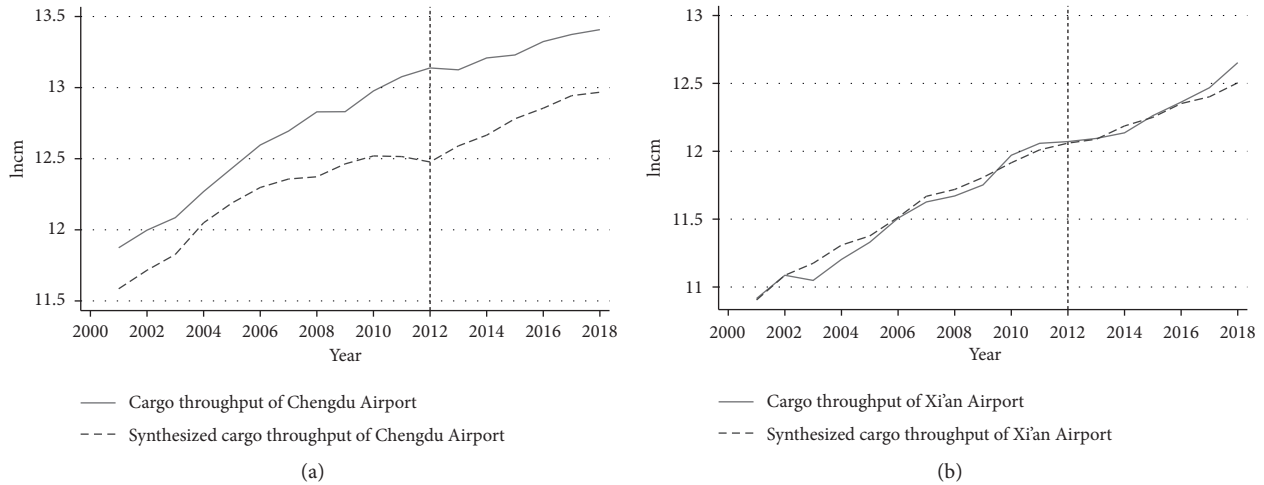
Figure 3: False experiment of cargo throughput at Xinzheng Airport. (a) The maximum weight and (b) the area with zero weight.
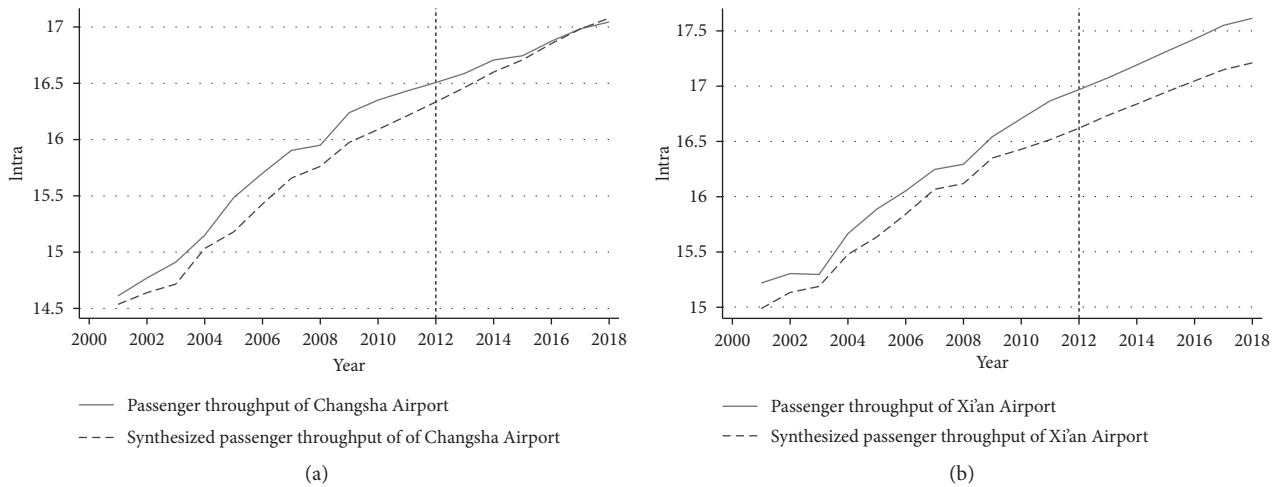
Figure 4: False experiment of passenger throughput at Xinzheng Airport. (a) The maximum weight and (b) the area with zero weight.

variation trend of the false experimental group of Xinzheng Airport passenger flow, Changsha and Xi'an, is similar to that of Xinzheng Airport, which is consistent with the conclusion of the ranking test, and further illustrates that the preferential policy only had an impact on the cargo transportation volume of the experimental airport. The reason for this phenomenon is easy to explain. First, the industry transferred from the airport in eastern China to the central and western is cargo transportation; compared with passenger transport, freight transportation can better improve the regional industrial structure and promote economic development. Secondly, since the airport ownership reform in 2001, the contribution rate of air cargo transport has exceeded that of passenger transport [46]. Air cargo transport has become the engine of regional economic growth.

Since then, the research results of SCM showed that preferential policies have a positive impact on the development of airports, especially on cargo transportation. H_2 is proved to be correct.

4.2. The Empirical Results of the Spatial Econometric Model.
The above content has verified that the preferential behavior of the government will increase the cargo volume at the local airport. Furthermore, we will analyze the spatial spillover effect of airport freight volume through the SDM. If there is a strong siphon relationship in cargo flow between airports, then the implementation of preferential policies will intensify this competition.

Based on the research purpose of this paper, we conduct a subsample study on the airports in the eastern, central, and western of China. However, the coefficient of independent variable in the SDM model does not represent the elastic coefficient, so direct, spatial spillover, and total effect need to be calculated. The results are presented in Table 5. For brevity, the result reports only the variables we care about.

From the direct effects in Table 5, it can be concluded that, overall, the cargo throughput and passenger throughput of China's airports have a positive impact on the local economy. However, the impact of flight takeoffs and

TABLE 5: Direct, indirect, and total effects of the SDM.

Spatial effect	Area	lntra	lncm	lnrf
Direct effect	The whole country	0.0292*** (−3.34)	0.0224*** (−4.38)	−0.0235*** (−3.22)
	Eastern region	0.0157* (−1.7)	0.0113* (−1.83)	0.0135 (−1.53)
	Central and western	0.0571*** (−3.77)	0.007 (−0.85)	−0.0579*** (−5.07)
Indirect effect/spatial spillover effect	The whole country	0.0318 (−1.26)	−0.0059 (−0.41)	−0.025 (−1.07)
	Eastern region	0.0176 (−1.07)	0.0092 (−0.65)	0.0001 (0.00)
	Central and western	0.1356** (−2.35)	−0.0685*** (−2.93)	−0.1131* (−1.90)
Total effect	The whole country	0.0610** (−2.12)	0.0165 (−0.97)	−0.0485* (−1.81)
	Eastern region	0.0333* (−1.65)	0.0206 (−1.16)	0.0136 (−0.65)
	Central and western	0.1927*** (−3.09)	−0.0615** (−2.27)	−0.1710*** (−2.63)

t statistics in parentheses. $^{*}p < 0.1$, $^{**}p < 0.05$, and $^{***}p < 0.01$.

landings on the regional economy is significantly negative. To a certain extent, aircraft takeoffs and landings reflect the strength of government support to airports; from the negative impact of the increase in aircraft takeoffs and landings at the airport on the regional economy, it can be inferred that these preferential policies may also induce airlines to use large aircraft and increase the number of flights to obtain high subsidy standards, regardless of low occupancy rates, which are equivalent to using financial subsidies to make up for the problem of inefficient operation. It increases the burden of regional finance and hinders economic growth. In the subsample estimation, the passenger and cargo throughput of the eastern airport plays a significant role in promoting the regional economy. However, in the central and western regions, only the airport passenger flow has a significant promoting effect on the regional economy, while the cargo traffic volume has no obvious pulling effect on the regional economy. It is preliminarily inferred that the eastern region is the Chinese economic center and high-end manufacturing area, so the demand for air transport in the eastern region is very large, which can significantly promote regional economic growth, while the high-end manufacturing industry in the central and western regions is underdeveloped, and the freight volume is slightly inadequate. As a result, its pulling effect on the economy is not obvious.

From the decomposition of spatial spillover effects, it can be found that the spatial spillover effects of various indicators of airports, in the whole country and the eastern region, are not significant, which may be because the development of the eastern airport has entered a mature period, the route network layout and market division have been completed, and the competitive relationship has been transformed into a cooperative relationship, which leads to the fact that the spatial spillover effect of an airport on other airports around is weak. In contrast, the central and western regions of China are vast and have yet to complete their route network layout; airports in each region already have made different efforts to grab market share. The economic spillover effect of passenger flow from airports in the central and western on surrounding areas is significantly positive. But, the spatial spillover effect of cargo traffic in the central and western airports, which we are concerned about, is significantly negative, indicating that the airports in the central and western regions are still in a state of fierce competition in cargo.

From the total effect of Table 5, we can summarize that the overall spatial spillover effect of airport cargo traffic in China is significantly negative, which shows that the competition of local airports in freight transport did not promote the development of the local economy. On the contrary, the overall economic income is negative due to disorderly vicious competition.

The result of the spatial econometric model is closely related to the selection of the weight matrix. Drawing on related research experience [32, 34, 37], we select the 0-1 matrix, based on the 800 km distance threshold, and the matrix, based on the reciprocal of geographical distance, to study the spatial spillover effect of the airport again. The results are consistent with the previous studies, so the empirical results of the SDM are robust. The rationality of H₃has been proved, and the cargo throughput of airports in central and western China shows a siphon effect.

4.3. Discussion Combined with the Results of the SCM and SDM. From the previous analysis of the SCM, it is concluded that the preferential policy implemented by Zhengzhou to the aviation economic zone is finally reflected in the increase of airport cargo (hypothesis 2), which shows that the current competition focus on airports in central and western China lies in cargo volume. Furthermore, the research results of SDM show that the spatial spillover indirect

effect of airport cargo transportation in central and western China is negative ((hypothesis 3), and there is a significant siphon effect between airports in central and western China. It indicates that the implementation of preferential policies in one area will increase the cargo throughput of the local airport but will correspondingly take goods from other areas. To offset this impact, other regions have also introduced policies to reduce the cost of transportation at local airports.

Taking Xi'an as an example, according to incomplete statistics, the total amount of foreign trade import and export air cargo, which is diverted by other provinces in Xi'an every year, amounts to 15000 tons, accounting for 40% of the stock of international air logistics in Xi'an. To recover this part of the lost goods, Xi'an issued the *Support Measures for Accelerating the Development of General Aviation Industry* and the *Incentive Measures for Investment and Tax Introduction of Xi'an National Civil Aerospace Industry Base* in July 2019. The preferential treatment, given to airports in terms of attracting investment and operation, far exceeds that of other central and western regions. In the process of the transfer of eastern airports to the central and western regions, such a policy is undoubtedly very attractive, so aerospace companies are likely to choose these places with more preferential policies. At the same time, Xi'an, Chengdu, Zhengzhou, and Wuhan, which belong to the mutual radiation circle, have a competition in aviation resources. If a place heavily subsidizes the air routes, it will seize the freight resources that originally belong to other regions. To avoid the local aviation industry that was excessively squeezed, other regions will inevitably adopt corresponding preferential policies to offset the impact of the existing preferential policies. The production cost of each airport has been temporarily reduced, the cargo volume has increased, and the cost of goods originally taken by land has also been reduced to acceptable air transport. But overall, the cost of air cargo in the central and western regions is on the rise. Obviously, it is not conducive to the sustainable development of the region and the air transport industry. This can explain why the increase in cargo throughput at airports in central and western China has a negative impact on the economy.

Since then, H_1 has been proved, the implementation of preferential policies has accelerated the convergent competition in the construction of aviation hubs in the central and western regions and adversely affected the development of the regional economy.

4.4. The Working Mechanism of Preferential Policies. The airports can accelerate the flow of labor capital between regions and promote the upgrading of industrial structure and regional economic transformation [26, 28]. Therefore, we will test the working mechanism of preferential policy from two aspects of human capital and industrial structure. The model is as follows:

$$Y_{it} = \alpha_1 + \beta_i D \times \theta_i + \delta_i X_i + \mu_i + \nu_t + \varepsilon_{it},$$
$$D = d_i \times d_t. \tag{3}$$

Here, Y is the regional economic level, α_1 is the constant, policy effect (D) is the interactive term of the time virtual variable d_t (1 after 2011, otherwise 0) and the regional virtual variable d_i (preferential areas take 1, otherwise 0), and θ is the coefficient of the interaction term of the core explanatory variable (human capital, industrial structure). In this paper, the interaction term of policy effect D and the two variables is used to test the mechanism of policy action. X is a series of control variables, such as airport cargo flow, passenger flow, takeoff and landing times, and government intervention. Besides, the model controls the regional effect and time effect. The test results are shown in Table 6.

The first column does not include interaction terms, which is treated as a comparison. In the second column, the estimated results of policy effect and human capital are both significantly positive, and the implementation of policies can promote regional economic development by improving human capital. The interaction term of the two variables is significantly negative. With the improvement of regional human capital, the promotion effect of preferential policies on the regional economy is increasingly weak. Similarly, in the third column, industrial structure has a positive impact on the regional economy, but the interaction term between policy effect and industrial structure is negative, indicating that preferential policies can hardly play a good effect on the improvement of industrial structure. This result is consistent with the conclusion of existing studies. Preferential policies can play a good supporting role in areas with poor human capital and industrial level. To some extent, this confirms the motivation of the central and western regional governments to adopt preferential policies for airports. However, with the development of the economy and society, the promoting role of preferential policies on the economy gradually decreases and such measures may not achieve the desired results [11].

5. Further Discussion on the Causes of the Preferential System

The rapid growth of China's economy is inseparable from the rapid growth of airports in various regions. However, under the interactive influence of multiple factors, such as the rise in the price of factors of production in the eastern coastal areas, the continuous appreciation of the RMB exchange rate, the reduction of the proportion of export tax rebates, and the tightening of trade policies, the cost of airport operation in these areas remains high, and the restrictions on resources and environment are becoming more and more significant, so the cargo transport activities at the eastern airport began to shift to the central and western. In recent years, many aviation hub cities in China have proposed the concept of building airport economic zones or aviation metropolises. As the factor-intensive economies move from the east to the west, China has positioned Zhengzhou, Wuhan, Xi'an, and other cities as vital logistics hubs in the country. Among them, the goal of Xinzheng Airport in Zhengzhou is to become an international aviation logistics center, while Wuhan Airport proposed the development task of building an airport economic zone to catch up with Beijing, Shanghai, and Guangzhou, while Xi'an and other places are positively influenced by Belt and Road Initiative and strongly supported by the local government.

Table 6: The mechanism test of preferential policy.

	(1)	(2)	(3)
D	0.0651*	10.3513***	1.1473***
	(1.90)	(9.29)	(9.12)
lntra	0.0283	0.0284	0.0288
	(1.47)	(1.47)	(1.49)
lncm	0.0232	0.0232	0.0227
	(1.35)	(1.35)	(1.32)
lnrf	−0.0256	−0.0256	−0.0256
	(−1.51)	(−1.51)	(−1.51)
gov	−0.0436***	−0.0436***	−0.0435***
	(−2.90)	(−2.90)	(−2.89)
lnta	0.0839***	0.0839***	0.0842***
	(2.74)	(2.74)	(2.74)
lnpop	0.4652***	0.4664***	0.4749***
	(3.82)	(3.83)	(3.92)
pd	0.1787	0.1891	0.2546
	(0.19)	(0.20)	(0.28)
esis	−0.0976	−0.1002	−0.1179
	(−0.35)	(−0.36)	(−0.42)
sec	0.0118***	0.0118***	0.0119***
	(5.13)	(5.14)	(5.19)
lntea	0.0546	0.0549	0.0547
	(1.56)	(1.58)	(1.57)
proad	0.0045	0.0045	0.0045
	(1.09)	(1.09)	(1.09)
Dxlntea		−0.9480***	
		(−9.17)	
Dxsec			−0.0221***
			(−8.56)
Provincial effect	Yes	Yes	Yes
Time effect	Yes	Yes	Yes
_cons	11.1517***	11.1411***	11.0849***
	(14.52)	(14.52)	(14.47)
R^2	0.971	0.971	0.971
N	1404	1404	1404

t statistics in parentheses. $^{*}p < 0.1$, $^{**}p < 0.05$, and $^{***}p < 0.01$.

Thus, the impact of the airport economy is not limited to industrial development; spatial planning is imperative.

The practice of China's aviation economic zone construction has surpassed related theoretical research in time, and the air economic zone in the central and western has unknowingly entered the fiery construction stage. In 2013, the State Council of China approved the Development Plan of Zhengzhou Airport Economic Comprehensive Experimental Zone (2013–2025), and the construction of Zhengzhou Airport has become a national development strategy. After that, the Civil Aviation Administration of China approved the Development Plan of Xi'an Aviation City Experimental Zone (2013–2025). Xi'an strives to build the Silk Road aviation hub. Wuhan Aviation Economic Zone covers an area of about 1000 square kilometers, relying on the advantages of transportation, industry, and talents, and it has put forward the goal of building a modern waterfront aviation city. Also, Chongqing Jiangbei International Airport has put forward an overall plan for the construction of an airport metropolitan area, and the Shuangliu area in Chengdu strives to build a modern airport new city. Changsha Airport Economic Zone was approved in 2017, to build a green, ecological, and smart aviation city. From the

development goals and overall strategy of the airport economic zones in the central and western, we can see that the goal of these airport economic zones is to build a modern aviation city.

Based on the above content, we can understand the differences in the degree of subsidies to the aviation economy, which was implemented by the provincial and municipal governments in China in terms of time and space.

First, the preferential system has an outstanding policy effect. In the initial period of the industry, if enterprises follow the rules, many processes may encounter obstacles. However, a small number of enterprises had received support from the government in the process of development, and then they could overcome the obstacles of the system to the enterprises, rapidly accumulate development strength in a short time, and gradually form the pillar of the regional economy with market competitiveness. For this reason, in the initial stage of airport construction, it is feasible for the government to give it policy support to help it tide over the difficult times.

With the rapid development of China's economy, the original economic operation mode and industrial linkages need to be reintegrated, while the airport economy has improved the efficiency of the use of information, knowledge, capital, and technology and reorganized the traditional mode of production in the aspects of passenger flow, logistics, and information flow, which plays a prominent role in improving the timeliness and added value of products. Therefore, the airport economy is not a separate economic region of each province and city, but a concentrated embodiment of the overall local economic development level. Almost all regions attach great importance to the construction speed, convenience, intelligence, and coordination of the airport economy. The tradition of supporting airport policy has not disappeared but has become more obvious and intensive.

Second, the development level of the airport economy in the central and western is close. Most of the airport economic zones in the central and western regions of China already have mature plans. According to the report of *China Airport Economic Development Index (2019)*, the top 10 hub driving indices of the 36 airport economic zones, which are under construction and planned by the end of 2018, are Shanghai, Beijing, Guangzhou, Chengdu, Wuhan, Shenzhen, Zhengzhou, Chongqing, Hangzhou, and Kunming. Cities in the central and western account for half of them. In the central and western, Chengdu, Chongqing, and Zhengzhou are among the top three in the overall index, while the total index levels of other provincial capitals are also very close to them. For airports in the central and western regions, the earliest ones to receive relevant policy supports from the local governments will be more competitive. Therefore, the relatively close level of development, as well as local attention to the airport economy, has become one of the important reasons for the continuous strengthening of the preferential system.

Currently, for gaining more flights and becoming a major regional aviation hub, key cities in the central and western have issued flight subsidy policies. The result will be

three effects. First, the resources obtained by the airport are too concentrated, which is relatively not conducive to the development of other industries and resulting in a crowding-out effect. Second, the preferential model will produce a certain degree of dependence, making specific industries wait for the arrival of local protection or preferential conditions, but cannot involve in the larger-scale market competition, affecting the long-term development of the industry. Third, on the one hand, this measure will increase the financial burden of the city, which is not conducive to the healthy development of the regional economy. On the other hand, the preferential policy will not make the region have a better space for development; on the contrary, it will increase the vicious competition of the airport economy. To cope with the flight subsidies of neighboring provinces and cities, all localities must constantly increase their preferential conditions. Owing to the fact that the preferential system cannot bring the expected high income and forms the resource distortion, it will produce a result, which is contrary to the initial desire of the implementation of the preferential system, and finally affect the development of the regional economy. All these indicate the aviation hub dispute trend towards more intense competition.

6. Main Conclusions and Policy Recommendations

At present, the governments of the central and western regions have issued policies to vigorously develop aviation hubs, but it may lead to repeated construction and convergent competition. We collected sample data from 78 airports of Chinese mainland from 2001 to 2018. By using the SCM, we found that the preferential policy had a positive effect on airport cargo traffic, and the results passed the robustness test. Furthermore, we used SDM to study the spatial spillover effect of airports. The results show that the spatial spillover effect of airport cargo traffic in central and western China is significantly negative, and there is fierce competition in cargo transport among airports. The implementation of preferential policies has intensified this competition and further led to the growth of cargo transport volume which harms the regional economy. At the same time, the results of mechanism analysis show that the airport has a greater role in promoting the economy in areas with insufficient human capital and industrial development, which also proves the motivation of the central and western regions to carry out competitive subsidies for airports. Judging from the current situation, the preferential policy in the aviation economy will accelerate the vicious competition in the aviation economic zones in the central and western regions, which is not conducive to the optimization, upgrading, transformation, and development of the regional economic structure in the long run. At the same time, after more than ten years of construction and accumulation, the national airport economic zone has entered a stage of deep development. As a new economic form and an important part of the regional economy, blindly giving preferential treatment to it is likely to disturb the market order.

Based on the above conclusions, we put forward the following policy recommendations.

First, the GDP championship system needs to be improved. The GDP tournament system is the direct reason for the formation of the preferential system. To improve it, it is necessary to improve the promotion system of government officials. The country cannot merely take the growth of GDP as the only political achievement nor judge the economic development of the provinces simply by the level of GDP. Second, the policies for large multinational enterprises must be transparent. The aviation preferential policies of various regions for large multinational enterprises need to be announced to the public, so as to reduce regional unfair competition and prevent foreign enterprises from obtaining unfair subsidies in China, which will reduce the negative impact on the national economy and promote fair competition. Third, the Civil Aviation Administration of China has better continued to deepen the market-oriented reform of civil aviation domestic freight rates, strengthen the market price determination mechanism, and gradually liberalize the passenger transport prices and cargo transport prices of more routes in order to finally realize the transportation price determined by market competition. Fourth, multiple airports need to form a regional consultative mechanism for subsidy policies. There is no real winner in the price war, and the central and western regions need to realize the harm of malicious competition; according to the characteristics and advantages of the local economy, they need to formulate the key development path of the aviation economy, take the path of differentiation, and form a transparent and efficient regional consultation mechanism. Particularly, the release of local subsidy policies is the best to fully communicate with the surrounding airports in advance.

Data Availability

The data selected in this paper are mainly from Civil Aviation from the Perspective of Statistics (2001–2018), China Urban Statistical Yearbook (2002–2019), and the annual Statistical Bulletin of Civil Aviation Airport Production. Some of the missing values are made up by consulting the National Economic Development Bulletin and the website of the Bureau of Statistics.

Disclosure

Chengyu Li and Guangliang Zhou are co-first authors.

Conflicts of Interest

The authors declare that they have no known competing financial interests or personal relationships that could have appeared to influence the work reported in this study.

Authors' Contributions

Chengyu Li and Guangliang Zhou contributed equally to the work.

Acknowledgments

References

[1] A. Mačiulis, A. V. Vasiliauskas, and G. Jakubauskas, "The impact of transport on the competitiveness of national economy," *Transport*, vol. 24, no. 2, pp. 93–99, 2009.

[2] S. J. Appold and J. D. Kasarda, "The airport city phenomenon evidence from large US airports," *Urban Studies*, vol. 50, no. 6, pp. 1239–1259, 2013.

[3] S. J. Appold, "Airport cities and metropolitan labor markets an extension and response to Cidell," *Journal of Economic Geography*, vol. 15, no. 6, pp. 1145–1168, 2015.

[4] E. Heymann, A. Karollus, L. Slomka, D. B. AG, and R. Hoffmann, *Germany's Regional Airports Under Political And Economic Pressure*, pp. 1–15, Deutsche Bank Research, Frankfurt, Germany, 2015.

[5] K. Button and S. Taylor, "International air transportation and economic development," *Journal of Air Transport Management*, vol. 6, no. 4, pp. 209–222, 2000.

[6] N. Sheard, "Airports and urban sectoral employment," *Journal of Urban Economics*, vol. 80, no. 3, pp. 133–152, 2014.

[7] J. Cidell, "The role of major infrastructure in subregional economic development an empirical study of airports and cities," *Journal of Economic Geography*, vol. 15, no. 6, pp. 1125–1144, 2015.

[8] E. L. F. A. Association, *Liberalisation of European Air Transport The Benefits of Low Fares Airlines to Consumers, Airports, Regions and the Environment*, pp. 13–16, European Low Fares Airlines Association, Brussels, Belgium, 2004.

[9] P. Breidenbach, "Ready for take-off? The economic effects of regional airport expansions in Germany," *Regional Studies*, vol. 54, no. 8, pp. 1084–1097, 2020.

[10] L. Zhou, "Governing China's local officials an analysis of promotion tournament model," *Economic Research Journal*, vol. 7, pp. 36–50, 2007.

[11] C. E. Bai, "The preferential mode is not sustainable," *Money China*, vol. 1, pp. 56–58, 2015.

[12] J. Zhang, "Decentralization and growth China context," *China Economic Quarterly*, vol. 1, pp. 21–52, 2008.

[13] X. Y. Fan, "The calculation of the rate of return on industrial capital in China and the analysis of regional and industry structure," *The Journal of World Economy*, vol. 5, pp. 48–57, 2004.

[14] Y. Y. Jiang and R. E. Ren, "The rate of return of industrial capital in China," *China Economic Quarterly*, vol. 3, pp. 877–888, 2004.

[15] T. Shao and J. K. Li, "Distorted capital market, rate of return on capital and differences in ownership," *Economic Science*, vol. 5, pp. 35–45, 2010.

[16] T. Shao, "Financial mismatch, ownership structure and return on capital a case of industrial enterprises in China from 1999 to 2007," *Journal of Financial Research*, pp. 51–68, 2010.

[17] C. E. Bai and L. Ma, "Government intervention, optimal taxation and structural adjustment," *Taxation Research*, vol. 6, pp. 46–50, 2015.

[18] C. E. Bai, Z. J. Qian, and K. P. Wu, "Determinants of factor shares in China's industrial sector," *Economic Research Journal*, vol. 8, pp. 16–28, 2008.

[19] C. E. Bai and Z. J. Qian, "Factor income share in China the story behind the statistics," *Economic Research Journal*, vol. 44, no. 3, pp. 27–41, 2009.

[20] Y. C. Cao, Y. R. Xi, and W. W. Li, "Analysis on the formation of airport economy from the perspective of new economic geography," *Inquiry Into Economic Issues*, vol. 2, pp. 49–54, 2009.

[21] C. Fershtman, "The interdependence between ownership status and market structure the case of privatization," *Economica*, vol. 57, no. 227, pp. 319–328, 1990.

[22] H. Cremer, M. Marchand, and J.-F. Thisse, "Mixed oligopoly with differentiated products," *International Journal of Industrial Organization*, vol. 9, no. 1, pp. 43–53, 1991.

[23] W. C. Merrill and N. Schneider, "Government firms in oligopoly industries a short-run analysis," *The Quarterly Journal of Economics*, vol. 80, no. 3, pp. 400–412, 1966.

[24] M. D. Irwin and J. D. Kasarda, "Air passenger linkages and employment growth in U.S. Metropolitan areas," *American Sociological Review*, vol. 56, no. 4, pp. 524–537, 1991.

[25] J. K. Brueckner, "Airline traffic and urban economic development," *Urban Studies*, vol. 40, no. 8, pp. 1455–1469, 2003.

[26] W. Song and K. Yang, "The impacts of air transportation and airport on regional economic development," *Scientia Geographica Sinica*, vol. 6, pp. 649–657, 2006.

[27] X. Y. Yang, S. Y. Mao, and N. Zhang, "The analysis of the airport developments' contribution to regional tourism," *Statistics & Information Forum*, vol. 26, no. 6, pp. 85–89, 2011.

[28] F. David and G. Saporito, *The Impact of a New Airport on International Tourism The Case of Ragusa (Sicily)*, Bank of Italy, Economic Research and International Relations Area, Rome, Italy, 2017.

[29] D. Baker, R. Merkert, and M. Kamruzzaman, "Regional aviation and economic growth cointegration and causality analysis in Australia," *Journal of Transport Geography*, vol. 43, pp. 140–150, 2015.

[30] Y.-H. Lee, G.-U. Yu, and M.-S. Kim, "Economic spillover effects of airport investment on regional production," *Journal of Korean Society of Transportation*, vol. 23, no. 2, pp. 37–50, 2005.

[31] L. Zhang, W. Chen, Z. N. Song, and J. F. Xue, "Study on the relationship between airport operation and regional economic growth," *Progress in Geography*, vol. 29, no. 12, pp. 1570–1576, 2010.

[32] Q. L. Wang, "Research on the relationship between China's airport economic zone and the hinterland regional economy based on dynamic spatial model," *Geographical Research*, vol. 36, no. 11, pp. 2141–2155, 2017.

[33] N. B. Li, *Research of the Airport Spacial Spillover Effect and its Regional Difference*, Southeast University, Dhaka, Bangladesh, 2013.

[34] X. Chen, J. Yuan, and L. Dai, "Airport network spillover effect with spatial econometric models," *Journal of Transportation Systems Engineering and Information Technology*, vol. 19, no. 4, pp. 211–217, 2019.

[35] A. Abadie and J. Gardeazabal, "The economic costs of conflict a case study of the Basque Country," *American Economic Review*, vol. 93, no. 1, pp. 113–132, 2003.

[36] H. L. Zhang, J. C. Huang, F. Jia, and A. Han, "Research on the spatial spillover effect of economic development of 288 cities

in China," *Statistics & Decision*, vol. 35, no. 24, pp. 141–144, 2019.

[37] L. Gao, *Research on Economic Spillover Effect of Airport Based on Spatial Econometric Model*, pp. 13–16, Civil Aviation Flight University of China, Deyang, China, 2020.

[38] L. Zhang and W. Shi, "The evolution and driving mechanism of spatial structurein airport economic zone Taking Shanghai Hongqiao International Airport as an example," *Geographical Research*, vol. 33, no. 1, pp. 57–70, 2014.

[39] N. Baltaci, O. Sekmen, and G. Akbulut, "The relationship between air transport and economic growth in Turkey cross-regional panel data analysis approach," *Journal of Economics and Behavioral Studies*, vol. 7, no. 1, pp. 89–100, 2015.

[40] M. Chen, Q. H. Gui, M. Lu, and Z. Chen, "How to maintain China's high growth rate via scale economy-an empirical study of economic opening and domestic market segmentation," *China Economic Quarterly*, vol. 1, pp. 125–150, 2008.

[41] Z. Y. Fan and J. Zhang, "Fiscal decentralization, intergovernmental transfer and market integration," *Economic Research Journal*, vol. 45, no. 3, pp. 53–64, 2010.

[42] B. B. Yu, "Economic growth effects of industrial restructuring and productivity improvement—analysis of dynamic spatial panel model with Chinese city data," *China Industrial Economics*, vol. 12, pp. 83–98, 2015.

[43] R. J. Duan, "Technological progress, technological efficiency and industrial structure upgrading—based on spatial econometric analysis of 285 cities in China," *R&D Management*, vol. 30, no. 6, pp. 106–116, 2018.

[44] M. Percoco, "Airport activity and local development evidence from Italy," *Urban Studies*, vol. 47, no. 11, pp. 2427–2443, 2010.

[45] A. Abadie, A. Diamond, and J. Hainmueller, "Synthetic control methods for comparative case studies estimating the effect of California's tobacco control program," *Journal of the American Statistical Association*, vol. 105, no. 490, pp. 493–505, 2010.

[46] S. F. Sun and Y. J. Li, "An empirical analysis on influence of air transport development to chinese economic growth," in *Proceedings of the 2011 International Conference on E-Business and E-Government (ICEE)*, pp. 1–4, Shangai, China, May 2011.

Research Article

Multiobjective Contactless Delivery on Medical Supplies under Open-Loop Distribution

Huilin Li [iD], Ke Xiong, and Xiuming Xie

Southern University of Science and Technology Yantian Hospital, Shenzhen 518081, Guangdong, China

Correspondence should be addressed to Huilin Li; 1228587935@qq.com

With the development and popularity of intelligent store terminals, contactless distribution has been a hot talk on medical supplies using intelligent express boxes. Based on the traditional vehicle routing problem, this paper considers the sharing economy and open-loop distribution reality hotspots and considers the optimization of carbon emissions in contactless distribution. The travel distance and load capacity are the key factors affecting carbon emissions. The carbon emission model proposes dual goals of minimizing distribution costs and carbon emissions. It constructs a distribution path planning model with multiple distribution stations. To solve this problem with multidepot optimization, we design a hybrid genetic algorithm, and according to the strategy of customer distance clustering analysis, the dispatching of vehicles is divided into three steps. The principle of elite crossing is applied to avoid the solution to fall into local optimum. The experimental results show that the proposed model and optimization algorithm can get a tradeoff between the logistics cost and carbon emissions.

1. Introduction

To solve the problems of fast allocation of medical supplies in the prevention of COVID-19, employing external vehicles to realize logistics distribution has become an important strategy and measure under the background of sharing economy. In addition, contactless terminal equipment (such as self-pickup boxes) also is applied for receiving medical supplies to avoid infection [1]. Finally, the distribution vehicle does not have to return to the original distribution center after completing the distribution task, it can continue to serve other distribution center or demand points, so the distribution problem can be simulated as an open-vehicle routing problem (OVRP), which not only reduces delivery time significantly but also ensures the safety of distribution in COVID-19 [1, 2].

In medical supplies, Liu et al. focus on integrated planning for public health emergencies and build a modified model for controlling H1N1 pandemic [3]. Garza-Reyes et al. focus on the improvement of transport and logistics performance of the medical service system; they build mathematical models to optimize medical supplies

distribution [4]. Zhang et al. reveal the critical role of timely supply of medical resources to avoid great infection [5]. Zhou et al. and He et al. focus on the semantic match of medical supplies to transport the medical resources to required places in an efficient way; this paper studies the medical transportation resource discovery mechanism, leading to efficiency improvement and operational innovation [6–8].

At present, in logistics distribution, most research on OVRP mainly focuses on reducing logistics costs or reducing the number of vehicles used [9–12]. With people's attention to energy conservation, emission reduction, and green logistics, how to protect the environment while reducing logistics costs has become a hot issue in academia and environmental protection departments. Bektas and Laporte [13] empirically studied the influencing factors of carbon emissions and weighed the relationship between the driving distance, driver's salary, and fuel consumption. Xiao et al. [14] described the carbon emission in the process of logistics distribution from a microperspective and compared the distribution routes under three different target situations: carbon emission, logistics distribution cost, and total

distribution distance. Considering the impact of road congestion on carbon emissions, Woensel et al. [15] compared and analyzed the carbon emissions under different driving speeds. Demir et al. [16] proposed that vehicle load, engine type and size, road slope, and other factors have a certain relationship with fuel consumption of distribution vehicles and further affect carbon emissions. Niu et al. [17] considered carbon emission cost into logistics cost, established a green open-loop vehicle routing problem, and designed a hybrid tabu search algorithm to solve the model.

From the existing research point of view, the research on the vehicle routing problem of minimizing carbon emissions mostly considers the case of a single distribution station, while the research on the vehicle routing problem of the logistics distribution system with multiple distribution stations is less. At the same time, in the study of the impact of carbon emissions on the logistics distribution system, the vast majority of research is still based on the weighted sum of single-objective optimization, and the research on the vehicle routing problem of the logistics distribution system is not enough. Carbon emissions multiplied by the carbon price coefficient and weighted to the logistics cost, in essence, is still to minimize the logistics cost as the goal and get a single decision-making result. In practical application, decision makers often need to obtain an optimal solution set and select a satisfactory logistics distribution scheme according to their preferences. Therefore, it is more practical to study the multiobjective open-loop vehicle routing problem with the objective of minimizing carbon emissions and logistics costs in the case of multiple distribution stations. Considering that the carbon emission of vehicles has a positive correlation with mileage and actual load [18, 19], an optimization model of carbon emission is established, a multiobjective multidistribution station vehicle routing problem is proposed to minimize logistics cost and carbon emission, and a mixed-integer programming model of the problem is established. Furthermore, a multiobjective genetic algorithm based on decomposition is designed to solve the problem. The simulation results show that the algorithm can solve the problem effectively.

2. Problem Description and Model

A city logistics distribution system has m distribution centers and n consumers. Considering the constraints of vehicle fuel consumption and the driver's workload, the maximum carrying capacity of the distribution vehicle is Q, and the driving distance of the distribution vehicle is not more than L. In order to minimize the logistics cost and carbon emissions of vehicle distribution, it is required to arrange the distribution vehicles and their driving paths reasonably under the constraints of vehicle load and driving distance. A feasible distribution scheme needs to meet the following conditions:

(1) The number of vehicles in each distribution center is limited, and the vehicles are rental vehicles

(2) Vehicles can only start from the distribution center and deliver the loaded goods to the designated

customers along a distribution route without returning to the original distribution center

(3) One delivery vehicle can serve multiple customers, but each customer is only served once by one vehicle

(4) Each vehicle has the constraints of capacity and maximum driving distance, and all distribution vehicles are homogeneous

In order to establish the mathematical model of the problem, the symbols are defined as follows:

2.1. Symbol Definition. In this section, we describe some symbols used in this model.

(1) Sets:

C: consumer set, $C = \{c_1, c_2, \ldots, c_n\}$, the number of N consumers
D: distribution center set, $D = \{d_1, d_2, \ldots, d_m\}$, the number of M distribution stations
N: distribution station and consumer set, $N = C \cup D$
K: distribution vehicle set, $K = \{k_1, k_2, \ldots, k_m\}$

(2) Parameters:

q_i: demand for consumer $i (0 \leq q_i \leq Q)$
d_{ij}: Euclidean distance between any two points i and j, $i, j = 1, 2, \ldots, n, \ldots, m + n$
w: empty net weight of delivery vehicle
Q: maximum loading capacity of distribution vehicles
L: maximum distance of distribution vehicles
C_f: rental fee per delivery vehicle
C_v: variable cost of vehicle unit (including workers' wages, vehicle daily maintenance fees, etc.)

(3) Decision variables:

x_{ijk}: if the vehicle k goes arc (i, j); otherwise, it is 0
f_{ijk}: the cargo loading capacity of distribution vehicle k going by (i, j)

2.2. Description Method of Vehicle Carbon Emission.
Existing research results show that there is a positive correlation between vehicle carbon emissions and fuel consumption, so fuel consumption can be used to describe its carbon emissions [20, 21]. Considering the relationship between the actual load and distance of the vehicle and the fuel consumption, the paper determines using the following method to calculate the fuel consumption:

$$F_{ij} = \left(\rho^0 + \frac{\rho^* - \rho^0}{Q} y_{ij}\right) d_{ij}, \tag{1}$$

where ρ^* and ρ^0 are the fuel consumption rates of full-load and no-load vehicles, respectively, and F_{ij} represents the fuel consumption of vehicles passing through the path. Therefore, according to the relationship between carbon emissions and fuel consumption, the calculation method of vehicle carbon emissions is as follows:

$$EM_{ij} = FE \cdot F_{ij}, \qquad (2)$$

where FE represents the carbon emissions per unit of fuel consumption.

2.3. Multiobjective Multidepot OVRP.

According to the abovementioned symbol definition and carbon emission calculation method, the multidepot open vehicle routing problem (MDOVRP) model for minimizing logistics cost and carbon emission is as follows:

$$\text{Min } C_f \sum_{k \in K} \sum_{i \in D} \sum_{j \in C} x_{ijk} + C_v \sum_{k \in K} \sum_{i \in N} \sum_{j \in N} x_{ijk} d_{ij}, \qquad (3)$$

$$\text{Min FE} \sum_{k \in K} \sum_{i \in N} \sum_{j \in N} x_{ijk} d_{ij} \left(\rho^0 + \frac{\rho^* - \rho^0}{Q} y_{ij} \right), \qquad (4)$$

subject to

$$\sum_{k \in K} \sum_{i \in N} x_{ijk} = 1, \quad \forall j \in C, \qquad (5)$$

$$\sum_{k \in K} \sum_{j \in N} x_{ijk} = 1, \quad \forall i \in C, \qquad (6)$$

$$\sum_{i \in N} x_{ihk} - \sum_{j \in N} x_{hjk} = 0, \quad \forall k \in K; h \in N, \qquad (7)$$

$$\sum_{i \in N} q_i \sum_{j \in N} x_{ijk} \leq Q, \quad \forall k \in K, \qquad (8)$$

$$\sum_{i \in N} \sum_{j \in N} d_{ij} x_{ijk} \leq L, \quad \forall k \in K, \qquad (9)$$

$$\sum_{i \in D} \sum_{j \in C} x_{ijk} \leq 1, \quad \forall k \in K, \qquad (10)$$

$$\sum_{j \in D} \sum_{i \in C} x_{ijk} \leq 1, \quad \forall k \in K, \qquad (11)$$

$$\sum_{i \in N} f_{ijk} - \sum_{i \in N} f_{jik} = q_j, \quad \forall j \in N, \forall k \in K, \qquad (12)$$

$$\sum_{k \in K} q_j x_{ijk} \leq \sum_{k \in K} f_{ijk}, \quad \forall i \in N, \forall j \in D, \qquad (13)$$

$$f_{ijk} \leq (Q_k - q_i) x_{ijk}, \quad \forall i \in N, \forall j \in D, \forall k \in K, \qquad (14)$$

$$x_{ijk} \in \{0, 1\}. \qquad (15)$$

The objective function in eq. (3) represents the minimum logistics distribution cost, including the rental cost and variable cost of distribution vehicles. The objective function in eq. (4) represents the minimum carbon emission. The constraints in eqs. (5) and (6) indicate that each consumer is only served once by only one vehicle. The constraint in eq. (7) ensures the continuity of vehicle driving. The constraints in eqs. (8) and (9), respectively, indicate the capacity constraints and mileage constraints of vehicles. The constraints in eqs. (10) and (11) indicate the availability constraints of vehicles, that is, determining the vehicle's driving capacity whether it is used or not. The constraints in eqs. (12)–(14) indicate the load limit of the vehicle driving on the side. The constraint in eq. (15) indicates the 0-1 variables.

3. Algorithm Design

Genetic algorithm is a population-based search algorithm, which can get multiple nondominated solutions in one run. It is widely used in NP-hard problems such as VRP [22, 23]. The algorithm designed in this paper is as follows.

3.1. Decomposition of Multiobjective Optimization Problems.

The decomposition-based multiobjective optimization algorithm decomposes the multiobjective optimization problem into several single-objective subproblems to solve. The weighted sum method and Chebyshev method are the commonly used decomposition methods. The weighted sum method depends on the characteristics of the problem and is not suitable for solving the optimization problem with a nonconvex front. Therefore, this paper uses the Chebyshev method to solve the multiobjective problem line decomposition.

3.2. Expression of Solution.

Considering the coding characteristics of the MDVRP, natural number coding is adopted to avoid the conversion between decimal and binary and the Hamming cliff problem in binary coding due to the inability to estimate the interval of independent variables [24–26]. As shown in Figure 1, distribution center 1 and distribution center 2 each have two distribution vehicles. Each distribution vehicle performs the distribution task under the constraints of capacity and mileage. For example, the distribution vehicle 1 in distribution center 1 provides distribution services for consumers 4 and 7, and the distribution route is distribution center 1 $\longrightarrow$ 4 $\longrightarrow$ 7 $\longrightarrow$ distribution center 1.

3.3. Algorithm Steps.

In the initialization phase, the algorithm parameters, such as population size and maximum number of iterations, are determined, and the initial position of each individual in the population is initialized. In the specific initialization stage, the MDOVRP is transformed into multiple VRPs by distance clustering, and then, the vehicles are allocated and the driving route is designed.

Genetic evolution strategy: in order to expand the search scope and improve the optimization ability of the solution, the search operator used in this paper is a sequential crossover operator (as shown in Figure 2). Specifically, a gene sequence in parent 1 is randomly selected, and the gene sequence selected by parent 1 is deleted in parent 2. Child 1 inherits the gene sequence selected by parent 1, and the remaining genes are copied according to the gene sequence of parent 2. Similarly, child 2 can be obtained after the transformation and crossover of parent 1 and parent 2. Among them, the elite
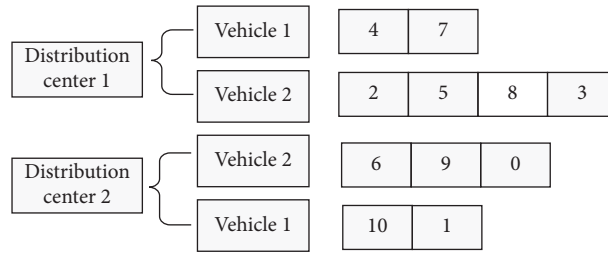
FIGURE 1: Expression of a solution.
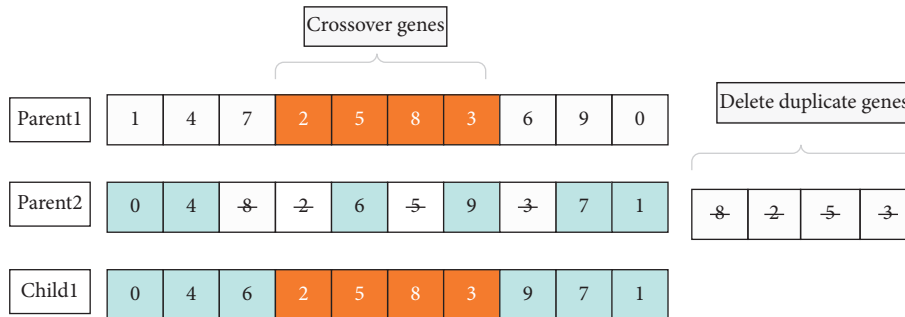
FIGURE 2: Crossover operations.

principle is introduced in the cross stage; that is, the elite individuals are selected for cross operation through the binary tournament principle. As shown in Figure 2, the genes selected by parent 1 are 2, 5, 8, and 3. The corresponding genes in parent 2 are deleted, and the genes 2, 5, 8, and 3 in parent 1 are obtained by offspring 1. The remaining genes are inserted in the sequence of genes in parent 2.

At the same time, in order to improve the diversity of drosophila individuals, three mutation operators, swap, insert, and invert, are used in the algorithm design. Among them, exchange mutation is to randomly select two different locations and then exchange customers in two locations, while shift mutation is to randomly select customers in one location and insert them into another random location. According to the coding method in this paper, the two locations selected by exchange mutation operation and shift mutation operation can be either two locations on the same subpath or two locations on the same subpath It can be two positions on different subpaths, so that different paths can smoothly realize "information exchange" and increase the search scope of solution space. Inversion mutation first randomly selects a subpath (i.e., a distribution route), then randomly selects two different locations on the subpath, and reverses the order of customers between the two locations.

4. Case Analysis

In this part, random initialization data are used for numerical experiments. Suppose there are four distribution centers, and each distribution center has two distribution

vehicles. The maximum carrying capacity and maximum driving distance of each vehicle are 120 and 400, respectively. The positions of 48 customers are randomly generated in the interval, and the demand of consumers is randomly generated in the interval. The distribution center and customer information are shown in Tables 1 and 2, respectively.

According to Suzuki [19], if $\rho^0 = 1$, $\rho^* = 2$; at the same time, Li et al. [21] pointed out that every liter of fuel consumption releases 2.32 kg of carbon emissions, the unit carbon emission cost is 2 yuan, the daily fixed cost of distribution vehicles is 500 yuan, and the unit variable cost of vehicle distribution is 7.56 yuan.

4.1. Open-Loop and Closed-Loop Distribution. In order to compare the differences between open-loop distribution and closed-loop distribution and to verify the effectiveness of the algorithm, the population 60 is set, the crossover rate and mutation rate are set to 0.9 and 0.1, respectively, and the number of iterations is 500. The algorithm is implemented in Java language and run on Intel (R) core (TM) i5-10210U CPU@1.6 GHz, the three algorithms are run 30 times independently, and the optimal results are shown in Figures 3 and 4.

4.2. Multiobjective Solutions. In Figure 5, it can be found that there is an inverse proportional relationship between logistics cost and carbon emission. Therefore, it can be said that, in the actual distribution, the carbon emission of logistics distribution vehicles can be realized by increasing a certain distribution cost; that is, there is a certain turnover

TABLE 1: Depot information.

No.	X-coor	Y-coor	Number of vehicles
1	4.159812	13.598909	2
2	21.397101	17.109821	2
3	−36.118921	42.980109	2
4	25.498080	−21.199321	2

TABLE 2: Customer information.

No.	X-coor	Y-coor	Demand
1	−29.729819	44.142146	10
2	−30.659302	5.460902	9
3	22.639003	5.470913	17
4	−13.169832	19.344121	6
5	−27.409815	38.320117	11
6	48.897125	6.268915	3
7	5.237919	22.259910	15
8	−44.987113	27.230912	18
9	−4.178921	−1.571234	15
10	23.029109	11.640331	15
11	25.276904	6.280612	20
12	−42.620903	−26.290111	7
13	−36.667907	10.138901	10
14	−20.668721	32.889810	8
15	−33.039931	6.570115	15
16	−41.379823	10.820217	20
17	−21.940114	27.590334	13
18	−35.188015	30.209832	15
19	18.601902	26.719131	12
20	−10.938610	43.208921	14
21	−37.760013	−33.329813	22
22	23.769120	29.076910	12
23	−43.029112	20.449001	9
24	−35.299321	−24.897812	17
25	−44.759801	14.367914	10
26	−19.328702	33.365912	10
27	7.397704	23.819004	16
28	37.397810	13.819821	18
29	−26.624912	43.336715	21
30	−38.559823	−3.709410	10
31	−16.779124	19.539005	12
32	−11.559014	11.619802	17
33	−46.547919	8.897315	17
34	16.228901	9.319218	23
35	1.789202	17.349817	15
36	−26.398132	29.530914	9
37	4.348926	14.679831	13
38	−20.670919	−23.129821	18
39	−22.826112	−9.807818	10
40	−31.097636	−18.619302	17
41	−7.848103	32.067509	17
42	11.876909	−24.927802	20
43	−18.927903	−23.726919	26
44	−11.918734	11.757612	13
45	29.839435	11.629012	20
46	12.267825	−35.808921	17
47	−37.927816	−21.607910	19
48	41.983101	−6.963910	12
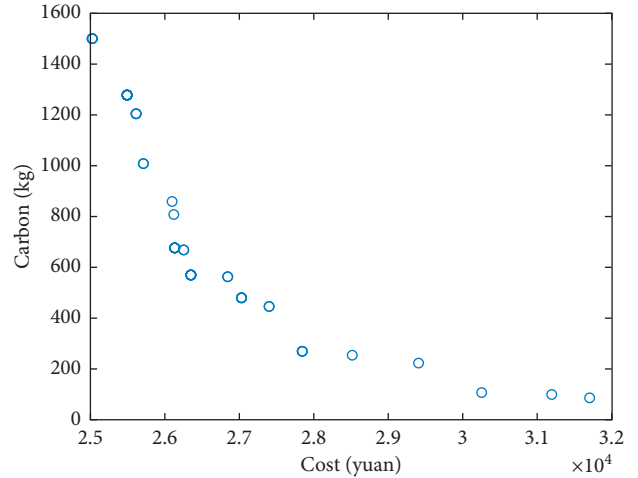
FIGURE 3: Pareto optimality.
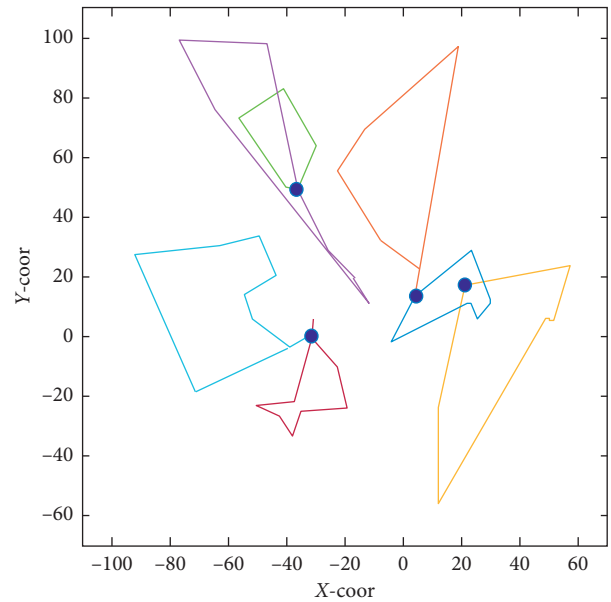
FIGURE 4: Routes for closed loop.

profit and loss phenomenon between the two. Logistics companies need to weigh the relationship between economic benefits and social benefits when making decisions. It is necessary to realize the unity of economic benefit and social benefit without hindering economic benefit.
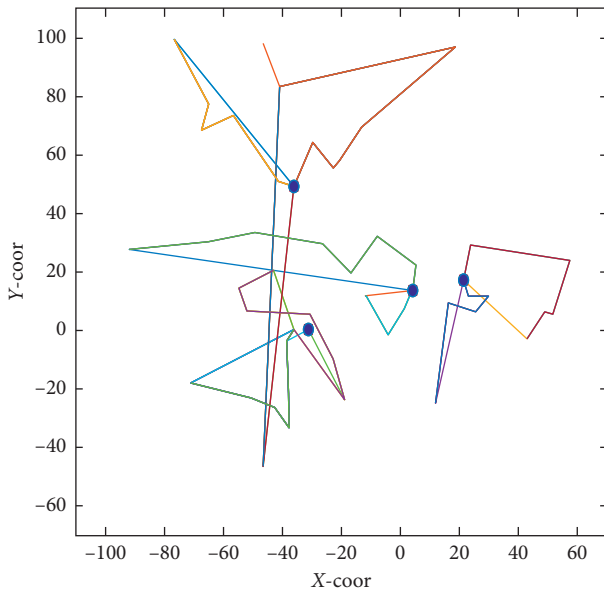
Figure 5: Routes for open loop.

5. Conclusions

With the rapid development of e-commerce industry, logistics distribution has become the difficulty of express delivery industry. Based on the traditional vehicle routing problem, considering the sharing economy and the hot spot of open-loop distribution, and considering the optimization of carbon emission in logistics distribution, this paper takes the driving distance and load capacity as the key factors to affect carbon emission, establishes a carbon emission model, and puts forward the most effective measures. To solve the dual objective problem of minimizing logistics distribution cost and minimizing logistics carbon emissions, a logistics distribution path planning model with multiple distribution stations is constructed. Aiming at the difficulties of the multiobjective solution and multidistribution station optimization problem coding, a strategy of clustering analysis based on customer distance is designed to schedule distribution vehicles in three steps, which ensures the satisfaction of customers' orders and the smooth operation. The elite crossover principle is used to avoid the solution falling into local optimum. The experimental results show that the solution results of the proposed logistics model and optimization algorithm can take into account the logistics cost and carbon emissions. This study provides theoretical and methodological guidance for the logistics distribution problem considering the open-loop distribution problem and carbon emission cost. At the same time, the algorithm also provides a way to solve this kind of NP-hard problem.

The next step is to study the logistics distribution optimization problem with uncertain characteristics and customer return and exchange.

Data Availability

Data are included in this paper.

Conflicts of Interest

The authors declare that they have no conflicts of interest.

Acknowledgments

References

[1] Y. He, M. Qi, F. Zhou, and J. Su, "An effective metaheuristic for the last mile delivery with roaming delivery locations and stochastic travel times," *Computers & Industrial Engineering*, vol. 145, Article ID 106513, 2020.

[2] L. Schrage, "Formulation and structure of more complex/realistic routing and scheduling problems," *Networks*, vol. 11, no. 2, pp. 229–232, 1981.

[3] M. Liu, X. Xu, J. Cao, and D. Zhang, "Integrated planning for public health emergencies: a modified model for controlling H1N1 pandemic," *Journal of the Operational Research Society*, vol. 71, no. 5, pp. 748–761, 2020.

[4] J. A. Garza-Reyes, B. Villarreal, V. Kumar, and J. Diaz-Ramirez, "A lean-TOC approach for improving emergency medical services (EMS) transport and logistics operations," *International Journal of Logistics Research and Applications*, vol. 22, no. 3, pp. 253–272, 2019.

[5] Z. Zhang, W. Yao, Y. Wang, C. Long, and X. Fu, "Wuhan and Hubei COVID-19 mortality analysis reveals the critical role of timely supply of medical resources," *Journal of Infection*, vol. 81, no. 1, pp. 147–178, 2020.

[6] F. Zhou, Y. He, P. Ma, and R. V. Mahto, "Knowledge management practice of medical cloud logistics industry: transportation resource semantic discovery based on ontology modelling," *Journal of Intellectual Capital*, vol. 22, no. 2, pp. 360–383, 2020.

[7] Y. He, X. Wang, Y. Lin, F. Zhou, and L. Zhou, "Sustainable decision making for joint distribution center location choice," *Transportation Research Part D-Transport and Environment*, vol. 55, pp. 202–216, 2017.

[8] Y. He, F. Zhou, M. Qi, and X. Wang, "Joint distribution: service paradigm, key technologies and its application in the context of Chinese express industry," *International Journal of Logistics Research and Applications*, vol. 23, no. 3, pp. 211–227, 2020.

[9] J. Brandão, "A tabu search algorithm for the open vehicle routing problem," *European Journal of Operational Research*, vol. 157, no. 3, pp. 552–564, 2004.

[10] F. Li, B. Golden, and E. Wasil, "The open vehicle routing problem: algorithms, large-scale test problems, and computational results," *Computers & Operations Research*, vol. 34, no. 10, pp. 2918–2930, 2007.

[11] P. P. Repoussis, C. D. Tarantilis, O. Bräysy, and G. Ioannou, "A hybrid evolution strategy for the open vehicle routing problem," *Computers & Operations Research*, vol. 37, no. 3, pp. 443–455, 2010.

[12] E. Cao, M. Lai, and H. Yang, "Open vehicle routing problem with demand uncertainty and its robust strategies," *Expert Systems With Applications*, vol. 41, no. 7, pp. 3569–3575, 2014.

[13] T. Bektaş and G. Laporte, "The pollution-routing problem," *Transportation Research Part B-Methodological*, vol. 45, no. 8, pp. 1232–1250, 2011.

[14] Y. Xiao and A. Konak, "The heterogeneous green vehicle routing and scheduling problem with time-varying traffic

congestion," *Transportation Research Part E-Logistics and Transportation Review*, vol. 88, pp. 146–166, 2016.

[15] T. Woensel, R. Creten, and N. Vandaele, "Managing the environmental externalities of traffic logistics: the issue of emissions," *Production and Operations Management*, vol. 10, no. 2, pp. 207–223, 2009.

[16] E. Demir, T. Bektaş, and G. Laporte, "A comparative analysis of several vehicle emission models for road freight transportation," *Transportation Research Part D: Transport and Environment*, vol. 16, no. 5, pp. 347–357, 2011.

[17] Y. Niu, Z. Yang, P. Chen, and J. Xiao, "Optimizing the green open vehicle routing problem with time windows by minimizing comprehensive routing cost," *Journal of Cleaner Production*, vol. 171, pp. 962–971, 2018.

[18] Y.-J. Kwon, Y.-J. Choi, and D.-H. Lee, "Heterogeneous fixed fleet vehicle routing considering carbon emission," *Transportation Research Part D: Transport and Environment*, vol. 81, pp. 89–971, 2013.

[19] Y. Suzuki, "A dual-objective metaheuristic approach to solve practical pollution routing problem," *International Journal of Production Economics*, vol. 176, pp. 143–153, 2017.

[20] E. Jabir, V. V. Panicker, and R. Sridharan, "Design and development of a hybrid ant colony-variable neighbourhood search algorithm for a multi-depot green vehicle routing problem," *Transportation Research Part D: Transport and Environment*, vol. 57, pp. 422–457, 2017.

[21] J. Li, D. Wang, and J. Zhang, "Heterogeneous fixed fleet vehicle routing problem based on fuel and carbon emissions," *Journal of Cleaner Production*, vol. 201, pp. 896–908, 2018.

[22] K. Deb, A. Pratap, S. Agarwal, and T. Meyarivan, "A fast and elitist multi-objective genetic algorithm: NSGA-II," *IEEE Transactions on Evolutionary Computation*, vol. 6, no. 2, pp. 182–197, 2002.

[23] H. Rai and A. Yadav, "Iris recognition using combined support vector machine and hamming distance approach," *Expert Systems With Applications*, vol. 41, no. 2, pp. 588–593, 2014.

[24] Y. He, X. Wang, F. Zhou, and Y. Lin, "Dynamic vehicle routing problem considering simultaneous dual services in the last mile delivery," *Kybernetes*, vol. 49, no. 4, pp. 1267–1284, 2019.

[25] F. Zhou, Y. He, and L. Zhou, "Last mile delivery with stochastic travel times considering dual services," *IEEE Access*, vol. 7, pp. 159013–159021, 2019.

[26] F. Zhou, M. K. Lim, Y. He, and S. Pratap, "What attracts vehicle consumers' buying: a saaty scale-based VIKOR (SSC-VIKOR) approach from after-sales textual perspective?" *Industrial Management and Data Systems*, vol. 120, no. 1, pp. 57–78, 2019.

Research Article

An Effective Heuristic for Multidepot Low-Carbon Vehicle Routing Problem

LiLing Liu [ID][1] **and LiFang Lai** [ID][2]

[1]Ji'an Vocational and Technology College, Ji'an, China
[2]Tsinghua Shenzhen International Graduate School, Shenzhen, China

Correspondence should be addressed to LiFang Lai; lai.lifang@sz.tsinghua.edu.cn

Low-carbon economy has been a hot research topic in recent years. This paper firstly considers the vehicle load weight, the key factors affecting the fuel consumption, to establish the fuel consumption model, and then constructs the vehicle routing planning model in the last mile delivery with multiple depots within time windows. In order to solve this problem, we improve the classical fruit fly algorithm which is easy to fall into the local optimum, and the improved fruit fly optimization algorithm is designed and integrated with genetic algorithm. Computational results show that our solution approach is capable of solving instances with up to 48 customers and 4 different depots. The effectiveness and efficiency of the model and multigroup fruit fly algorithm are verified through case study.

1. Introduction

In recent years, the scale of online retail market continues to expand in China, accounting for a large proportion of the total retail sales of social consumer goods. In 2018, the national online retail sales exceeded 9 trillion yuan, of which the online retail sales of physical goods reached 7 trillion yuan in China. At the same time, the rapid development of online shopping industry also puts forward higher requirements for the construction of e-commerce logistics distribution system. In the distribution process of online shopping goods, the "last mile" distribution speed directly affects the user experience of consumers [1]. Therefore, e-commerce enterprises strive to deliver products to consumers in the shortest time and are committed to the innovation and competition of terminal distribution mode. For example, Jingdong has set up 300000 terminal service outlets nationwide, launched various time effective distribution services such as "the next day delivery" and "the same day delivery", and upgraded the delivery time to half an hour through "jingzhunda" service; Suning has established 19 large-scale logistics centers and 60 regional logistics distribution centers nationwide, providing consumers with various services such as second delivery, half day delivery, on-time delivery, and next day delivery "Last mile" distribution service.

"Last mile" terminal distribution is essentially a multidepot vehicle routing problem (MDVRP). At present, MDVRP is becoming a research hotspot in academic circles. In order to minimize the total logistics cost, Renaud et al. [2] proposed MDVRP with vehicle capacity and mileage as constraints and designed tabu search algorithm to solve the problem. Mirabi et al. [3] studied MDVRP with the goal of minimum delivery time and proposed a random hybrid heuristic algorithm. Kuo et al. [4] designed a three-stage variable neighborhood search algorithm for MDVRP with loading cost. Liu et al. [5] studied MDVRP in the case of multicarrier cooperation and proposed a two-stage greedy heuristic algorithm. Salhi et al. [6] established the MDVRP model of heterogeneous vehicles and extended it on whether the stations are shared, the number limit of each type of vehicles, and the capacity limit of each depot. Oliveira et al. [7] transformed MDVRP into multiple VRPs for solving and designed a coevolutionary algorithm for solving.

With the rapid development of e-commerce logistics, the carbon emissions in distribution activities are also increasing, especially the high energy consumption and pollution. According to the International Energy Association report released in 2016, transportation is the second largest industry causing CO_2 emissions [8]. In February 2018, the general office of the State Council issued the opinions on promoting the collaborative development of e-commerce and express logistics, which advocated the construction of a low-carbon green logistics system. Therefore, well-known e-commerce enterprises such as Jingdong and Alibaba are also publishing their own green logistics plans. Bektas et al.'s [9] research shows that the carbon emission of distribution vehicles is mainly proportional to the fuel consumption, so the carbon emission can be reduced by optimizing the fuel consumption. Therefore, the author studies many factors affecting the fuel consumption of distribution vehicles and finds that the driving speed and driving distance of distribution vehicles will have a significant impact on the fuel consumption. Klapp et al. [1] proposed that vehicle load, engine type and size, road slope, and other factors have a certain relationship with fuel consumption of distribution vehicles and further affect carbon emissions. Considering the proportional relationship between fuel consumption and carbon emissions, Demir et al. [10] proposed that the fuel consumption can be effectively reduced by reasonably scheduling distribution vehicles and optimizing distribution routes, so as to reduce the fuel cost and carbon emissions in logistics distribution, ultimately reduce the logistics cost of distribution companies, and improve social benefits. Therefore, this paper attempts to consider the impact of fuel consumption on the distribution route in the "last mile" distribution and strive to achieve the purpose of reducing fuel consumption and carbon emissions by optimizing the distribution route.

In the e-commerce shopping environment, there is a lack of direct contact between customers and products, so consumers will have the insecurity of online shopping [11]. Funches's [12] research shows that when the waiting time of online shopping consumers exceeds the expected waiting time, customers tend to think that e-commerce does not keep its promise, resulting in lower consumption experience. Therefore, the timeliness of distribution has become the key to the logistics service quality of online shopping industry and the biggest problem faced by the development of e-commerce enterprises. When consumers place orders, e-commerce enterprises often promise to deliver goods to customers within a certain deadline. In this situation, the promised delivery mechanism of logistics distribution can provide psychological expectation of delivery time for consumers and enhance the security of online shopping. McNabb et al. [13] considered the limitation of delivery time window and established a distribution vehicle scheduling model based on ant colony algorithm, in order to reduce customer waiting time. Qureshi et al. [14] established a mixed-integer programming model considering the latest receiving time limit of customers.

So, how will the policy requirements of low-carbon emission affect the operation of terminal distribution?

Considering the latest receiving time limit of consumers, how should e-commerce enterprises optimize the terminal distribution path? In order to deeply analyze and answer the above questions, this paper attempts to propose an MDVRP considering the consumers' overtime payment penalty and fuel consumption optimization under the condition of consumers' latest receiving time and designs a multi-population fruit fly algorithm to solve the problem.

2. Formulation

2.1. Fuel Consumption Model.
Sahin et al. found that the fuel consumption cost accounts for 60% of total logistics cost with the full load of 20 t per 1000 km. In addition, the reduction of the fuel consumption is good for the environment [15]. Xiao et al. [16] and Suzuk [17] established the fuel consumption model considering travel distance and load which is two main factors affecting the fuel consumption through investigation, and the fuel consumption can reduce by optimizing the vehicle routing. Based on the above research, ρ^* and ρ^0 represent the fuel consumption rate with full load and empty load, respectively, Q stands for maximum loading capacity, and $\rho(Q_1)$ stands for fuel consumption per km with a load of Q_1 (kg):

$$\rho(Q_1) = \left(\rho^0 + \frac{\rho^* - \rho^0}{Q} Q_1 \right). \tag{1}$$

2.2. Problem Description and Formulation.
A city logistics distribution system has distribution centers and customers. In order to minimize the logistics cost and driving distance, it is required to arrange the distribution vehicles and their driving routes reasonably under the constraints of vehicle load and driving distance. In order to establish the mathematical model of the problem, the symbol is defined as follows.

2.2.1. Symbol Description

C: Set of consumers $C = \{v_1, v_2, \ldots, v_n\}$, representing a consumer

D: Set of distribution centers, $D = \{v_{n+1}, v_{n+2}, \ldots, v_{n+m}\}$

N: Set of consumers and distribution centers, $N = C \cup D$

A: Path set, $A = \{(i, j) \mid i, j \in N, i \neq j\}$

K: Set of distribution vehicles, $K = \{k_1, k_2, \ldots, k_S\}$, representing the total number of vehicles

ω: The empty net weight of the delivery vehicle

Q_k: The maximum loading capacity of distribution vehicles

L_k: The maximum driving distance of distribution vehicles k ($k \in K$)

q_i: Consumer demand ($0 \leq q_i \leq Q$, $i \in C$)

s_i: The service time of distribution vehicles in providing distribution services for consumers

T_i: The latest delivery time promised by e-commerce platform to consumers

d_{ij}: The Euclidean distance between any two points, $d_{ij} = d_{ji}$, $i, j \in N$, indicating the symmetric path

C_{hc}: Rental cost per vehicle

C_{vc}: Variable cost of vehicle unit mileage (mainly including variable cost such as driver's salary cost)

C_{fe}: Unit fuel consumption cost

C_{pi}: The delay penalty coefficient to be paid to consumers when delivery is delayed

V: Average speed of delivery vehicles

ρ_{ij}: Fuel consumption rate of vehicles on and between Routes (i, j)

x_{ijk}: 0–1 variable, if the vehicle passes by a route value of 1; otherwise it is zero

g_{ijk}: The amount of goods to be transported when the delivery vehicle passes the route (i, j)

a_i: Ready time of consumer i, $i \in C$

l_i: Delivery vehicle departure time from consumer i to next consumer j, $i, j \in C$

P_i: Delayed service time for consumer i, $i \in C$

2.2.2. Model considering Fuel Consumption. The model built in this paper is as follows:

$$\text{Min}\, C_{hc} \sum_{k \in K} \sum_{i \in D} \sum_{j \in C} x_{ijk} + C_{vc} \sum_{k \in K} \sum_{i \in N} \sum_{j \in N} d_{ij} x_{ijk}$$
$$+ C_{fc} \sum_{k \in K} \sum_{i \in N} \sum_{j \in N} \left(\rho^0 + \frac{\rho^* - \rho^0}{Q} f_{ijk} \right) d_{ij} x_{ijk} + C_{pi} \sum_{i \in C} P_i, \tag{2}$$

$$\text{s.t.} \sum_{k \in K} \sum_{j \in N} x_{ijk} = \sum_{k \in K} \sum_{i \in N} x_{ijk} = 1, \quad \forall i, j \in C, \tag{3}$$

$$\sum_{i \in N} x_{ihk} - \sum_{j \in N} x_{hjk} = 0, \quad \forall k \in K; h \in N, \tag{4}$$

$$\sum_{i \in N} q_i \sum_{j \in N} x_{ijk} \leq Q_k, \quad \forall k \in K, \tag{5}$$

$$\sum_{i \in N} \sum_{j \in N} d_{ij} x_{ijk} \leq T_k, \quad \forall k \in K, \tag{6}$$

$$q_j x_{ijk} \leq g_{ijk} \leq (Q - q_i) x_{ijk}, \quad \forall (i, j) \in A, k \in K, \tag{7}$$

$$lpta_j \geq l_j + \sum_{k \in K} \sum_{i \in N} \frac{x_{ijk} d_{ij}}{V}, \quad \forall j \in C, \tag{8}$$

$$a_i + s_i \leq l_i, \quad \forall i \in C, \tag{9}$$

$$P_i \geq a_i - T_i, \quad \forall i \in C, \tag{10}$$

$$x_{ijk} \in \{0, 1\}, \quad \forall i, j \in N, k \in K, \tag{11}$$

$$a_i, p_i, l_i, f_{ijk} \geq 0, \quad \forall i, j \in C; k \in K. \tag{12}$$

Formula (2) denotes the minimization objective function; formula (3) denotes that every consumer is served only once by a vehicle; formula (4) ensures the continuity of the vehicle's driving path; formulas (5) and (6) denote the capacity constraints and travel time constraints of the vehicle; formula (7) denotes the weight constraints on each segment of the driving path during the vehicle's driving process; formulas (8) and (9) indicate the actual delivery time limit; formula (10) indicates the delay delivery time limit of a consumer; formula (11) indicates the 0–1 variable constraint; formula (12) indicates the nonnegative limit of a variable.

3. Improved Fruit Fly Algorithm Based on Multiple Populations

VRP is a NP-hard problem. Researchers usually use heuristic or metaheuristic algorithms to solve [18–20]. This model involves multiple distribution centers and fuel consumption optimization, which make the solution more difficult [21]. Pan [22] proposed a fruit fly optimization (FFO) algorithm inspired by fruit fly feeding behavior. Because of its few parameters and fast convergence, it has become an important method to solve optimization problems [23, 24], which makes it possible to solve this model effectively.

FFO simulated the process of fruit fly using sensitive olfactory and visual search for food, including three phases: population initialization, olfactory foraging, and visual foraging. Firstly, the algorithm parameters, the number of populations, and the initialization location of fruit fly are initialized; second, a new fruit fly individual is obtained by simulating its olfactory feeding behavior; then, the optimal fruit fly individual location is updated by simulating the behavior of fruit fly through visual feeding; finally, when the iteration process reaches certain criteria, the output algorithm solves the result. However, fruit fly population has the disadvantage of easily falling into local optimum [25], so this paper tries to improve it. Based on the basic FFA, an improved fruit fly optimization algorithm (IFFO) based on multiple populations is designed to solve this model.

3.1. Coding. Considering that MDVRP is a typical discrete optimization problem, this paper uses natural number encoding to represent the scheduling scheme and sets up a scheduling scheme $X = (x_1^T, x_2^T, \ldots, x_k^T)^T$, where k represents the number of vehicles, $x_k = (0, r_1, r_2, \ldots, r_s, 0)$ represents the route of the first vehicle, and 0 represents the subscript of the depot. In the specific encoding phase, MDVRP is first converted into multiple VRPs to solve in parallel, then each customer is assigned a distribution vehicle, and the driving route of the distribution vehicle is designed. Assuming that there are three depots, you can see that the number of distribution vehicles is not the same at

each depot; that is, the number of distribution routes is also different. For example, there are two vehicles participating in the distribution, one of which provides distribution services for consumer 3, consumer 1, and consumer 7, and the distribution routes are Depot 1 ⟶ Consumer 3 ⟶Consumer 1 ⟶ Consumer 7 ⟶ Depot 1, or if there is only one vehicle at depot 2 participating in the distribution, the distribution routes are Depot 2 ⟶ Consumer 8 ⟶ Consumer 9 ⟶ Consumer 11 ⟶ Depot 2 (as shown in Figure 1).

3.2. Multiple-Population Methods.

The multipopulation method, which enables the algorithm to obtain more than one optimal solution in one run, has been widely used in NP-hard problem such as flow shop scheduling [26, 27]. In order to overcome the disadvantage of local optimum in the process of solving fruit fly algorithm, this paper divides the individuals in fruit fly population into several subpopulations by using the strategy of simultaneous evolution of multiple populations. At the same time, in order to effectively utilize the advantageous information of the dominant solution in each subpopulation and strengthen the communication and cooperation among subpopulations, interactive strategies between subpopulations are designed during the iteration process of fruit fly algorithm. Slightly, the search efficiency and accuracy of the optimal solution are enhanced by information interaction between the optimal individuals in the subpopulation. Figure 2 shows the strategy for information exchange between subpopulations. In subpopulation 1, a fruit fly individual is randomly selected, such as one in neutron population 1, as parent 1, and then probability, and selecting individuals in the same population, individuals in other subpopulations, and globally optimal individuals to perform crossover operations. This way of information interaction between subpopulations improves the ability to search for the optimal solution to the problem. At the same time, the excellent genes of the best individuals in the population are transferred to the current individuals with a certain probability to achieve rapid convergence.

3.3. Genetic Evolution Strategies in Fruit Fly Individuals.

In the original fruit fly algorithm, individual updates are obtained by constant comparisons of old and new optimal values, which can easily lead to premature convergence. In the IFFO designed in this paper, a crossover operation in the genetic algorithm is introduced to obtain new fruit fly individuals. For this reason, in order to improve the search ability of the solution, a crossover strategy for fruit fly individuals was designed according to their coding style. As shown in Figure 3, a gene was randomly selected from parent 1 and parent 2, the selected parent 1 gene was deleted from parent 2, and then the selected gene from parent 1 was inserted into parent 2, where the insertion position was the position where the function value of parent 2 was lowered the most, resulting in offspring 1. Similarly, progeny 2 can be obtained.

At the same time, in order to improve the diversity among fruit fly individuals, swap, insert, and invert mutators were used in IFFO. The three mutators are shown
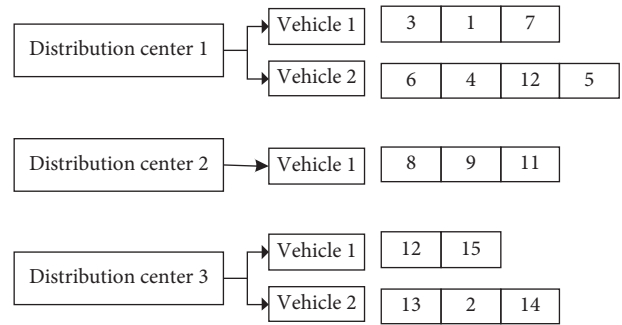
Figure 1: Coding diagram.
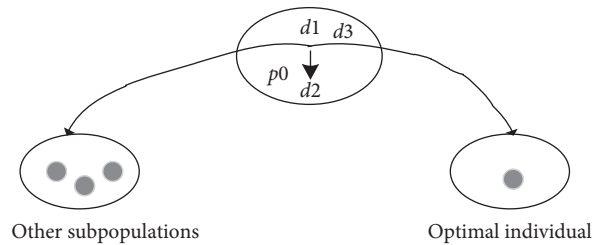
Figure 2: Information exchange between subpopulations.

in Figure 4. The swap mutation is to randomly select two different locations and then swap the consumers at two locations. The shift mutation is to randomly select the consumers at one location and insert them into another random location. According to the encoding method in this paper, the two locations selected by the swap mutation operation and the shift mutation operation can be both locations on the same subpath. It can also be two locations on different subpaths, which enables different paths to smoothly achieve "information exchange" and increase the search scope of solution space. Inverted mutation first randomly selects a subpath (that is, a distribution route), then randomly selects two different locations on the subpath, and flips the order of consumers between the two locations.

New fruit fly individuals generated by crossover and mutation are placed in the corresponding population, and better individuals with this subproblem are inherited to the next generation at the selection stage based on elite retention strategies.

3.4. Improved Fruit Fly Algorithm Steps

3.4.1. Initialization.

The initialization stage is mainly divided into two steps: the initialization of algorithm parameters and the initialization of the individual population.

> Step 1: the main parameters of the algorithm are as follows: the number of fruit fly subpopulations (N), the number of fruit fly individuals of subpopulations (popsize), the number of iterations of the algorithm (MaxIter), and the interaction criteria of subpopulations (Interaction).
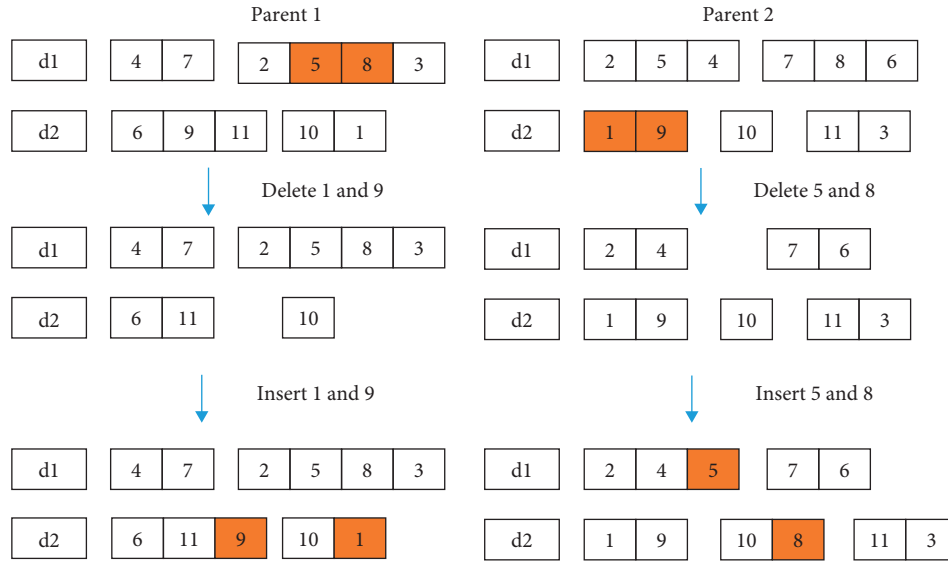
FIGURE 3: Crossover operation.
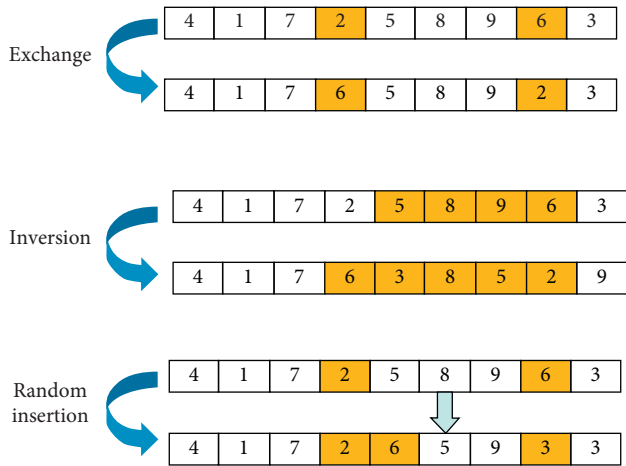
FIGURE 4: Exchange, inversion, and random insertion operation.

Step 2: in order to expand the search scope of the solution, this paper adopts the method of random initialization. Specifically, when distributing distribution vehicles to consumers, a distribution vehicle is randomly selected. If a distribution vehicle is selected, the consumer is assigned to the distribution vehicle, and the distribution vehicle is assigned to the distribution vehicle. When the capacity and driving path of the distribution vehicle exceed the maximum constraints, another vehicle is randomly selected again until all consumers get the distribution vehicle to perform the distribution task, and then the initialization phase of the individual population is completed.

3.4.2. Olfactory Search and Visual Search Stage. In the olfactory search phase, for each subpopulation, *popsize* new fruit fly individuals are generated by the genetic evolution strategy described in Section 3.3. If the new fruit fly

individual *r* generated by the genetic evolution strategy at the current position (X^r_{currt}) of the subpopulation is set as ($X^r_1, X^r_2, \ldots, X^r_{\text{popszie}}$), and the optimal individual in the new individuals is X^r_{best}, then the updating of fruit fly individuals is performed in the visual search stage. If the objective function value is $f(X^r_{\text{best}}) < f(X^r_{\text{currt}})$, the current position X^r_{currt} is replaced by the optimal position X^r_{best}; that is $X^r_{\text{currt}} = X^r_{\text{best}}$.

3.4.3. The Stage of Interaction between Subpopulations. For the population-based intelligent optimization algorithm, the communication and cooperation among individuals in the population can expand the search space of the solution, accelerate the convergence speed, and improve the efficiency and accuracy of the algorithm. The multipopulation fruit fly algorithm designed in this paper has multiple subpopulations. Each subpopulation updates the solution of the population, respectively, which is a lack of communication between the populations. So, it is proposed to use the subpopulation communication mechanism shown in Figure 2. In the iterative process of the fruit fly algorithm, after Interaction, the interaction between the populations is performed once. Selectively introducing the excellent genes of the external population or the optimal individual for the subpopulation can improve the searchability for the optimal solution of the problem.

4. Case Study

In order to verify the effectiveness of the model and IFFO algorithm, this paper takes an e-commerce logistics company as an example for numerical simulation. The logistics company has four distribution centers, the maximum carrying capacity of each distribution vehicle is 200 kg, the maximum driving distance of each vehicle is 500 km, the rental cost of each distribution vehicle is 600 yuan/vehicle, the variable cost of unit mileage is 5 yuan/km, and the fuel

cost is 7.5 yuan/L. Four depots need to provide logistics distribution services to 48 consumers. Euclidean distance is used to represent the distance between any points. Given the demand of each consumer, it is assumed that the logistics distribution vehicles start from the morning of that day to carry out the distribution task and promise to deliver the goods before that day, allowing a certain delay in distribution, but not more than the latest. The average speed of the vehicle is 60 km/h. It is required to reduce the cost of logistics distribution and customers' delayed receiving time and design reasonable scheduling and logistics distribution routes. The coordinates of depot information (unit: km) are (4.163, 13.559), (21.387, 17.105), (−36.118, 49.097), and (−31.201, 0.235), and the consumer information is shown in Table 1.

4.1. Performance Analysis of IFFO.

4.1. Performance Analysis of IFFO. Genetic algorithm (abbreviated form GA) has the advantage of fast convergence in solving NP-hard problems, so it has become an important method for solving vehicle routing problems [28–31]. In order to verify the effectiveness of IFFO, the paper compares the solution results of FFO, IFFO, and GA and draws the distribution route map of the three algorithms. Among them, the population number of GA and FFO is set to 60, and the number of IFFO subpopulations is set to 5. Each population has 12 individuals, the crossover rate and mutation rate of GA are set to 0.9 and 0.1, respectively, IFFA carries out information interaction among subpopulations every 10 iterations, and the total number of iterations of the three algorithms is 500. The algorithm programs are written in C++ programming language and run on Intel (R) Core (TM) i5−8250@1.6 GHz on a Dell laptop with 8.0 GB CPU and 8.0 GB memory. Each of the three algorithms runs 20 times independently, and the optimal calculation results are shown in Figures 5–7.

From the analysis of Figures 5 to 7, we can see that both GA and FFO get 8 distribution routes after the operation, while in this paper the multipopulation fruit fly algorithm IFFA designed gets 7 distribution routes after the operation, because it reduces the use of a distribution vehicle; that is, it reduces the fixed cost, which further shows that the reasonable design of logistics distribution routes can reduce the distribution cost.

As can be seen from Figure 8, compared with GA, the basic logistics cost, fuel cost, and overtime compensation cost are reduced by 25.5%, 32.8%, and 23.3%, respectively. Compared with the basic fruit fly algorithm FFO, the basic logistics cost and fuel cost calculated by IFFO are reduced by 8.4% and 5.1%, respectively, and the overtime compensation penalty is increased by 11.6%. This is mainly because IFFO has obtained 7 distribution routes. Because of the lack of a distribution vehicle, the distribution task of each vehicle is increased, the waiting time of customers is increased, and the amount of delay penalty is increased. By analyzing Figure 9, it can be found that in the iterative process of the algorithm, the gap between the solution results of GA and FFO and that of IFFO is increasing, which indicates that the multipopulation mechanism proposed in this paper can expand the search

TABLE 1: Customer information.

No.	X-axis (km)	Y-axis (km)	Demand (kg)
1	−29.730	64.136	12
2	−30.664	5.463	8
3	51.642	5.469	16
4	−13.17	69.336	5
5	−67.413	68.323	12
6	48.907	6.274	5
7	5.243	22.260	13
8	−65.002	77.234	20
9	−4.175	−1.569	13
10	23.029	11.639	18
11	25.482	6.287	7
12	−42.615	−26.392	6
13	−76.672	99.341	9
14	−20.673	57.892	9
15	−52.039	6.567	4
16	−41.376	50.824	25
17	−91.943	27.588	5
18	−65.118	30.212	17
19	18.597	96.716	3
20	−40.942	83.209	16
21	−37.756,	−33.325	25
22	23.767	29.083	21
23	−43.030	20.453	14
24	−35.297	−24.896	19
25	−54.755	14.368	14
26	−49.329	33.374	6
27	57.404	23.822	16
28	−22.754	55.408	9
29	−56.622	73.340	20
30	−38.562	3.705	13
31	−16.779	19.537	10
32	−11.560	11.615	16
33	−46.545	97.974	19
34	16.229	9.320	22
35	1.294	7.349	14
36	−26.404	29.529	10
37	4.352	14.685	11
38	−50.665	−23.126	15
39	−22.833	−9.814	13
40	−71.100	−18.616	15
41	−7.849	32.074	8
42	11.877	−24.933	22
43	−18.927	−23.730	24
44	−11.920	11.755	3
45	29.840	11.633	25
46	12.268	−55.811	19
47	−37.933	−21.613	21
48	42.883	−2.966	10

range of the solution and improve the optimization speed and accuracy of the solution.

4.2. Consider the Importance of Carbon Emissions.

4.2. Consider the Importance of Carbon Emissions. Figure 10 shows that the cost of logistics distribution in an open-loop distribution scenario is reduced by 19.70% compared with the total cost of closed-loop distribution. That is, after the distribution task is completed, the distribution vehicle does not have to return to the original distribution center but can be
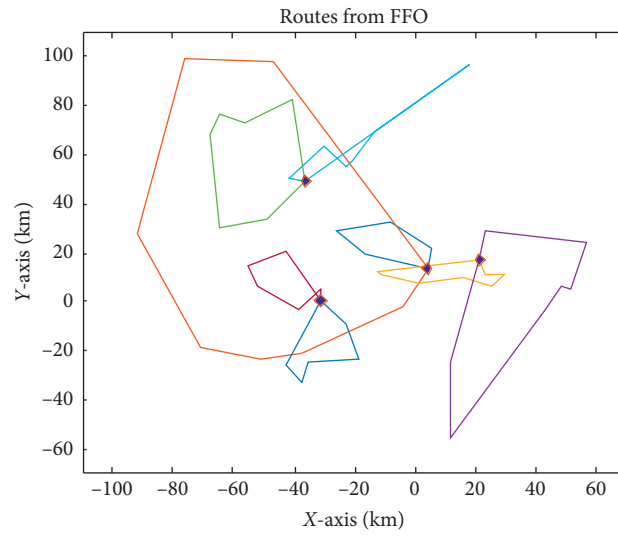
Figure 5: Routes from FFO.
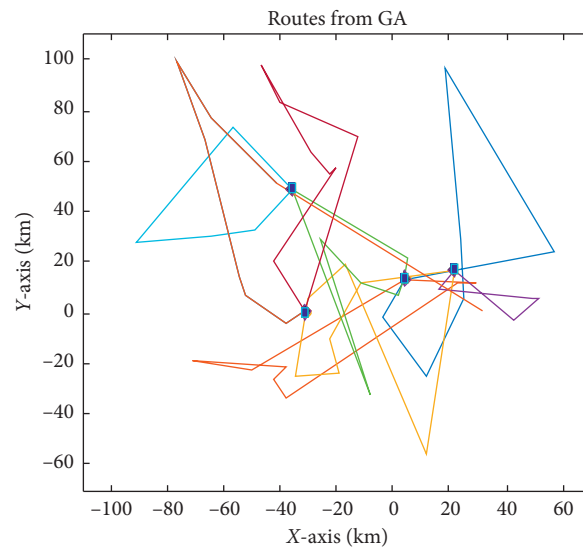
Figure 6: Routes from GA.
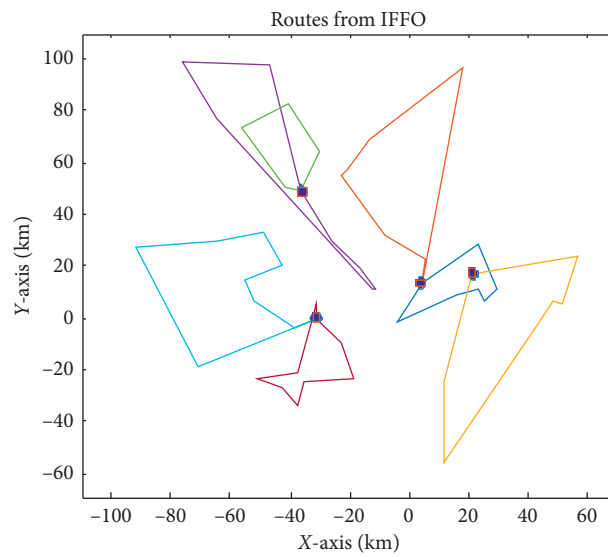
Figure 7: Routes from IFFO.
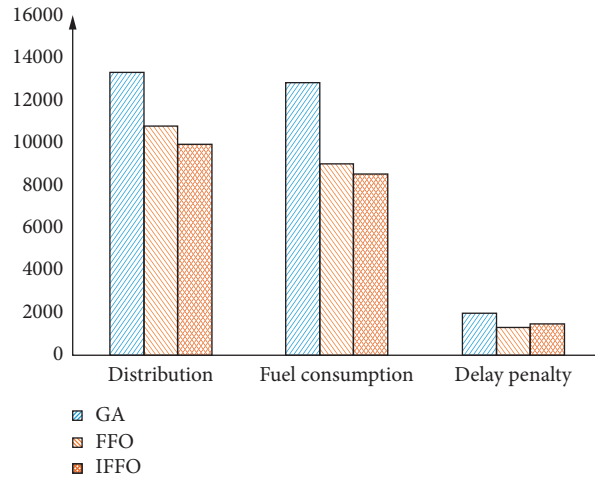
FIGURE 8: Cost comparison among 3 algorithms.
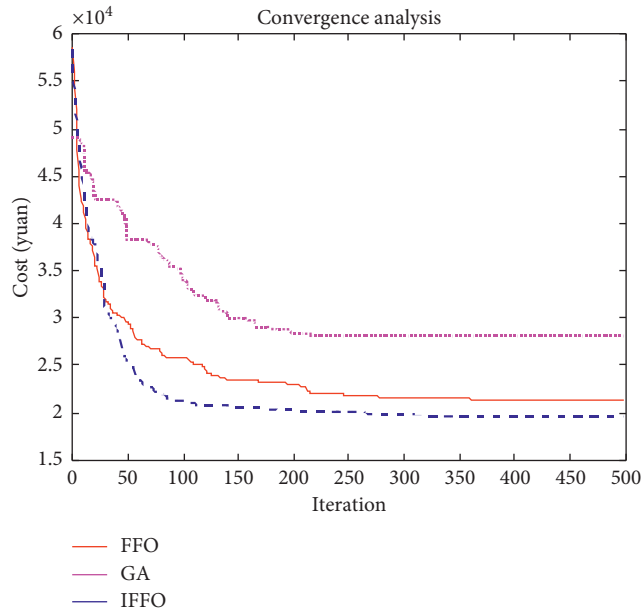
FIGURE 9: Convergence analysis among 3 algorithms.
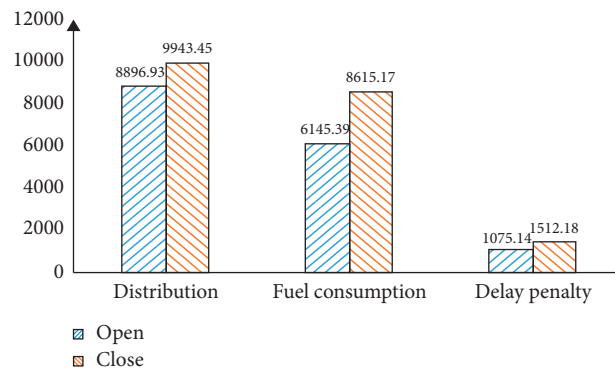
FIGURE 10: Cost comparison between open and close loop.

assigned nearby. This is mainly because when the open-loop distribution is completed, the vehicle does not have to return to the distribution center, thus avoiding empty driving of the vehicle, thus reducing the fuel consumption cost. Thus, the total distribution cost has been reduced, which indicates that in the actual logistics distribution process, the empty vehicles should be minimized, the full load rate of vehicles should be increased, and the logistics distribution costs such as fuel consumption costs should be reduced through reasonable optimization of distribution routes.

5. Conclusion

In this paper, the driving distance and load of distribution vehicles are considered as the key factors affecting fuel consumption, a fuel consumption model is established, and a terminal distribution route planning model with multiple depots is constructed under the time limit of receipt by consumers, and the coding method of the problem is designed. Considering that the traditional fruit fly algorithm is easy to fall into local optimum, multiple fruit fly algorithms are designed. The multipopulation evolution mechanism of simultaneous population evolution and the interaction mechanism between individual subpopulations are designed. The model is solved by genetic algorithm, fruit fly algorithm, and improved fruit fly algorithm. The effectiveness of the improved multipopulation fruit fly algorithm is verified, the cost of logistics distribution is reduced, and the vehicle routing rules of multiple depots with delivery time constraints for customers are solved. NP-hard problems such as delimitation problems provide a way to solve them.

Admittedly, this paper also has some drawbacks, such as whether the customer's order can be dynamically changed, whether the customer's time window can be changed, and so on. This will be the work to be studied hereinafter.

Data Availability

All data used to support the findings of the study are included within the article.

Conflicts of Interest

The authors declare that they have no conflicts of interest.

Acknowledgments

References

[1] M. A. Klapp, A. L. Erera, and A. Toriello, "The dynamic dispatch waves problem for same-day delivery," *European Journal of Operational Research*, vol. 271, no. 2, pp. 519–534, 2018.

[2] J. Renaud, F. F. Boctor, and G. Laporte, "An improved petal heuristic for the vehicle routeing problem," *Journal of the Operational Research Society*, vol. 47, no. 2, pp. 329–336, 1996.

[3] M. Mirabi, S. M. T. Fatemi Ghomi, and F. Jolai, "Efficient stochastic hybrid heuristics for the multi-depot vehicle routing problem," *Robotics and Computer-Integrated Manufacturing*, vol. 26, no. 6, pp. 564–569, 2010.

[4] Y. Kuo and C.-C. Wang, "A variable neighborhood search for the multi-depot vehicle routing problem with loading cost," *Expert Systems With Applications*, vol. 39, no. 8, pp. 6949–6954, 2012.

[5] R. Liu, Z. Jiang, R. Y. K. Fung, F. Chen, and X. Liu, "Two-phase heuristic algorithms for full truckloads multi-depot capacitated vehicle routing problem in carrier collaboration," *Computers & Operations Research*, vol. 37, no. 5, pp. 950–959, 2010.

[6] S. Salhi, A. Imran, and N. A. Wassan, "The multi-depot vehicle routing problem with heterogeneous vehicle fleet: formulation and a variable neighborhood search implementation," *Computers & Operations Research*, vol. 52, pp. 315–325, 2014.

[7] F. B. de Oliveira, R. Enayatifar, H. Javedani Sadaei, F. Gadelha Guimarães, and J.-Y. Potvin, "A cooperative coevolutionary algorithm for the multi-depot vehicle routing problem," *Expert Systems With Applications*, vol. 43, pp. 117–130, 2016.

[8] International Energy Agency, CO_2 *Emissions from Fuel Combustion-Highlights*, International Energy Agency (IEA), Paris, France, 2016.

[9] T. Bektaş and G. Laporte, "The pollution-routing problem," *Transportation Research Part B-Methodological*, vol. 45, no. 8, pp. 1232–1250, 2011.

[10] E. Demir, T. Bektaş, and G. Laporte, "A comparative analysis of several vehicle emission models for road freight transportation," *Transportation Research Part D: Transport and Environment*, vol. 16, no. 5, pp. 347–357, 2011.

[11] Y. He, F. Zhou, M. Qi, and X. Wang, "Joint distribution: service paradigm, key technologies and its application in the context of Chinese express industry," *International Journal of Logistics Research and Applications*, vol. 23, no. 3, pp. 211–227, 2020.

[12] V. Funches, "The consumer anger phenomena: causes and consequences," *Journal of Services Marketing*, vol. 25, no. 6, pp. 420–428, 2011.

[13] M. E. McNabb, J. D. Weir, R. R. Hill, and S. N. Hall, "Testing local search move operators on the vehicle routing problem with split deliveries and time windows," *Computers & Operations Research*, vol. 56, pp. 93–109, 2015.

[14] A. G. Qureshi, E. Taniguchi, and T. Yamada, "An exact solution approach for vehicle routing and scheduling problems with soft time windows," *Transportation Research Part E: Logistics and Transportation Review*, vol. 45, no. 6, pp. 960–977, 2009.

[15] B. Sahin, H. Yilmaz, Y. Ust, A. F. Guneri, and B. Gulsun, "An approach for analysing transportation costs and a case study," *European Journal of Operational Research*, vol. 193, no. 1, pp. 1–11, 2009.

[16] Y. Xiao, Q. Zhao, I. Kaku, and Y. Xu, "Development of a fuel consumption optimization model for the capacitated vehicle routing problem," *Computers & Operations Research*, vol. 39, no. 7, pp. 1419–1431, 2012.

[17] Y. Suzuki, "A dual-objective metaheuristic approach to solve practical pollution routing problem," *International Journal of Production Economics*, vol. 176, pp. 143–153, 2016.

[18] R. Liu, X. Xie, V. Augusto, and C. Rodriguez, "Heuristic algorithms for a vehicle routing problem with simultaneous

delivery and pickup and time windows in home health care," *European Journal of Operational Research*, vol. 230, no. 3, pp. 475–486, 2013.

[19] F. Zhou, Y. He, P. Ma, and R. V. Mahto, "Knowledge management practice of medical cloud logistics industry: transportation resource semantic discovery based on ontology modelling," *Journal of Intellectual Capital*, vol. 22, no. 2, pp. 360–383, 2020.

[20] F. Zhou, M. K. Lim, Y. He, and S. Pratap, "What attracts vehicle consumers' buying," *Industrial Management & Data Systems*, vol. 120, no. 1, pp. 57–78, 2019.

[21] J. R. Montoya-Torres, J. López Franco, S. Nieto Isaza, H. Felizzola Jiménez, and N. Herazo-Padilla, "A literature review on the vehicle routing problem with multiple depots," *Computers & Industrial Engineering*, vol. 79, pp. 115–129, 2015.

[22] W.-T. Pan, "A new fruit fly optimization algorithm: taking the financial distress model as an example," *Knowledge-Based Systems*, vol. 26, no. 26, pp. 69–74, 2012.

[23] Q.-K. Pan, H.-Y. Sang, J.-H. Duan, and L. Gao, "An improved fruit fly optimization algorithm for continuous function optimization problems," *Knowledge-Based Systems*, vol. 62, no. 62, pp. 69–83, 2014.

[24] X. Zhu, A. Garcia-Diaz, M. Jin, and Y. Zhang, "Vehicle fuel consumption minimization in routing over-dimensioned and overweight trucks in capacitated transportation networks," *Journal of Cleaner Production*, vol. 85, pp. 331–336, 2014.

[25] H.-Z. Li, S. Guo, C.-J. Li, and J.-Q. Sun, "A hybrid annual power load forecasting model based on generalized regression neural network with fruit fly optimization algorithm," *Knowledge-Based Systems*, vol. 37, pp. 378–387, 2013.

[26] Y. Marinakis and M. Marinaki, "A hybrid multi-swarm particle swarm optimization algorithm for the probabilistic traveling salesman problem," *Computers & Operations Research*, vol. 37, no. 3, pp. 432–442, 2010.

[27] J. J. Liang, Q.-K. Pan, C. Tiejun, and L. Wang, "Solving the blocking flow shop scheduling problem by a dynamic multi-swarm particle swarm optimizer," *The International Journal of Advanced Manufacturing Technology*, vol. 55, no. 5-8, pp. 755–762, 2011.

[28] F. Zhou, Y. He, and L. Zhou, "Last mile delivery with stochastic travel times considering dual services," *IEEE Access*, vol. 7, pp. 159013–159021, 2019.

[29] Y. He, M. Qi, F. Zhou, and J. Su, "An effective metaheuristic for the last mile delivery with roaming delivery locations and stochastic travel times," *Computers & Industrial Engineering*, vol. 145, Article ID 106513, 2020.

[30] Y. He, X. Wang, F. Zhou, and Y. Lin, "Dynamic vehicle routing problem considering simultaneous dual services in the last mile delivery," *Kybernetes*, vol. 49, no. 4, pp. 1267–1284, 2019.

[31] Y. He, X. Wang, Y. Lin, F. Zhou, and L. Zhou, "Sustainable decision making for joint distribution center location choice," *Transportation Research Part D: Transport and Environment*, vol. 55, pp. 202–216, 2017.

[32] R. Dekker, J. Bloemhof, and I. Mallidis, "Operations Research for green logistics-an overview of aspects, issues, contributions and challenges," *European Journal of Operational Research*, vol. 219, no. 3, pp. 671–679, 2012.

Research Article

Contactless Distribution Path Optimization Based on Improved Ant Colony Algorithm

Feng Wu [ID]

College of Information Engineering, Xinyang Agriculture and Forestry University, Xinyang 464000, China

Correspondence should be addressed to Feng Wu; 3306792320@qq.com

In the context of the normalization of the epidemic, contactless delivery is becoming one of the most concerned research areas. In the severe epidemic environment, due to the frequent encounter of bayonet temperature measurement, road closure, and other factors, the real-time change frequency of each traffic information is high. In order to improve the efficiency of contactless distribution and enhance user satisfaction, this paper proposes a contactless distribution path optimization algorithm based on improved ant colony algorithm. First of all, the possible traffic factors in the epidemic environment were analyzed, and the cost of each link in the distribution process was modeled. Then, the customer satisfaction is analyzed according to the customer service time window and transformed into a cost model. Finally, the total delivery cost and user satisfaction cost were taken as the optimization objectives, and a new pheromone updating method was adopted and the traditional ant colony algorithm was improved. In the experiment, the effectiveness of the proposed model and algorithm is verified through the simulation optimization and comparative analysis of an example.

1. Introduction

Contactless distribution refers to placing goods in a designated location, such as delivery cabinets and doorsteps. Customers then pick up the goods themselves, thus achieving contactless delivery of goods. Compared with traditional delivery methods, contactless delivery reduces the contact between people [1]. During the COVID-19 outbreak, contactless delivery effectively reduced the risk of cross-infection between delivery personnel and customers. In the context of the normalization of the epidemic, the demand for contactless delivery is increasing day by day. When the epidemic control policy is strict, considering the factors of safety and necessity of life, most of the goods distributed without contact are fresh goods. Therefore, the contactless distribution of fresh goods has important research significance. Reasonable planning of fresh goods logistics distribution path not only can reduce the logistics distribution cost and ensure the freshness of fresh products, but also can increase customer satisfaction and enhance the competitiveness of enterprises.

Since the vehicle routing problem was proposed [2], a large number of research achievements have been generated. Desrocherst and Verhoog [3] proposed a hybrid vehicle path model. Solomon and Desrosiers incorporated the concept of time windows into the vehicle routing problem [4]. On this basis, Jabali et al. solved the time window constraint [5] by punishing the cost, introduced the concepts of soft time window and hard time window and established the vehicle routing problem of soft time window. In recent years, advocating green development, with the goal of reducing energy consumption and carbon emissions, green vehicle routing has attracted the attention of academic circles. Tabu search algorithms based on particle swarm optimization (PSO), simulated annealing, and path partition are often used to solve the green vehicle routing problem model [6]. In order to highlight the impact of vehicle energy consumption and carbon emissions on the environment, literature [7] puts forward the problem of pollution path. Literature [8] analyzed the influence of vehicle departure time on vehicle speed, built a time-dependent single target pollution path model, and solved it by using tabu search algorithm and

departure time and speed optimization algorithm, respectively. Literature [9] designed a Wolf swarm algorithm to solve the vehicle routing problem of multiple distribution centers. Yan et al. [10] studied the two-dimensional packing vehicle routing problem including time window and multiple vehicle field factors and proposed the quantum particle swarm optimization algorithm to solve the problem. Literature [11] designed a variable neighborhood search algorithm for solving the VRP model. Literature [12] used dynamic programming algorithm to solve the vehicle routing problem.

The research on the contactless distribution path of fresh goods is mainly applied to the field of cold chain logistics and transportation. At present, there have been a series of research results in the field of cold chain logistics and transportation. Tarantilis and Kiranoudis [13] took the distribution of meat and milk in Greece as an example to study the vehicle routing problem of open cold chain logistics distribution with multiple models and multiple distribution centers. Amorim et al. [14] constructed a multitime window and multivehicle routing problem for a food distribution problem in Portugal. Yang and Sun [15] studied the VRP model of perishable goods in cold chain logistics and optimized the distribution path by using genetic algorithm. Zhang et al. [16] designed a mathematical model of vehicle path of cold chain logistics with multiple depots and models and solved it through genetic algorithm and elite selection method. Ma et al. [17] studied the vehicle routing optimization model of cold chain logistics based on random demand. Lan et al. [18] analyzed the impact of urban road congestion on the vehicle distribution cost of cold chain logistics, built the corresponding vehicle path optimization model, and designed a hybrid genetic algorithm to solve the problem. In the case of uncertain demand, Li and Wang [19] established the distribution path optimization problem of perishable products with time windows with random customer demand.

To sum up, research on the distribution of vehicles in cold chain logistics has produced certain research results, which lays a good foundation for the research on the green vehicle routing problem in cold chain logistics. However, there are also some limitations, mainly reflected in the following three aspects: (1) The existing cold chain logistics distribution does not consider the real-time impact of road closure, bayonet temperature measurement, and traffic congestion on path planning. (2) At present, the relevant literature of cold chain logistics vehicle routing optimization mainly discusses the economy, and seldom involves the green benefits of vehicle energy saving and emission reduction. (3) Less consideration is given to the impact on user satisfaction.

On this basis, the possible traffic factors in the epidemic environment are analyzed in this paper, and the cost of each link is modeled in the distribution process. The fixed cost, transportation cost, refrigeration cost, carbon emission cost, penalty cost, and user satisfaction cost of the vehicle were taken as objective functions to build the model. Based on the traditional ant colony algorithm, the updating method of pheromone is improved, and a path planning algorithm

which is more consistent with the contactless distribution model is obtained. The improved post-ant colony algorithm for path planning can adjust the path according to the real-time traffic situation, which can not only improve the efficiency of contactless distribution, but also improve user satisfaction.

2. Distribution Problem Modeling

2.1. Description of Distribution Problem. In actual application scenarios, distribution companies will not set up too many distribution centers due to cost constraints [20]. In an epidemic situation, the number of distribution centers set up will be more limited. Therefore, in order to be more consistent with the actual situation, the hypothetical situation of the distribution problem in this paper is as follows.

(1) There is only one distribution center, which has multiple distribution vehicles.

(2) The distribution scope is the residential areas, shopping malls, and other places near the distribution center. The same community or shopping mall will have multiple goods at the same time distribution needs. For the convenience of description, the same residential area, shopping mall, and other residential areas are collectively referred to as the same residential area in the following description.

(3) The location coordinates of each customer can be accurate to the specific community, the demand of each customer is known, and the sum of the demand of the same community is known.

(4) In order to save distribution resources, generally only one vehicle will be arranged to meet the needs of customers in the same location at a time; that is, customers in the same community will only be provided with distribution services by one delivery vehicle.

(5) In this paper, it is assumed that each vehicle starts from the distribution center and returns to the distribution center after completing certain distribution tasks. During the distribution process, the vehicle is only responsible for delivering goods and contacting customers for self-collection. Delivery personnel are not responsible for face-to-face inspection, return, and other services.

(6) If the goods are not delivered within the specified time, its quality will decline, and the customer can ask for compensation after receiving the goods. Therefore, if the delivery is not within the time frame required by the customer, there will be a penalty fee.

(7) Assume that the distribution center has enough vehicles to complete all the distribution tasks, and the distribution vehicles have the same model and are equipped with refrigeration equipment. The maximum loading capacity of the vehicle is known. The customer demand on each distribution route

cannot exceed the maximum loading capacity of the distribution vehicle.

Based on the above assumptions, the cold chain distribution problem of contactless distribution studied in this paper can be described as follows. A fresh goods distribution center distributes fresh goods to the surrounding customer groups, using refrigerated trucks as transportation tools. The demand and geographical location of each customer is known, and each customer has a certain limit on the delivery time of goods. The vehicle shall return to the distribution center after completing certain distribution tasks. In order to optimize the objective function, the driving route is arranged reasonably under the condition of satisfying the customer's demand. Figure 1 is a basic distribution diagram of the problem.

2.2. Signs and Variables

M: the number of communities served by the logistics distribution center

M_i: the number of customers in the ith community

N: the number of customers served by the logistics distribution center

W: the number of refrigerated vans owned by the distribution center

d_{ij}: the distance that vehicles travel directly from community i to community j

q_i: the quantity demanded by all customers in community i

p: unit price of fresh goods

Q_w: maximum load capacity of the delivery vehicle

Q_{ij}: the load of a vehicle when it travels directly from community i to community j

$\rho(Q_{ij})$: fuel consumption per unit distance of goods transporting Q_{ij} when the vehicle travels from community i to community j

t_i^k: the time it takes for vehicle k to reach customer i

$U(t_i)$: customer's i satisfaction with goods distribution

$[\mathrm{ET}_i, \mathrm{LT}_i]$: the best service window for customer i

$[\mathrm{ET}_i^*, \mathrm{LT}_i^*]$: the service time window acceptable to customer i

ε_1: penalty cost per unit time of the vehicle serving customer i before the time ET_i

ε_2: penalty cost per unit time of the vehicle serving customer i after the time LT_i

t_i: the time that vehicle k serves customer i, where $t_0 = 0$

α_{ijk}: a path factor; when vehicle k drives directly from customer i to customer j, its value is 1; otherwise, its value is 0

β_{ik}: the vehicle distribution factor; when the goods of customer i are delivered by vehicle k, the value is 1; otherwise, the value is 0

$C1$: fixed operating cost of the vehicle

$C2$: unit transport cost of the vehicle

$C3$: environmental cost per unit CO_2 of emissions consumed

C_{e1}: refrigeration cost per unit time during the distribution process

C_{e2}: refrigeration cost per unit time during loading and unloading

ω: the emission coefficient of CO_2

r_{ij}: the road condition factor of vehicles driving directly from community i to community j

2.3. Road Traffic Factor.

In the severe epidemic environment, due to the frequent encounter of bayonet temperature measurement, road closure, and other factors, the real-time performance of each road condition information changes greatly. In order to improve the efficiency of contactless distribution, these factors need to be considered in the distribution path optimization model. In order to meet the practical application scenarios and facilitate the establishment of the subsequent cost model, the road traffic situation is divided into four situations.

Situation 1: the road condition is good and does not affect the normal work of the delivery vehicle. In this case, the road condition factor r_{ij} is constant 1.

Situation 2: the road condition is good, but there is a temperature measuring bayonet in the road section of the distribution vehicle. Because the temperature measurement and registration of bayonet need a certain time, the distribution of vehicles will be affected to a certain extent. At this point, the road condition factor r_{ij} is a constant greater than 1, and its size is related to the number of specific temperature measuring bayonets. Here, the temperature measurement bayonet information can be obtained by the relevant government departments. In general, temperature bayonet conditions do not change very frequently and generally do not change on the same day, such as $r_{ij} \in (1, 3]$.

Situation 3: the road condition is normal, and the road section of the delivery vehicle will encounter congestion. In this case, the road condition factor r_{ij} is a variable greater than 1, and the specific value is determined by the degree of traffic congestion. Traffic congestion is assumed to be captured by real-time information released by the Department of Transportation. In general, traffic jams are highly correlated with the time of day. For example, in the morning and evening peak hours, when the road condition is poor, the value of the road condition factor is large, such as $r_{ij} \in (3, 5]$.

Situation 4: in case of severe epidemic, some road sections may be closed in order to control access to the area. When the road is closed, in order to realize the distribution of goods, only a detour can be taken. In this case, the road condition factor r_{ij} will be reassigned according to the detour distance and the traffic
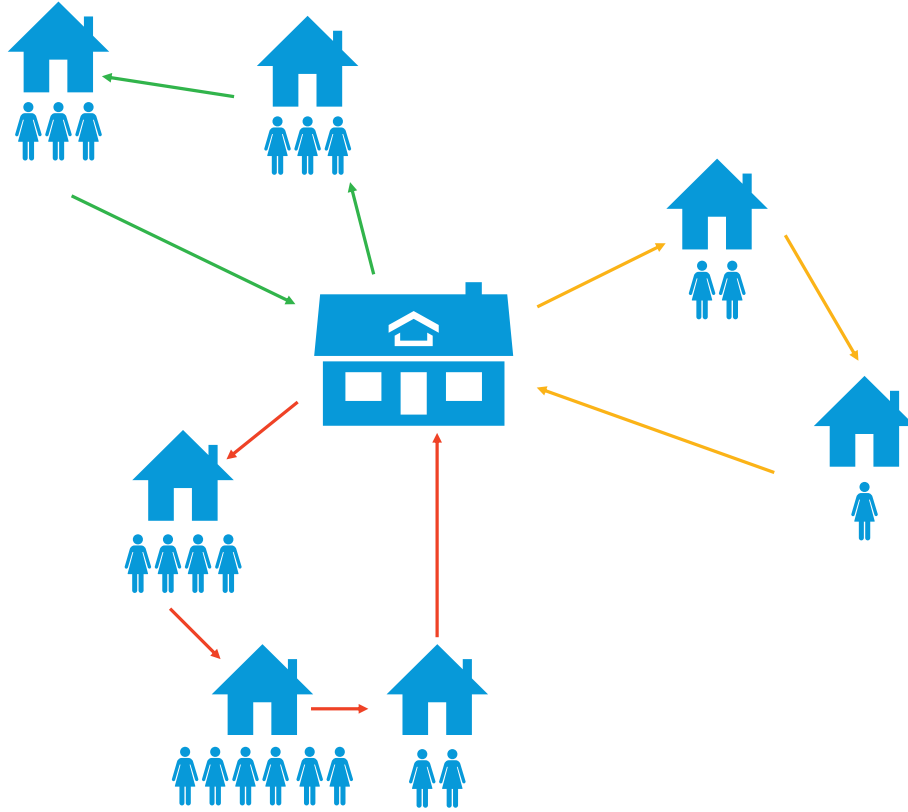
Figure 1: The basic distribution diagram.

condition, and its value is usually larger, such as $r_{ij} \in (5, 10]$.

2.4. Distribution Cost Analysis. In the context of epidemic environment, in order to better reflect the actual situation of contactless distribution, this paper adds carbon emission, customer satisfaction, and traffic conditions on the basis of vehicle cost, refrigeration cost, and penalty cost. Among them, carbon emission and customer satisfaction are calculated as separate cost functions. Route traffic factors affect the cost of each of the above items, but in order to simplify the calculation model, this paper converts the path traffic factors into the influence coefficient of distance. That is, when the road conditions encounter temperature checkpoints, traffic jams, and road closures, the distance assumption becomes larger, so that the vehicle cost, refrigeration cost, and time cost will all increase.

2.4.1. Fixed Costs of Vehicles. The fixed cost of using a vehicle is usually constant, including fixed wear and tear on the vehicle and costs related to the use of the vehicle, such as the driver's salary, independent of the vehicle's mileage and the number of customers served. The fixed cost $V1$ of the vehicle is shown as follows:

$$V1 = C1 \sum_{j=1}^{M} \sum_{k=1}^{W} \alpha_{0jk}. \tag{1}$$

2.4.2. Transportation Costs of Vehicles. The transportation cost of a vehicle mainly refers to the fuel consumption cost, which is usually proportional to the mileage of a vehicle. Therefore, the transportation cost $V2$ of a vehicle can be expressed as follows:

$$V2 = C2 \sum_{k=1}^{W} \sum_{i=0}^{M} \sum_{j=0}^{M} r_{ij} d_{ij} \alpha_{ijk}. \tag{2}$$

2.4.3. Costs of Refrigeration. The refrigeration cost should be considered in the transportation process of cold chain model. Cooling costs include the energy consumed to keep the vehicle cool during transportation and the cost of additional energy provided by the cooling system during offloading.

Therefore, in the process of transportation, the refrigeration cost $V31$ of the refrigerated truck is shown as follows:

$$V31 = C_{e1} \sum_{k=1}^{W} \sum_{i=0}^{M} \sum_{j=0}^{M} \alpha_{ijk} t_{ij}^{k}. \tag{3}$$

During the unloading process, the refrigeration cost $V32$ of the refrigerated truck can be expressed as follows:

$$V32 = C_{e2} \sum_{k=1}^{W} \sum_{i=0}^{M} \beta_{jk} \omega_{j}. \tag{4}$$

Therefore, the refrigeration cost of the whole process is

$$V3 = V31 + V32 = C_{e1} \sum_{k=1}^{W} \sum_{i=0}^{M} \sum_{j=0}^{M} \alpha_{ijk} t_{ij}^{k} + C_{e2} \sum_{k=1}^{W} \sum_{i=0}^{M} \beta_{jk} \omega_{j}. \tag{5}$$

2.4.4. Costs of Carbon Emission. Carbon emission cost mainly refers to the CO_2 emission cost generated by vehicle fuel consumption in the distribution process, carbon emission = fuel consumption $\times CO_2$ emission coefficient. Fuel consumption is related to both transport distance and vehicle load capacity. The fuel consumption per unit distance ρ can be expressed as a linear function dependent on the cargo carrying capacity of the truck X. Divide the total vehicle weight into vehicle dead weight Q_0 and cargo capacity X; then the unit distance fuel consumption $\rho(X)$ is shown as follows:

$$\rho(X) = a(Q_0 + X) + b. \tag{6}$$

The maximum cargo capacity of the vehicle is set as Q, the fuel consumption per unit distance is ρ^* when full load, and the fuel consumption per unit distance is ρ_0 when no load.

$$\rho_0 = aQ_0 + b,$$
$$\rho^* = a(Q_0 + Q) + b, \tag{7}$$
$$a = \frac{\rho^* - \rho_0}{Q}.$$

Thus, fuel consumption per unit distance $\rho(X)$ can be expressed as

$$\rho(X) = \rho_0 + \frac{\rho^* - \rho_0}{Q} X. \tag{8}$$

Therefore, in the process of fresh agricultural products distribution, if the goods of ij are transported from customer i to customer j, then the carbon emissions generated when driving between (i, j) can be expressed as

$$E_1 = \omega\rho(Q_{ij})r_{ij}d_{ij}, \tag{9}$$

where ω is the CO_2 emission coefficient, Q_{ij} represents the deadweight when the vehicle travels directly from customer i to customer j, $\rho(Q_{ij})$ represents the fuel consumption per unit distance when the vehicle travels between (i, j), and the deadweight is Q_{ij}. In this paper, the carbon emission cost is calculated through the carbon tax mechanism, that is, carbon emission cost = carbon tax $\times$ carbon emission. If the carbon tax is set as $C3$, then the total carbon emission cost $V4$ in the distribution process can be expressed as

$$V4 = C3 \cdot \omega \sum_{k=1}^{W} \sum_{i=0}^{M} \sum_{j=0}^{M} r_{ij}d_{ij}\alpha_{ijk}\rho(Q_{ij}). \tag{10}$$

2.4.5. Penalty Costs. The quality of fresh products is greatly affected by the time factor, so in the process of distribution,

each customer has characteristic requirements for the service time window, which is divided into acceptable service time window $[ET_i^*, LT_i^*]$ and optimal service time window $[ET_i, LT_i]$ according to the service level. If the delivery time is not within the optimal delivery time, it may lead to the loss of subsequent business. At the same time, the optimal time window is related to the time when distribution starts to serve, so the penalty cost function can be expressed as

$$V5(t_i^k) = \begin{cases} \text{Max } E, & t_i^k < ET_i^*, \\ \varepsilon_1(ET_i - t_i^k), & ET_i^* \le t_i^k < ET_i, \\ 0, & ET_i \le t_i^k \le LT_i, \\ \varepsilon_2(t_i^k - LT_i), & LT_i < t_i^k \le LT_i^*, \\ \text{Max } E, & t_i^k > LT_i^*. \end{cases} \tag{11}$$

where $\text{Max } E$ is a constant, representing the maximum loss caused outside the acceptable delivery time window.

2.4.6. User Satisfaction. The customer satisfaction with the service $U(t_i^k)$ also depends on the time window when the customer starts the service. The specific function is as follows:

$$U(t_i^k) = \begin{cases} 0, & t_i^k < ET_i^*, \\ \dfrac{t_i^k - ET_i^*}{ET_i - ET_i^*}, & ET_i^* \le t_i^k < ET_i, \\ 1, & ET_i \le t_i^k \le LT_i, \\ \dfrac{LT_i^* - t_i^k}{LT_i^* - LT_i}, & LT_i < t_i^k \le LT_i^*, \\ 0, & t_i^k > LT_i^*. \end{cases} \tag{12}$$

In order to take user satisfaction into account in the overall loss function, the loss cost of user satisfaction is defined as follows:

$$V6 = \sum_{k=1}^{W} \sum_{i=1}^{N} \frac{1}{1 + U(t_i^k)}. \tag{13}$$

2.5. Construction of Distribution Model. To sum up, considering the influence of traffic path factors and user satisfaction, the final optimization model of distribution path is as follows:

$$\min V = V1 + V2 + V3 + V4 + V5 + V6, \tag{14}$$

where

$$\sum_{i=1}^{M} q_i \beta_{ik} \le Q_k, \tag{15}$$

$$\sum_{k=1}^{W} \beta_{ik} = 1, \tag{16}$$

$$\sum_{i=0}^{M} \alpha_{ijk} = \beta_{jk}, \tag{17}$$

$$\sum_{j=0}^{M} \alpha_{ijk} = \beta_{ik}, \tag{18}$$

$$\sum_{i,j \in S \times S} \alpha_{ijk} \le |S| - 1, \quad S \in \{1, 2, \ldots, N\}, \tag{19}$$

$$t_j = t_i + t_{ij}, \tag{20}$$

where the objective equation (14) represents the comprehensive cost formula of cold chain logistics transportation including carbon emissions. Equation (15) is the constraint of vehicle carrying capacity. Equation (16) ensures that each customer is only served by one vehicle. Equations (17) and (18) restrict that for any customer, only one vehicle can arrive and depart once. Equation (19) is the elimination condition of secondary loop. Equation (20) represents the continuity of the distribution process.

3. Improved Ant Colony Algorithm

Because VRP belongs to NP-hard problem, heuristic algorithm is usually used to solve it. The optimization of the distribution path of fresh agricultural products considering carbon emission is also a NP-hard problem. Because its complexity is higher than that of VRP, the algorithm is required to solve it. Ant colony algorithm is a kind of simulated evolutionary algorithm inspired by real ant colony behavior in nature. Ant colony algorithm has shown good performance in many aspects, such as positive feedback, strong robustness, distributed computing, and easy to be combined with other methods. Its positive information feedback mechanism enables it to quickly find better solutions. Distributed computing makes it easy to implement algorithms in parallel and avoid falling into local optimality. Therefore, this paper uses the improved ant colony algorithm to solve the model.

3.1. Basic Step of the Algorithm. The basic flow of ant colony algorithm is as follows.

Step 1. Initialize parameters. There are m ants; start from the distribution center at the same time and select the first access point according to certain conditions, respectively.

Step 2. List all unvisited points for each ant and set the number of them as $S1$.

Step 3. Judge the value of $S1$. If $S1 = 0$, it means that the ant has completed all the distribution tasks and should return to the distribution center to end the distribution of this line. If $S1 > 0$, then $S2$ ($S2 \le S1$) is selected from $S1$ unaccessed points that meet the access conditions. If $S2 = 0$, it means that no optional point meets the conditions, and the vehicle returns to the distribution center. If $S2 > 0$, then $S = \min(S1, S2)$, and add the distribution center to the candidate access points. Select one point as the next service point according to a certain probability, and return to Step 2.

Step 4. Judge whether all ants have completed the delivery task. If so, calculate the total route length of each ant, select the shortest route and record it, and update the pheromone according to the rules.

Step 5. Calculate the minimum value of routes passed by each ant in each operation, denoted as L_i ($i = 1, 2, \ldots, N$); after multiple calculations, the iterative optimal solution can be obtained as $\min(L_i)$.

3.2. Heuristic Factor. Heuristic factor is the key factor inspiring ant to select nodes and the core part of ant colony algorithm, which can directly affect the algorithm's solution quality. The influence of vehicle load is taken into account in the model built for the optimization of fresh agricultural products distribution path considering carbon emissions. If only the distance is taken as a heuristic factor, the solution results will be affected, resulting in fuel waste and cost increase. Therefore, the customer's demand for goods is introduced into the heuristic factor, which makes the algorithm take into account the influencing factors of fuel consumption when selecting the next node. The heuristic factors for the optimization of the distribution path of fresh agricultural products considering carbon emissions are shown as follows:

$$\varphi_{ij} = \frac{q_j}{d_{ij}}. \tag{21}$$

As shown in equation (21), on the premise of satisfying the vehicle load and time constraints, the ant individual will comprehensively calculate the heuristic factor according to the current load and distance. The distance is in the denominator, so the smaller the distance, the larger the heuristic factor, and the greater the probability that the ant will choose this customer point. Similarly, the load weight is at the molecular position, so the greater the demand for goods at the next customer point is, the greater the value of heuristic factor is, and the greater the selection probability is. In other words, the customer point with large demand is given priority for delivery, so as to reduce the load weight of the delivery vehicle and reduce fuel consumption.

3.3. Improved Pheromone Update Strategy. In the classical model, the specific updating mode of the pheromone left by the kth ant from i to j is as follows [21].

The ant quantity system is

$$\Delta\tau_{kij} = \begin{cases} \dfrac{Q}{d_{ij}}, \\ 0. \end{cases} \tag{22}$$

The ant density system is

$$\Delta\tau_{kij} = \begin{cases} Q, \\ 0. \end{cases} \tag{23}$$

The ant circle system is

$$\Delta\tau_{kij} = \begin{cases} \dfrac{Q}{L^k}, \\ 0. \end{cases} \tag{24}$$

Inspired by the ideas of genetic algorithm, such as genetic inheritance, recombination and mutation, a new pheromone updating method is proposed in this paper. The new pheromone updating method can effectively retain the better route segments and combine reasonably between different route segments, so as to facilitate the rapid generation of the optimal solution. The pheromone left by the kth ant from i to j changes to

$$\Delta\tau_{kij} = \begin{cases} \left(K_{kij}\right)^{\omega 1}\left(L_{kij}\right)^{\omega 2}\left(R_{kij}\right)^{\omega 3}\left(d_{kij}\right)^{\omega 4} + \dfrac{Q}{R_k}, \\ 0, \end{cases} \tag{25}$$

where $\omega 1$, $\omega 2$, $\omega 3$, and $\omega 4$ need to be determined according to specific problems. In general, $\omega 1$ is positive, $\omega 2$, $\omega 3$, and $\omega 4$ are negative, and $\omega 1 = 2.0$, $\omega 2 = \omega 3 = \omega 4 = -0.5$ are used in the calculation of this paper. The value of equations (22)–(25) is based on whether the k ant passes through sections i and j.

After improvement, new symbols need to be defined as follows:

K_{kij}: the number of temperature measuring points at bayonet of the subline where the segment from point i to point j passed by the k ant

L_{kij}: the length of the subline from point i to point j that the k ant passes

R_k: the total length of the route traveled by the k ant

The indicator K_{kij} can strengthen the pheromone in the excellent subsegments. The indicator L_{kij} can distinguish between subpaths with the same or similar number of access points. Indicator R_k reflects the advantages and disadvantages of the general routes passed by different ants. Through such pheromone updating method, the unblocked road sections can fully retain the relative stability, thus generating a better combination. On this basis, a small correction factor is added to all the road pheromones to ensure certain variation effect and avoid the algorithm falling into local optimal prematurely.

$$p_k(i,j) = \begin{cases} \dfrac{[\tau(i,j)^\alpha][\eta(i,j)^\beta]}{\sum_{\mu \in J_k(i)}[\tau(i,j)^\alpha][\eta(i,j)^\beta]}, & j \in J_k(i), \\ 0, & j \notin J_k(i), \end{cases} \tag{26}$$

$$\tau(i,j) = (1-\rho) \times \tau(i,j) + \sum_{k=1}^{m} \Delta\tau_k(i,j), \tag{27}$$

$$\tau(i,j) = \tau(i,j) + \tau_0. \tag{28}$$

where α is the relative importance of residual information and β is the relative importance of heuristic information. In this paper, let $\alpha = 1$, $\beta = 1$. ρ is the pheromone volatilization parameter; ρ is set as 0.5. τ_0 is the pheromone correction factor to increase the probability of choosing different routes and avoid the precocity of the algorithm. In this paper, τ_0 is set as 0.1. Equations (25)–(28) represent the updating steps of pheromone. Equation (26) represents the probability that the kth delivery vehicle starts from community i and takes different community j as the target point.

The 2-opt local optimization algorithm is mixed into the ant colony algorithm. After all ants have completed the construction of the solution, the best solution of each generation is locally improved before the pheromone on each path is updated, so as to accelerate the convergence speed of the ant colony algorithm.

4. The Experiment

4.1. The Experimental Setup. In consideration of various factors of vehicle distribution in cold chain logistics, data of class C (centralized distribution), class R (random distribution), and class RC (mixed distribution) in Solomon's VRPTW database were used as the test data [22] in this paper. Each example had 100 customer points and 1 distribution center. In order to better fit the reality, the initial time of the model is set as 6:00 a.m., which is the earliest service time of the distribution center and is set as time 0. According to the law of urban traffic, 7:00 to 9:00 and 17:00 to 19:00 in the afternoon are set as traffic jam periods, and the traffic in other periods is smooth. The temperature measuring bayonet points are randomly distributed on each route, and there is only one at most for each plot location, and the road is closed at most once for each plot location. The selected vehicle no-load weight is 5000 kg; capacity is 1000 weight units. If a weight unit is 2 kg, then the vehicle capacity is 2 t, and the corresponding carbon emission rate coefficient is $\omega 0 = 110$, $\omega 1 = 0$, $\omega 2 = 0$, $\omega 3 = 3.75 \times 10^{-4}$, $\omega 4 = 8\ 702$, $\omega 5 = 0$, and $\omega 6 = 0$. Corresponding coefficient of load correction factor for [22] is $\chi_0 = 1.27$, $\chi_1 = 0.0614$, $\chi_2 = 0$, $\chi_3 = 0.001\ 1$, $\chi_4 = -0.00235$, $\chi_5 = 0$, $\chi_6 = 0$, and $\chi_7 = -1.33$. The values of other parameters involved in the model are shown in Table 1, and those of algorithm parameters are shown in Table 2 [8]. The algorithm was programmed by MATLAB R2020 and calculated on 16 GB PC with CPU3.0 GHz memory.

TABLE 1: Model parameter values.

Parameter	Parameter value
g_k	150 yuan/units
μ	5 yuan/h
ψ	10 yuan/h
p	5 yuan/kg
gf	7 yuan/L
cf	0.0528 yuan/kg
θ_1	0.0010 h
θ_2	0.0015 h
ez	0.0066 g/(kg·km)
θ_3	15 yuan/h
θ_4	20 yuan/h
ch	12 yuan/h

TABLE 2: Ant colony algorithm parameters.

Parameter	Parameter value
NCmin	40
NCmax	400
M	15
α	1
β	3
γ	3
φ	2
Q	100

4.2. Large Data Case for Path Optimization. The RC204 dataset was used to calculate path optimization. Its program running time is 290.3 s, and the total distribution cost is 10052.8 yuan. A total of 9 vehicles are used for distribution, and the cost of manpower and vehicle use is 2943.9 yuan, the cost of refrigeration is 2656.6 yuan, the cost of fuel consumption is 3904.1 yuan, the cost of carbon emission is 50.1 yuan, the cost of waiting for punishment at the customer point early is 395.7 yuan, and the cost of customer satisfaction loss is 102.4 yuan. The specific path optimization scheme is shown in Table 3. In Table 3, SN represents the vehicle number, VR (vehicle driving) represents the vehicle driving path (0 represents the distribution center and 1–100 represents the customer point), and VAT (vehicle driving time) represents the time of the vehicle arriving at each customer point.

The calculation results show the following contents:

(1) The algorithm in this paper can obtain the optimal planning path in a relatively short time.

(2) By combining VR and VAT, it can be seen that due to the influence of road factors, customer service time window, vehicle load, and other constraints, there are obvious differences in the distribution routes of cold chain logistics vehicles. Vehicle 2 served the largest number of customer points, reaching 21. Vehicles 8 and 9 serve the least number of customer points. The reason for this is that each requirement point has a different time window, and vehicle routing planning must meet customer point time window requirements while ensuring minimum fitness.

(3) From VAT, it can be seen that both vehicle 1 and vehicle 2 start to distribute from the distribution center at 0, while the departure time of other vehicles is different. If you start at 0, you need to bear a large time window penalty. It shows that it is necessary to consider time dependence when planning the path of logistics enterprises. The route should be planned scientifically according to the actual situation of the road network, the time window of the customer points, and the cost of refrigeration and fuel consumption in the transportation process.

(4) According to VAT, vehicle 4 completely avoids the congestion period. Vehicles 1, 3, 6, 7, and 8 only enter the morning rush hour, not the evening rush hour. However, vehicles 2, 5, and 9 only entered the evening rush hour and did not enter the morning rush hour. This indicates that the method proposed in this paper can reasonably avoid the traffic jam period and improve the efficiency of vehicle distribution.

4.3. Path Planning for Different Distribution Examples. Different types of dataset were used to calculate the path optimization. Each dataset was calculated 10 times, and the average value was taken as the final result. The experimental results are shown in Table 4, where EX represents the type of calculation example, TC represents the total cost of distribution, TMC represents the cost of manpower and vehicle start-up and rental, CC represents refrigeration cost, FC represents fuel consumption, CF represents carbon emission cost, PC represents the penalty cost of time window, UC represents the cost of customer satisfaction loss, and VN represents the number of vehicles.

As shown in Figure 2 and Table 4, the following can be obtained:

(1) In the solution process of different calculation examples, the algorithm can reach the optimal solution and achieve stability within 400 iterations. It indicates that the algorithm can solve the model in this paper well, and the convergence is good.

(2) The total distribution cost, vehicle use and labor cost, refrigeration cost, and vehicle use number of *C*-type dataset are the highest among all types, but the fuel consumption cost is the lowest compared with other types. The main reason is that the *C*-type distribution customer points are mainly concentrated in several areas and the driving distance is short, so the fuel consumption cost is relatively low. However, the customer time window is relatively narrow. As the customer point service time of the *C*-type dataset in Solomon's database is 90 min, which is different from the 10 min service time of *R* and RC customers, the vehicle can only serve fewer customers, and the total delivery travel time is longer.

(3) The total distribution cost, vehicle rental and labor cost, and number of vehicles of *R*-type and RC-type categories are less than those of *C*-type categories,

TABLE 3: The vehicle path planning of RC204 dataset.

SN	VR	VAT
1	0-1-2-6-7-3-5-45-46-16-15-10-11-0	0-37.98-57.92-73.85-90.25-125.02-139.01-155.01-171.12-228.94-240.79-260.52-272.72-305.02
2	0-8-73-47-17-9-12-14-59-97-24-22-13-18-19-20-49-21-48-25-77-58-0	326.83-366.21-401.42-426.22-438.68-462.00-481.22-496.22-529.97-546.69-590.98-603.25-654.63-755.24-775.63-792.74-807.75-824.82-836.02-853.04-874.97-896.24-943.77
3	0-23-51-85-26-28-30-32-27-29-31-33-34-35-36-37-0	131.4-200.99-236.53-253.28-295.83-310.03-324.03-356.38-375.48-391.27-401.27-423.79-441.97-506.03-518.06-531.03-572.63
4	0-38-39-40-41-42-43-0	239.27-277.87-288.92-304.42-324.23-340.64-355.35-393.92
5	0-44-50-63-76-89-64-52-53-54-81-72-71-55-56-57-74-86-75-61-68-0	182.77-218.1-277.03-304.49-323.01-343.21-387.07-417.17-447.75-492.17-508.43-534.24-554.43-601.74-641.76-678.46-712.82-731.07-788.76-872.03-889.78-897.94
6	0-62-95-65-66-80-91-67-0	107.9-168-194.03-225.78-242.18-263.81-279.17-304.67-329.76
7	0-69-70-88-98-82-83-90-99-87-79-84-0	137.83-158-195.52-223.14-239.42-258.12-282.89-308.83-334.34-364.23-418.42-492.82-517.94
8	0-92-93-94-96-0	0-14.65-35.72-53.47-69.79-98.93
9	0-4-60-78-100-0	608.03-643.98-680.41-704.24-780.97-799.62

TABLE 4: Experimental data results of different distribution examples.

| EX	C103	C104	R203	R204	RC204	RC208
TC/yuan	17180.60	15914.90	13386.20	11642.70	10051.90	11504.80
TMC/min	6889.20	6553.40	4460.00	3946.90	2843.00	3493.00
CC/yuan	5698.90	5007.50	3866.90	3057.00	2655.80	3450.90
FC/yuan	3822.90	3785.94	4727.10	4050.50	3903.40	4167.80
CF/yuan	48.70	45.40	61.10	52.50	50.00	53.00
PC/yuan	506.70	506.70	506.70	432.20	394.60	228.50
UC/yuan	210.49	248.88	66.74	99.80	101.30	107.85
VN	25	23	15	13	9	13
((TMC + CC)/TC)/%	73.27	72.64	62.21	60.16	54.70	60.36
(FC/TC)/%	22.25	23.79	35.31	34.79	38.83	36.23
(CF/TC)/%	0.28	0.29	0.46	0.45	0.50	0.46
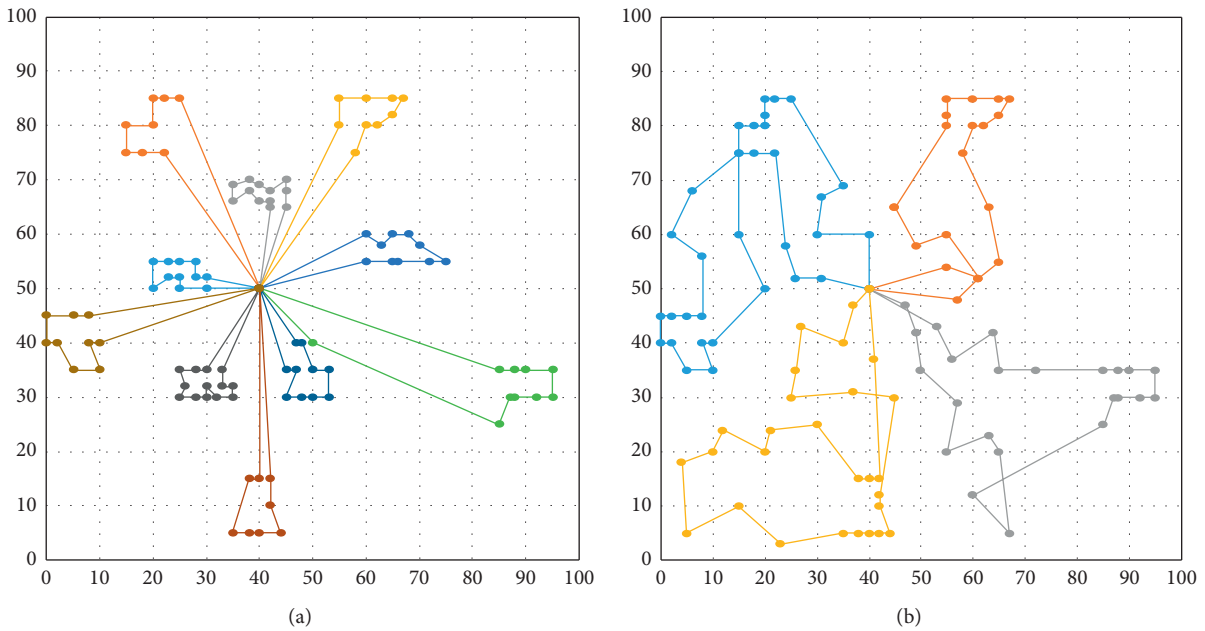
FIGURE 2: Example of vehicle path planning. (a) C104. (b) RC208.

mainly because the service time of these two types is only 10 min, customers are randomly distributed, and the time window requirements of customers are relatively loose, so the vehicles can deliver to multiple customers, and the total driving time is shorter.

(4) In the total cost composition of distribution, all types of TMC and CC account for a relatively high proportion, accounting for more than half of the total cost, while C accounts for more than 70%. This shows that the cost of logistics distribution mainly comes from vehicle use cost, manpower cost, and refrigeration cost. The main influencing factor is the travel time, so to reduce the logistics cost, the most important thing is to reduce the total transportation time.

(5) The proportion of fuel consumption cost in logistics is low, the highest is only about 38% of the total cost of RC-type dataset, and the lowest is only about 22% of C-type dataset. The carbon emission ratio is very low, accounting for only 0.2% to 0.4% of the total cost. It shows that from the economic point of view of logistics enterprises, the carbon emission cost generated by the current carbon tax can hardly effectively promote the energy conservation and emission reduction of enterprises.

4.4. Simulation under Different Traffic Factors. On the premise that other conditions of the algorithm remain unchanged, the traffic factors r_{ij} are set as 1.5, 3.5, and 8.5 to simulate the situation of temperature measuring jam, traffic jam, and road closure. Then, the path planning was performed on RC204 dataset. Each case was solved for 10 times, and the average value was taken as the final result. The optimized results obtained are shown in Table 5, where CP represents the carbon emissions and TT represents the traveling time.

By observing the recognition results in Table 5, the following can be seen:

(1) With the increase of traffic factors, the total cost of distribution, vehicle use cost, labor cost, and refrigeration cost will increase to varying degrees, indicating that these costs are positively correlated with congestion.

(2) With the increase of traffic factor, fuel consumption and carbon emissions increase, indicating that congestion will affect the greenness of cold chain logistics distribution path. The driving time also increases, indicating that traffic congestion will affect the speed and thus affect vehicle path planning.

(3) Although traffic factors change significantly, TC, TMC, CC, FC, CP, and VN have little change because the model constructed in this paper can make most vehicles effectively avoid the traffic jam period, which demonstrates the effectiveness of the model and solving algorithm in this paper.

Table 5: Simulation results under different traffic factors.

Traffic factors r_{ij}	1.5	3.5	8.5
TC/yuan	9871.5	1051.7	10383.1
TMC/min	2798.6	2842.8	2960.3
CC/yuan	2647.1	2655.5	2689.2
CF/yuan	3888.4	3903	4005.1
PC/yuan	905.6	947.7	990.1
UC/yuan	98	101.3	106.7
VN	9	9	10
TT/min	4759	4836	4902

5. Conclusion

Under the background of normal epidemic situation, the contactless distribution of fresh goods has important research significance. Reasonable planning of fresh goods logistics distribution path can not only reduce the distribution cost in logistics, but also increase customer satisfaction. This paper studies the possible traffic factors in the epidemic environment and comprehensively considers the vehicle management cost, fuel consumption and carbon emission cost, refrigeration cost, time window penalty cost, and user satisfaction cost. An optimization model for this problem is built, and an improved ant colony algorithm model based on path partitioning strategy is designed. The heuristic factor and pheromone updating strategy of basic ant colony algorithm are improved. The simulation results show that the model can deal with various traffic factors effectively. The proposed algorithm can achieve better optimization results in different distributed data cases.

Data Availability

The labeled dataset used to support the findings of this study are available from the corresponding author upon request.

Conflicts of Interest

The author declare that they have no conflicts of interest regarding the publication of this paper.

Acknowledgments

References

[1] C. Luo, L. Wu, and N. Liu, "Study based on contactless distribution patterns under the outbreak," *IOP Conference Series: Earth and Environmental Science. IOP Publishing*, vol. 526, no. 1, Article ID 12204, 2020.

[2] G. B. Dantzig and J. H. Ramser, "The truck dispatching problem," *Management Science*, vol. 6, no. 1, pp. 80–91, 1959.

[3] M. Desrochers and T. W. Verhoog, "A new heuristic for the fleet size and mix vehicle routing problem," *Computers & Operations Research*, vol. 18, no. 3, pp. 263–274, 1991.

[4] M. M. Solomon and J. Desrosiers, "Survey paper-time window constrained routing and scheduling problems," *Transportation Science*, vol. 22, no. 1, pp. 1–13, 1988.

[5] O. Jabali, R. Leus, T. Van Woensel, and T. de Kok, "Self-imposed time windows in vehicle routing problems," *OR Spectrum*, vol. 37, no. 2, pp. 331–352, 2015.

[6] R.-M. Chen, Y.-M. Shen, and W.-Z. Hong, "Neural-like encoding particle swarm optimization for periodic vehicle routing problems," *Expert Systems with Applications*, vol. 138, Article ID 112833, 2019.

[7] R. Kramer, A. Subramanian, T. Vidal, and L. d. A. F. Cabral, "A matheuristic approach for the pollution-routing problem," *European Journal of Operational Research*, vol. 243, no. 2, pp. 523–539, 2015.

[8] Y. Xiao and A. Konak, "The heterogeneous green vehicle routing and scheduling problem with time-varying traffic congestion," *Transportation Research Part E: Logistics and Transportation Review*, vol. 88, pp. 146–166, 2016.

[9] Q. K. Cao, K. W. Yang, and X. Y. Ren, "Vehicle routing optimization with multiple fuzzy time windows based on improved wolf pack algorithm," *Advances in Production Engineering & Management*, vol. 12, no. 4, pp. 401–411, 2017.

[10] R. Yan, X. N. Zhu, and Q. Zhang, "Research of the model and algorithm for two-dimensional multi-depots capacitated vehicle routing problem with time window constrain," *Chinese Journal of Management Science*, vol. 25, no. 7, pp. 67–77, 2017.

[11] S. Huber and M. J. Geiger, "Order matters—a variable neighborhood search for the swap-body vehicle routing problem," *European Journal of Operational Research*, vol. 263, no. 2, pp. 419–445, 2017.

[12] J. D. Camm, M. J. Magazine, S. Kuppusamy, and K. Martin, "The demand weighted vehicle routing problem," *European Journal of Operational Research*, vol. 262, no. 1, pp. 151–162, 2017.

[13] C. D. Tarantilis and C. T. Kiranoudis, "A meta-heuristic algorithm for the efficient distribution of Perishable foods," *Journal of Food Engineering*, vol. 50, no. 1, pp. 1–9, 2001.

[14] P. Amorim, S. N. Parragh, F. Sperandio, and B. Almada-Lobo, "A rich vehicle routing problem dealing with perishable food: a case study," *TOP*, vol. 22, no. 2, pp. 489–508, 2014.

[15] J. Yang and H. Sun, "Battery swap station location-routing problem with capacitated electric vehicles," *Computers & Operations Research*, vol. 55, pp. 217–232, 2015.

[16] Y. M. Zhang, Y. M. Li, and H. O. Liu, "Research on VRP optimization of multi-type vehicle cold-chain logistics with satisfaction constraint," *Statistics and Decision*, vol. 35, no. 4, pp. 176–181, 2019.

[17] X. G. Ma, T. J. Liu, P. Z. Yang et al., "Vehicle routing optimization model of cold chain logistics based on stochastic demand," *Journal of System Simulation*, vol. 8, pp. 1824–1832, 2016.

[18] H. Lan, Q. F. He, and Z. Bian, "Distribution routing optimization of cold chain logistics with consideration of road traffic conditions," *Journal of Dalian Maritime University*, vol. 41, no. 11, pp. 67–74, 2015.

[19] N. Li and S. B. Wang, "Production and distribution optimization model for perishable products in uncertain demand," *Application Reseach of Computers*, vol. 28, no. 3, pp. 927–929, 2011.

[20] J. Dai, L. Xie, and Q. Wang, "The impact of the third party logistics integration on logistics service quality, partnership and corporate operational performance," *Management Review*, vol. 27, no. 5, pp. 188–197, 2015.

[21] H. B. Duan, *Ant Colony Algorithms: Theory and Applications*, pp. 33–38, Science Press, Beijing, China, 2005.

[22] A. J. Hickman, "Methodology for calculating transport emissions and energy consumption," Report, Transport Research Laboratory, Crowthorne, UK, 1999.

Research Article

Masked Face Recognition Algorithm for a Contactless Distribution Cabinet

GuiLing Wu (ID)

Xinyang Agriculture and Forestry University, Xinyang 464000, China

Correspondence should be addressed to GuiLing Wu; wgl@xyafu.edu.cn

A contactless delivery cabinet is an important courier self-pickup device, for the reason that COVID-19 can be transmitted by human contact. During the pandemic period of COVID-19, wearing a mask to take delivery is a common application scenario, which makes the study of masked face recognition algorithm greatly significant. A masked face recognition algorithm based on attention mechanism is proposed in this paper in order to improve the recognition rate of masked face images. First, the masked face image is separated by the local constrained dictionary learning method, and the face image part is separated. Then, the dilated convolution is used to reduce the resolution reduction in the subsampling process. Finally, according to the important feature information of the face image, the attention mechanism neural network is used to reduce the information loss in the subsampling process and improve the face recognition rate. In the experimental part, the RMFRD and SMFRD databases of Wuhan University were selected to compare the recognition rate. The experimental results show that the proposed algorithm has a better recognition rate.

1. Introduction

The contactless delivery scene is becoming increasingly normal, since COVID-19 can be transmitted by contact. In the scene of contactless express delivery, a self-pickup cabinet is an important piece of terminal express delivery equipment, and face recognition is one of the effective way to achieve contactless express delivery. During the pandemic of COVID-19, nearly everyone wears masks, which makes the traditional face recognition technology almost ineffective on face recognition self-pickup cabinets. Therefore, it is greatly urgent to improve the performance of existing face recognition technology for face mask recognition.

In recent years, face recognition technology has made great breakthroughs in both theoretical progress and practical applications. It has become a frontier research direction in the field of pattern recognition. However, the recognition problem of occluded face images, such as mask, hairstyle, sunglasses, and hat occlusions, often appears in the process of face processing. These occlusions greatly interfere with the correct recognition of human faces. The low-rank representation [1], however, can quickly solve the occlusion problem. A new iterative method is used to effectively improve the recognition rate and the robustness of large-area image occlusion recognition. Literature [2] proposed a method combining structured occlusion coding and sparse representation-based classifier [2], which cleverly used structured sparse coding to deal with image occlusion problems. In addition, the long and short-term memory network autoencoder [3] was also commonly used to solve the problem of facial occlusion, which better improved the robustness of image noise reduction. However, the occlusion problem has not been completely solved.

Face recognition with occlusion has attracted extensive attention in academic circles. Occlusion processing methods are generally divided into video occlusion processing and image occlusion processing methods. Object tracking is usually used to deal with the occlusion problem in dynamic video. For example, a tracking method based on video monitoring is proposed in literature [4], which can automatically detect and process occlusion objects. Literature [5] proposed a new object tracking technology, which can track

people's dynamic behaviors and actions and maintain pixel tracking allocation even under large shielding. It has been used in different experiments of indoor human behavior supervision due to its robustness. The methods for processing occluded images can be divided into five categories: low-rank representation, image restoration, fuzzy analysis, robust principal component analysis, and structural occlusion coding. Literature [6] proposed a robust low-rank representation method to solve the problem of face recognition with occlusion. This method mainly combines robust representation and low error estimation. At present, the multiscale fractal coding and reconstruction method of image restoration has been proposed in literature [7], which has a good effect on texture images and images with large holes. Literature [8] proposed a method based on fuzzy principal component analysis to detect the occlusion area and restore the face area. However, the fuzzy principal component analysis has a large amount of computation and is not ideal for large-area occlusion processing.

Low-rank robust principal component analysis is a mainstream occlusion face feature extraction method, which combines structural occlusion coding with sparse representation classification. Literature [9] proposed a new nonnegative sparse representation method for robust face recognition in large-scale databases. However, this algorithm has a large amount of computation and a complex structure. Literature [10] proposed an occlusion dictionary method, which plays an increasingly important role in face recognition and can effectively deal with various occlusion objects. It can distinguish the features of nonoccluded and occluded regions and encode the corresponding parts of the dictionary, respectively. The occlusion problem is resolved by using detection/mask scores in literature [11]. And it introduced a plug-and-play occlusion handling algorithm to deal with the occlusion between different object instances. Occlusion face recognition problem is the most critical step towards the practical face recognition technology.

Face recognition systems must solve the problem of occlusion. Objects like hats, scarves, and sunglasses are very common. Sometimes, a large area of occlusion will seriously destroy the information of the original image, resulting in the failure of large image recognition. Literature [12] proposed the method of sparse error and graphical model to continuously overlap and finally display the mask. The Markov random field model is transformed into the calculation of the sparse representation of the training image, so as to find the occlusion area accurately. Therefore, great research significance lies in how to separate the blocked face images from blocking images.

A masked face recognition algorithm based on attention mechanism is proposed in the paper, in order to improve the face recognition rate of masks. First, the masked image is separated by local constrained dictionary learning method; that is, the mask and the face image are separated. Then, dilated convolution is adopted to reduce the problem of resolution reduction in the process of subsampling, and an attention mechanism is designed to reduce information loss in the process of subsampling. Finally, according to the important feature information of the face image, the attention mechanism neural network algorithm is used for face recognition.

2. Materials and Methods

2.1. Relevant Work.
In recent years, researchers have been devoted to the study of effective face recognition with occlusion [10] and proposed many effective algorithms. It mainly includes three methods: the generation model of the occlusion problem, the discriminant model, and robust feature extraction. These three methods will be introduced in the following paragraphs.

2.1.1. Generation Model.
In the robust learning process of occluded face image data, dictionary atom, low-rank structure of face image, and occluded structure are used to represent the occluded part of the image to be recognized. The local feature loss in face image is processed by reconstruction of noise such as occlusion to correct its influence on recognition performance. By fully understanding the content of the occlusion part, the recognition efficiency is improved. Generating models mainly include robust subspace regression and robust structured error coding.

Robust subspace regression is established by projecting the high-dimensional feature data of different categories of face images into the low-dimensional subspace in a linear or nonlinear way. Then, an independent subspace is established for the occlusion part, and the existing dictionary atoms are used to represent the occlusion in the face image, which can achieve robust recognition effect for the occlusion face. At present, robust subspace solutions to occlusion face recognition mainly include sparse representation, collaborative representation, and occlusion dictionary learning.

(1) *Sparse Representation.* The study in [12] first applies the sparse representation to the field of face recognition and proposes a method based on sparse representation classification (SRC). The sparsity nonzero principle is used to select the most appropriate sparse matrix to represent the image to be recognized more flexibly and comprehensively. Thus, face image classification can be achieved, and the error caused by occlusion and damage can be handled uniformly.

(2) *Collaborative Representation Classification.* The essence is to use training samples from all categories to jointly represent the image to be recognized. The study in [13] through the analysis of the SRC method can effectively enhance the capacity of classification difference, on the basis of classification based on collaborative said method for face recognition.

(3) *Occlusion Dictionary Learning.* The purpose is to learn a new set of dictionaries from the original training samples, which can well represent the ability of the original training samples. Then, it is used for image processing and classification. The study in [14] uses low-rank matrix restoration to train relatively clean face images from face images to be recognized

as a new feature dictionary. Then, the feature dictionary is learned using Fisher's criterion dictionary learning method. Ensure that subdictionaries of the pending class in the new dictionary are well represented for samples in the same category, but not for samples in other categories. This method can effectively reduce the reconstruction error and improve the performance of face recognition with occlusion.

Because of the spatial continuity and locality of occlusion, the error caused by occlusion region has its specific spatial structure, and occlusion will destroy the low-rank structure of face image. Therefore, it is crucial to improve the performance of occluded face recognition to effectively and accurately reconstruct the low-rank structure of the face image from the data damaged by occlusion. And robust structured error coding is to use the low-rank structure of face image to recognize face. Face images in natural environments are affected by different kinds of occlusion noises, leading to great differences between actual low-rank structures of face images and low-rank structures processed by PCA. In order to improve the robustness of occlusion face recognition, the study in [15] proposed robust principal component analysis (RPCA). After decomposition of all training sample matrix Y by low-rank matrix, low-rank content matrix Z and sparse content matrix E were obtained. Thus, the recovery of the low-rank subspace of the training sample is realized. The method takes into account how to recover the low-rank structure from the training samples with large errors but sparse structure, so the effect of sparse noise is effectively suppressed and has strong robustness. To increase the interclass information between low-rank matrices of different categories of faces, literature [16] expressed all training samples as an observation matrix D. After matrix D is decomposed, the low-rank matrix A without occlusion and the sparse error matrix E are obtained. RPCA is applied to the low-rank matrix A, and the subspace obtained is used as the occlusion dictionary of face images. Then, the image reconstruction was identified and the error size was classified according to the sparse representation classification and occlusion dictionary.

2.1.2. Discriminant Model.
There are two error indexes that are used as the main discriminant model to estimate the occlusion location. One is the local similarity error between the occlusion image and the original image, and the other is the spatial local error caused by the occlusion. The occluded face image is regarded as the Mosaic of occluded area and unoccluded area, and the unoccluded area is given a larger weight to code. In the process of recognition, the occlusion area may be directly discarded or the image reconstruction may be carried out according to the occlusion area. The key consideration is how to accurately detect the occlusion position, without understanding the content of the occlusion area, so as to eliminate or suppress the impact of occlusion on face recognition. Compared with the generation model, the discriminant model can save a lot of reconstruction time and avoid the introduction of new noise and other problems during reconstruction. The discriminant models mainly include error weight measurement based on local similarity and occlusion error support estimation.

The error weight measurement based on local similarity is to obtain the error information of the occluded image and its original image by comparing the local similarity. The error is given different weights to measure the occlusion position. When human eyes judge the similarity of two images, they only judge their similar areas and directly ignore the contents of nonsimilar areas. For the recognition of occluded face image, the local similarity between the occluded image and its original image is compared first. Then, the error information obtained is weighted with different weights to code the error, and the occlusion location is estimated. Thus, the occluded area can be detected and only the unoccluded area can be identified. The error weight measurement model based on robust sparse coding and the error weight measurement model based on correlation entropy are used to measure the occlusion region through the local similar errors of the two images. Then, the weight of occlusion features is allocated adaptively to suppress or eliminate the influence of occlusion on the performance of face recognition. However, both of these algorithms have some shortcomings. For example, the two algorithms give different weights adaptively according to the error caused by occlusion, but neither of them provides any technology to guarantee that the error caused by occlusion must be large. Moreover, a new noise is introduced in the iterative weighting process, which reduces the efficiency of occlusion face recognition.

Occlusion error support estimation is used to estimate the occlusion position for the spatial local error structure caused by occlusion. In practical face recognition applications, the original images with occluded images may not always exist, so most methods need to reconstruct the original unoccluded images for the occluded face images to be recognized. This will lead to uncertain reconstruction errors in the reconstructed image, resulting in poor detection effect of occluded areas.

Therefore, in order to accurately and directly detect the occlusion region, it is necessary to make full use of the spatial local continuity of occlusion error.

2.1.3. Robust Feature Extraction.
Robust face image feature extraction is low-order function, such as color, texture, brightness and expression, age, and gender. Such multiscale decomposition features more orientation to avoid interference between various features. To extract image features, suppress or eliminate the impact of obstacle features on recognition performance and achieve robust recognition effect. Existing robust feature extraction methods for occlusion face recognition mainly include "shallow" feature extraction and "deep" feature extraction.

Shallow robust feature extraction is the traditional robust feature extraction method applied to the occlusion case. The most effective and representative features unrelated to occlusion are extracted, so as to achieve robust feature extraction from occlusion face images. Based on image

gradient direction (IGD), feature extraction shaded face images can be measured between the relationships. In order to solve the actual occlusion face recognition problem, literature [17] proposed a low-order model based on adaptive sparse gradient direction. The generalized gradient direction is used to extract effective features and enhance the continuity of the model to maintain the robustness of face recognition. Literature [18] proposed the subspace learning framework of image gradient direction. The occluded test samples and training samples are mapped into the gradient face space. The image gradient feature is robust to the image noise in the gradient face space. It can extract robust face features without the effect of occlusion to a large extent. Mapping the test samples into the image gradient PCA subspace will result in a reconstructed image with almost no occlusion. Thus, robust feature extraction can be realized for occluded face images, and the extracted features can be used for recognition and classification. This method is implemented under the condition that the difference of the occlusion region of two completely different images approximately obeying the uniform distribution. In practice, the difference between the occluded image and its original image is not uniformly distributed. This method is not suitable for face image recognition with arbitrary occlusion because of its poor performance in the real environment.

Deep learning has the characteristics of automatic learning features, and the extracted "deep" features are more expressive and stable than those designed manually. Therefore, deep learning is used to acquire more abstract and expressive deep features. It is expected that the abstract semantic information of data can be represented by multilevel high-order features to obtain robust features. It was considered a good way to overcome the limitations of artificially designed "shallow" features. A robust "depth" feature should both minimize intraclass differences and maximize interclass differences in the image. In order to identify whether multiple face images belong to the same person, the DeepID2 neural network structure was proposed in literature [19]. The convolutional neural network is used for feature learning. Different face features are extracted through face recognition signals, and the interclass differences between different face images are increased. And through the face verification signal to extract the features of the same face, reduce the intraclass differences, so as to learn the strong ability to distinguish features. However, literature [20] adopted forward and backward greedy algorithms to select some effective complementary DeepID2 vectors due to the large number of features to be learned. The features after dimensionality reduction are input into the joint Bayesian model for face classification and recognition. Although the network structure is not designed to distinguish between occluded and nonoccluded faces, the features of deep learning are adaptively robust to occluding. In order to further extract better facial features, literature [21] improved the DeepID2 network and proposed the DeepID2+ network structure. Supervised signals are added in each convolution layer, and the 512-dimension features of the final output are binarized by using threshold values. Therefore, it not only ensures the accuracy of recognition but also improves the

speed of face retrieval. The results show that DeepID2+ is robust to mask human face from bottom to top and black blocks of different sizes. When the occlusion is less than 20% and the block is less than 30×30, the validation accuracy of the output of DeepID2+ is almost unchanged. Furthermore, it provides a new way to deal with the occlusion face recognition.

2.2. The Proposed Algorithm

2.2.1. Mask Separation with Locality Constraint Dictionary Learning Method.
Local constraint dictionary (LCD) means that, given the dictionary Q_H, x_i can be approximately represented by a linear combination of the atoms q_j in the dictionary; that is, $x_i = \sum_{j=1}^{k} c_{ji} q_j$. The embedded $y_i = p(x_i)$ in the d-dimensional space can be represented by the insertion of q_j in a low-dimensional space of $p(q_i)$ nearly linear; that is, $x_j = \sum_{j=1}^{k} c_{ji} p(q_j)$. According to the l_2 distance, in order to minimize the errors of the above two linear representations, the following two expressions should be minimized simultaneously with respect to Q_H and $C = [c_1, c_2, \ldots, c_N]$.

$$
\sum_{j=1}^{N} \left\| p(x_i) - \sum_{j=1}^{K} c_{ji} p(q_j) \right\|^2,
$$
$$
\sum_{j=1}^{N} \left\| x_i - \sum_{j=1}^{K} c_{ji} q_j \right\|^2.
\tag{1}
$$

To ensure choice invariance, constraints $\forall_i, \sum_{j=1}^{K} c_{ji} = 1$, $\|c_i\|_0 = \tau$. Furthermore, if q_j is not in the τ neighborhood of $x_i (i = 1, 2, \ldots, N)$, c_{ij} is equal to 0. If q_j is in the neighborhood of x_i, then $c_{ji} \neq 0$. The corresponding function is shown as

$$
\min_{C, Q_N} \|X - Q_H C\|_F^2 + \lambda \sum_{i=1}^{N} \sum_{j=1}^{K} c_{ji}^2 \left\| x_i - q_j \right\|^2 + \mu \|C\|_F^2,
\tag{2}
$$

where $I^T c_i = 0$, $c_{ji} = 0$, $\forall_i = 1, 2, \ldots, N$, and $q_j \notin \Omega_\tau(x_i)$. And i is the column vector with 1 entry. $\Omega_\tau(x_i) \in R^{n \times \tau}$ is the τ neighborhood of x_i, which contains τ nearest neighbors of x_i. λ is the parameter, $\lambda < 0$.

The form of a face image y blocked by an occlusion object v is $u = y + v$, which violates the low-dimensional linear lighting model and leads to SOC classification error. Occlusion categories in real scenes are predictable and can be collected in advance. Inspired by literature [22], the algorithm in this paper constructs a subdictionary of occlusion object $B = [B_1, B_2, \ldots, B_S]$, and different subscripts represent different categories. Then, add it to the original dictionary as $R = [Q, B]$. The mask v belonging to class t is then represented by the corresponding subdictionary V_t.

Specifically, if a face of the r-th object is occluded by the occlusion of the t-th category, then u is represented linearly by Q_r and B_t as $u = y + v = Q_r X_r + B_t C_t$. By looking for appropriate sparse solutions, a series of coefficients, whose nonzero terms represent faces and occluded objects, can be obtained. The specific form is as follows:

$$W = \left[x^T, c^T \right]^T$$
$$= \left[0, \ldots, 0, x_{r,1}, x_{r,2}, \ldots, x_{r,n}, 0, \ldots, 0, c_{r,1}, c_{r,2}, \ldots, c_{r,n_t}, 0, \ldots, 0 \right]^T. \tag{3}$$

It can be seen that a well-constructed dictionary can deal with all kinds of occlusion effectively and is highly robust in the actual scene. The equation for occlusion identification problem is as follows:

$$\widehat{\omega}_0 = \underset{w}{\arg \min} \| w \|_0 = \underset{x,c}{\arg \min} \| x; c \|_0,$$
$$\text{s.t.} \quad \left\| u - [Q, B] \begin{bmatrix} x \\ c \end{bmatrix} \right\|_2 = \| u - Rw \|_2 \le \varepsilon. \tag{4}$$

When the data are gradually increasing, it is not feasible to solve problem (4), so l_1 normal form is used to replace Al_0 normal form in problem (4), so problem (4) becomes the following problem:

$$\widehat{\omega}_1 = \underset{w}{\arg \min} \| w \|_1 = \underset{x,c}{\arg \min} \| x; c \|_1,$$
$$\text{s.t.} \quad \left\| u - [Q, B] \begin{bmatrix} x \\ c \end{bmatrix} \right\|_2 = \| u - Rw \|_2 \le \varepsilon. \tag{5}$$

Calculate the error between $\widehat{y}$ and $\widehat{y}_i$, where $\widehat{y}_i = Q\delta_i(\widehat{x})$. Even with occlusion, the minimum residual difference can be allocated to sample u. It makes up the occlusion dictionary and the clean face dictionary. The two dictionaries obtained are of considerable use for subsequent occlusion work, as Figure 1 shows. This separates the mask from the face. Compared with the original face, the pixel value of the separated face does not decrease, and the face dictionary composed is more conducive to the subsequent classification. In this paper, the recognition results are presented in a subsequent experiment.

2.2.2. Face Recognition Algorithm Using Attention Mechanism.
The overall network structure proposed in this paper uses two paths for secondary sampling, rather than the traditional U-shaped structure. Dilated convolution is used to obtain more detailed information. ResNet is used to extract features from feature context information, so as to obtain a larger sensory field of vision. Meanwhile, attention modules are designed to improve accuracy by imitating human visual mechanism [23]. Finally, a feature fusion module is designed to integrate the collected features of different sensory fields to obtain better results.

(1) Dilated Convolution. In order to improve the resolution while maintaining a fixed field of view, the algorithm in this paper uses dilated convolution in the spatial information path. The expression of ordinary convolution is as follows:

$$P(x, y) \cdot M(x, y) = \sum_{i=0}^{\omega} \sum_{j=0}^{m} K(i, j) \cdot P(x - i, y - j). \tag{6}$$

In the equation, $P(x, y)$ is the pixel value of the original image at the point (x, y) and $M(x, y)$ is the convolution kernel multiplied by it with the size of $\omega \times m$.

The dilated convolution is calculated as follows:

$$P(x, y) \cdot M'(x, y) = \sum_{i=0}^{\omega} \sum_{j=0}^{m} M'(i, j) \cdot P(x - l \times i, y - l \times j), \tag{7}$$

where l is the expansion factor and $M'(x, y)$ is the dilated convolution kernel. It can be seen from equations (6) and (7) that the dilated convolution is essentially 0 filling of the convolution kernel. It can increase the perception field of the convolution kernel, while retaining the original pixel information, thus increasing the resolution. If the size of the convolution kernel is k and the expansion rate is l, then the actual effective size of the dilated convolution is $k + (k - 1) \times (l - 1)$. Compared with ordinary convolution of the same size, expansive convolution not only expands the perception field but also maintains the same resolution as ordinary convolution.

(2) Attention Mechanism. An attention mechanism is adopted in this paper in order to make up for the loss of details caused by subsampling and better guide model training. It can enhance the target features and suppress the background through the weighted processing of feature map [24]. The target features here are the contour and texture information of the eyes, eyebrows, and face due to the features of the face of the mask. The attention mechanism is mainly composed of spatial attention mechanism, channel attention mechanism, and pyramid attention mechanism, as shown in Figure 2.

(3) Spatial Attention Mechanism. The mechanism of spatial attention is mainly put forward by imitating human visual mechanism. When the human eye sees an image, it automatically gives greater attention to key locations. When you see a rabbit, for example, you pay more attention to the rabbit's ears. Therefore, different parts of the image feature map should have different weights [25]. The spatial attention mechanism proposed in this paper is shown in Figure 3.

The resulting feature graph uses maximum and mean global pooling on the channel dimensions. The feature information of different positions on the feature map is compared and extracted, and the feature weight of each position is obtained.

The maximum global pooling expression is

$$P(i, j) = \max \left(I_t(i, j) \right), \quad t \in (1, c), \tag{8}$$

where $I_t(i, j)$ is the eigenvalue of the feature graph on channel t-th at position (i, j), $P(i, j)$ is the feature graph after maximum pooled, and c is the number of channels.

The global pooling of the mean value is expressed as

$$Q(i, j) = \frac{1}{d} \sum_{n=1}^{d} T_n(i, j). \tag{9}$$

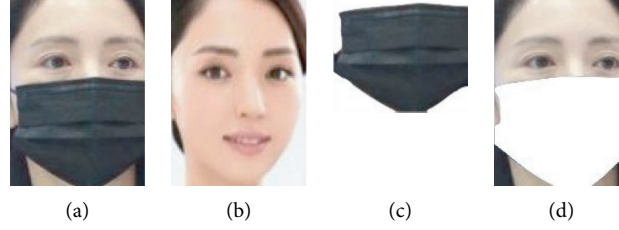(a)   (b)   (c)   (d)

FIGURE 1: The example of mask separation. (a) Mask face image. (b) Reference image. (c) Separated mask. (d) Separated face.

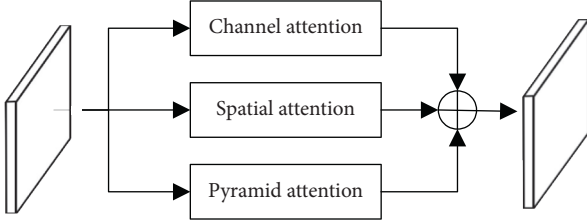FIGURE 2: Structure of attention mechanism.

In the equation, $T_n(i, j)$ is the eigenvalue of the nth channel feature graph at the position (i, j). $Q_n(i, j)$ is the feature graph after averaging pooling, and d is the number of channels.

The two feature maps are connected in channel dimension by means of channel connection. In order to better integrate the information extracted by the two methods, the size of 1×1 convolution kernel is used for learning. The final weight of attention of the obtained feature map was calculated by sigmoid function [26], so as to avoid errors caused by excessive weight coefficient.

The sigmoid function is expressed as follows:

$$SF(x) = \frac{1}{1 + e^{-x}}, \tag{10}$$

where SF (x) is the response of the output and x is the input.

Spatial attention mechanism can effectively extract salient information of each position in the feature map. Based on this, a weight is assigned to the eigenvalue of each position to extract the main feature of the target effectively.

(4) Channel Attention Mechanism. Each channel of the feature map extracted by convolutional neural network (CNN) represents an image feature, such as texture and shape. The target features here are the contour and texture information of the eyes, eyebrows, and face due to the features of the face of the mask. In the image, each feature contains different information, and its contribution to image segmentation is also different. Therefore, different attention should be paid to each different feature [27] and different weights should be assigned. Channel attention mechanism is designed to assign weight to features so that the network can focus on important features, as shown in Figure 4.

By using global maximum pooling and global average pooling, the channel information is modeled in spatial dimension and the characteristic information of each channel is obtained.

The calculation process of maximum pooling is

$$Q_c = \max(I_c(i, j)). \tag{11}$$

In the equation, $i \in (1, h)$, $j \in (1, \omega)$, c represents c-th feature graph, and Q_c represents the output of the feature graph after maximum pooling.

The calculation process of average pooling is

$$Q_t = \frac{1}{\omega} \frac{1}{h} \sum_{i=1}^{t} \sum_{j=1}^{\omega} I_t(i, j). \tag{12}$$

In the equation, $i \in (1, h)$, $j \in (1, \omega)$, t represents the m-th feature graph, and Q_t represents the output of the feature graph after average pooling.

In order to use less computation to integrate the feature graphs obtained by global pooling, the two feature graphs are, respectively, passed through a convolution kernel of size 1×1. Then, nonlinear components are added through BN layer and ReLU layer to make the model fit better. This method can prevent the occurrence of overfitting phenomenon to a certain extent. Finally, the two feature graphs obtained are fused and the final weight is obtained through the sigmoid function.

(5) Pyramid Attention Mechanism. Human vision tends to integrate a variety of information when discriminating objects. For example, distinguishing a rabbit from a cat pays more attention to the shape of its ears, and distinguishing a panda from a bear pays more attention to its color. It can be seen that different features in different positions on the feature map should receive different attention. In order to obtain different information of different position of image better, a pyramid type attention model is proposed. By extracting the feature map of different perceptual field, the image information under different perceptual field is obtained. This information was fused to obtain the final weight coefficient, as shown in Figure 5.

The feature graphs are, respectively, passed through 3×3, 1×1, and 5×5 convolution kernels. Because these convolution kernels are used in low-resolution high-level feature maps, there is not much computational burden. Then the feature images are collected by convolution kernels of different sizes. In this way, contextual information can be better integrated and feature information can be obtained at different scales. Through these convolution kernels of different sizes, the characteristic information under different perceptual fields is obtained. Based on the above feature
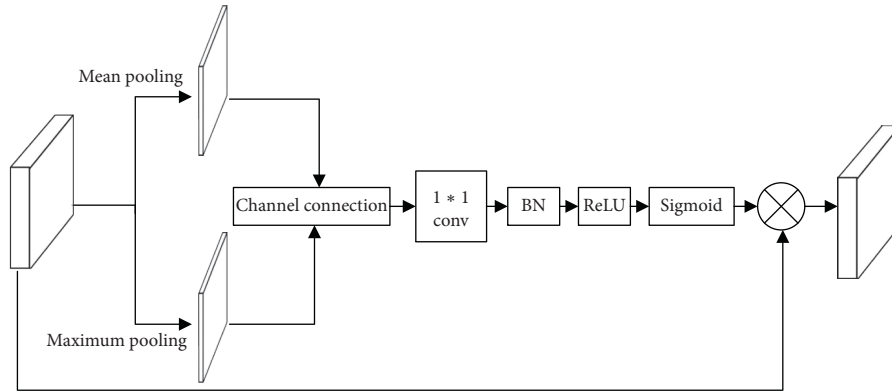
Figure 3: Spatial attention mechanism.
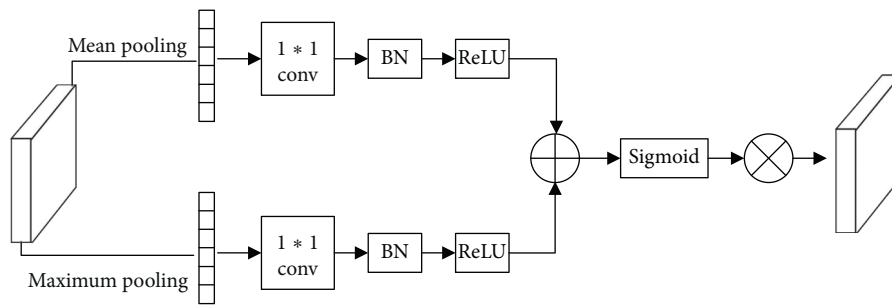
Figure 4: Channel attention mechanism.
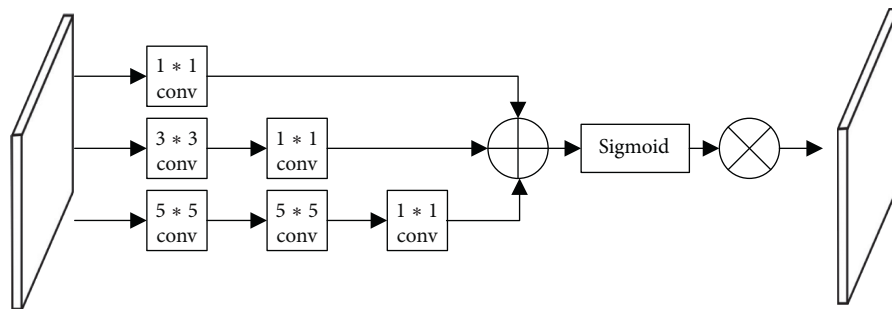
Figure 5: Pyramid attention mechanism.

information, the feature weights of different positions are obtained through a 1×1 convolution kernel. Finally, the obtained feature graphs are added for fusion, and the final weight is obtained through the sigmoid function.

(6) Feature Fusion Module. For different types of objects, the importance of vision perception is different. For larger objects, the features acquired from the larger visual field are more important. For smaller objects, the features of larger visual field will collect too much peripheral information and lead to errors. The traditional feature fusion methods are generally cascade or addition, which does not take into account the different sensory field of different feature graphs and ignores the specificity of features. In view of this, the

feature fusion module designed in this paper assigns different weights to feature images with different perception fields to achieve better feature fusion, as shown in Figure 6.

First, the two input feature maps are linked at the channel dimension level. Secondly, the cascaded feature image is fused by a 3×3 convolution kernel to realize the preliminary fusion of feature image information. Global pooling operation is carried out to extract the information of each feature map. Then, the obtained feature image is passed through the convolution kernel of size of 1×1, so that the network learns the weight according to the overall information of each feature image. Finally, the sigmoid function is used to get the final weight, which is multiplied by the original feature graph. Through the feature fusion module,
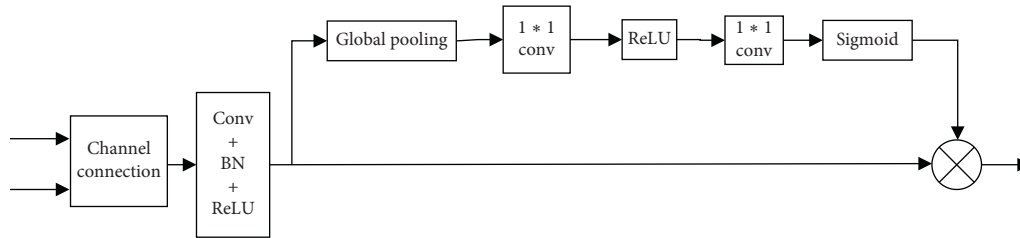
Figure 6: Feature fusion module.

(a)

(b)
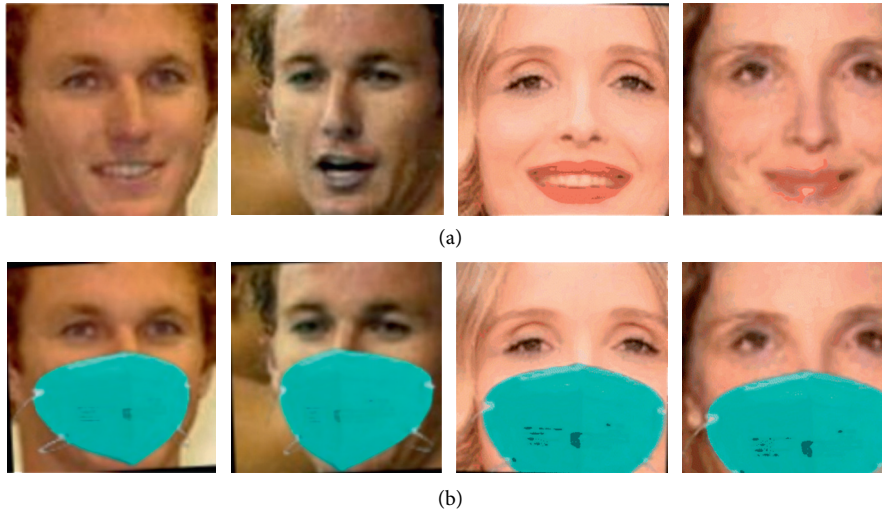
Figure 7: The face images of SMFRD. (a) Face image without mask. (b) Masked face images.

weight is assigned to the feature images under different perceptual fields, so that the feature specificity under different perceptual fields can be reflected, and the features can be fused better.

3. Results and Discussion

In this paper, the RMFRD (real-world face recognition dataset) and SMFRD (simulated face recognition dataset) [28] opened by Wuhan University are selected as the experimental databases. RMFRD and SMFRD are the first real face mask dataset in the world, and the simulated masked image data in SMFRD are based on LFW [29] and Webface [30] datasets. The experiment in this paper is carried out on a 16 GB memory NVIDIA GeForce GTX1080TI GPU workstation.

3.1. Experiment on SMFRD Dataset. The SMFRD database simulates wearing a mask on the existing public large-scale face dataset to obtain a large number of face images. Among them, public large-scale face datasets include commonly used LFW and Webface datasets. In this way, a simulated masked face dataset was constructed, covering 500,000 face images from 10,000 subjects. Figure 7 shows multiple pairs of face images.

In the training process, 5000 people were randomly selected from 10000 people as the training set. Among them,

a normal image without a mask was selected as the baseline image for recognition. During the training process, other normal images without masks were first selected for training. Then, all face images wearing masks were selected for training.

In the test phase, the remaining 5000 people were selected as the test set. During the test, a normal image without a mask was selected as the baseline image for recognition. During the test, other normal images without masks were selected for identification tests. Then, all faces wearing masks were selected for recognition tests.

In this paper, the PCA + SVM [31], SRC [32], CNN, and DCGAN + CNN [33] are selected for comparison. In the DCGAN + CNN method, DCGAN is used to fill the occlusion face image, and CNN is also a fine-tuned VGGFACE model for face recognition. All methods were tested on the RMFRD dataset, and the results are shown in Table 1. It can be seen that the expression recognition accuracy of the proposed method in this paper is high, regardless of whether the face image is covered by a mask or not. In the deep learning method, although DCGAN + CNN method also fills the face image, the consistency of the image obtained is poor, which affects the accuracy of expression recognition. The proposed algorithm in this paper has already separated the mask part before face recognition and then extracted the important features such as eyes and eyebrows by using the attention mechanism, so the algorithm in this paper has higher stability.

TABLE 1: Comparison of recognition rates with different algorithms.

Methods	Image without mask	Image with mask
PCA + SVM [31]	91.22	68.63
SRC [32]	92.80	72.42
CNN [33]	97.52	69.63
DCGAN + CNN [33]	97.59	75.85
Proposed	98.39	95.31

FIGURE 8: The images of RMFRD. (a) Masked face images. (b) and (c) Face images without mask.

3.2. Experiment on RMFRD Dataset. The face images of RMFRD dataset come from Internet resources, in which the front image of public figures and their corresponding face mask images are captured by the crawler tool. Then, the unreasonable face images were manually removed and a tagging tool was experimented with to crop the exact face areas. The dataset consisted of 5,000 photos of 525 people wearing masks and 90,000 photos of 525 people not wearing masks. Figure 8 shows multiple pairs of face images.

In the training process, 300 people were randomly selected from 525 people as the training set. Among them, a normal image without a mask was selected as the baseline image for recognition. During the training process, other normal images without masks were first selected for training. Then, all face images wearing masks were selected for training.

In the test phase, the remaining 325 people were selected as the test set. During the test, a normal image without a

TABLE 2: Comparison of recognition rates with different algorithms.

Methods	Image without mask	Image with mask
PCA + SVM [31]	90.14	67.82
SRC [32]	91.92	72.37
CNN [33]	97.21	68.69
DCGAN + CNN [33]	97.36	75.21
Proposed	98.10	95.22

TABLE 3: Comparison of time consuming with different algorithms.

Methods	Image without mask (%)	Image with mask (%)
PCA + SVM [31]	0.92	0.93
SRC [32]	1.20	1.20
CNN [33]	0.87	0.89
DCGAN + CNN [33]	1.23	1.25
Proposed	0.91	0.98

mask was selected as the baseline image for recognition. During the test, other normal images without masks were selected for identification tests. Then, all faces wearing masks were selected for recognition tests.

PCA + SVM, SRC, CNN, and DCGAN + CNN algorithms were selected, and experiments were carried out on RMFRD dataset at the same time as the proposed algorithm. The recognition results are shown in Table 2. It can be seen that the expression recognition accuracy of the method presented in this paper is higher than other methods.

3.3. The Algorithm Efficiency. In order to compare the efficiency of the algorithm, the time consumption of the recognition process is compared. The time consumption of different face recognition methods is compared, which is as shown in Table 3. It can be seen from the table that the recognition time of the algorithm in this paper is less than 1 second, which can meet the experiment of actual use scenarios.

4. Conclusions

Since COVID-19 can be spread by contact, contactless delivery cabinets are becoming increasingly normal. The self-delivery cabinet is an important piece of terminal express delivery equipment in the contactless express delivery scenario, and the masked face recognition is one of the effective way to achieve the contactless express delivery. In this paper, the local constrained dictionary learning method firstly is used to separate the masked face image, and the parts of the mask are separated to reduce the impact on the recognition algorithm. Then, the dilated convolution method is used to reduce the impact of resolution reduction in the sampling process. According to the important features of face images, such as eyes and eyebrows, multiple features are extracted by using attention machine neural network. Finally, the algorithm comparison experiment is carried out through the simulation face masked image database and the real face masked image database. Experimental results show

that the proposed algorithm has a better recognition rate and also has important application value in contactless express delivery scenarios.

Data Availability

The RMFRD (real-world face recognition dataset) and SMFRD (simulated face recognition dataset) opened by Wuhan University are selected as the experimental databases. The data can be downloaded from https://github.com/X-zhangyang/Real-World-Masked-Face-Dataset. Because of the programmer's reason, the source code of this algorithm is not convenient to provide directly. The readers can program if interested, according to the idea of the paper.

Conflicts of Interest

The author declares no conflicts of interest.

Acknowledgments

References

[1] J. Qian, J. Yang, F. Zhang, and Z. Lin, "Robust low-rank regularized regression for face recognition with occlusion," in *Proceedings of the IEEE Conference on Computer Vision and Pattern Recognition Workshops*, Columbus, OH, USA, June 2014.

[2] Y. Ouyang, N. Sang, and R. Huang, "Accurate and robust facial expressions recognition by fusing multiple sparse representation based classifiers," *Neurocomputing*, vol. 149, pp. 71–78, 2015.

[3] F. Zhao, J. Feng, J. Zhao, W. Yang, and S. Yan, "Robust LSTM-autoencoders for face de-occlusion in the wild," *IEEE Transactions on Image Processing*, vol. 27, no. 2, pp. 778–790, 2017.

[4] H. Possegger, T. Mauthner, P. M. Roth, and H. Bischof, "Occlusion geodesics for online multi-object tracking," in *Proceedings of the IEEE Conference on Computer Vision and Pattern Recognition*, pp. 1306–1313, Columbus, OH, USA, June 2014.

[5] L. A. Camuñas-Mesa, T. Serrano-Gotarredona, S. H. Ieng, R. Benosman, and B. Linares-Barranco, "Event-driven stereo visual tracking algorithm to solve object occlusion," *IEEE Transactions on Neural Networks and Learning Systems*, vol. 29, no. 9, pp. 4223–4237, 2017.

[6] M. Iliadis, H. Wang, R. Molina, and A. K. Katsaggelos, "Robust and low-rank representation for fast face identification with occlusions," *IEEE Transactions on Image Processing*, vol. 26, no. 5, pp. 2203–2218, 2017.

[7] Z. Ying, G. Jun, C. Guo, and F. Wengang, "Multi-scale and multi-orientation texture feature extraction method based on fractal theory," *Chinese Journal of Scientific Instrument*, vol. 29, no. 4, p. 787, 2008.

[8] N. Naik, P. Jenkins, and N. Savage, "A ransomware detection method using fuzzy hashing for mitigating the risk of occlusion of information systems," in *Proceedings of the 2019 International Symposium on Systems Engineering (ISSE)*, pp. 1–6, IEEE, Edinburgh, UK, October 2019.

[9] S. Zeng, J. Gou, and L. Deng, "An antinoise sparse representation method for robust face recognition via joint l_1 and l_2 regularization," *Expert Systems with Applications*, vol. 82, pp. 1–9, 2017.

[10] W. Ou, X. You, D. Tao, P. Zhang, Y. Tang, and Z. Zhu, "Robust face recognition via occlusion dictionary learning," *Pattern Recognition*, vol. 47, no. 4, pp. 1559–1572, 2014.

[11] Y. Chen, G. Lin, S. Li et al., "BANet: bidirectional aggregation network with occlusion handling for panoptic segmentation," in *Proceedings of the IEEE/CVF Conference on Computer Vision and Pattern Recognition*, pp. 3793–3802, Seattle, WA, USA, August 2020.

[12] J. Wright, A. Y. Yang, A. Ganesh, S. S. Sastry, and Y. Ma, "Robust face recognition via sparse representation," *IEEE Transactions on Pattern Analysis and Machine Intelligence*, vol. 31, no. 2, pp. 210–227, 2008.

[13] X. Song, Y. Chen, Z.-H. Feng, G. Hu, T. Zhang, and X.-J. Wu, "Collaborative representation based face classification exploiting block weighted LBP and analysis dictionary learning," *Pattern Recognition*, vol. 88, pp. 127–138, 2019.

[14] H. Zhang, W. He, L. Zhang, H. Shen, and Q. Yuan, "Hyperspectral image restoration using low-rank matrix recovery," *IEEE Transactions on Geoscience and Remote Sensing*, vol. 52, no. 8, pp. 4729–4743, 2013.

[15] Z. Gao, L.-F. Cheong, and Y.-X. Wang, "Block-sparse RPCA for salient motion detection," *IEEE Transactions on Pattern Analysis and Machine Intelligence*, vol. 36, no. 10, pp. 1975–1987, 2014.

[16] C.-P. Wei, C.-F. Chen, and Y.-C. F. Wang, "Robust face recognition with structurally incoherent low-rank matrix decomposition," *IEEE Transactions on Image Processing*, vol. 23, no. 8, pp. 3294–3307, 2014.

[17] Q. Xu and Y. Xu, "Extremely low order time-fractional differential equation and application in combustion process," *Communications in Nonlinear Science and Numerical Simulation*, vol. 64, pp. 135–148, 2018.

[18] G. Tzimiropoulos, S. Zafeiriou, and M. Pantic, "Subspace learning from image gradient orientations," *IEEE Transactions on Pattern Analysis and Machine Intelligence*, vol. 34, no. 12, pp. 2454–2466, 2012.

[19] Y. Sun, D. Liang, X. Wang, and X. Tang, "Deepid3: face recognition with very deep neural networks," 2015, https://arxiv.org/abs/1502.00873.

[20] M. Fachrurrozi, A. Wijaya, and M. N. Rachmatullah, "New optimization technique to extract facial features," *IAENG International Journal of Computer Science*, vol. 45, no. 4, 2018.

[21] Y. Sun, X. Wang, and X. Tang, "Deeply learned face representations are sparse, selective, and robust," in *Proceedings of the IEEE Conference on Computer Vision and Pattern Recognition*, pp. 2892–2900, Boston, MA, USA, June 2015.

[22] Y. Wen, W. Liu, M. Yang, Y. Fu, Y. Xiang, and R. Hu, "Structured occlusion coding for robust face recognition," *Neurocomputing*, vol. 178, pp. 11–24, 2016.

[23] A. Vaswani, N. Shazeer, N. Parmar et al., "Attention is all you need," in *Proceedings of Advances in Neural Information Processing Systems*, pp. 5998–6008, Long Beach, CA, USA, December 2017.

[24] A. Gilra and W. Gerstner, "Non-linear motor control by local learning in spiking neural networks," in *Proceedings of the International Conference on Machine Learning*, Stockholm, Sweden, July 2018.

[25] K. He, X. Zhang, S. Ren, and J. Sun, "Deep residual learning for image recognition," in *Proceedings of 2016 IEEE Conference on Computer Vision and Pattern Recognition*, pp. 770–778, IEEE, Las Vegas, NV, USA, June 2016.

[26] X. Yin, J. A. N. Goudriaan, E. A. Lantinga, J. Vos, and H. J. Spiertz, "A flexible sigmoid function of determinate growth," *Annals of Botany*, vol. 91, no. 3, pp. 361–371, 2003.

[27] S. Woo, J. Park, J.-Y. Lee, and I. S. Kweon, "Cbam: convolutional block attention module," in *Proceedings of the European Conference on Computer Vision (ECCV)*, pp. 3–19, Munich, Germany, July 2018.

[28] Z. Wang, G. Wang, B. Huang et al., "Masked face recognition dataset and application," 2020, https://arxiv.org/abs/2003.09093.

[29] Y. Guo, L. Zhang, Y. Hu, X. He, and J. Gao, "Ms-celeb-1m: a dataset and benchmark for large-scale face recognition," in *Proceedings of the European Conference on Computer Vision*, pp. 87–102, Springer, Amsterdam, Netherlands, July 2016.

[30] S. Pepin and C. Körner, "Web-FACE: a new canopy free-air CO_2 enrichment system for tall trees in mature forests," *Oecologia*, vol. 133, no. 1, pp. 1–9, 2002.

[31] Y. Luo, C. Wu, and Y. Zhang, "Facial expression recognition based on principal component analysis and support vector machine applied in intelligent wheelchair," *Application Research of Computers*, vol. 29, no. 8, pp. 3166–3168, 2012.

[32] M. Zhu, S. Li, and H. Ye, "An occluded facial expression recognition method based on sparse representation," *Public Relations & Artificial Intelligence*, vol. 27, no. 8, pp. 708–712, 2014.

[33] R. Yeh, C. Chen, T. Y. Lim, and M. Hasegawa-Johnson, "Semantic image inpainting with perceptual and contextual losses," in *Proceedings of IEEE Conference on Computer Vision and Pattern Recognition*, pp. 6882–6890, Honolulu, HI, USA, July 2017.

Research Article

Unrestricted Face Recognition Algorithm Based on Transfer Learning on Self-Pickup Cabinet

Zhixue Liang ⓘ

School of Computer and Software, Nanyang Institute of Technology, Nanyang 473000, China

Correspondence should be addressed to Zhixue Liang; 3161015@nyist.edu.cn

In the contactless delivery scenario, the self-pickup cabinet is an important terminal delivery device, and face recognition is one of the efficient ways to achieve contactless access express delivery. In order to effectively recognize face images under unrestricted environments, an unrestricted face recognition algorithm based on transfer learning is proposed in this study. First, the region extraction network of the faster RCNN algorithm is improved to improve the recognition speed of the algorithm. Then, the first transfer learning is applied between the large ImageNet dataset and the face image dataset under restricted conditions. The second transfer learning is applied between face image under restricted conditions and unrestricted face image datasets. Finally, the unrestricted face image is processed by the image enhancement algorithm to increase its similarity with the restricted face image, so that the second transfer learning can be carried out effectively. Experimental results show that the proposed algorithm has better recognition rate and recognition speed on the CASIA-WebFace dataset, FLW dataset, and MegaFace dataset.

1. Introduction

At present, the global epidemic prevention and control has become normal, so it is necessary to develop effective prevention and control measures. In the field of logistics distribution, terminal contactless distribution has become the focus of the public [1]. At present, the main research technology of terminal contactless matching is face recognition technology. In the contactless scene, the face images are often interfered by unrestricted environmental factors such as light, occlusion, and expression. For the face image affected by the unrestricted environment, the quality is poor, so it is difficult to recognize, and the recognition accuracy is low [2]. Therefore, the study of the fast face image recognition algorithm in unconstrained environment is of great significance for the field of terminal contactless distribution.

In computer vision, face recognition is one of the most important research directions. Face recognition can be used in digital cameras, access control systems, identity recognition network applications and entertainment applications, and other fields. With the rapid development of artificial intelligence and image analysis technology, face recognition

technology has been widely used in many fields [3]. However, face images collected under an unrestricted environment are subjects to the mixed interference of illumination, occlusion, expression, and other factors, so that the face recognition accuracy is greatly reduced. At the same time, because the original image exists in high dimensional data, the speed of face recognition is also affected. Therefore, it is of great significance to study the fast face image recognition algorithm in unrestricted environment.

The face recognition method can be divided into the traditional method and deep neural network method. The traditional methods are mainly composed of the geometric feature-based method, local feature analysis method, and eigenface method. In recent years, with the rapid development of deep learning theory, the deep neural network has become the most widely used algorithm in face recognition. The first deep neural network model that attracted attention in face recognition was the Facebook's DeepFace [4] model in 2014. The DeepFace model is the first study to use deep learning to approach human performance in face recognition. It achieves an average accuracy of 97.35% on the LFW dataset, approaching the human limit of 97.5%. DeepFace

extracts highly compressed facial features, and models facial features with the 3D model. The model assumes that the feature parts of all faces are fixed at the pixel level, and the faces are aligned by region-based affine transformation. Finally, a deep neural network is used as a feature extractor to extract the face features from the image. This model contains a very large number of parameters due to the use of the full connection layer. Subsequently, Professor Tang et al. developed a series of new deep neural network structures of DeepID. DeepID1 [5] is a small network consisting of four convolutional layers and two fully connected layers. The output DeepID feature of the penultimate layer contains 160 dimensions. The higher the number of layers is, the larger the receptive field is in the features of the convolutional neural network. So the connection mode takes into account both the local features of the face and the global features of the whole face. DeepID2 [6] added the loss function of face verification on the basis of DeepID1 and learned the discriminant features of faces through two objective functions. In the final loss function, the importance of face classification and face verification is adjusted by changing the weight of the two loss functions. The final loss function is composed of the weighted sum of the two loss functions of face classification and face verification. The subsequent DeepID2+ [7] network continues to change the network structure on the basis of DeepID2, from 160 dimensions to 512 dimensions. The second is that a lot of structural analysis has been performed, and it turns out that neurons at the higher levels are more sensitive to faces. DeepID2+ achieves results that exceed human performance on LFW datasets and is robust to appropriate face occlusion. Compared with the DeepID2+ model, the latest DeepID3 model further deepens the number of layers and achieves better results.

In recent years, it has become a trend to train models to complete face recognition based on the deep neural network using larger labeled datasets. For example, Google used 200 million face images containing 8 million different individuals in FaceNet [8]. However, the cost of collecting and tagging such datasets is enormous, and training them through deep neural networks requires better hardware support. Larger and larger datasets are used to train better models, but this is not a good development direction. For example, when the face verification accuracy on the LFW dataset increased from 99.47% to 99.77%, the number of trained images increased from 200,000 to 1.2 million. However, in most realistic scenarios, only a small amount of data can be used, and how to learn rich knowledge from these limited data is a problem to be solved. There is growing interest in the research and development of technologies in different fields, such as domain adaptive and transfer learning [9], and the personalized search model achieved amazing results [10]. In a study [11], a transfer learning algorithm combining a large number of source domain samples with a relatively small number of target domain data is proposed. In a study [12], a deep transfer metric learning method for cross-domain visual recognition is proposed by transferring recognition knowledge from the labeled source domain to the unlabeled target domain. Therefore, the best way to guide the face representation learning of a few

samples through deep learning can be knowledge transfer or domain adaptation. In other words, you can learn some preknowledge from other large databases and then fine-tune that knowledge in your target domain.

Therefore, compared with traditional machine learning methods, deep learning methods have great advantages in the field of feature extraction. In other words, the convolutional neural network algorithm can automatically extract the features of the image content layer by layer without any prior knowledge [13]. When the number of samples is large enough and the number of network layers is large enough, the data can be fully excavated to extract excellent features with resolution. However, deep learning is driven by data, and it is difficult to extract features with generalization ability when the amount of data is insufficient. In the unrestricted environment, the number of face images is small and the acquisition cost is high, so the data scale is not enough to support the training of the network.

In this study, the transfer learning method is used to solve the problem of insufficient number of face images in unrestricted environment. First, the faster RCNN algorithm is improved to improve the recognition speed of the algorithm. Then, the network parameters trained by the ImageNet large-scale dataset [14] are used for initialization by using one transfer learning. Second, the network parameters are tuned through the face images under restricted conditions with relatively sufficient data volume, and the face images under restricted conditions are trained to be able to recognize. Finally, the face image is enhanced under unrestricted conditions, such as attitude alignment, illumination brightness enhancement, and angle rotation. Therefore, it can increase its similarity with the face image under the restricted condition. After secondary transfer learning of the previously obtained restricted face image recognition network, the network that can accurately recognize the unrestricted face image is obtained.

The rest of this article is organized as follows. The second section introduces the face recognition model of the improved faster RCNN algorithm. The third section introduces the enhancement method of unrestricted face image. The fourth section gives the transfer learning method and experimental results. The fifth section is the conclusion of this study.

2. Materials and Methods

2.1. Face Recognition Model with the Improved Faster RCNN Algorithm. Faster RCNN is an improvement object detection framework over the existing RCNN algorithm framework. RCNN combines CNN with a regional candidate box. On this basis, a faster RCNN algorithm appears [15]. The basic idea of these algorithms is to divide the original image into different candidate boxes. The convolutional neural network CNN is used as a feature extractor, and a feature vector is extracted from the candidate box. Then, a classifier is trained to classify the feature vectors. Finally, the target detection framework consists of three parts as shown in Figure 1.
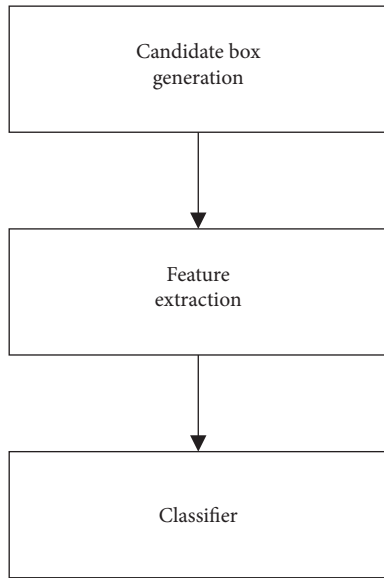
Figure 1: The target detection framework.

The faster RCNN proposes a region proposal network (RPN) to generate candidate boxes based on the convolutional neural network. In this network, the faster RCNN is still used as the detector. RPN and faster RCNN actually share a convolutional layer to extract features; thus, RPN and faster RCNN combine to form a single unified a faster RCNN network. As shown in Figure 2, it can be roughly divided into four parts: convolutional trunk network, RPN micronetwork, faster RCNN detector, and multitask loss.

In order to speed up the detection process of the model, the convolutional backbone network and the multitask loss function are adjusted; at the same time, the RPN micronetwork of faster RCNN is improved in this study.

2.2. The Adjusted Convolution Backbone. The convolutional layer in faster RCNN borrows the convolutional layer architecture of the classical classification model and its pretrained weight. The pretrained model of the classification task was applied to a similar detection task, and the weight of the classification model was directly adjusted, which greatly reduced the training amount of the model.

As shown in Figure 3, the convolutional layer part of the VGG-16 classification model [16] is adopted by the convolutional backbone network in this study. The feature map is not pooled before output, which changes slightly. The step length of all convolution operations is 1, and the boundary filling is 1. The width and height of convolution kernel is 3×3, which ensures that the width and height of the image remain unchanged before and after convolution. The pooling layer adopts the maximum pooling of 2×2 with a step size of 2. The pooling layer does not affect the number of channels in the image. However, after each pooling, the width and height of the image will be halved. The number of channels for convolution is 64, 128, 256, 512, and so on. The number of channels represents the number of feature images extracted by convolution. After each convolutional layer, the rectified

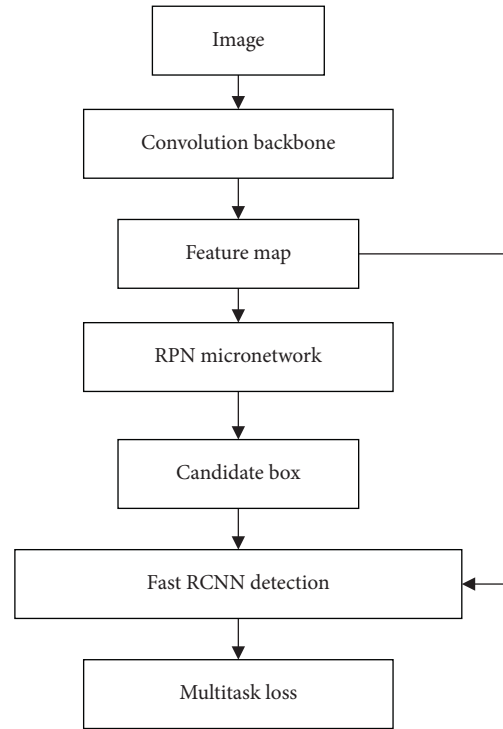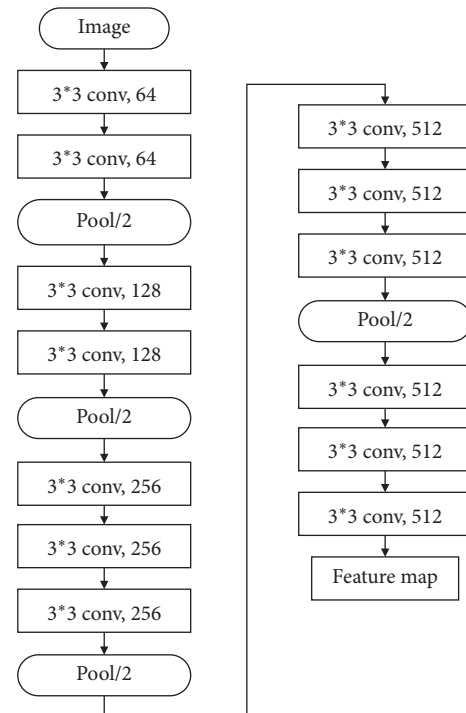Figure 2: The algorithm framework of faster RCNN.

Figure 3: The convolution backbone of faster RCNN.

linear unit (ReLU) activation function performs nonlinear transformation, which does not affect the width and height of the feature and the number of channels. Therefore, after the input image is convolved with 13 layers and pooled with 4 layers, the width and height of the output feature map

obtained will become 1/16 of the original image, and the number of channels will change from RGB 3 channels to 512.

2.3. Improved RPN Micronetwork.

The RPN micronetwork adopts the sliding window mode to generate 9 anchors in the input image for each point on the feature map. As shown in Figure 4, it is the anchor point corresponding to the center point of the feature map on the input image. The outer black box is the original image of 800×600 pixels. The inside, the middle, and the outside of the three thick and thin boxes, respectively, represent the size of 128, 256, and 512. In each scale, there are three situations of aspect ratio of $1:2$, $1:1$, and $2:1$, so each sliding window corresponds to 9 anchors.

In the original anchor, 128, 256, and 512 are set in order to ensure that the target object can adapt to various scales. As for anchor settings with three scales and three proportions, this is equivalent to a point in the feature map that can correspond to 9 regions in the original image perception field. Each area corresponds to an anchor. With supervised learning parameter training, the model can adjust the parameters, so that the calculated feature map can correspond to the object in the original picture. Smaller scales can capture small differences between objects, which allow different classes of objects to be distinguished. The larger scale can ensure that the original image is covered, that is, all the receptive fields, so that the original image will not miss the undetected objects.

The RPN network structure is shown in Figure 5. For a given input image, the convolutional layer generates the convolutional feature map. The RPN micronetwork slides a small window of 3×3 on the feature map after convolution. Each window maps to a 256-dimensional eigenvector, which is then fed into two branch networks: Cls classification network and Reg regression network. Here, the original 512-dimension eigenvector is improved to a 256-dimension eigenvector, which accelerates the detection speed.

Cls classifier classifies the feature vectors of window mapping. It predicts a foreground probability and background probability for each anchor, so there will be $2 \times 9 = 18$ probability values, which are represented by 18 neurons. The Reg regression performs regression on the eigenvectors of the window map. It predicts the center point coordinates and offset of width and height of each anchor, which is represented by (t_x, t_y, t_w, t_h). So there are $4 \times 9 = 36$ offsets, represented by 36 neurons. Note that the processing of the feature map is carried out in a sliding window mode, so these processes can be realized by convolution operation.

2.4. Multitasking Loss.

For RPN training, the multitask loss is adopted in this study to combine the cross entropy loss of the classifier with the Smooth$_{L1}$ loss of the regression. In order to get the multitask loss, suppose that its classification loss is $L_{cls}(p_i, p_i^*)$ and regression loss is $L_{reg}(t_i, t_i^*)$, then the multitask loss $L(\{p_i\}, \{t_i\})$ of all samples is calculated as follows:
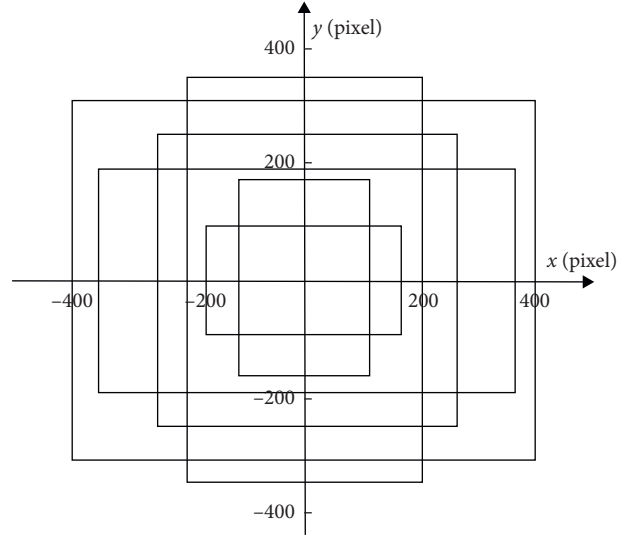
Figure 4: Anchor corresponding to the center point of the feature map.
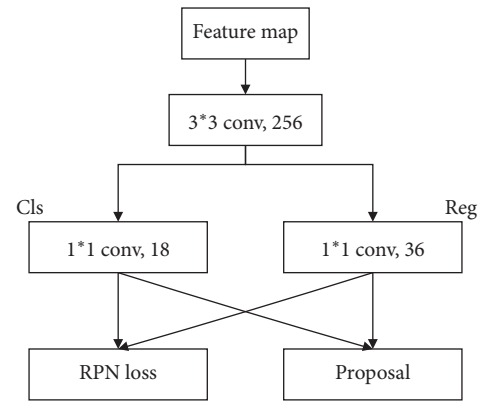
Figure 5: The RPN micronetwork.

$$\frac{1}{N_{cls}} \sum_i L_{cls} + \lambda \frac{1}{N_{reg}} \sum_i p_i^* L_{reg}, \tag{1}$$

where N_{cls} and N_{reg} are the standardized terms, and λ is the tradeoff coefficient. Consider the classification loss of a single sample

$$L_{cls}(p, p^*) = -\log p_{p^*}, \tag{2}$$

where p^* is the category tag corresponding to anchor, and p is the prediction probability of its corresponding category tag.

In the multitask loss, only the regression loss of the anchor marked as positive is calculated, and the regression loss function is considered separately.

$$L_{reg}(t_i, t_i^*) = \text{Smooth}_{L1}(t_i - t_i^*), \tag{3}$$

where

$$\text{Smooth}_{L_1}(x) = \begin{cases} 0.5x^2, & \|x\| < 1, \\ \|x\| - 0.5, & \text{others,} \end{cases} \tag{4}$$

where t_i and t_i^* are represented by a source of four groups. In order to express the simplicity of above, the subscript i is removed. And only the regression under a single sample is considered for the predicted offset t_i of anchor and the true offset t_i^* of ground truth for anchor.

$$t = (t_x, t_y, t_w, t_h),$$
$$t^* = (t_x^*, t_y^*, t_w^*, t_h^*), \tag{5}$$

where

$$t_x = \frac{(x - x_a)}{w_a},$$

$$t_x^* = \frac{(x^* - x_a)}{w_a},$$

$$t_y = \frac{(y - y_a)}{h_a},$$

$$t_y^* = \frac{(y^* - y_a)}{h_a},$$

$$\tag{6}$$

$$t_w = \log\left(\frac{w}{w_a}\right),$$

$$t_w^* = \log\left(\frac{w^*}{w_a}\right),$$

$$t_h = \log\left(\frac{h}{h_a}\right),$$

$$t_h^* = \log\left(\frac{h^*}{h_a}\right).$$

The SGD method [17] is used in the RPN network to optimize the multitask loss function to minimize the loss function $L(\{p_i\}, \{t_i\})$. In the optimization process, the model adjusts the parameters to find a local optimal solution. During the test, RPN is used to predict the category probability of each anchor and the regression offset of the anchor marked as positive. The candidate box of regression offset correction is obtained by using the nonmaximal suppression method from the output of the RPN micronetwork.

3. The Enhancement Method of Unrestricted Face Image

3.1. Face Posture Alignment through Image Rotation.
Because of the complicated attitude problem, the image in nature brings great challenge to the key point positioning. Therefore, face image posture clustering is needed, and then, different categories of images are trained. For an image I, the goal of face alignment is to learn a nonlinear mapping

function D from features to key points. Due to the large difference in attitude, D's learning process is complex, so D is divided into several simple subtasks $\{D_1, D_2, \ldots, D_n\}$. In this way, in each subtask D_k, faces have similar postures, which simplifies the learning of D.

Because of the diversity of posture, affine transformation is used to adjust face pose before clustering. Affine transformation matrix M is given in equation (7). Affine transformation only needs two sets of three-point coordinates to obtain the matrix M. The three coordinates are the coordinates of the two eyes and the middle position of the mouth. For each image, one is the coordinates $(x, y, 1)^T$ in the original coordinate system, and the other is the coordinates $(u, v, 1)^T$ in the target seat system. Notice that the position of the eyes in the target coordinate system is on the same horizontal line. Once the transformation matrix M is calculated, it can be used to affine transform the entire image. The result is shown in Figure 6. The first row is before the affine transformation, and the second row is after the transformation. There are only three kinds of corrected facial posture: positive face, left face, and right face.

$$\begin{bmatrix} u \\ v \\ 1 \end{bmatrix} = \begin{bmatrix} a_1 b_1 c_1 \\ a_2 b_2 c_2 \\ 000 \end{bmatrix} \begin{bmatrix} x \\ y \\ 1 \end{bmatrix}. \tag{7}$$

Considering that no real labels about poses are provided in the dataset, the K-means unsupervised clustering algorithm [18] is used to realize pose clustering. Then, a better initial position is provided closer to the true position for all samples in each class. The adaptive SDM model is used to extract discriminative features, and each category is trained separately to obtain three different training models. Since the key point position is corrected by affine transformation, the final output key point position needs to be converted to the source coordinate system by an inverse transformation. As shown in formula (8), x_t' is the position coordinate in the coordinate system after affine transformation, and x_t is the coordinate of the key point position in the source coordinate system.

$$x_t = M^{-1} x_t'. \tag{8}$$

3.2. The Alignment of Face Images.
In face alignment processing, a regression function is learned to predict the position increment between the current position and the real position. Considering that the regression function is a complex nonlinear mapping function, a linear regression method is used by SDM instead of complex nonlinear regression to predict the position. The objective function is as follows:

$$\min f(x_0 + \Delta x) = \|h(d(x_0 + \Delta x)) - \Phi_*\|_2^2. \tag{9}$$

Suppose that a picture has m pixels $d \in R^{m \times 1}$, and $d(x) \in R^{p \times 1}$ is the p key points on the picture. $x_0 \in R^{p \times 2}$ represents the initial position, and h is a nonlinear feature extraction function. In the experiment of this study, the

(a) (b) (c)

(d) (e) (f)

FIGURE 6: Face posture before and after affine transformation.

HOG feature is used. $\Phi_* = h(d(x_*))$ represents the feature extracted based on the real position. For each sample, there is an initial position x_0. According to Newton's gradient descent criterion, it is only needed to iterate on formula (7) repeatedly to obtain a sequence of Δx, $\{\Delta x_1, \Delta x_2, \ldots, \Delta x_k\}$. And after each iteration, $x_k = x_{k-1} + \Delta x_k$ is corrected. After several iterations, x_k will converge to the optimal position x_*.

Taylor's expansion was carried out on equation (9); then, Δx is derived. Let the derivative be 0; then, equation (10) is obtained as follows:

$$\Delta x = -H^{-1}J_f = -2H^{-1}J_h^T(\Phi_0 - \Phi_*). \qquad (10)$$

Let $R_0 = -2H^{-1}J_h^T$, $b_0 = 2H^{-1}J_h^T\Phi_*$, and the first iteration can be expressed as follows:

$$\Delta x_1 = R_0\Phi_0 + b_0, \qquad (11)$$

where R_0 is seen as the direction of decline. A series of descending directions R_k and b_k need to be calculated and expressed as equation (12). The features extracted at each stage constitute a set $\Phi = \{\Phi_1, \Phi_2, \ldots, \Phi_k\}$.

$$\Delta x_k = R_{k-1}\Phi_{k-1} + b_{k-1}. \qquad (12)$$

The adaptive feature extraction is embodied in Φ_k. As shown in Figure 7, here are five key points as an example. The red dot represents the position obtained at each stage, the green dot represents the real position, and the red circle represents the radius r of the feature extraction frame. Figure 7(a) shows the transformation trend of the radius r of the SDM model. It can be seen that the size of r is constant. This will extract useless features that affect the positioning of key points.

Face alignment is a process from coarse to fine. The size of the radius r of the feature extraction frame is related to the position increment Δx generated in each stage.

When Δx in the training sample is widely distributed, it is more inclined to use large r to extract features. Follow the rule from coarse to fine and adaptively change the size of r to obtain discriminative features. As shown in Figure 7(b), in the initial stage, the obtained position x_k is far from the real position x_*, and Δx is widely distributed. The use of large feature boxes near key points to extract more useful information is conducive to handling large differences in face shape and ensuring robustness. As the stage increases, the distance between x_k and x_* becomes smaller and smaller, and the use of a gradually reduced feature extraction frame can effectively obtain discriminative features. Especially in the later stages, a small feature extraction frame can reduce noise and ensure accuracy. Equation (13) expresses the acquisition process of the radius r_k of the adaptive feature extraction frame, and x_k^{ij} represents the position of the jth key point of the ith sample in the k stage.

(a) Fixed feature block size
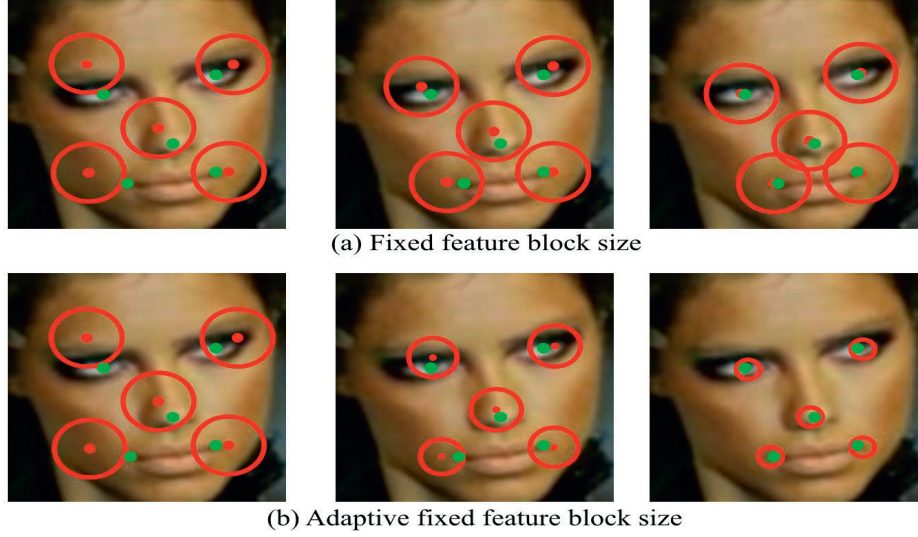

(b) Adaptive fixed feature block size

FIGURE 7: Trend of feature extraction block size with the number of stage. (a) Fixed feature block size. (b) Adaptive fixed feature block size.

$$r_k = \max\left(\left\|x_k^{ij} - x_*^{ij}\right\|\right), \quad j = 1, 2, \ldots, p, i = 1, 2, \ldots, N.$$

(13)

Although r_k is gradually decreasing, the strategy is tough, and it does not take into account the distribution of position increments Δx generated at each stage of the training sample. In the experiment of this study, the radius r_k of the feature extraction frame is adaptively obtained according to the Δx produced in each stage. At each stage, each sample will produce Δx with a dimension of $p \times 2$. Calculate the distance between the current position of each key point and the real position to obtain P distances. N samples will produce $N \times p$ distances. The maximum distance is selected among $N \times p$ distances, which is regarded as the size of the feature extraction frame r of each key point of all samples at this stage. The reason for the largest selection is to extract useful features around the real key points. In this way, the size of the feature extraction frame selected at each stage fully considers the distribution of the current position and the true position of the sample. As the stage increases, it will gradually decrease, and the extracted features can be extracted at the real position to the greatest extent, and the interference of redundant features is also reduced.

By obtaining the radius r of the adaptive feature extraction frame, the discriminative feature $\Phi = \{\Phi_1, \Phi_2, \ldots, \Phi_k\}$ is obtained. The values of R_k and b_k can be calculated by minimizing the difference between the current position increment and the actual position increment, which is shown as follows:

$$\arg \min_{R_k, b_k} \sum_{d^i} \left\|\Delta x_*^i - R_k \Phi_k - b_k\right\|.$$

(14)

This equation is a typical linear least squares problem, and an analytical solution can be obtained. Then, according to formula (12), the position increment Δx_k of the kth stage can be obtained. Then, the key point position x_k of the kth

stage can be obtained. After the iteration is completed, R_k and b_k obtained at each stage can be saved.

In a test sample, the attitude of the face image is first determined, and the corresponding initial position x_0 is given. Then, a series of R_k and b_k obtained in the training stage are used to predict the position of key points.

3.3. Enhancement of the Face Image. It is difficult and costly to obtain sufficient samples of unrestricted face images, and it is difficult to train a satisfactory model based on the number of existing samples. When encountering the problem of insufficient data volume, the common method is to expand the dataset by random cropping, color conversion, and other methods. Although this method can improve the recognition accuracy of the network, the improvement is limited. In this study, the method of transfer learning is adopted with the aid of the daytime aerial photography dataset with relatively sufficient data volume. Fine-tune the daytime vehicle recognition network model through nighttime data to realize the recognition of nighttime targets.

Since restricted face images and unrestricted face images have great similarity, the features extracted by the network are also very similar. Transfer learning takes advantage of this similarity to transplant the restricted face training model to the unrestricted face recognition network. Then, we use the unrestricted face data to enhance the image to make the algorithm more suitable for the recognition of unrestricted face images. The higher the similarity of two objects connected by transfer learning is, the more conducive to transfer learning is. By comparing restricted face data with nonrestricted face data, the main difference lies in the interference of illumination, occlusion, expression, and other factors. Therefore, in order to improve the similarity between restricted face data and unrestricted face data, it can be processed from multiple perspectives such as illumination, occlusion, and expression to improve the similarity. In this study, illumination enhancement is selected for image processing to

improve the similarity between restricted and unrestricted face data. In the algorithm of illumination enhancement, the Retinex algorithm is adopted in this study because it can weaken the influence of light on the object in the image and restore the original color, edge, and other information of the object.

In Retinex theory, images are thought to be composed of incident and reflected light [19]. The basic idea of the image enhancement method is to remove the influence of the illuminating light and retain the reflection properties of the object itself. The Frankle-McCann Retinex iterative algorithm is used in this study. The iterative piecewise linearization based on spiral structure and compares paths to estimate illumination is adopted in this algorithm. The spiral structure path is that the pixel correction result at point $(0, 0)$ will be jointly determined by the pixel value of the inflection point of the path. The number of selected reference points is moderate. The closer to the target point, the more intensive the sampling, the better the result. The color images are used in this study, so the three channels of RGB are processed separately. Finally, the three channels are merged and output.

(1) The early stage of the data conversion

In order to reduce the amount of calculation in subsequent calculations, the pixel value of the original image is converted from the integer domain to the logarithmic domain. To avoid negative values, the original image is added with 1 to the pixel value as a whole, which is expressed as follows:

$$s(x, y) = \log[1 + S(x, y)]. \tag{15}$$

Then, the constant matrix r can be initialized. The constant value takes the average value of the original image pixels, and the size is the same as the original image.

(2) Comparison and correction between pixels

For an image with a pixel size of $m \times n$, the coordinate change between the two comparison points at the furthest distance from the target point is expressed as follows:

$$D = 2^P, \tag{16}$$

where

$$P = \text{fix}[1b \min(m, n) - 1], \tag{17}$$

where fix is the rounding function. Then, the distance between the two comparison points in each next step is shortened to half of the previous step, and the direction is rotated clockwise, which is shown as follows:

$$D = -\frac{D}{2}. \tag{18}$$

And the direction is rotated until the interval of the comparison points is less than 1.

Assuming that $r_n(x, y)$ is the result of the previous iteration, $r_{n+1}(x, y)$ is the result of this iteration. If $D > 0$, then

$$\begin{cases} r_{n+1}(x + D, y) = r_n(x, y) + s(x + D, y) - s(x, y), \\ r_{n+1}(x, y + D) = r_n(x, y) + s(x, y + D) - s(x, y). \end{cases} \tag{19}$$

Otherwise, if $D < 0$, then

$$\begin{cases} r_{n+1}(x, y) = r_n(x - D, y) + s(x, y) - s(x - D, y), \\ r_{n+1}(x, y) = r_n(x, y - D) + s(x, y) - s(x, y - D). \end{cases} \tag{20}$$

(3) Image output display

After the iterative operation, the gray value of the reflected image is often a floating point number, which needs to be linearly converted to an effective gray value:

$$R(x, y) = \frac{r_{n+1}(x, y) - r_{(n+1)\min}(x, y)}{r_{(n+1)\max}(x, y) - r_{(n+1)\min}(x, y)} \times 255, \tag{21}$$

where $r_{(n+1)\max}(x, y)$ and $r_{(n+1)\min}(x, y)$ are the maximum and minimum values of the iteration result $r_{n+1}(x, y)$, respectively, and $R(x, y)$ is the final enhancement result.

4. Results and Discussion

4.1. Method of Transfer Learning. In order to effectively recognize face images in an unrestricted environment, an unrestricted face recognition algorithm based on transfer learning is proposed. The region extraction network of the faster RCNN algorithm is improved to improve the recognition speed of the algorithm. In order to improve the detection accuracy, a transfer learning method is adopted, in which network parameters trained by large-scale datasets are used for initialization. Then, the network parameters trained by the face dataset under unrestricted conditions are fine-tuned. The specific steps are expressed as follows.

Step 1. Large ImageNet dataset and face image dataset are transferred for the first time. The improved faster RCNN network in this study is trained by using the large ImageNet dataset and face image dataset. The parameters obtained from the training are used for network initialization.

Step 2. The secondary transfer learning of face image datasets under unconstrained conditions is carried out. The network parameters trained by the face dataset can be fine-tuned under unrestricted conditions.

Step 3. The initialized network is used to train the RPN and generate ROI

Step 4. According to the ROI obtained in Step 3, the source domain dataset is used to conduct classification and regression training for the initialized network

Step 5 . The network obtained in Step 4 is used to train RPN, adjust only the network layer parameters specific to RPN, and generate ROI

Step 6 . The generated ROI training network was used for classification and regression, and the shared convolutional layer parameters were kept fixed. So far, the training of the faster RCNN network for the target domain data detection model is completed.

4.2. Restricted Face Image Recognition Experiment.
In order to verify the effectiveness of the face recognition algorithm proposed in this study, the recognition experiment is conducted on the CASIA-WebFace face dataset [16], LFW dataset [20], and MegaFace dataset [21] under unrestricted conditions.

4.2.1. CASIA-WebFace Dataset.
CASIA-WEBFACE is one of the most important large-scale datasets in the field of face recognition. It contains more than 494,000 face images with labels of 10,575 people, and the size of its training set is only 0.49 MB. In this study, face images belonging to the same person as LFW and MegaFace were first removed from the dataset. A total of 122,875 face images of 2580 people were selected from the rest of the dataset, and these images were divided into training set, verification set, and test set according to the ratio of 7:2:1. The face image in the training set is preprocessed. Obtain the largest face region in the face image and remove the interference outside the face region. Key points were set in the image, and affine transformation was carried out according to the nose and eyes, so as to make the eyes flush and the nose centered. Then, the face image is further processed to make its size as 112×112. Among them, the face image of the training set is shown in Figure 8.

4.2.2. Recognition Results of Restricted Face Images.
The network model trained by ImageNet is used to initialize the network parameters of the algorithm in this study, and the restricted face image set in the CASIA-WebFace dataset is used to fine-tune the algorithm network in this study, and the target recognition of the restricted face image based on one transfer learning is completed. In this experiment, the recognition effects of different networks are compared on CASIA-WebFace. The results are given in Table 1.

By observing the recognition results in Table 1, it can be seen that the network model in this study can accurately identify restricted face images, and the proposed algorithm has a faster recognition speed.

4.3. Unrestricted Face Image Recognition Experiment.
In order to verify the effectiveness of the proposed algorithm for unrestricted face image recognition, this experiment was tested on LFW and MegaFace datasets under unrestricted conditions. In the model training of CASIA-WebFace datasets, face images belonging to the same person as those in LFW and MegaFace datasets have been removed.

The low-level convolution layer of the network model is used to extract shallow features such as edges, colors, and textures, which has little influence on different datasets. In this study, the parameters of the low 3-layer convolutional network are fixed for the trained constrained face image recognition model. According to the dataset of unrestricted face images, only the parameters of the deeper network are fine-tuned.

4.3.1. LFW Dataset Experiment.
The LFW dataset contains more than 13,000 facial pictures of 5749 people in the natural environment. In the natural environment, human faces are often affected by illumination, expression, and occlusion, which bring great challenges to recognition. In the experiment, a View2 test set containing 6000 pairs of faces was used. In this dataset, it contains a total of 10 folds, and each fold contains 300 pairs of matched and mismatched faces. The random sample of the LFW dataset is shown in Figure 9.

Comparison tests were performed on unrestricted datasets, and the results are shown in Table 2. Through experimental comparison in Table 2, it can be found that the algorithm proposed in this study achieves a quite good recognition effect in the FLW dataset, which is 3.20% higher than Ouamane in the same small dataset. Even in the big data training set, the recognition efficiency is higher than that of DeepFace and DDML. The accuracy is similar to that of Face Net with large training data, which shows that the algorithm framework in this study has a good recognition rate. And the recognition speed of the algorithm in this study has a very good application value for actual engineering applications because of other algorithms.

4.3.2. MegaFace Dataset Experiment.
MegaFace is a public face test dataset with millions of interference items added. MegaFace dataset includes multiple application scenarios such as face verification, face training, and face confirmation.

MegaFace specifies that a training set below 0.5 MB is a small dataset, while a training set above 0.5 MB is a large dataset. However, the network proposed in this study is trained and evaluated under a small dataset. The random sample of MegaFace dataset is shown in Figure 10.

As can be seen from the experimental comparison in Table 3, the recognition rate of the algorithm proposed in this study is 2.10% higher than that of the Ouamane algorithm in the same test results. At the same time, the algorithm in this study exceeds the recognition rate of FaceNet in large-scale data, which is enough to show that the proposed algorithm has good robustness under unconstrained conditions. At the same time, the proposed algorithm has a faster recognition speed.
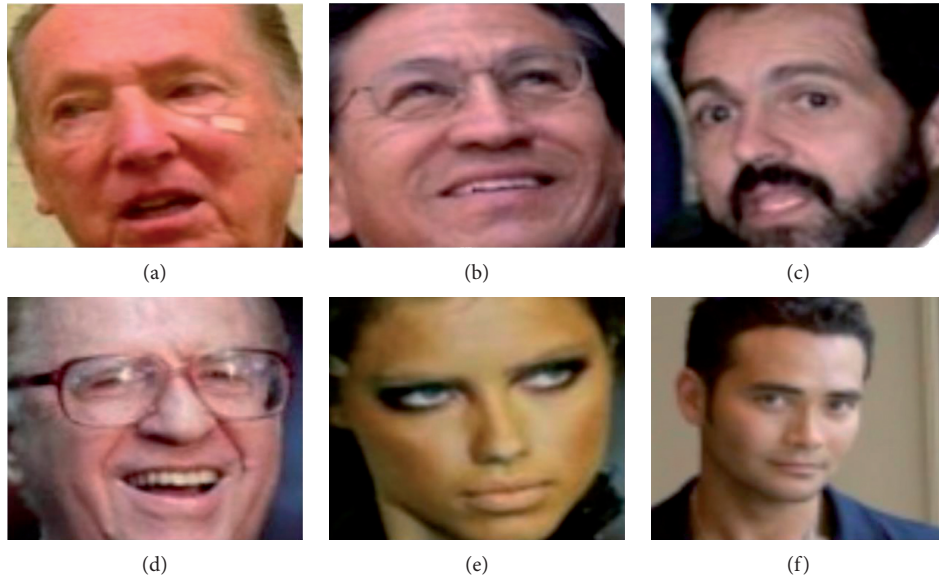
FIGURE 8: The random sample of the CASIA-WebFace dataset.

TABLE 1: Comparison of recognition rate on the CASIA-WebFace dataset.

Methods	Training set size/MB	Test of time/s	Recognition rate/%
FaceNet [8]	199.8	0.61	99.18
DeepFace [22]	3.99	0.29	97.27
DDML [23]	2.53	0.38	98.81
Ouamane [24]	0.68	0.52	98.99
DeepID2 [6]	0.27	0.32	98.87
Faster RCNN [15]	0.49	0.185	97.42
Proposed	0.49	0.049	99.52

FIGURE 9: The random sample of the LFW dataset.

TABLE 2: Comparison of recognition rate on the LFW dataset.

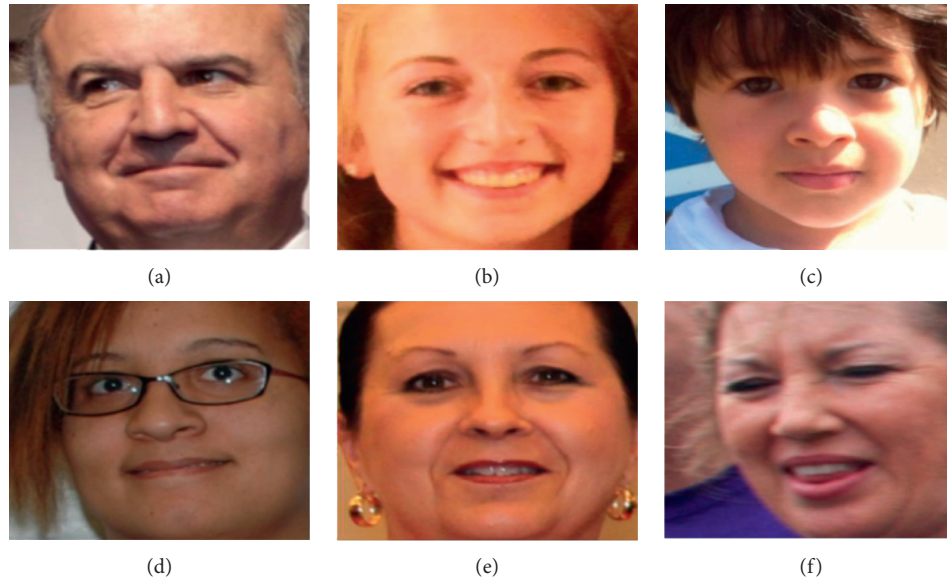| Methods	Training set size/MB	Test of time/s	Recognition rate
FaceNet [8]	199.8	0.62	98.02
DeepFace [22]	3.99	0.29	92.29
DDML [23]	2.53	0.39	93.73
Ouamane [24]	0.68	0.58	94.99
DeepID2 [6]	0.27	0.35	94.82
Faster RCNN [15]	0.49	0.188	91.45
Proposed	0.49	0.051	98.19

(a)　(b)　(c)

(d)　(e)　(f)

FIGURE 10: The random sample of the MegaFace dataset.

TABLE 3: Comparison of recognition rate on the MegaFace dataset.

Methods	Training set size/MB	Test of time/s	Recognition rate
FaceNet [8]	199.8	0.61	91.01
DeepFace [22]	3.99	0.29	86.25
DDML [23]	2.53	0.38	87.76
Ouamane [24]	0.68	0.57	90.10
DeepID2 [6]	0.27	0.34	88.85
Faster RCNN [15]	0.49	0.188	85.42
Proposed	0.49	0.050	92.20

5. Conclusions

In this study, the first transfer learning is completed from the large-scale dataset ImageNet to medium-scale restricted face image set, and the effective recognition of restricted face image set is realized. Then, the secondary transfer learning from the medium-scale restricted face image set to the small-scale unrestricted face image set is completed. The image enhancement methods, such as pose alignment, illumination brightness enhancement, and angle rotation, are applied to the unrestricted face image set to facilitate the smooth transfer learning. Experimental results show that the proposed algorithm has high identification accuracy and can meet the requirements of rapid detection and has the engineering application value for the field of terminal contactless distribution.

Data Availability

The source code of this algorithm cannot be provided directly because of the programmer's reason.

Conflicts of Interest

The author declares that there are no conflicts of interest.

References

[1] C. Cao and G. Wang, "Evaluation of intelligent speech technology in epidemic prevention: take iflytek input software in Chinese and Japanese recognition as an example," *Journal of Physics: Conference Series*, vol. 1631, no. 1, 2020.

[2] L. Hui-Ying and S. Yu-Guo, "Research on unconditioned face recognition based on residual network," *Computer Engineering & Software*, vol. 40, no. 11, pp. 143–147, 2019.

[3] S. V. Dharsini, B. Balaji, K. S. K. Hari et al., "Music recommendation system based on facial emotion recognition," *Journal of Computational and Theoretical Nanoscience*, vol. 17, no. 4, pp. 1662–1665, 2020.

[4] Y. Taigman, M. Yang, M. Ranzato, and L. Wolf, "Deepface: closing the gap to human-level performance in face

verification," in *Proceedings of the IEEE Conference on Computer Vision and Pattern Recognition*, pp. 1701–1708, Columbus, OH, USA, June 2014.

[5] Yi Sun, X. Wang, and X. Tang, "Deep learning face representation from predicting 10,000 classes," in *Proceedings of the IEEE Conference on Computer Vision and Pattern Recognition*, Columbus, OH, USA, June 2014.

[6] Y. Chen, Y. Chen, X. Wang et al., "Deep Learning Face Representation by Joint Identification- verification," in *Proceedings of the International Conference On Neural Information Processing Systems*, MIT Press, Cambridge; MA, USA, June 2014.

[7] Yi Sun, X. Wang, and X. Tang, "Deeply learned face representations are sparse, selective, and robust," in *Proceedings of the IEEE Conference on Computer Vision and Pattern Recognition*, Boston, MA, USA, June 2015.

[8] Y. Zhao, AiP. Yu, and D.T. Xu, "Person recognition based on FaceNet under simulated prosthetic vision," *Journal of Physics: Conference Series*, vol. 1437, no. 1, 2020.

[9] Q. Wang, G. Michau, and O. Fink, "Domain adaptive transfer learning for fault diagnosis," in *Proceedings of the 2019 Prognostics And System Health Management Conference*, Qingdao, China, October 2019.

[10] Y. Song, H. Wang, and X. He, "Adapting deep ranknet for personalized search," in *Proceedings of the 7th ACM International Conference on Web Search and Data Mining*, pp. 83–92, ACM, New York, NY, USA, February 2014.

[11] X. Cao, "A practical transfer learning algorithm for face verification," in *Proceedings of the IEEE International Conference on Computer Vision*, Sydney, Australia, April 2013.

[12] J. Hu, J. Lu, and Y.-P. Tan, "Deep transfer metric learning," in *Proceedings of the IEEE Conference on Computer Vision and Pattern Recognition*, pp. 325–333, Seattle, WA, USA, June 2015.

[13] A. G. Guo, A. H. Wang, A. Y. Yan et al., "A fast face detection method via convolutional neural network," *Neurocomputing*, vol. 395, pp. 128–137, 2020.

[14] F. Cen and G. Wang, "Boosting occluded image classification via subspace decomposition-based estimation of deep features," *IEEE Transactions on Cybernetics*, vol. 99, pp. 1–14, 2019.

[15] R. Girshick, "Fast R-CNN," *Computer Science*, vol. 1, 2015.

[16] T. Kaur and T. K. Gandhi, "Automated brain image classification based on VGG-16 and transfer learning," in *Proceedings of the 2019 International Conference On Information Technology (ICIT)*, IEEE, Bhubaneswar, India, August 2019.

[17] Y. Koga, H. Miyazaki, and R. Shibasaki, "A CNN-based method of vehicle detection from aerial images using hard example mining," *Remote Sensing*, vol. 10, no. 1, p. 124, 2018.

[18] W. U. Yaqin and W. Xiaodong, "Hybrid differential evolution *K*-means unsupervised clustering algorithm in big data mining," Chongqing University of Technology (Natural Science), Chongqing, China, 2019.

[19] W. Chen, L. Wang, Y. Zhang et al., "Anti-disturbance grabbing of underwater robot based on retinex image enhancement," in *Proceedings of the 2019 Chinese Automation Congress (CAC)*, IEEE, Hangzhou, China, February 2020.

[20] P. A. Deshmukh, "Optimal face retrieval from LFW dataset," *IJARCCE*, vol. 6, no. 3, pp. 452–455, 2017.

[21] Z. Wang, K. He, Y. Fu et al., "Multi-task deep neural network for joint face recognition and facial attribute prediction," in *Proceedings of the ACM on international Conference on multimedia retrieval*, pp. 365–374, ACM, Ottawa, ON, Canada, June 2017.

[22] Y. Taigman, M. Yang, M. Ranzato et al., "DeepFace: closing the gap to human-level performance in face verification," in *Proceedings of the IEEE Conference on Computer Vision and Pattern Recognition*, pp. 1701–1708, IEEE Computer Society, Columbus, DC, USA, June 2014.

[23] J. Hu, J. Lu, and Y. P. Tan, "Discriminative deep metric learning for face verification in the wild," in *Proceedings of IEEE Computer Society Conference on Computer Vision and Pattern Recognition*, pp. 1875–1882, Washington, DC, USA, June 2014.

[24] A. Ouamane, "Side-information based exponential discriminant analysis for face verification in the wild," in *Proceedings of the 2015 11th IEEE international conference and workshops on automatic face and gesture recognition (FG)*, IEEE, Ljubljana, Slovenia, May 2015.